Title
Identification of host genetic determinants required for intoxication by cytolethal distending toxins

Author
Eshraghi, Aria

Publication Date
2013

Peer reviewed|Thesis/dissertation

UNIVERSITY OF CALIFORNIA

Los Angeles

Identification of host genetic determinants required for intoxication by cytolethal distending toxins

A dissertation submitted in partial satisfaction of the requirements for the degree

Doctor of Philosophy in Microbiology, Immunology and Molecular Genetics

By

Aria Eshraghi

2013

ABSTRACT OF THE DISSERTATION

Identification of host genetic determinants required

for intoxication by cytolethal distending toxins

by

Aria Eshraghi

Doctor of Philosophy in Microbiology. Immunology and Molecular Genetics

University of California, Los Angeles 2013

Professor Kenneth A. Bradley, Chair

Cytolethal distending toxins (CDTs) are tripartite protein exotoxins produced by a diverse group of pathogenic Gram-negative bacteria. Based on their ability to induce DNA damage, cell cycle arrest and apoptosis of cultured cells, CDTs are proposed to enhance virulence by blocking cellular division and/or directly killing epithelial and immune cells. Despite the widespread distribution of CDTs among several important human pathogens, our understanding of how these toxins interact with host cells is limited. This dissertation identifies and characterizes host factors that confer sensitivity to CDTs from *Aggregatibacter actinomycetemcomitans, Haemophilus ducreyi, Escherichia coli*, and *Campylobacter jejuni.* Host plasma membrane cholesterol supported intoxication and was found to be limiting for sensitivity to CDT in CHO-K1 cells. In contrast, a role for host glycans and the membrane protein TMEM181, which were previously implicated as receptors for

binding of CDT to host cells, were found to be dispensable or play a negative role in sensitivity to CDT. Characterization of CDT-resistant mutants from two independent forward genetic screens identified a series of genes that play a role in CDT intoxication. One of these genes, Derlin-2 (Derl2), is a central component of endoplasmic reticulum associated degredation (ERAD) pathway, suggesting that CDT utilizes ERAD to escape from the lumen of the ER. Derl2 deficient cells are resistant to CDT due to decreased retrotranslocation of CDT from the lumen of the ER. Further, the mechanism of Derl2-dependent of escape of CDTs from the ER is distinct from previously described Derl2-dependent retrotranslocation of ERAD substrates. Specifically, two independent requirements for Derl2-mediated ERAD of misfolded proteins, a conserved WR motif and interaction with the AAA-ATPase p97, are dispensable for retrotranslocation of CDT and another retrograde trafficking toxin, ricin. This previously undescribed mechanism demonstrates a novel Derl2-dependent ERAD pathway exploited by retrograde trafficking toxins. In total, the findings presented here provide insight into the molecular and cellular basis of CDT-host interactions.

The dissertation of Aria Eshraghi is approved.

Linda Baum

Wenyuan Shi

Benhur Lee

Kenneth A. Bradley, Committee Chair

University of California, Los Angeles

2013

DEDICATION

This dissertation is dedicated to my dearest wife Leah, who has filled my life with joy and comfort and whose endless love and support over the years has allowed me to indulge in my scientific curiosity. To my mother and father, Azita and Manou, who worked so hard to provide the opportunities that have led to my success. To my sister, Anita, who inspired a tenacity that gave me the power to never resign in the face of adversity.

TABLE OF CONTENTS

TABLE OF CONTENTS (cont.)

TABLE OF CONTENTS (cont.)

TABLE OF CONTENTS (cont.)

LIST OF FIGURES

LIST OF FIGURES (cont.)

LIST OF TABLES

LIST OF ACRONYMS

Aa – *Aggregatibacter actinomycetemcomitans*

ATM – ataxia telangiectasis-mutated

CDT – cytolethal distending toxin

Cj – *Campylobacter jejuni*

ConA – concanavalin A

CRAC – cholesterol recognition amino acid consensus

Ec – *Escherichia coli*

ENU – N-ethyl-N-nitrosourea

FRET – fluorescence resonance energy transfer

GalNAc – N-acetylgalactosamine

GlcNAc – N-acetylglucosamine

GS-II – Griffonia simplicifolia lectin II

Hd – *Haemophilus ducreyi*

HRP – horseradish peroxidase

K_d – dissociation constant

LCA – *Lens culinaris* agglutinin

LUV – large unilamellar vesicle

MβCD – methyl beta cyclo dextrin

MGC – mammalian gene collection

MLV – murine leukemia virus

MPA – *Maclura pomifera* agglutinin

MSCV – murine stem cell virus

LIST OF ACRONYMS (cont.)

ORF – open reading frame

PEI – polyethyleneimine

RNAi – ribonucleic acid interference

SCID – severe combined immunodeficiency

SGMS1 – sphingomyelin synthase 1

SPR – surface plasmon resonance

TMB – tetramethylbenzidine

UEA – Ulex europaeus agglutinin

WGA – Wheat germ agglutinin

ACKNOWLEDGEMENTS

Special appreciation goes to Dr. Ken Bradley, who has not only served as a mentor, but has been a close friend through my doctoral studies. Several students were integral in the efforts that resulted in this dissertation: Emily Jin-Kyung Kim, Joanna Ruhl, Ashley Tetlow, Somya Jalan, and Julia Kulik all have bright futures ahead of them. Two former members of Dr. Bradley's lab deserve acknowledgement: Dr. Francisco Maldonado-Arocho for propelling me into this project and Dr. David Banks for technical advice in the early years. Other members of Dr. Bradley's lab were sources of intellectual stimulation and day to day shenanigans that made the lab a pleasure: Dr. Jill Terra (formerly Pottratz), Dr. Eugene Gillespie, Mr. Bryan France, and Mr. Charlie (Chi-Lee) Ho. Dr. Steven Blanke and members of his lab at the University of Illinois, Urbana-Champaign provided a fruitful close collaboration for which I am thankful. I am thankful for technical assistance and reagents from Dr. Peter Bradley, Dr. Fuyuhiko Tamanoi and members of their labs. Thanks to Dr. Robert Damoiseaux and the staff of the UCLA Molecular Screening Shared Resource for help with the high-throughput screens. I am grateful to Dr. David Wong for encouraging me to seek out independent NIH funding for my project. The UCLA T32 oral health-scientist predoctoral training grant (T32DE007296) and Ruth L. Kirschstein National Research Service Award (F31DE022485) provided funding for my doctoral studies.

A version of chapter 2 was originally published in the *Journal of Biological Chemistry* by Aria Eshraghi, Francisco J. Maldonado-Arocho, Amandeep Gargi, Marissa M. Cardwell, Michael G. Prouty, Steven R. Blanke, and Kenneth A. Bradley.

Cytolethal Distending Toxin Family Members Are Differentially Affected by Alterations in Host Glycans and Membrane Cholesterol." *The Journal of Biological Chemistry*. 2010; Vol. 285,No. 24, pp.18199–18207. © the American Society for Biochemistry and Molecular Biology. Chapter 5 is a manuscript in preparation entitled "Derlin-2 is required for intoxication by cytolethal distending toxins" and is currently under review for publication. As of the writing of this dissertation, the intended authors are Aria Eshraghi, Emily Jin-Kyung Kim, Batcha Tamilselvam, Julia Cherise Kulik, Amandeep Gargi, Robert Damoiseaux, Steven R. Blanke and Kenneth A. Bradley. The appendix contains a paper that was originally published in the *Journal of Biological Chemistry* by Amandeep Gargi, Batcha Tamilselvam, Brendan Powers, Michael G. Prouty, Tommie Lincecum, Aria Eshraghi, Francisco J. Maldonado-Arocho, Brenda A. Wilson, Kenneth A. Bradley, and Steven R. Blanke. entitled "Cellular Interactions of the Cytolethal Distending Toxins from *Escherichia coli* and *Haemophilus ducreyi*." 2013, January 10 (Epub ahead of print); © the American Society for Biochemistry and Molecular Biology.

VITA

Education

University of California, Los Angeles
Ph.D., Microbiology, Immunology and Molecular Genetics 2006-2013
University of California, Berkeley
B.A. Integrative Biology (High Honors) 2002-2004

Research

Doctoral Research
University of California, Los Angeles 2006-2013
Advisor: Dr. Kenneth A. Bradley, Ph.D.
Laboratory Rotations
University of California, Los Angeles Spring 2007
Advisor: Dr. Kenneth A. Bradley, Ph.D.
University of California, Los Angeles Winter 2007
Advisor: Dr. Wenyuan Shi, Ph.D.
University of California, Los Angeles Fall 2006
Advisor: Dr. Srinivasa Reddy, Ph.D.
Honors Undergraduate Research
University of California, Berkeley 2002-2004
Advisor: Dr. Bruce Ames, Ph.D.
Research Associate
Children's Hospital Oakland Research Institute; Oakland, CA 2004-2006
Advisor: Dr. Bruce Ames, Ph.D. and Dr. Mark Shigenaga, Ph.D.
Pacific Biolabs Hercules, CA (formerly Northview Pacific Labs) 1999-2003
Director: Dr. Gurpreet Ratra Ph.D.

Publications

Eshraghi, A., Kim, E., Batcha, T., Kulik, J., Gargi, A., Blanke, S.R., Bradley, K.A. *Derlin-2 is required for intoxication by cytolethal distending toxin.* (Manuscript *in prep*aration)

Gargi, A., Tamilselvam, B., Powers, B., Prouty, M.G., Lincecum, T., **Eshraghi, A.**, Maldonado-Arocho, F.J., Wilson, B.A., Bradley, K.A., and Blanke, S.R. *Cellular interactions of the cytolethal distending toxins from Escherichia coli and Haemophilus ducreyi.* Journal of Biological Chemistry. Epub 2013 Jan 10

Eshraghi, A., Maldonado-Arocho, F.J., Gargi, A., Cardwell, M., Prouty, M., Blanke, S.R., and Bradley, K.A. *Cytolethal distending toxin family members are differentially affected by alterations in host glycans and membrane cholesterol.* Journal of Biological Chemistry. 285(24): p 18199-207, 2010.

Fellowships/Grants/Awards

- NIH-NIDCR (F31DE022485) Ruth L. Kirschstein National Research Service Award — 3/2012 – 2/2013
  Role: Principal Investigator
  Title: Host determinants governing interactions with cytolethal distending toxins
- NIH-NIDCR (T32DE007296) Oral Health Scientist Predoctoral Training Grant — 1/2010 – 2/2012
  Role: Trainee
  Title: Characterizing interactions between Aggregatibacter actinomycetemcomitans cytolethal distending toxin and host cells
- Howard Hughes Medical Institute Biology Fellows Program (UC Berkeley) — 7/2003 – 6/2004
  Role: Trainee
  Title: A molecular probe to investigate bacterial translocation across the gastrointestinal barrier

Research Seminars

- Micro Club, University of California, Los Angeles — 11/2012
  Title: Totally eRAD! Cytolethal distending toxins exploit protein dislocation to cause nuclear destruction.
- Molecular Biology Retreat, University of California, Los Angeles — 10/2011
  Title: Identification of a host genetic determinant required for intoxication by cytolethal distending toxin.

Posters Presented

- Gordon Conference: Microbial Toxins and Pathogenicity. Waterville Valley, NH — 2012
  Poster title: Host determinants governing interactions with cytolethal distending toxins
- Microbial Pathogenesis and Host Response Conference. Cold Spring Harbor, NY — 2011
  Poster title: Host determinants governing interactions with cytolethal distending toxins
- American Society for Microbiology General Meeting. San Diego, CA — 2010
  Poster title: Cytolethal distending toxins from divergent bacteria have distinct host cell requirements for intoxication

Teaching Experience

- Affiliated Global Faculty – Department of Biology — 2010 – Present
  Animal Physiology; Bahai Institute of Higher Education, Online
- Graduate Student Instructor – Department of Microbiology, Immunology and Molecuar Genetics — Fall 2009
  Teaching Assistant Training Course; University of California, Los Angeles
- Teaching Assistant – Department of Microbiology, Immunology and Molecuar Genetics — Spring 2008 & Fall 2007
  Microbiology Lab; University of California, Los Angeles

CHAPTER 1

INTRODUCTION

1.1 BACKGROUND

In 1987 and 1988 the laboratory of Dr. Hermy Lior discovered a new heat labile toxin in the culture supernatants of *Escherichia coli* and *Campylobacter* species (Anderson et al., 1987; Johnson and Lior, 1988a; Johnson, 1987). Filtrates of culture supernatants from E. coli (O55:K59:H4), *C. jejuni*, *C. coli*, *C. fetus* subspecies *fetus*, and *C. laridis* caused a marked distention of Chinese hamster ovary (CHO-K1), Vero, HeLa and HEp-2 cells followed by cell death after prolonged exposure. Based on the lethality of the toxin and marked distention of intoxicated cells, it was named cytolethal distending toxin (CDT). CDTs are part of a recently described class of bacterial proteins and effectors that cause cell cycle arrest in host cells called cyclomodulins (Nougayrede et al., 2005). CDTs are hypothesized to modulate host cellular function by inducing "limited damage"; that is, the well-adapted pathogen may use the strategy of not inducing overt toxicity to allow the host to live, yielding a niche for the pathogen to proliferate (Lara-Tejero and Galan, 2002). Since Johnson and Lior discovered CDT in 1998, a number of other CDT-expressing pathogens have been identified (reviewed in (Smith and Bayles, 2006) and (Gargi et al., 2012)). This dissertation focuses on the CDTs expressed by four pathogens: *Aggregatibacter actinomycetemcomitans* (Aa-CDT), *Haemophilus ducreyi* (Hd-CDT), *Escherichia coli* (Ec-CDT) and *Campylobacter jejuni* (Cj-CDT).

CDTs are important virulence factors for several pathogens. Wildtype *C. jejuni* were more invasive and had greater pro-inflammatory capabilities in SCID and NFκB-deficient mice than *C. jejuni* mutants that lack CDT expression (Fox et al., 2004; Purdy et al., 2000). Infection with *Helicobacter hepaticus* CDT mutants caused

reduced levels of inflammation in murine models of inflammatory bowel disease and hepatic dysplasia (Ge et al., 2007; Young et al., 2004). Wildtype *H. hepaticus* and mutants lacking CDT expression initially colonized IL-10-deficient mice equivalently, but only wildtype *H. hepaticus* produced long-term infection and typhlocolitis (Pratt et al., 2006). Further, *C. jejuni* lacking CDT expression were unable to colonize mucin-deficient mice (McAuley et al., 2007). The purified toxin itself is able to cause pathogenic symptoms. Intragastric administration of recombinant *Shigella dysenteriae* CDT in the suckling mouse model caused diarrhea, necrosis of intestinal mucosa and sloughing of the epithelia in the descending colon (Okuda et al., 1997).

The role of CDTs as virulence factors in infection studies in animals is supported by epidemiological studies in humans that reveal a significant association of *cdt* genes with increased virulence. The presence of Aa-CDT is significantly associated with strains that cause aggressive periodontitis (Tan et al., 2002). Clinical isolates from patients with the sexually transmitted disease chancroid reveal that 83% of the chancroid causing *H. dureyi* isolates encode the CDT operon and are cytotoxic. Further, sonicates from 89 out of 100 strains of *H. ducreyi* isolated from various geographic areas demonstrated cytotoxic activity, likely due to CDT (Purven et al., 1995). The presence of CDT genes was found to be significantly associated with *E. coli* induced hemolytic uremic syndrome, characterized by haemolysis and renal failure (Bielaszewska et al., 2004). One hundred out of 114 (87.7%) *C. jejuni* isolates from Danish broiler chickens had CDT activity on Vero cells and all but one of these 114 isolates contained the cdt genes (Bang et al., 2001). These data suggest that CDT is an important virulence factor that contributes to pathogenesis.

1.1.1 The host – toxin relationship

Based on the ability to induce DNA damage, cell cycle arrest and apoptosis of cultured cells, CDTs have been proposed to function *in vivo* by blocking cellular division and/or directly killing epithelial and immune cells. Because of this, identification and characterization of specific host factors that support intoxication may lead to development of therapeutics to block toxin action, thereby limiting the pathogenic ability of the bacteria. For example, if CDT mediates immune evasion by the pathogen, toxin inhibitors can aid in pathogen detection and clearance. Identifying host factors that are required by the toxin, especially receptors, and characterization of the molecular determinants of these host-toxin interactions can lead to the development of toxin inhibitors. For example, soluble receptors or peptides that imitate the amino acids that mediate binding of a proteinacious toxin can be used to block toxin binding to the host cell surface (Rainey and Young, 2004). Characterization of the mechanisms that mediate toxin entry and intracellular trafficking can lead to development of dominant negative protein constructs or small molecule inhibitors that block these processes required for intoxication (Rainey and Young, 2004).

An additional benefit provided by the investigation of bacterial and plant toxin trafficking is to reveal novel and unexpected mechanisms by which pathogens subvert existing host systems. These studies have historically provided valuable insights into fundamental host cellular processes (Sandvig and van Deurs, 2005). Since CDTs are the first known bacterial effectors targeted to the host cell nucleus

(Nishikubo et al., 2003), they represent a tool to study a previously unknown trafficking pathways usurped by bacterial virulence factors to gain entry into the nucleus.

1.2 CDT IS A TRIPARTITE TOXIN

CDT consists of a hetero-trimeric complex of three proteins encoded by a single operon. CdtA, CdtB and CdtC form the holotoxin in a 1:1:1 stoichiometry by following the AB_2 type toxin model, consisting of one catalytically Active subunit, CdtB, and two Binding subunits, CdtA and CdtC (Figure 1.1).

1.2.1 The binding subunits: CdtA and CdtC

Several lines of evidence suggest that CdtA and CdtC make up the CDT binding moiety. CdtA and CdtC facilitate binding of CdtB to the cell surface of HeLa cells (Lee et al., 2003; McSweeney and Dreyfus, 2004). Pre-binding HeLa and U937 cells only with both CdtA and CdtC, not CdtA or CdtC alone, allowed for uptake of CdtB (Deng and Hansen, 2003; McSweeney and Dreyfus, 2004, 2005; Mise et al., 2005). Further, pre-binding cells with a combination of CdtA and CdtC, but not CdtA or CdtC alone, inhibited binding and/or intoxication by the holotoxin (Deng and Hansen, 2003; Lee et al., 2003). CdtB/CdtC dimers have partial activity, but full activity requires the complete trimer (Akifusa et al., 2005; Lara-Tejero and Galan, 2001; Lee et al., 2003; Nesic et al., 2004).

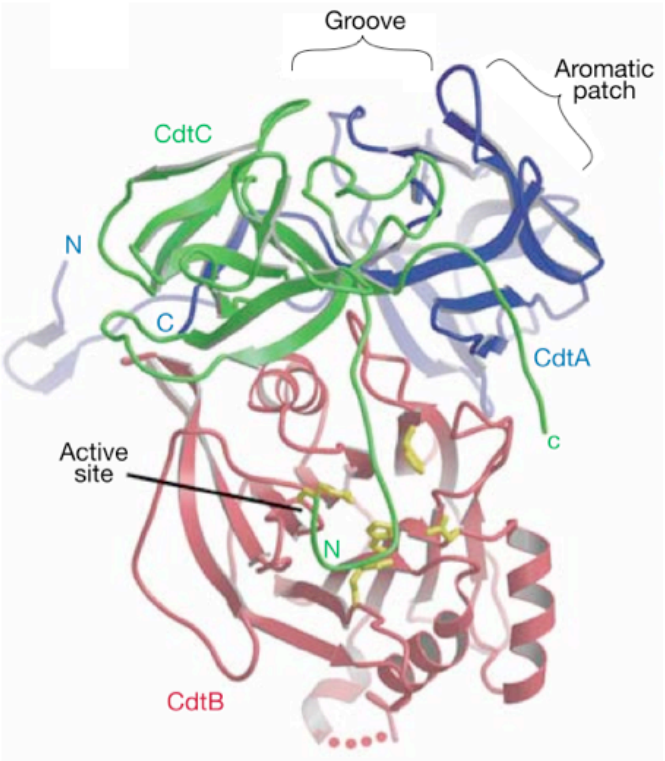

Figure 1.1 Crystal structure of Hd-CDT.
Shown as a ribbon cartoon, the blue ribbon shows CdtA, red CdtB, green CdtC and the active site in yellow. The red dots indicate CdtB peptide not modeled due to disorder. N- and C-termani are indicated. Reprinted by permission from Macmillan Publishers Ltd: (Nesic et al., 2004), copyright 2004.

Without CdtA and CdtC, CdtB is harmless to host cells unless it is microinjected into the cytoplasm, expressed ectopically or electroporated (Lara-Tejero and Galan, 2000; McSweeney and Dreyfus, 2004).

CdtA and CdtC both adopt lectin-like structures resembling ricin, an unrelated retrograde trafficking AB toxin expressed by the castor oil plant *Ricinus communis*. Structural alignment of Hd-CdtA and Hd-CdtC with the ricin B-chain results in root mean square deviations of 2.3 angstroms and 3.7 angstroms over 119 and 108 amino acids, respectively (Nesic et al., 2004). Close examination of Hd-CdtA and Hd-CdtC in the crystal structure reveals two marked surface elements. First, there is a large patch of eight closely packed aromatic amino acids in Hd-CdtA and second, a deep groove is formed at the interface of the two proteins away from where they interact with Hd-CdtB. For Hd-CDT, simultaneous mutagenesis of four of the residues in the aromatic patch on Hd-CdtA (W91G/W98G/W100G/Y102A) or the four residues that make up the deep groove between Hd-CdtA and Hd-CdtC (CdtA: P103A/Y106A; CdtC R43K/Q49A) had no effect on holotoxin assembly. Although holotoxin structure was unaffected, the aromatic and deep groove mutants displayed blocked or severely diminished ability to bind and intoxicate HeLa cells, respectively (Nesic et al., 2004; Nesic and Stebbins, 2005). Mutagenesis of the Aa-CdtA residues that make up the aromatic patch resulted in loss of binding to CHO-K1 cells for the residues that don't affect holotoxin formation (Y140A, Y188A, and Y189A but not Y105A, which prevented holotoxin formation) (Cao et al., 2008). This suggests that the aromatic patch in CdtA and the deep groove formed at the interface

between CdtA and CdtC are involved in binding to the receptor that is present on HeLa and CHO-K1 cells.

1.2.2 The catalytically active subunit: CdtB

CdtB shares structural homology with a class of Mg^{2+} dependent phosphoesterase enzymes, including DNAse I and phosphatidylinositol 3,4,5-triphosphate (PI-3-4-5-P_3) phosphatase (Dlakic, 2000, 2001). The predominantly studied activity of CdtB is that of a DNAse I-like enzyme causing DNA double strand breaks. Indeed, performing a structural alignment of the active sites of Hd-CdtB and DNAse I reveals an almost perfect superimposition with a root mean square deviation of 3.3 angstroms over 209 amino acids (Figure 1.2) (Nesic et al., 2004). Mutation of the CdtB residues that are homologous to DNase I catalytic residues, residues that mediate contact with DNA, or residues that support Mg^{2+} binding, renders the toxin unable to cleave DNA in cell free systems and unable to intoxicate cells (Elwell et al., 2001; Elwell and Dreyfus, 2000; Guerra et al., 2005; Lara-Tejero and Galan, 2000; Shenker et al., 2007).

The field has predominantly focused on the DNAse activity of CdtB; however, several reports have characterized the PI-3-4-5-P_3 phosphatase activity. Comparison of the Aa-CdtB active site with that of inositol polyphosphate-5 phosphatase reveals a high degree of homology for the residues required for activity (Figure 1.3). Aa-CdtB hydrolyzes PI-3-4-5-P_3 to PI-3-4-5-P_2 in cell free systems by cleaving off a single phosphate, similar to phosphatidylinositol 5-phosphatases (Shenker et al., 2007).

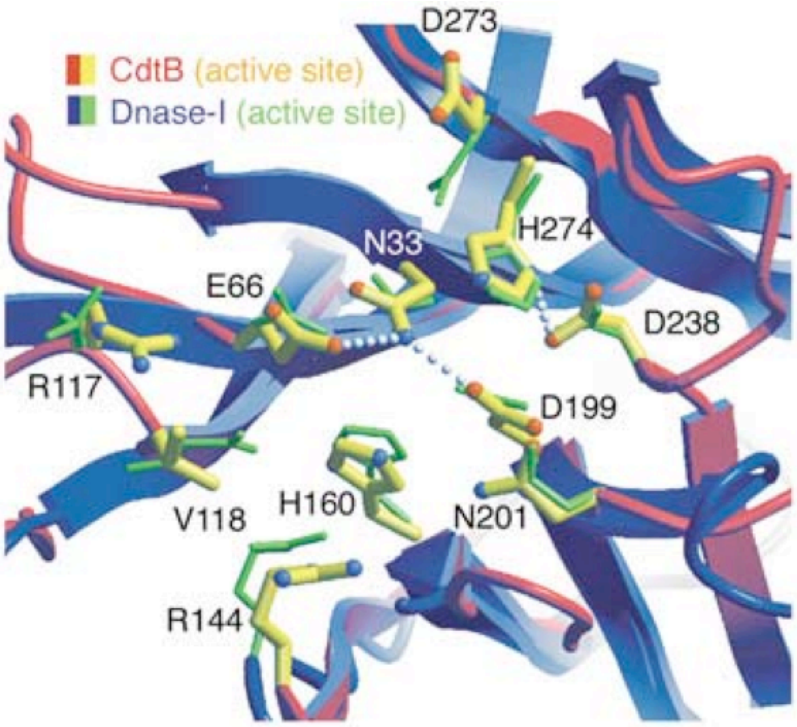

Figure 1.2 Structural alignment of the active sites of Hd-CdtB with DNase I. Main-chain/side-chain atoms of Hd-CdtB are shown in red/yellow and Main-chain/side-chain atoms of DNase I are shown in blue/green. Reprinted by permission from Macmillan Publishers Ltd: (Nesic et al., 2004), copyright 2004.

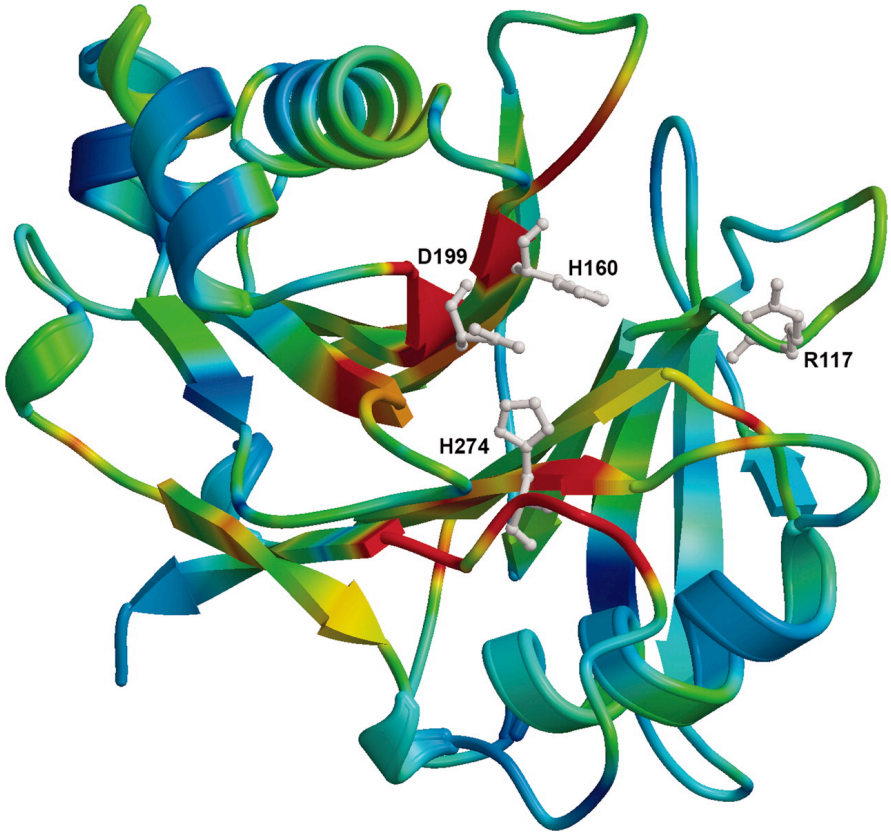

Figure 1.3 Structural comparison of the active sites of Hd-CdtB with IP5P. Residues that are most conserved between the two proteins are shown in red with color changing toward green for intermediated conservation and blue for lack of conservation. Despite overall lack of homology between these proteins, the active sites are very similar, suggesting that they share functional similarity. Figure from (Shenker et al., 2007).

Aa-CDT intoxication of Jurkat cells causes time dependent reduction of cellular PI-3-4-5-P_3. The two catalytic histidines that are required for activity in CdtB and DNase I are also present in PI-3-4-5-P_3 phosphatases. Further, mutation of these histidines or other residues that are homologous to those required for PI-3-4-5-P_3 phosphatase function renders CDT unable to intoxicate Jurkat cells (Shenker et al., 2007). Pre-treatment of Jurkat cells with the PI3K inhibitors Wortmannin and LY290004 lowering cellular PI-3-4-5-P_3 levels resulted in protection from Aa-CDT intoxication (Shenker et al., 2007).

It is still unclear which of the two CdtB activities are the most important to pathogenesis. The phosphatase activity has only been studied in the CDT encoded by *A. actinomycetemcomitans* (Rabin et al., 2009; Shenker et al., 2007). One possibility is that the predominant activity is specific to the species expressing that CDT. Alternatively, it is possible that CDTs have both activities but based on the host cell being targeted, one activity is predominant over the other. Indeed, by inducing mutations that inhibit the phosphatase activity and not the DNAse activity, it was determined that intoxication of differentiated nonproliferating U937 cells was independent of phosphatase activity. In contrast, proliferating U937 cells were resistant to holotoxins that were comprised of Aa-CdtB with mutations that cause reduced phosphatase activity or reduced phosphatase and DNase activity, suggesting that proliferating U937 cells require phosphatase or phosphatase and DNase activity for intoxication (Rabin et al., 2009). This suggests that CDT intoxication of proliferating and nonproliferating U937 cells occurs by distinct

mechanisms and is an experimental model that can be applied to other cell lines and CDTs expressed by other bacteria.

1.2.3 CdtC inhibits CdtB activity

The crystal structure of CDT reveals that each of the three CDT subunits interfaces with the two others to form the stable holotoxin. Further Hd-CdtA and Hd-CdtC subunits display non-globular amino acid extentions at the N- and C-termini (Nesic et al., 2004). Of particular interest is the N-terminal tail of CdtC. Thirteen amino acids in the N-terminal tail of Hd-CdtC are in close proximity with the Hd-CdtB residues modeled to interact with DNA, thereby blocking the active site of CdtB and rendering the toxin inactive in cell free assay systems (Nesic et al., 2004). Deletion of these 13 amino acids (CdtCΔ21-35) results in renewed activity in a plasmid relaxation assay. Interestingly, holotoxins assembled with either wildtype Hd-CdtC or Hd-CdtCΔ21-35 have similar activity in cellular intoxication assays. This suggests that CdtB activity is inhibited by the N-terminal tail of CdtC and this inhibition is removed during intracellular trafficking (discussed below).

1.3 CDT HOST CELL BINDING AND INTRACELLULAR TRAFFICKING

1.3.1 Cell binding

For toxins that act on intracellular targets, binding to the cell surface is an important first step. Because of this, many groups focus on the requirements for toxin binding. Both CdtA and CdtC play an important role in CDT binding the receptor. Although there are some examples that show that the CdtB-CdtC dimer is

sufficient to cause a low-level intoxication, the holotoxin is much more efficient (Akifusa et al., 2005; Lara-Tejero and Galan, 2001; Lee et al., 2003; Nesic et al., 2004). For both Ec-CDT and Cj-CDT, binding of CdtA and CdtC to the surface of HeLa cells was saturable and specific, as an excess of unlabeled CdtA or CdtC was able to inhibit the binding of the labeled proteins (Lee et al., 2003; McSweeney and Dreyfus, 2005). Interestingly, Cj-CdtC was able to competitively inhibit binding of Cj-CdtA and vise versa, also. This suggests that a specific receptor for Cj-CDT exists on the surface of HeLa cells and that both binding subunits use the same receptor. The binding of Hd-CDT to the surface of HeLa cells has a disassociation constant (K_d) of 270 nM (A. Gargi and S. Blanke, personal communication). This high affinity binding is functionally relevant: incubation of HEp-2 cells with holotoxin for as little as 15 minutes on ice, which allows for binding but not internalization, followed by thorough washing and warming to 37ºC to allow internalization, results in efficient intoxication (Cortes-Bratti et al., 1999). The identification and characterization of these receptors would be a significant advance in the CDT field. Though uncharacterized, some cell surface molecules have been suggested to play a role in Aa-CDT and Ec-CDT binding; however, no specific receptors have been identified for Hd-CDT and Cj-CDT.

One report suggests that the receptor for Aa-CDT on lymphocytes is cholesterol (Boesze-Battaglia et al., 2009). Extraction of cholesterol from the plasma membranes of Jurkat cells by incubation with the cholesterol chelator methyl beta cyclodextrin (MβCD) abolished Aa-CDT binding and internalization. Aa-CDT bound to large unilamellar vesicles (LUVs) constructed of cholesterol and not to LUVs that

contain other similar sterols. Increasing the cholesterol concentration in LUVs resulted in greater binding of Aa-CDT in a dose dependent fashion as assessed by fluorescence resonance energy transfer (FRET) and surface plasmon resonance (SPR). Finally, a cholesterol recognition/interaction amino acid consensus (CRAC) domain was found on Aa-CdtC and mutation of this CRAC domain resulted in reduced binding to cholesterol containing LUVs and reduced ability to bind and intoxicate Jurkat cells. Since this finding, an atypical CRAC domain was identified in CdtC from *Haemophilus parasuis* (Zhou et al., 2012) and cholesterol depletion of CHO-K1 cells by treatment with MβCD was shown to inhibit binding and intoxication by Cj-CDT (Lin et al., 2011). Although depletion of cholesterol may alter CDT internalization or trafficking, the studies described above reveal that cholesterol extraction led to reduced CDT binding in addition to inhibited intoxication. This suggests that reduction in intoxication from MβCD resulted, at least in part, from inhibition of binding (Zhou et al., 2005).

Due to the presence of ricin-like lectin domains in CdtA and CdtC, host glycoconjugates may play a role in CDT binding and intoxication (Hu et al., 2006; Hu and Stebbins, 2006; Lara-Tejero and Galan, 2001; Nesic et al., 2004). Pre-treatment of CHO-K1 cells with an inhibitor of asparagine-linked glycosylation, tunicamycin, made them resistant to Ec-CDT intoxication (McSweeney and Dreyfus, 2005). However, for some proteins, inhibition of glycosylation results in misfolding and turnover. If the receptor for CDT is a glycoprotein that requires glycosylation, tunicamycin treatment may cause CDT resistance via reduced receptor presentation. Further, tunicamycin has been shown to inhibit the rate-limiting

enzyme of cholesterol biosynthesis, HMG-CoA reductase (Volpe and Goldberg, 1983); therefore, tunicamycin treatment may inhibit intoxication via cholesterol depletion-induced reductions in CDT binding, internalization and trafficking. Next, there is evidence that lectins block CDT binding and intoxication. Pre-binding HeLa cells with lectins that bind fucose or fucose-containing glycans inhibited binding by Ec-CdtA and Ec-CdtC and prevented intoxication by Ec-CDT (McSweeney and Dreyfus, 2005). Using a lectin to block CDT from accessing the cell surface may also result in blocking access to the protein component of a cell surface glycoprotein; therefore, this experiment cannot conclude if fucose or a fucosylated protein serves as the receptor.

A sub-class of glycoconjugates, glycoproteins with asparagine-linked glycans, may play a role in CDT binding. Ec-CdtA and Ec-CdtC bind to immobilized glycoproteins and this binding is abolished if the immobilized glycoproteins are pre-treated with Peptide-N-Glycosidase F (PNGase F), an enzyme that cleaves the covalent bond between asparagine and the innermost N-acetylglucoseamine (GlcNAc) (McSweeney and Dreyfus, 2005). Pre-treatment of HeLa cells with PNGase F prior to CDT intoxication made them resistant to intoxciation by Ec-CDT (McSweeney and Dreyfus, 2005). In contrast, pre-treatment of HeLa cells with O-glycosidase, which cleaves the covalent bond between serines or threonines and the innermost N-Acetylgalactosamine (GalNAc), had no effect on Ec-CDT intoxication (McSweeney and Dreyfus, 2005). These data suggest that asparagine linked glycans support CDT binding.

There is also evidence that host glycosphongolipids support CDT intoxication. Glycosphongolipids are composed of membrane embedded ceramide covalently linked to a glycan; the most common first linkage to the ceramide is to a glucose molecule. Pre-incubation of monocytic U937 cells with 1-phenyl-2-palmitoylamino-3-morpholino-1-propanol (PPMP), an inhibitor of glucosylceramide synthesis, results in inhibition of Aa-CDT intoxication (Mise et al., 2005). Further, CHO-K1 cells deficient in ceramide biosynthesis (LY-B cells), and therefore deficient in glycosphingolipids, were reported to be resistant to Aa-CDT intoxication compared to their complemented counterparts (Mise et al., 2005). GM3 containing liposomes were able to bind and precipitate Aa-CDT prior to intoxication of U937 cells, while liposomes containing a variety of other glycosphingolipids were not. Based on these data, glycosphingolipids may play a role in CDT intoxication, at least for Aa-CDT and monocytes.

More recently, a forward somatic cell genetic approach identified two cell surface factors that support Ec-CDT intoxication (Carette et al., 2009). A human chronic myeloid leukemia cell line (KBM7) with a nearly haploid karyotype (except chromosome 8) was mutagenized with a gene trapping retrovirus, selected with Ec-CDT and proviral integrations in resistant clones were mapped by sequencing gene-trapped host DNA. Cells deficient in sphingomyelin synthase 1 (SGMS1) were resistant to intoxication, and complementation with *SGMS1* cDNA restored sensitivity. SGMS1 deficient cells were deficient in sphingomyelin, as judged by resistance to a lysenin, a sphingomyelin specific toxin derived from the coelomic fluid of the earthworm *Eisenia foetida* (Yamaji et al., 1998). Since sphingomyelin is

an integral part of lipid rafts, depletion is thought to result in destruction of lipid raft structure leading to the prevention of receptor clustering and functional endocytosis (Miyaji et al., 2005). The second gene identified in the screen was *TMEM181*, a putative G-protein coupled receptor present at the cell surface (Carette et al., 2009; Wollscheid et al., 2009). Like SGMS1, complementation of TMEM181 deficient cells with TMEM181 cDNA resulted in renewed sensitivity to Ec-CDT. Flag-tagged Ec-CDT was able to co-immunoprecipitate HA-tagged TMEM181, indicating a binding interaction between the molecules. Lastly, overexpressing TMEM181 in mouse embryo NIH3T3 fibroblast cells, human osteosarcoma U2OS cells, and HeLa cells made them hypersensitive to Ec-CDT intoxication. Although TMEM181 may be required for Ec-CDT intoxication and has previously been shown to be present on the cell surface, there is still no indication that knockdown results in decreased binding; therefore, TMEM181 may play a role other than cell binding.

1.3.2 Internalization

After binding, CDT is internalized into the endosomal network dependent on several host factors. Clustering of the receptor into clathrin coated pits is required for efficient intoxication by Hd-CDT. Potassium depletion from the media resulted in removal of clathrin coats and inhibition of Hd-CDT activity 40-80% on HEp-2 cells (Cortes-Bratti et al., 2000; Moya et al., 1985). Pharmacological inhibitors of clathrin assembly into coated pits, chlorpromazine and imipramine, inhibited Hd-CDT intoxication of HEp-2 cells by 80% (Cortes-Bratti et al., 2000; Sofer and Futerman, 1995). Internalization of CDT is dependent on dynamin. Overexpression of a

dominant negative dynamin, which is required for clathrin dependent endocytosis, inhibited Hd-CDT intoxication of HeLa cells (Cortes-Bratti et al., 2000; Damke et al., 1994).

Depletion of cholesterol from the plasma membrane results in reduced CDT intoxication (Boesze-Battaglia et al., 2009; Guerra et al., 2005; Lin et al., 2011; Zhou et al., 2012). Cholesterol depletion has been shown to alter of lipid raft organization and receptor uptake (Kabouridis et al., 2000; Mahammad et al., 2010), which could lead to inhibition of CDT intoxication (Boesze-Battaglia et al., 2006; Lin et al., 2011). Alternatively, inhibition of intoxication may occur via reduced binding to the cell surface (as described above) or through altered trafficking. Indeed, vesicular trafficking of another retrograde trafficking toxin, ricin, is inhibited by cholesterol depletion or supplementation (Grimmer et al., 2000).

1.3.3 Trafficking

Several protein toxins expressed by bacteria and plants must access intracellular targets to exert an action on host cells. Based on the functions of their subunits, one class of these toxins is known as the “AB” toxins and is composed of multiple subunits that have two main functions. The “B” subunit(s) is responsible for binding to the cell membrane and the “A” subunit(s) contains the active or catalytic activity. All of these toxins face the formidable challenge of crossing a biological membrane in order to gain access to their intracellular targets. The AB toxins can be split into two groups (Table 1.1). Both groups of toxins are endocytosed into the endosomal network. The toxins in one of theses subgroups, including diphtheria

toxin, anthrax lethal toxin, anthrax edema toxin and clostridial neurotoxins, enter the cytoplasm through the endosomal membrane (Figure 1.4). The translocation across the endosomal membrane is due to conformational changes in the toxin molecules mediated by acidification of the endosomal lumen which results in exposure of hydrophobic residues that insert into the membrane (Draper and Simon, 1980; Sandvig and Olsnes, 1980, 1981, 1988).

The second subgroup of AB toxins, which includes Shiga toxin, cholera toxin, *Pseudomonas* exotoxin A, ricin and CDT, is retrograde trafficked through the Golgi apparatus and into the ER. All characterized retrograde trafficking toxins are thought to retrotranslocate across the ER membrane into the cytosol to reach their intracellular targets. This retrotranslocation process is currently an active area of investigation for CDT. CDT is unique in this subgroup in that the final cellular target is in the nucleus and not the cytosol (Nishikubo et al., 2003).

Interestingly, there are some differences in trafficking between the CDTs encoded by divergent pathogens. Pre-treatment of HeLa cells with ammonium chloride and bafilomycin A1, inhibitors of endosomal acidification, prevented trafficking and intoxication by Hd-CDT, but not Ec-CDT (Gargi et al., 2013). Further, Hd-CDT required functional Rab7 for trafficking through the endosomal network and colocalizes with Rab9, while Ec-CDT did not. These data suggest that Hd-CDT requires trafficking through late endosomes that are acidified, while Ec-CDT does not. These different trafficking pathways correlate with the high level of divergence between Hd-CDT and Ec-CDT.

Table 1.1 Examples of AB toxins that are either translocated across the endosomal membrane or that are trafficked through the Golgi and ER.

Toxins that cross the endosomal membrane to gain access to the cytosol	Toxins that are retrograde trafficked through the Golgi apparatus and ER
Bacillus anthracis Lethal Toxin	Shiga toxin
Bacillus anthracis Edema Toxin	Ricin
Diptheria Toxin	Cholera toxin
Clostridial neurotoxins	*Pseudomonas* exotoxin A
Cytotoxin necrotizing factor 1	
Clostridium botulinum C2 toxin	
Clostridium difficile toxin B	
Pasturella multodica toxin	

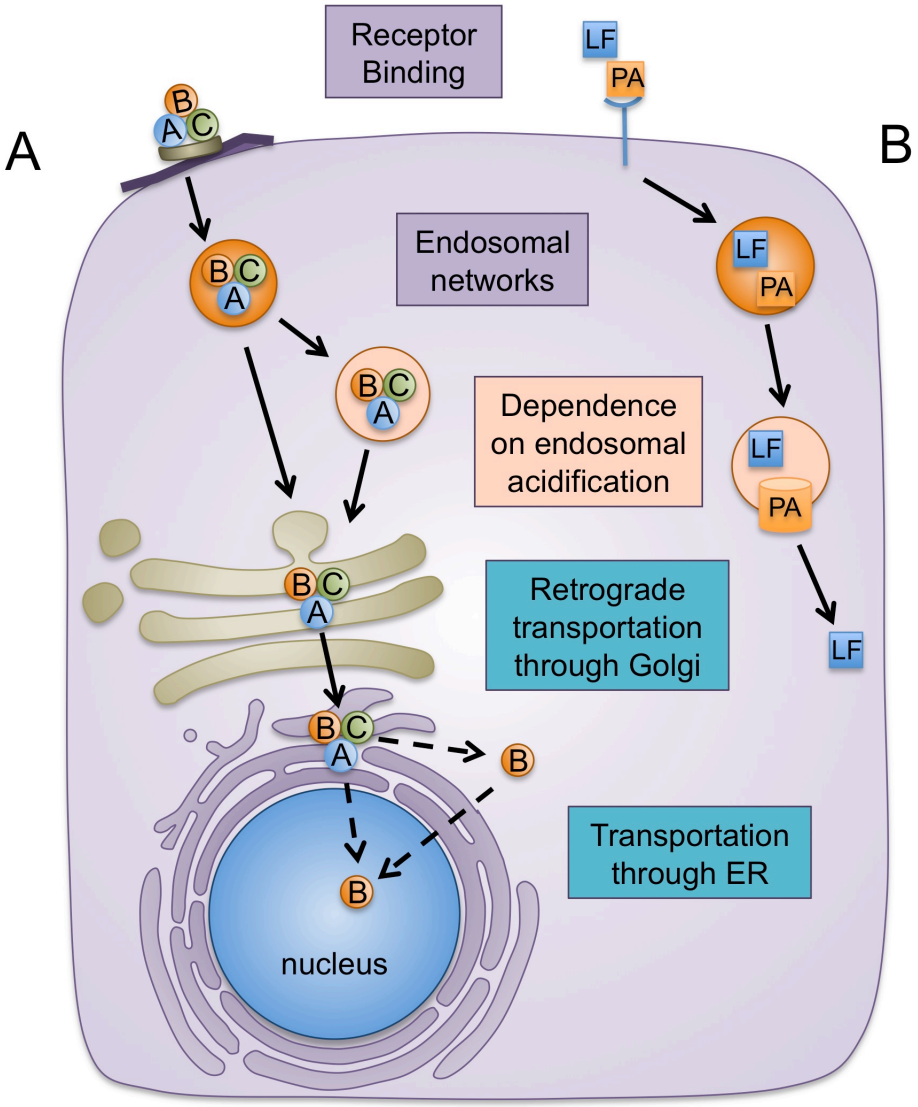

Figure 1.4 Toxin trafficking (Adapted from (Gargi et al., 2012)).
(A) CDTs bind a cell surface receptor and are endocytosed. Some CDTs require trafficking through an acidified endosome. CDTs are retrograde trafficked through the Golgi apparatus into the lumen of the ER. CDTs are then translocated through the ER membrane either directly into the lumen of the nucleus or are translocated into the cytosol and are imported into the nucleus via a nuclear localization signal. (B) The trafficking of anthrax lethal toxin is shown in contrast. After binding to a cell surface receptor and internalization, acidification of the endosome causes a conformational change in protective antigen which causes formation of a pore, through which lethal factor translocates to gain access to the cytosol.

A series of intricate experiments has demonstrated that CDT is retrograde trafficked through the Golgi and ER before reaching the final cellular target in the nucleus. Two pharmacological inhibitors block the endosomal trafficking. Bafilomycin A1 inhibits vacuolar proton ATPases, raising the vesicular pH and blocking protein transport from early to late endosomes (Bayer et al., 1998). Nocodazole disrupts microtubules blocking the fusion of endosomes with downstream vesicles such as late endosomes, lysosomes and the Golgi (Bayer et al., 1998). Pre-treating HEp-2 cells with either of these drugs prior to intoxication with Hd-CDT resulted in a complete block to intoxication (Cortes-Bratti et al., 2000). Incubation of cells at 18°C prevented endosomal transport of proteins to the lysosomes or Golgi and blocks intoxication of HEp-2 cells by Hd-CDT (Cortes-Bratti et al., 2000). Further, an intact Golgi apparatus is required for trafficking of CDT. Brefeldin A and ilimaquinone disrupts the Golgi complex resulting in redistribution of the Golgi membranes and proteins throughout the cell or to the ER (Chardin and McCormick, 1999; Nambiar and Wu, 1995; Takizawa et al., 1993). Treatment of HeLa and MDCK cells with either of these inhibitors resulted in resistance to Hd-CDT intoxication (Akifusa et al., 2005; Cortes-Bratti et al., 2000; Guerra et al., 2005). Finally, a biochemical approach was taken to illustrate the trafficking of CDT through the Golgi. Taking advantage of the fact that protein sulfation occurs exclusively in the trans-Golgi, a CdtB sulfation assay was used to determine if CDT is trafficked through the Golgi. HeLa cells were pre-incubated with radiolabeled sulfate and intoxicated with Hd-CDT holotoxin containing Hd-CdtB with a sulfation tag (SAEDYEYPS). Detection of radiolabeled CdtB demonstrated that CDT was

trafficked through the Golgi (Guerra et al., 2005). Using a similar method, Hd-CDT was shown to traffic through the ER, where protein mannosylation occurs. Mannosylation of Hd-CdtB tagged with three glycosylation sites $(NGTKNNTSQ)_3$ demonstrated that CDT was trafficked through the ER (Guerra et al., 2005).

Perhaps the most controversial step in the mechanism of CDT intoxication is the trafficking of CDT downstream of the ER. As discussed above, all of the characterized retrograde trafficking toxins are believed to be retrotranslocated from the lumen of the ER to the cytoplasm to reach their intracellular targets. Based on this dogma, many believed that CDT undergoes a similar process to reach the cytosol and is subsequently trafficked into the nucleus. Supporting this hypothesis is the presence of putative nuclear localization signals (NLS) on both Aa-CdtB and Ec-CdtB, (McSweeney and Dreyfus, 2004; Nishikubo et al.). Interestingly, the nuclear localization signals on Aa-CdtB and Ec-CdtB are in different locations, but mutagenesis of any of the residues conserved residues results in an inactive toxin. Direct visualization of CdtB in the cytoplasm has proven elusive, and only one study has provided evidence for this. Fluorescence microscopy revealed diffuse Aa-CdtB staining across what seems to be the cytosol (Damek-Poprawa et al., 2012); however, such an experimental approach is difficult to interpret. Biochemical evidence, like the experiments described above, would be more convincing; however, such data does not exist. Alternatively, some evidence suggests that CDT is trafficked from the ER directly to the nucleus, without an intermediate step in the cytoplasm. First, a series of CHO cell lines selected to be resistant to ricin, *Pseudomonas* exotoxin A and cholera toxin and presumed to be deficient in the ER

associated degradation (ERAD) pathway (Teter and Holmes, 2002; Teter et al., 2003) are not resistant to Hd-CDT (Guerra et al., 2005). Second, transfection of HeLa cells with dominant negative versions of Derlin-1 and Derlin-2, proteins involved in ERAD, did not inhibit intoxication by Hd-CDT (Guerra et al., 2005). Third, a farnesylation assay similar to the sulfation and glycosylation assays described above shows that Hd-CdtB with a farnesylation tag is not farnesylated in the cytoplasm, although the lack of a signal is not necessarily conclusive (Guerra et al., 2009). Last, confocal microscopy of HeLa cells intoxicated with Hd-CDT composed of epitope tagged Hd-CdtB demonstrated spike-like projections into the nucleus. These projections were composed of the ER membrane and epitope tagged Hd-CdtB, which led the authors to conclude that CDT is trafficked directly from the ER to nucleus (Guerra et al., 2009); however, the resolution of this data is not convincing. The mechanism by which CdtB traffics out of the ER lumen is the topic of chapter 5.

1.4 THE EFFECTS OF CDT INTOXICATION ON HOST CELLS

1.4.1 The eukaryotic cell cycle

Eukaryotic cells posses an intricate system of development and division that is generally organized into four distinct steps (Figure 1.5)(reviewed in (Alberts, 2002)). The first step, termed the gap-1 or G_1 phase, occurs after the previous division and before DNA synthesis. The G_1 phase is a period of growth toward the end of which the chromosomes are prepared for duplication. In the next step, termed the synthesis or S phase, the chromosomes are duplicated but each daughter chromosome remains attached to the other.

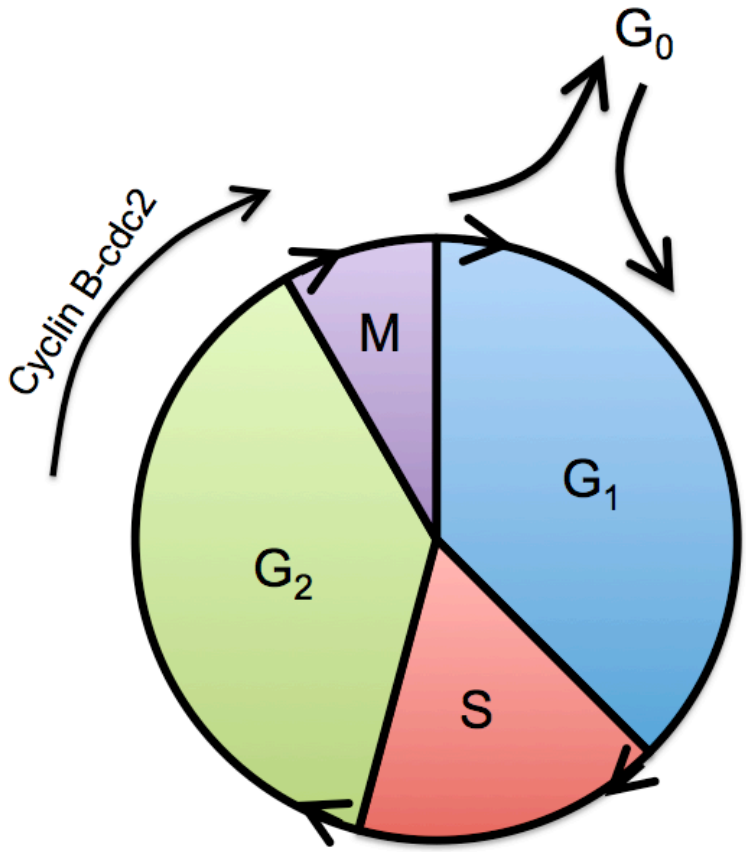

Figure 1.5 The Eukaryotic Cell Cycle.
The eukaryotic cell cycle is composed of four distinct steps. The gap-1 phase (G_1) is characterized as a period of growth and preparation for DNA synthesis. The synthesis phase (S) is characterized by duplication of the DNA. The gap-2 phase (G_2) is another period of growth resulting in a cellular size roughly twice the size at the beginning of G_1. The entry into the mitosis phase (M) step is controlled by a complex of Cyclin B and cdc2. Following M, the cells can enter a quiescent state called G_0, when the cell is not preparing to divide.

After DNA synthesis during the S phase, there is another growth phase, termed gap-2 or G_2, after which the cells are about twice the size as they were at the beginning of G_1. During the last phase, mitosis, several events occur that result in two daughter cells. The chromosomes condense and the nuclear envelope dissolves to allow for a spindle apparatus to form. This spindle apparatus attaches to each chromosome and pulls each of the daughter chromosomes to an opposite corner of the elongating cell. In the middle of the elongated cell, the cell membrane pinches off to result in two daughter cells, each containing a single complete complement of chromosomes in a newly formed nucleus. This process repeats over and over in dividing cells; however, in some cases where there is an absence of a growth signal or the presence of a growth inhibitory signal, the cells enter a period of called G_0 following mitosis, exhibited by the lack of growth.

The progression through the cell cycle is controlled by the expression of a series of proteins called cyclins. Expression of each cyclin occurs at a specific point of the cell cycle, resulting in oscillating concentrations in synchrony with the cell cycle. Once the cyclin reaches a critical concentration, it associates with a specific member of the cyclin dependent kinase (CDK). Activation of the CDK requires two events. First, a phosphatase dephosphorylates CDK and second, dephosphorylated CDK associates with a cyclin to form an active CDK (Alberts, 2002; Smits and Medema, 2001). Activated CDKs drive progression through the cell cycle.

Molecular mechanisms that control progression through the cell cycle provide the assurance that one step has completed with fidelity before the next step commences (reviewed in (Elledge, 1996)). A series of these checkpoint

mechanisms are responsible for halting the cell cycle if DNA integrity has been compromised and loss of checkpoint function can lead to mutagenesis, replicative gaps and chromosomal aberrations (Kaufmann and Paules, 1996). Although these checkpoints can halt the cell cycle at one of three times during the cell cycle, during G_1, during S or during G_2, the double stranded breaks caused by CDT most often cause arrest in the G_2 phase.

The cyclin B-cdc2 complex controls progression from G_2 into S phase (Figure 1.6)(Smits and Medema, 2001). Mammalian cells begin to synthesize cyclin B at the end of S phase via cell cycle regulated transcription (Piaggio et al., 1995; Pines and Hunter, 1989). An additional mechanism that explains G_2-specific expression of cyclin B is that cyclin B mRNA is more stable in G_2 versus G_1 (Pines and Hunter, 1989). Cyclin B binds to its associated CDK, cdc2, and is held in an inactive state by phosphorylation of cdc2 by the Wee1/Mik1 family of kinases (Atherton-Fessler et al., 1993; Endicott et al., 1994; Lundgren et al., 1991; Parker and Piwnica-Worms, 1992). Cdc25C dephosphorylates the cyclin B/cdc2 complex during late G_2 to result in the initiation of mitosis (Dunphy, 1994). Further, the cyclin B/cdc2 phosphorylates Cdc25C to activate it, leading to a feedback activation mechanism that results in rapid progression into mitosis (Hoffmann et al., 1993; Izumi and Maller, 1993).

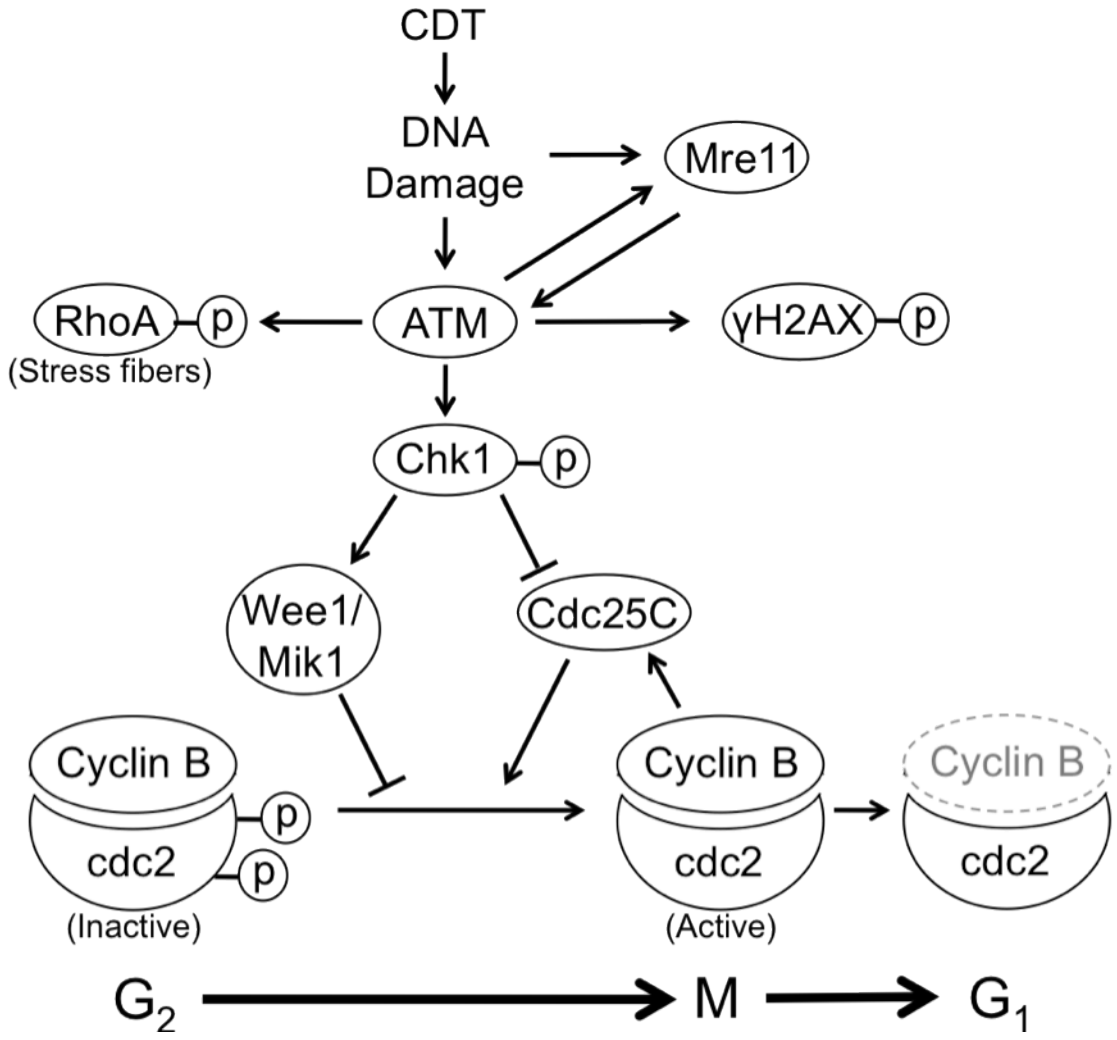

Figure 1.6 Control of the progression from G_2 to Mitosis.
Double stranded DNA damage is recognized by the Mre11 complex and ATM. The Mre11 complex recruits ATM to the sites of DNA damage and ATM further activates the Mre11 complex to recruit DNA repair enzymes. ATM phosphorylates RhoA to induce stress fiber formation and phosphorylates the histone H2AX to further recruit DNA repair enzymes. ATM also phosphorylates Chk1 that induces a signal transduction cascade that leads to cell cycle arrest at the G_2/M interface. Activated Chk1 activates Wee1/Mik1 kinase that sequesters cdc2 in the inactive state. Activated Chk1 inhibits Cdc25C phosphatase activity that, again, sequesters cdc2 in the inactive state. In the absence of DNA damage, active Cyclin B-cdc2 further activates Cdc25C that results in an autoactivation loop, leading to a rapid progression into mitosis. Finally, after mitosis is well under way, Cyclin B is degraded.

1.4.2 CDT intoxication causes cell cycle arrest

Cells have evolved a complex set of DNA damage responses in response to a constant barrage of environmental factors like ionizing radiation and oxidative free radicals liberated by ongoing metabolism. These responses upregulate mechanisms of DNA repair and delay the cell cycle to avoid propagating genetic damage to daughter cells. The cellular response to DNA damage caused by CDT intoxication has been likened to that caused by ionizing radiation. Indeed, both CDT intoxication and ionizing radiation caused DNA double strand breaks, resulting in activation of similar DNA damage responses (Cortes-Bratti et al., 2001; Li et al., 2002).

CDT possesses weak DNase I activity that causes limited DNA damage in the host nucleus. In an *in vitro* assay, the CDT DNAse activity had approximately 0.01% of the activity reported for human or bovine DNase (Elwell et al., 2001). This relatively weak DNase activity correlates with the limited damage caused by CDT rather than an overt toxicity (Lara-Tejero and Galan, 2002). Further, this suggests that the CdtB phosphatase activity may play an important roll in toxicity that that has yet to be studied thoroughly. The relatively weak DNAse activity is sufficient to cause DNA damage both *in vitro* and *in vivo*. Incubating purified CDT with supercoiled plasmid DNA resulted in degradation to relaxed or linear forms within 12 hours (Elwell et al., 2001; Elwell and Dreyfus, 2000; Nesic et al., 2004). Ectopic expression of CdtB in HeLa cells resulted in nuclear fragmentation (Lara-Tejero and Galan, 2000). Intoxication of HeLa cells with CDT or ectopic expression of CdtB in

yeast resulted in a marked DNA fragmentation as judged by pulse field gel electrophoresis (Frisan et al., 2003; Hassane et al., 2001).

The response to double stranded DNA breaks is regulated by a well-studied mechanism of signal transduction (Figure 1.6)(reviewed in (Kaufmann and Paules, 1996) and (Dasika et al., 1999)). The DNA damage caused by CDT was recognized by the Mre11 complex which is composed of Mre11, Rad50 and Xrs2 proteins and serves to stimulate DNA repair via either homologous recombination or non-homologous end joining (Boulton and Jackson, 1998; Li et al., 2002). The Mre11 complex also functions to arrest the cell cycle to allow for DNA repair to occur prior to progression through the cell cycle via activation of ataxia telangiectasis-mutated kinase (ATM) (Uziel et al., 2003). ATM is a tumor suppressor protein and a central regulator of the DNA damage response. Upon recognition of DNA damage and stimulation by the Mre11 complex, ATM became activated via autophosphorylation (Carson et al., 2003; Lee and Paull, 2005).

Activated ATM has a number of known targets. First, CDT-mediated ATM activation caused induction of RhoA-mediated stress fiber formation (Frisan et al., 2003). Consistent with previous literature demonstrating cell survival with functional RhoA expression, stress fiber formation in CDT-intoxicated cells inhibited cell death (Fiorentini et al., 1998; Frisan et al., 2003). Second, ATM phosphorylates histone H2AX at the sites near the double strand breaks caused by CDT, thereby recruiting other proteins involved in DNA repair (Burma et al., 2001; Li et al., 2002). Last, ATM phosphorylates Chk1, which inhibits Cdc25C activity. Therefore, ATM activation results in a signal transduction pathway that results in cell cycle arrest at the G_2/M

boundry. ATM-deficient cells displayed reduced sensitivity to CDT, demonstrating the importance of ATM to the host cellular response to CDT (Cortes-Bratti et al.; Frisan et al., 2003).

1.4.3 CDT intoxication causes apoptosis in some cell lines

The role of CDT in the induction of apoptosis has yet to be elucidated; however, several studies have begun to characterize CDT-mediated induction of apoptotic markers in monocytes and T cells. The DNase activity of CdtB was required for caspase-3 dependent induction of apoptosis in proliferating U937 cells. In contrast, CDT induced apoptosis in differentiated nonproliferating U937 cells in an uncharacterized caspase-independent manner (Rabin et al., 2009). CDT intoxicated Jurkat T cells displayed increased caspase-2 and -7 activity and increased cell surface presentation of phosphatidylserine as judged by staining with Annexin V (Ohara et al., 2004). One interesting report suggested that DNA fragmentation occured via the apoptotic cascade and not directly due to DNA damage induced by CDT (Shenker et al., 2006). This report hypothesized that the CdtB phosphatase activity leads to induction of apoptosis and subsequent activation of endogenous nucleases, which result in DNA fragmentation. In this study, two inhibitors of apoptosis, overexpression of Bcl-2 and the caspase-3 inhibitor zvad, blocked apoptosis, DNA fragmentation as judged by the TUNEL assay and histone H2AX phosphorylation but had no effect on G_2 arrest. Together, these data suggest that CDT may cause apoptosis in monocytes and T cells to limit the host immune system.

1.4.4 CDT induced cytokine secretion

Hosts have evolved many mechanisms to detect and combat pathogens. Although cytokine release plays a role in many of these mechanisms, there are only a few studies investigating the role that CDT plays in induction of these mediators. These studies suggest that CDT expression is responsible for at least some of the inflammation caused by these pathogens. *C. jejuni* infection induced IL-8 secretion, which is responsible for many of the symptoms associated with *Campylobacter*-induced colitis. IL-8 induction by *Campylobacter* was dependent on CDT expression (Hickey et al., 2000). IL-8 was also induced by intoxication of monocyte derived dendritic cells (MDDC) with Hd-CDT (Xu et al., 2004). Treatment of peripheral blood mononuclear cells with the CDT subunits from *Aggregatibacter actinomycetemcomitans* induced secretion of IL-1β, IL-6, and IL-8, and in some cases, co-treatment with multiple subunits was synergistic in cytokine secretion (Akifusa et al., 2001). In this same study, IFNγ was only induced upon treatment with the holotoxin (Akifusa et al., 2001). This cytokine expression was not due to co-purification of bacterial lipopolysaccharide because blocking the LPS coreceptor with an anti-CD14 antibody that blocks LPS-mediated cytokine expression did not attenuate CDT-mediated cytokine expression. A/JCr mice were infected with wildtype *Helicobacter hepaticus* and isogenic mutants unable to express CDT. Of the mice that had established infections, only wildtype mice had induced IFNγ mRNA expression in the gastrointestinal tract (Ge et al., 2005). Likewise, the mice infected with wildtype *H. hepaticus* had higher Th1 associated IgG2a, Th2 associated IgG1,

and mucosal associated IgA responses. It remains unclear whether cytokine secretion is advantageous to pathogenesis or to immune mediated clearance of the infection.

Pathogens expend significant efforts to evade the host immune system. If expression of CDT could block cytokine release, this would be a certain advantage to the pathogens. *H. ducreyi* mediated IL-12 induction is blocked by pre-treating monocyte derived dendritic cells (MDDC) with Hd-CDT (Xu et al., 2004). MDDC and macrophages pre-treated with Hd-CDT and stimulated with *H. ducreyi* lipooligosaccharide are unable to cause T-cell proliferation (Xu et al., 2004). Taken together, these results suggest that expression of CDT may provide an advantage to the pathogen by hampering the immune response.

1.4.5 CDT induced carcinogenesis

Chronic exposure to DNA damaging agents, such as reactive oxygen species produced during cellular metabolism and ionizing radiation causes genomic instability, which leads to tumor induction. Chronic inflammation is associated with increased risk of tumor development and progression (Grivennikov et al., 2010; Karin et al., 2006). The genotoxic and proinflammatory capability of CDT suggest that this toxin may be associated with carcinogenesis (reviewed in (Guerra et al., 2011)). CDT expression enhances colonization and persistence, which are hallmarks of chronic infections. Wildtype *H. hepaticus* colonized a higher percentage of outbred Swiss Webster mice than isogenic CDT deficient mutants (Ge et al., 2005). Further, 10 months after persistent infection of A/JCr mice with *H. hepaticus*,

only mice infected with wildtype developed hepatic dysplasic nodules and displayed increased hepatocyte proliferation, even though both groups had similar numbers of *H. hepaticus* in the liver (Ge et al., 2007). The presence of hepatic dysplasia in mice infected with wildtype *H. hepaticus* correlated with enhanced expression of TNFα, IFNγ, Cox-2, and IL-6. Long-term chronic exposure of rat fibrobalsts and human colonic epithelial cells to sub-lethal doses of *H. hepaticus* CDT resulted in genomic instability and phenotypic properties of malignancy (Guidi et al., 2013). These cells had impaired DNA damage response and enhanced growth in semisolid media, characteristics of malignant cells. Although it is unclear whether the genotoxicity or the proinflammatory capability of CDT is responsible for progression towards carcinogenicity or malignancy, the data suggests a link between CDT and cancer.

1.5 EXPRESSION OF CDTs BY VARIOUS PATHOGENS

CDTs are expressed by a wide array of Gram-negative pathogens occupying diverse niches and causing a variety of diseases. The presence of CDT in unrelated pathogens suggests that the evolutionarily conserved cyclomodulatory activity of CDT is an effective virulence strategy. Our lab has studied CDTs expressed by four human and animal pathogens. Of the three proteins that make up CDT holotoxins, the active subunits, CdtB, encoded by these diverse pathogens, share relatively high levels of homology, while the binding subunits, CdtA and CdtC, range from closely related, as in comparing those from *A. actinomycetemcomitans* and *H. ducreyi*, to more distantly related, as in comparing those from *E. coli* and *C. jejuni* (Table 1.2; discussed in Chapter 2).

Studies presented here utilized four distinct CDTs with varying levels of homology. Using such an approach can elucidate common and differential host factors that support sensitivity to this class of toxins. Two models may exist. Host factors required for intoxication may be shared by closely related toxins that share a high degree of amino acid homology, but colonize very different tissues within the host, such as Aa-CDT and Hd-CDT. Alternatively, host factors required for intoxication may be shared by CDTs expressed by pathogens that share a common niche, like Ec-CDT and Cj-CDT. This hypothesis would be supported by the fact that these pathogens are exposed to the same environmental influences (host cell types, extracellular mileu, immune influences), they may have evolved CDTs that share common binding requirements and functions

In order to investigate host factors required by divergent CDTs, the studies presented here provide data on CDTs expressed by four distinct pathogens. The CDTs expressed by *A. actinomycetemcomitans* and *H. ducreyi* share a high degree of amino acid homology, while the CDTs expressed by *E. coli and C. jejuni* are unrelated. Not only do these diverse pathogens express divergent CDTs, they also inhabit diverse niches. For example, *A. actinomycetemcomitans* and *H. ducreyi*, which both belong to the Pasteurellaceae family, occupy the human oral cavity and the human external genitalia. It will be interesting to determine if common niches or amino acid homology plays a greater role in host factor requirements for CDT intoxication. A comparative understanding of the role for CDTs in the pathogenesis of these bacteria will provide a comprehensive knowledge of host factors required by this diverse family of toxins.

Table 1.2 Percentage of amino acid identity in cytolethal distending toxin families. (Figure adapted from (Pickett and Whitehouse, 1999)).

	Species			
CDT Protein	**Ec**	**Cj**	**Hd**	**Aa**
CdtA				
Ec	100	26.3	32.7	33.8
Cj		100	25.7	26.2
Hd			100	91.9
Aa				100
CdtB				
Ec	100	56.5	50.6	49.8
Cj		100	50.2	50.2
Hd			100	96.8
Aa				100
CdtC				
Ec	100	26.3	25.3	27.1
Cj		100	23.5	23.7
Hd			100	93.5
Aa				100

Aggregatibacter actinomycetemcomitans (formerly *Actinobacillus actinomycetemcomitans*)

A. actinomycetemcomitans is a non-motile facultatively anaerobic oral commensal coccobacillus. This opportunistic pathogen is associated with aggressive periodontitis, oral abscesses, osteoclastogenesis and several extra-oral pathologies such as osteomyelitis, synovitis, skin infections, urinary tract infections, pericarditis and endocarditis (Norskov-Lauritsen and Kilian, 2006; Sullivan et al., 2002; Tan et al., 2002; Wilson and Henderson, 1995). The connection to the heart is the strongest of the non-oral infections as *A. actinomycetemcomitans* causes 0.6% of endocarditis overall and has been found in 18% of atherosclerotic plaque samples (Das et al., 1997; Haraszthy et al., 2000).

The form of aggressive periodontitis caused by *A. actinomycetemcomitans* is characterized by inflammation and degeneration of the gingiva, alveolar bone (which forms tooth socket) and periodontal ligament (connective tissue that surrounds the root of the tooth), leading to the eventual loss of teeth (Suzuki, 1988). Epidemiological studies show the presence of Aa-CDT is significantly associated with strains that cause aggressive periodontitis (Tan et al., 2002). The ability of Aa-CDT to intoxicate T-cells is hypothesized to contribute to the ability of this pathogen to cause chronic infections, presumably by helping to suppress localized immune responses (Shenker et al., 1999). Aa-CDT also affects cell types other than lymphocytes, and may contribute to localized tissue destruction seen in oral

abscesses (Mayer et al., 1999; Sugai et al., 1998). T-cells and periodontal fibroblasts intoxicated with CDT upregulate RANKL, a key cytokine involved in bone resorption, implicating CDT as an important factor in osteoclastogenesis during periodontitis (Norskov-Lauritsen and Kilian, 2006). Also, topical application of Aa-CDT to the rat oral gingival epithelium *in vivo* resulted in cell cycle arrest (Ohara et al., 2011). Aa-CDT expression may allow immune evasion leading to proliferation, oral abscesses, dental caries, destruction of the periodontum and eventually tooth loss. These data provide evidence that CDT is a virulence factor that is important to oral health.

1.5.2 Haemophilus ducreyi

H. ducreyi is a Gram-negative bacillus that is the causative agent of the disease chancroid. Chancroid is characterized by slow-healing, soft, painful, pimple-like ulcers on the external genetalia that eventually burst to form open ulcers covered with purulent exudate. If left untreated, approximately half of patients develop inguinal bubos that burst and form deep craters (Morse, 1989). Since untreated chancroid results in open ulcers on the genitalia, clinicians have made it a priority to treat it in areas of high HIV prevalence (Trees and Morse, 1995).

Though a role for CDT in *Haemophilus ducreyi* pathogenesis has yet to be thoroughly tested, two studies have shown a correlation of CDT with clinical isolates from chancroid patients. Ahmed and colleagues found the presence of the CDT operon and cytotoxic activity was present of 83% of clinical isolates from chancroid patients (Ahmed et al., 2001). Another study found that sonicates from 89 out of 100

strains of *H. ducreyi* isolated from various geographic areas demonstrated cytotoxic activity, likely due to CDT activity (Purven et al., 1995). Several human cell lines are sensitive to Hd-CDT, including Jurkat T-cells, THP-1 monocytes and the epithelial-like cell lines HeLa and HEp-2 from the cervix and larynx, respectively (Wising et al., 2005a). A single animal study has explored recombinant Hd-CDT in a chancroid model. Intradermal co-administration of Hd-CDT with *H. ducreyi* exacerbated dermal lesions in a rabbit dermal model of chancroid, to a greater extent than *H. ducreyi* alone (Wising et al., 2005b). In contrast, one human study found no difference between the ability of wildtype *H. ducreyi* and isogenic CDT mutants to cause skin pustules (Young et al., 2001); however, this methodology can only investigate establishment of infection and not persistence or tissue penetration. Although the details of how Hd-CDT contributes to chancroid pathology is still unclear, the significant presence of the toxin in clinical isolates suggests that Hd-CDT plays a role in pathogenesis.

1.5.3 Escherichia coli

E. coli are rod-shaped bacteria associated with numerous diseases, including gastroenteritis and hemolytic-uremic syndrome. Several *E. coli* strains have been shown to produce CDTs. The CDTs expressed by these strains have been designated Ec-CDT-I (Scott and Kaper, 1994), Ec-CDT-II (Pickett et al., 1994), Ec-CDT-III (Peres et al., 1997), Ec-CDT-IV (Toth et al., 2003) and Ec-CDT-V (Bielaszewska et al., 2004; Janka et al., 2003). Culture filtrates from enterpathogenic *E. coli* were shown to have CDT activity on African green monkey

kidney Vero cells, human cervical carcinoma HeLa cells, human larynx carcinoma HEp-2 cells and CHO-K1 cells, but not effective on mouse adrenal tumor Y-1 cells (Bouzari and Varghese, 1990; Johnson and Lior, 1988a; Johnson, 1987).

Several studies have attempted to determine if CDT production in *E. coli* is significantly associated with strains that cause disease, especially from enteropathogenic isolates (Albert et al., 1996; Bouzari et al., 2005; Bouzari and Varghese, 1990; Clark et al., 2002; Guth et al., 1994; Johnson and Lior, 1988b; Okeke et al., 2000). To date, these efforts have identified a significant association of the presence of CDT genes in patients with *E. coli* induced hemolytic uremic syndrome (Bielaszewska et al., 2004).

1.5.4 Campylobacter jejuni

C. jejuni is a microaerophilic helical shaped Gram-negative bacteria that is part of the normal gastrointestinal flora of chickens. *C. jejuni* are the most common cause of food borne infection illness in industrial nations, estimated to cause up to 4 million cases each year (Friedman, 2000). Surveying 117 strains of *C. jejuni* isolated from Danish turkeys revealed CDT activity in 89.7 to 97.4% of isolates, depending on mammalian cell line intoxicated (Bang et al., 2004). Another study revealed that 100 out of 114 (87.7%) *C. jejuni* isolates from Danish broiler chickens had CDT activity on Vero cells and that all but one of these 114 isolates contained the *cdt* genes (Bang et al., 2001).

Similar to *E. coli*, culture filtrates from *C. jejuni* were shown to have CDT activity on African green monkey kidney Vero cells, human cervical carcinoma HeLa

cells, human larynx carcinoma HEp-2 cells and CHO-K1 cells, but not on mouse adrenal tumor Y-1 cells (Johnson and Lior, 1988a). Although *C. jejuni* expressing mutant forms of CDT were able to colonize the gastrointestinal tract of SCID mice to similar levels as wildtype *C. jejuni*, CDT mutants had impaired invasiveness into the blood, spleen and liver (Purdy et al., 2000). Similarly, both wildtype and CDT mutant *C. jejuni* were able to colonize NF-κB deficient mice, but only wildtype *C. jejuni* were able to induce gastroenteritis (Fox et al., 2004). Expression of Cj-CDT promoted invasion into blood, spleen and liver, and enhances inflammation in two mouse models (Fox et al., 2004; Purdy et al., 2000).

1.6 BIBLIOGRAPHY

Ahmed, H.J., Svensson, L.A., Cope, L.D., Latimer, J.L., Hansen, E.J., Ahlman, K., Bayat-Turk, J., Klamer, D., and Lagergard, T. (2001). Prevalence of cdtABC genes encoding cytolethal distending toxin among Haemophilus ducreyi and Actinobacillus actinomycetemcomitans strains. J Med Microbiol *50*, 860-864.

Akifusa, S., Heywood, W., Nair, S.P., Stenbeck, G., and Henderson, B. (2005). Mechanism of internalization of the cytolethal distending toxin of Actinobacillus actinomycetemcomitans. Microbiology *151*, 1395-1402.

Akifusa, S., Poole, S., Lewthwaite, J., Henderson, B., and Nair, S.P. (2001). Recombinant Actinobacillus actinomycetemcomitans cytolethal distending toxin proteins are required to interact to inhibit human cell cycle progression and to stimulate human leukocyte cytokine synthesis. Infect Immun *69*, 5925-5930.

Albert, M.J., Faruque, S.M., Faruque, A.S., Bettelheim, K.A., Neogi, P.K., Bhuiyan, N.A., and Kaper, J.B. (1996). Controlled study of cytolethal distending toxin-producing Escherichia coli infections in Bangladeshi children. J Clin Microbiol *34*, 717-719.

Alberts, B.J., Alexander; Lewis, Julian; Raff, Martin; Roberts, Keith; and Walter, Peter., ed. (2002). Molecular Biology of the Cell, 4th edition, 4th edition edn (New York, Garland Science).

Anderson, J.D., MacNab, A.J., Gransden, W.R., Damm, S.M., Johnson, W.M., and Lior, H. (1987). Gastroenteritis and encephalopathy associated with a strain of Escherichia coli 055:K59:H4 that produced a cytolethal distending toxin. Pediatr Infect Dis J *6*, 1135-1136.

Atherton-Fessler, S., Parker, L.L., Geahlen, R.L., and Piwnica-Worms, H. (1993). Mechanisms of p34cdc2 regulation. Mol Cell Biol *13*, 1675-1685.

Bang, D.D., Borck, B., Nielsen, E.M., Scheutz, F., Pedersen, K., and Madsen, M. (2004). Detection of seven virulence and toxin genes of Campylobacter jejuni isolates from Danish turkeys by PCR and cytolethal distending toxin production of the isolates. J Food Prot *67*, 2171-2177.

Bang, D.D., Scheutz, F., Ahrens, P., Pedersen, K., Blom, J., and Madsen, M. (2001). Prevalence of cytolethal distending toxin (cdt) genes and CDT production in Campylobacter spp. isolated from Danish broilers. J Med Microbiol *50*, 1087-1094.

Bayer, N., Schober, D., Prchla, E., Murphy, R.F., Blaas, D., and Fuchs, R. (1998). Effect of bafilomycin A1 and nocodazole on endocytic transport in HeLa cells: implications for viral uncoating and infection. J Virol *72*, 9645-9655.

Bielaszewska, M., Fell, M., Greune, L., Prager, R., Fruth, A., Tschape, H., Schmidt, M.A., and Karch, H. (2004). Characterization of cytolethal distending toxin genes and expression in shiga toxin-producing Escherichia coli strains of non-O157 serogroups. Infect Immun *72*, 1812-1816.

Boesze-Battaglia, K., Besack, D., McKay, T., Zekavat, A., Otis, L., Jordan-Sciutto, K., and Shenker, B.J. (2006). Cholesterol-rich membrane microdomains mediate cell cycle arrest induced by Actinobacillus actinomycetemcomitans cytolethal-distending toxin. Cell Microbiol *8*, 823-836.

Boesze-Battaglia, K., Brown, A., Walker, L., Besack, D., Zekavat, A., Wrenn, S., Krummenacher, C., and Shenker, B.J. (2009). Cytolethal Distending Toxin-induced Cell Cycle Arrest of Lymphocytes Is Dependent upon Recognition and Binding to Cholesterol. J Biol Chem *284*, 10650-10658.

Boulton, S.J., and Jackson, S.P. (1998). Components of the Ku-dependent non-homologous end-joining pathway are involved in telomeric length maintenance and telomeric silencing. Embo J *17*, 1819-1828.

Bouzari, S., Oloomi, M., and Oswald, E. (2005). Detection of the cytolethal distending toxin locus cdtB among diarrheagenic Escherichia coli isolates from humans in Iran. Res Microbiol *156*, 137-144.

Bouzari, S., and Varghese, A. (1990). Cytolethal distending toxin (CLDT) production by enteropathogenic Escherichia coli (EPEC). FEMS Microbiol Lett *59*, 193-198.

Burma, S., Chen, B.P., Murphy, M., Kurimasa, A., and Chen, D.J. (2001). ATM phosphorylates histone H2AX in response to DNA double-strand breaks. J Biol Chem *276*, 42462-42467.

Cao, L., Bandelac, G., Volgina, A., Korostoff, J., and DiRienzo, J.M. (2008). Role of aromatic amino acids in receptor binding activity and subunit assembly of the cytolethal distending toxin of Aggregatibacter actinomycetemcomitans. Infect Immun *76*, 2812-2821.

Carette, J.E., Guimaraes, C.P., Varadarajan, M., Park, A.S., Wuethrich, I., Godarova, A., Kotecki, M., Cochran, B.H., Spooner, E., Ploegh, H.L.*, et al.* (2009). Haploid genetic screens in human cells identify host factors used by pathogens. Science *326*, 1231-1235.

Carson, C.T., Schwartz, R.A., Stracker, T.H., Lilley, C.E., Lee, D.V., and Weitzman, M.D. (2003). The Mre11 complex is required for ATM activation and the G2/M checkpoint. Embo J *22*, 6610-6620.

Chardin, P., and McCormick, F. (1999). Brefeldin A: the advantage of being uncompetitive. Cell *97*, 153-155.

Clark, C.G., Johnson, S.T., Easy, R.H., Campbell, J.L., and Rodgers, F.G. (2002). PCR for detection of cdt-III and the relative frequencies of cytolethal distending toxin

variant-producing Escherichia coli isolates from humans and cattle. J Clin Microbiol *40*, 2671-2674.

Cortes-Bratti, X., Chaves-Olarte, E., Lagergard, T., and Thelestam, M. (1999). The cytolethal distending toxin from the chancroid bacterium Haemophilus ducreyi induces cell-cycle arrest in the G2 phase. J Clin Invest *103*, 107-115.

Cortes-Bratti, X., Chaves-Olarte, E., Lagergard, T., and Thelestam, M. (2000). Cellular internalization of cytolethal distending toxin from Haemophilus ducreyi. Infect Immun *68*, 6903-6911.

Cortes-Bratti, X., Karlsson, C., Lagergard, T., Thelestam, M., and Frisan, T. (2001). The Haemophilus ducreyi cytolethal distending toxin induces cell cycle arrest and apoptosis via the DNA damage checkpoint pathways. J Biol Chem *276*, 5296-5302.

Damek-Poprawa, M., Jang, J.Y., Volgina, A., Korostoff, J., and DiRienzo, J.M. (2012). Localization of Aggregatibacter actinomycetemcomitans cytolethal distending toxin subunits during intoxication of live cells. Infect Immun *80*, 2761-2770.

Damke, H., Baba, T., Warnock, D.E., and Schmid, S.L. (1994). Induction of mutant dynamin specifically blocks endocytic coated vesicle formation. J Cell Biol *127*, 915-934.

Das, M., Badley, A.D., Cockerill, F.R., Steckelberg, J.M., and Wilson, W.R. (1997). Infective endocarditis caused by HACEK microorganisms. Annu Rev Med *48*, 25-33.

Dasika, G.K., Lin, S.C., Zhao, S., Sung, P., Tomkinson, A., and Lee, E.Y. (1999). DNA damage-induced cell cycle checkpoints and DNA strand break repair in development and tumorigenesis. Oncogene *18*, 7883-7899.

Deng, K., and Hansen, E.J. (2003). A CdtA-CdtC complex can block killing of HeLa cells by Haemophilus ducreyi cytolethal distending toxin. Infect Immun *71*, 6633-6640.

Dlakic, M. (2000). Functionally unrelated signalling proteins contain a fold similar to Mg2+-dependent endonucleases. Trends Biochem Sci *25*, 272-273.

Dlakic, M. (2001). Is CdtB a nuclease or a phosphatase? Science *291*, 547.

Draper, R.K., and Simon, M.I. (1980). The entry of diphtheria toxin into the mammalian cell cytoplasm: evidence for lysosomal involvement. J Cell Biol *87*, 849-854.

Dunphy, W.G. (1994). The decision to enter mitosis. Trends Cell Biol *4*, 202-207.

Elledge, S.J. (1996). Cell cycle checkpoints: preventing an identity crisis. Science *274*, 1664-1672.

Elwell, C., Chao, K., Patel, K., and Dreyfus, L. (2001). Escherichia coli CdtB mediates cytolethal distending toxin cell cycle arrest. Infect Immun *69*, 3418-3422.

Elwell, C.A., and Dreyfus, L.A. (2000). DNase I homologous residues in CdtB are critical for cytolethal distending toxin-mediated cell cycle arrest. Mol Microbiol *37*, 952-963.

Endicott, J.A., Nurse, P., and Johnson, L.N. (1994). Mutational analysis supports a structural model for the cell cycle protein kinase p34. Protein Eng *7*, 243-253.

Fiorentini, C., Matarrese, P., Straface, E., Falzano, L., Fabbri, A., Donelli, G., Cossarizza, A., Boquet, P., and Malorni, W. (1998). Toxin-induced activation of Rho GTP-binding protein increases Bcl-2 expression and influences mitochondrial homeostasis. Exp Cell Res *242*, 341-350.

Fox, J.G., Rogers, A.B., Whary, M.T., Ge, Z., Taylor, N.S., Xu, S., Horwitz, B.H., and Erdman, S.E. (2004). Gastroenteritis in NF-kappaB-deficient mice is produced with wild-type Camplyobacter jejuni but not with C. jejuni lacking cytolethal distending toxin despite persistent colonization with both strains. Infect Immun *72*, 1116-1125.

Friedman, C.R., J. Neimann, H. C. Wegener, and R. V. Tauxe. (2000). Epidemiology of Campylobacter jejuni infections in the United States and other industrialized nations. (Washington DC, American Society for Microbiology).

Frisan, T., Cortes-Bratti, X., Chaves-Olarte, E., Stenerlow, B., and Thelestam, M. (2003). The Haemophilus ducreyi cytolethal distending toxin induces DNA double-strand breaks and promotes ATM-dependent activation of RhoA. Cell Microbiol *5*, 695-707.

Gargi, A., Reno, M., and Blanke, S.R. (2012). Bacterial toxin modulation of the eukaryotic cell cycle: are all cytolethal distending toxins created equally? Front Cell Infect Microbiol *2*, 124.

Gargi, A., Tamilselvam, B., Powers, B., Prouty, M.G., Lincecum, T., Eshraghi, A., Maldonado-Arocho, F.J., Wilson, B.A., Bradley, K.A., and Blanke, S.R. (2013). Cellular interactions of the cytolethal distending toxins from escherichia coli and haemophilus ducreyi. J Biol Chem.

Ge, Z., Feng, Y., Whary, M.T., Nambiar, P.R., Xu, S., Ng, V., Taylor, N.S., and Fox, J.G. (2005). Cytolethal distending toxin is essential for Helicobacter hepaticus colonization in outbred Swiss Webster mice. Infect Immun *73*, 3559-3567.

Ge, Z., Rogers, A.B., Feng, Y., Lee, A., Xu, S., Taylor, N.S., and Fox, J.G. (2007). Bacterial cytolethal distending toxin promotes the development of dysplasia in a model of microbially induced hepatocarcinogenesis. Cell Microbiol *9*, 2070-2080.

Grimmer, S., Iversen, T.G., van Deurs, B., and Sandvig, K. (2000). Endosome to Golgi transport of ricin is regulated by cholesterol. Mol Biol Cell *11*, 4205-4216.

Grivennikov, S.I., Greten, F.R., and Karin, M. (2010). Immunity, inflammation, and cancer. Cell *140*, 883-899.

Guerra, L., Guidi, R., and Frisan, T. (2011). Do bacterial genotoxins contribute to chronic inflammation, genomic instability and tumor progression? FEBS J *278*, 4577-4588.

Guerra, L., Nemec, K.N., Massey, S., Tatulian, S.A., Thelestam, M., Frisan, T., and Teter, K. (2009). A novel mode of translocation for cytolethal distending toxin. Biochim Biophys Acta *1793*, 489-495.

Guerra, L., Teter, K., Lilley, B.N., Stenerlow, B., Holmes, R.K., Ploegh, H.L., Sandvig, K., Thelestam, M., and Frisan, T. (2005). Cellular internalization of cytolethal distending toxin: a new end to a known pathway. Cell Microbiol *7*, 921-934.

Guidi, R., Guerra, L., Levi, L., Stenerlow, B., Fox, J.G., Josenhans, C., Masucci, M.G., and Frisan, T. (2013). Chronic exposure to the cytolethal distending toxins of Gram-negative bacteria promotes genomic instability and altered DNA damage response. Cell Microbiol *15*, 98-113.

Guth, B.E., Giraldi, R., Gomes, T.A., and Marques, L.R. (1994). Survey of cytotoxin production among Escherichia coli strains characterized as enteropathogenic (EPEC) by serotyping and presence of EPEC adherence factor (EAF) sequences. Can J Microbiol *40*, 341-344.

Haraszthy, V.I., Zambon, J.J., Trevisan, M., Zeid, M., and Genco, R.J. (2000). Identification of periodontal pathogens in atheromatous plaques. J Periodontol *71*, 1554-1560.

Hassane, D.C., Lee, R.B., Mendenhall, M.D., and Pickett, C.L. (2001). Cytolethal distending toxin demonstrates genotoxic activity in a yeast model. Infect Immun *69*, 5752-5759.

Hickey, T.E., McVeigh, A.L., Scott, D.A., Michielutti, R.E., Bixby, A., Carroll, S.A., Bourgeois, A.L., and Guerry, P. (2000). Campylobacter jejuni cytolethal distending

toxin mediates release of interleukin-8 from intestinal epithelial cells. Infect Immun *68*, 6535-6541.

Hoffmann, I., Clarke, P.R., Marcote, M.J., Karsenti, E., and Draetta, G. (1993). Phosphorylation and activation of human cdc25-C by cdc2--cyclin B and its involvement in the self-amplification of MPF at mitosis. Embo J *12*, 53-63.

Hu, X., Nesic, D., and Stebbins, C.E. (2006). Comparative structure-function analysis of cytolethal distending toxins. Proteins *62*, 421-434.

Hu, X., and Stebbins, C.E. (2006). Dynamics and assembly of the cytolethal distending toxin. Proteins *65*, 843-855.

Izumi, T., and Maller, J.L. (1993). Elimination of cdc2 phosphorylation sites in the cdc25 phosphatase blocks initiation of M-phase. Mol Biol Cell *4*, 1337-1350.

Janka, A., Bielaszewska, M., Dobrindt, U., Greune, L., Schmidt, M.A., and Karch, H. (2003). Cytolethal distending toxin gene cluster in enterohemorrhagic Escherichia coli O157:H- and O157:H7: characterization and evolutionary considerations. Infect Immun *71*, 3634-3638.

Johnson, W.M., and Lior, H. (1988a). A new heat-labile cytolethal distending toxin (CLDT) produced by Campylobacter spp. Microb Pathog *4*, 115-126.

Johnson, W.M., and Lior, H. (1988b). A new heat-labile cytolethal distending toxin (CLDT) produced by Escherichia coli isolates from clinical material. Microb Pathog *4*, 103-113.

Johnson, W.M., Lior H. (1987). Response of Chinese hamster ovary cells to a cytolethal distending toxin (CDT) of Escherichia coli and possible misinterpretation as a heat-labile (LT) enterotoxin. FEMS Microbiology Letters *43*, 19-23.

Kabouridis, P.S., Janzen, J., Magee, A.L., and Ley, S.C. (2000). Cholesterol depletion disrupts lipid rafts and modulates the activity of multiple signaling pathways in T lymphocytes. Eur J Immunol *30*, 954-963.

Karin, M., Lawrence, T., and Nizet, V. (2006). Innate immunity gone awry: linking microbial infections to chronic inflammation and cancer. Cell *124*, 823-835.

Kaufmann, W.K., and Paules, R.S. (1996). DNA damage and cell cycle checkpoints. Faseb J *10*, 238-247.

Lara-Tejero, M., and Galan, J.E. (2000). A bacterial toxin that controls cell cycle progression as a deoxyribonuclease I-like protein. Science *290*, 354-357.

Lara-Tejero, M., and Galan, J.E. (2001). CdtA, CdtB, and CdtC form a tripartite complex that is required for cytolethal distending toxin activity. Infect Immun *69*, 4358-4365.

Lara-Tejero, M., and Galan, J.E. (2002). Cytolethal distending toxin: limited damage as a strategy to modulate cellular functions. Trends Microbiol *10*, 147-152.

Lee, J.H., and Paull, T.T. (2005). ATM activation by DNA double-strand breaks through the Mre11-Rad50-Nbs1 complex. Science *308*, 551-554.

Lee, R.B., Hassane, D.C., Cottle, D.L., and Pickett, C.L. (2003). Interactions of Campylobacter jejuni cytolethal distending toxin subunits CdtA and CdtC with HeLa cells. Infect Immun *71*, 4883-4890.

Li, L., Sharipo, A., Chaves-Olarte, E., Masucci, M.G., Levitsky, V., Thelestam, M., and Frisan, T. (2002). The Haemophilus ducreyi cytolethal distending toxin activates sensors of DNA damage and repair complexes in proliferating and non-proliferating cells. Cell Microbiol *4*, 87-99.

Lin, C.D., Lai, C.K., Lin, Y.H., Hsieh, J.T., Sing, Y.T., Chang, Y.C., Chen, K.C., Wang, W.C., Su, H.L., and Lai, C.H. (2011). Cholesterol depletion reduces entry of Campylobacter jejuni cytolethal distending toxin and attenuates intoxication of host cells. Infect Immun *79*, 3563-3575.

Lundgren, K., Walworth, N., Booher, R., Dembski, M., Kirschner, M., and Beach, D. (1991). mik1 and wee1 cooperate in the inhibitory tyrosine phosphorylation of cdc2. Cell *64*, 1111-1122.

Mahammad, S., Dinic, J., Adler, J., and Parmryd, I. (2010). Limited cholesterol depletion causes aggregation of plasma membrane lipid rafts inducing T cell activation. Biochim Biophys Acta *1801*, 625-634.

Mayer, M.P., Bueno, L.C., Hansen, E.J., and DiRienzo, J.M. (1999). Identification of a cytolethal distending toxin gene locus and features of a virulence-associated region in Actinobacillus actinomycetemcomitans. Infect Immun *67*, 1227-1237.

McAuley, J.L., Linden, S.K., Png, C.W., King, R.M., Pennington, H.L., Gendler, S.J., Florin, T.H., Hill, G.R., Korolik, V., and McGuckin, M.A. (2007). MUC1 cell surface mucin is a critical element of the mucosal barrier to infection. J Clin Invest *117*, 2313-2324.

McSweeney, L.A., and Dreyfus, L.A. (2004). Nuclear localization of the Escherichia coli cytolethal distending toxin CdtB subunit. Cell Microbiol *6*, 447-458.

McSweeney, L.A., and Dreyfus, L.A. (2005). Carbohydrate-binding specificity of the Escherichia coli cytolethal distending toxin CdtA-II and CdtC-II subunits. Infect Immun *73*, 2051-2060.

Mise, K., Akifusa, S., Watarai, S., Ansai, T., Nishihara, T., and Takehara, T. (2005). Involvement of ganglioside GM3 in G(2)/M cell cycle arrest of human monocytic cells induced by Actinobacillus actinomycetemcomitans cytolethal distending toxin. Infect Immun *73*, 4846-4852.

Miyaji, M., Jin, Z.X., Yamaoka, S., Amakawa, R., Fukuhara, S., Sato, S.B., Kobayashi, T., Domae, N., Mimori, T., Bloom, E.T.*, et al.* (2005). Role of membrane sphingomyelin and ceramide in platform formation for Fas-mediated apoptosis. J Exp Med *202*, 249-259.

Morse, S.A. (1989). Chancroid and Haemophilus ducreyi. Clin Microbiol Rev *2*, 137-157.

Moya, M., Dautry-Varsat, A., Goud, B., Louvard, D., and Boquet, P. (1985). Inhibition of coated pit formation in Hep2 cells blocks the cytotoxicity of diphtheria toxin but not that of ricin toxin. J Cell Biol *101*, 548-559.

Nambiar, M.P., and Wu, H.C. (1995). Ilimaquinone inhibits the cytotoxicities of ricin, diphtheria toxin, and other protein toxins in Vero cells. Exp Cell Res *219*, 671-678.

Nesic, D., Hsu, Y., and Stebbins, C.E. (2004). Assembly and function of a bacterial genotoxin. Nature *429*, 429-433.

Nesic, D., and Stebbins, C.E. (2005). Mechanisms of assembly and cellular interactions for the bacterial genotoxin CDT. PLoS Pathog *1*, e28.

Nishikubo, S., Ohara, M., Ueno, Y., Ikura, M., Kurihara, H., Komatsuzawa, H., Oswald, E., and Sugai, M. (2003). An N-terminal segment of the active component of the bacterial genotoxin cytolethal distending toxin B (CDTB) directs CDTB into the nucleus. J Biol Chem *278*, 50671-50681.

Norskov-Lauritsen, N., and Kilian, M. (2006). Reclassification of Actinobacillus actinomycetemcomitans, Haemophilus aphrophilus, Haemophilus paraphrophilus and Haemophilus segnis as Aggregatibacter actinomycetemcomitans gen. nov., comb. nov., Aggregatibacter aphrophilus comb. nov. and Aggregatibacter segnis comb. nov., and emended description of Aggregatibacter aphrophilus to include V factor-dependent and V factor-independent isolates. Int J Syst Evol Microbiol *56*, 2135-2146.

Nougayrede, J.P., Taieb, F., De Rycke, J., and Oswald, E. (2005). Cyclomodulins: bacterial effectors that modulate the eukaryotic cell cycle. Trends Microbiol *13*, 103-110.

Ohara, M., Hayashi, T., Kusunoki, Y., Miyauchi, M., Takata, T., and Sugai, M. (2004). Caspase-2 and caspase-7 are involved in cytolethal distending toxin-induced apoptosis in Jurkat and MOLT-4 T-cell lines. Infect Immun *72*, 871-879.

Ohara, M., Miyauchi, M., Tsuruda, K., Takata, T., and Sugai, M. (2011). Topical application of Aggregatibacter actinomycetemcomitans cytolethal distending toxin induces cell cycle arrest in the rat gingival epithelium in vivo. J Periodontal Res *46*, 389-395.

Okeke, I.N., Lamikanra, A., Steinruck, H., and Kaper, J.B. (2000). Characterization of Escherichia coli strains from cases of childhood diarrhea in provincial southwestern Nigeria. J Clin Microbiol *38*, 7-12.

Okuda, J., Fukumoto, M., Takeda, Y., and Nishibuchi, M. (1997). Examination of diarrheagenicity of cytolethal distending toxin: suckling mouse response to the products of the cdtABC genes of Shigella dysenteriae. Infect Immun *65*, 428-433.

Parker, L.L., and Piwnica-Worms, H. (1992). Inactivation of the p34cdc2-cyclin B complex by the human WEE1 tyrosine kinase. Science *257*, 1955-1957.

Peres, S.Y., Marches, O., Daigle, F., Nougayrede, J.P., Herault, F., Tasca, C., De Rycke, J., and Oswald, E. (1997). A new cytolethal distending toxin (CDT) from

Escherichia coli producing CNF2 blocks HeLa cell division in G2/M phase. Mol Microbiol *24*, 1095-1107.

Piaggio, G., Farina, A., Perrotti, D., Manni, I., Fuschi, P., Sacchi, A., and Gaetano, C. (1995). Structure and growth-dependent regulation of the human cyclin B1 promoter. Exp Cell Res *216*, 396-402.

Pickett, C.L., Cottle, D.L., Pesci, E.C., and Bikah, G. (1994). Cloning, sequencing, and expression of the Escherichia coli cytolethal distending toxin genes. Infect Immun *62*, 1046-1051.

Pickett, C.L., and Whitehouse, C.A. (1999). The cytolethal distending toxin family. Trends Microbiol *7*, 292-297.

Pines, J., and Hunter, T. (1989). Isolation of a human cyclin cDNA: evidence for cyclin mRNA and protein regulation in the cell cycle and for interaction with p34cdc2. Cell *58*, 833-846.

Pratt, J.S., Sachen, K.L., Wood, H.D., Eaton, K.A., and Young, V.B. (2006). Modulation of host immune responses by the cytolethal distending toxin of Helicobacter hepaticus. Infect Immun *74*, 4496-4504.

Purdy, D., Buswell, C.M., Hodgson, A.E., McAlpine, K., Henderson, I., and Leach, S.A. (2000). Characterisation of cytolethal distending toxin (CDT) mutants of Campylobacter jejuni. J Med Microbiol *49*, 473-479.

Purven, M., Falsen, E., and Lagergard, T. (1995). Cytotoxin production in 100 strains of Haemophilus ducreyi from different geographic locations. FEMS Microbiol Lett *129*, 221-224.

Rabin, S.D., Flitton, J.G., and Demuth, D.R. (2009). Aggregatibacter actinomycetemcomitans cytolethal distending toxin induces apoptosis in nonproliferating macrophages by a phosphatase-independent mechanism. Infect Immun *77*, 3161-3169.

Rainey, G.J., and Young, J.A. (2004). Antitoxins: novel strategies to target agents of bioterrorism. Nat Rev Microbiol *2*, 721-726.

Sandvig, K., and Olsnes, S. (1980). Diphtheria toxin entry into cells is facilitated by low pH. J Cell Biol *87*, 828-832.

Sandvig, K., and Olsnes, S. (1981). Rapid entry of nicked diphtheria toxin into cells at low pH. Characterization of the entry process and effects of low pH on the toxin molecule. J Biol Chem *256*, 9068-9076.

Sandvig, K., and Olsnes, S. (1988). Diphtheria toxin-induced channels in Vero cells selective for monovalent cations. J Biol Chem *263*, 12352-12359.

Sandvig, K., and van Deurs, B. (2005). Delivery into cells: lessons learned from plant and bacterial toxins. Gene Ther *12*, 865-872.

Scott, D.A., and Kaper, J.B. (1994). Cloning and sequencing of the genes encoding Escherichia coli cytolethal distending toxin. Infect Immun *62*, 244-251.

Shenker, B.J., Demuth, D.R., and Zekavat, A. (2006). Exposure of lymphocytes to high doses of Actinobacillus actinomycetemcomitans cytolethal distending toxin induces rapid onset of apoptosis-mediated DNA fragmentation. Infect Immun *74*, 2080-2092.

Shenker, B.J., Dlakic, M., Walker, L.P., Besack, D., Jaffe, E., LaBelle, E., and Boesze-Battaglia, K. (2007). A novel mode of action for a microbial-derived immunotoxin: the cytolethal distending toxin subunit B exhibits phosphatidylinositol 3,4,5-triphosphate phosphatase activity. J Immunol *178*, 5099-5108.

Shenker, B.J., McKay, T., Datar, S., Miller, M., Chowhan, R., and Demuth, D. (1999). Actinobacillus actinomycetemcomitans immunosuppressive protein is a member of the family of cytolethal distending toxins capable of causing a G2 arrest in human T cells. J Immunol *162*, 4773-4780.

Smith, J.L., and Bayles, D.O. (2006). The contribution of cytolethal distending toxin to bacterial pathogenesis. Crit Rev Microbiol *32*, 227-248.

Smits, V.A., and Medema, R.H. (2001). Checking out the G(2)/M transition. Biochim Biophys Acta *1519*, 1-12.

Sofer, A., and Futerman, A.H. (1995). Cationic amphiphilic drugs inhibit the internalization of cholera toxin to the Golgi apparatus and the subsequent elevation of cyclic AMP. J Biol Chem *270*, 12117-12122.

Sugai, M., Kawamoto, T., Peres, S.Y., Ueno, Y., Komatsuzawa, H., Fujiwara, T., Kurihara, H., Suginaka, H., and Oswald, E. (1998). The cell cycle-specific growth-

inhibitory factor produced by Actinobacillus actinomycetemcomitans is a cytolethal distending toxin. Infect Immun *66*, 5008-5019.

Sullivan, P., Clark, W.L., and Kaiser, P.K. (2002). Bilateral endogenous endophthalmitis caused by HACEK microorganism. Am J Ophthalmol *133*, 144-145.

Suzuki, J.B. (1988). Diagnosis and classification of the periodontal diseases. Dent Clin North Am *32*, 195-216.

Takizawa, P.A., Yucel, J.K., Veit, B., Faulkner, D.J., Deerinck, T., Soto, G., Ellisman, M., and Malhotra, V. (1993). Complete vesiculation of Golgi membranes and inhibition of protein transport by a novel sea sponge metabolite, ilimaquinone. Cell *73*, 1079-1090.

Tan, K.S., Song, K.P., and Ong, G. (2002). Cytolethal distending toxin of Actinobacillus actinomycetemcomitans. Occurrence and association with periodontal disease. J Periodontal Res *37*, 268-272.

Teter, K., and Holmes, R.K. (2002). Inhibition of endoplasmic reticulum-associated degradation in CHO cells resistant to cholera toxin, Pseudomonas aeruginosa exotoxin A, and ricin. Infect Immun *70*, 6172-6179.

Teter, K., Jobling, M.G., and Holmes, R.K. (2003). A class of mutant CHO cells resistant to cholera toxin rapidly degrades the catalytic polypeptide of cholera toxin and exhibits increased endoplasmic reticulum-associated degradation. Traffic *4*, 232-242.

Toth, I., Herault, F., Beutin, L., and Oswald, E. (2003). Production of cytolethal distending toxins by pathogenic Escherichia coli strains isolated from human and animal sources: establishment of the existence of a new cdt variant (Type IV). J Clin Microbiol *41*, 4285-4291.

Trees, D.L., and Morse, S.A. (1995). Chancroid and Haemophilus ducreyi: an update. Clin Microbiol Rev *8*, 357-375.

Uziel, T., Lerenthal, Y., Moyal, L., Andegeko, Y., Mittelman, L., and Shiloh, Y. (2003). Requirement of the MRN complex for ATM activation by DNA damage. Embo J *22*, 5612-5621.

Volpe, J.J., and Goldberg, R.I. (1983). Effect of tunicamycin on 3-hydroxy-3-methylglutaryl coenzyme A reductase in C-6 glial cells. J Biol Chem *258*, 9220-9226.

Wilson, M., and Henderson, B. (1995). Virulence factors of Actinobacillus actinomycetemcomitans relevant to the pathogenesis of inflammatory periodontal diseases. FEMS Microbiol Rev *17*, 365-379.

Wising, C., Azem, J., Zetterberg, M., Svensson, L.A., Ahlman, K., and Lagergard, T. (2005a). Induction of apoptosis/necrosis in various human cell lineages by Haemophilus ducreyi cytolethal distending toxin. Toxicon *45*, 767-776.

Wising, C., Molne, L., Jonsson, I.M., Ahlman, K., and Lagergard, T. (2005b). The cytolethal distending toxin of Haemophilus ducreyi aggravates dermal lesions in a rabbit model of chancroid. Microbes Infect *7*, 867-874.

Wollscheid, B., Bausch-Fluck, D., Henderson, C., O'Brien, R., Bibel, M., Schiess, R., Aebersold, R., and Watts, J.D. (2009). Mass-spectrometric identification and relative quantification of N-linked cell surface glycoproteins. Nat Biotechnol *27*, 378-386.

Xu, T., Lundqvist, A., Ahmed, H.J., Eriksson, K., Yang, Y., and Lagergard, T. (2004). Interactions of Haemophilus ducreyi and purified cytolethal distending toxin with human monocyte-derived dendritic cells, macrophages and CD4+ T cells. Microbes Infect *6*, 1171-1181.

Yamaji, A., Sekizawa, Y., Emoto, K., Sakuraba, H., Inoue, K., Kobayashi, H., and Umeda, M. (1998). Lysenin, a novel sphingomyelin-specific binding protein. J Biol Chem *273*, 5300-5306.

Young, R.S., Fortney, K.R., Gelfanova, V., Phillips, C.L., Katz, B.P., Hood, A.F., Latimer, J.L., Munson, R.S., Jr., Hansen, E.J., and Spinola, S.M. (2001). Expression of cytolethal distending toxin and hemolysin is not required for pustule formation by Haemophilus ducreyi in human volunteers. Infect Immun *69*, 1938-1942.

Young, V.B., Knox, K.A., Pratt, J.S., Cortez, J.S., Mansfield, L.S., Rogers, A.B., Fox, J.G., and Schauer, D.B. (2004). In vitro and in vivo characterization of Helicobacter hepaticus cytolethal distending toxin mutants. Infect Immun *72*, 2521-2527.

Zhou, F., Xu, W., Hong, M., Pan, Z., Sinko, P.J., Ma, J., and You, G. (2005). The role of N-linked glycosylation in protein folding, membrane targeting, and substrate binding of human organic anion transporter hOAT4. Mol Pharmacol *67*, 868-876.

Zhou, M., Zhang, Q., Zhao, J., and Jin, M. (2012). Haemophilus parasuis encodes two functional cytolethal distending toxins: CdtC contains an atypical cholesterol recognition/interaction region. PLoS One *7*, e32580.

CHAPTER 2

CYTOLETHAL DISTENDING TOXIN FAMILY MEMBERS ARE DIFFERENTIALLY AFFECTED BY ALTERATIONS IN HOST GLYCANS AND MEMBRANE CHOLESTEROL

Aria Eshraghi[1,†], Francisco J. Maldonado-Arocho[1,A,†], Amandeep Gargi[2], Marissa Cardwell[1,B], Michael G. Prouty[2,C], Steven R. Blanke[2] and Kenneth A. Bradley[1,3]

From: [1]Department of Microbiology, Immunology and Molecular Genetics, University of California, Los Angeles, California, and [2]Department of Microbiology, Institute for Genomic Biology, University of Illinois at Urbana-Champaign, Urbana, Illinois

[†]Contributed equally to this work

Current Addresses: [A]Tufts University, Department of Microbiology, Boston, Massachusetts, [B]University of Chicago, Department of Microbiology, Chicago, Illinois, and [C]Department of Enterics/Infectious Disease Directorate, Naval Medical Research Center, Silver Springs, MD

Running Title: Host cellular interactions of CDTs

Address correspondence to: Kenneth A. Bradley, PhD, Department of Microbiology, Immunology, & Molecular Genetics, University of California at Los Angeles, 609 Charles E. Young Dr. East, Los Angeles, CA, 90095. Phone: 310-206-7465; Fax: 310-206-5231; E-mail: kbradley@microbio.ucla.edu

2.1 ABSTRACT

Cytolethal distending toxins (CDTs) are tripartite protein exotoxins produced by a diverse group of pathogenic Gram-negative bacteria. Based on their ability to induce DNA damage, cell cycle arrest and apoptosis of cultured cells, CDTs are proposed to enhance virulence by blocking cellular division and/or directly killing epithelial and immune cells. Despite the widespread distribution of CDTs among several important human pathogens, our understanding of how these toxins interact with host cells is limited. Here we demonstrate that CDTs from *Haemophilus ducreyi*, *Aggregatibacter actinomycetemcomitans, Escherichia coli*, and *Campylobacter jejuni* differ in their abilities to intoxicate host cells with defined defects in host factors previously implicated in CDT binding, including glycoproteins, and glycosphingolipids. The absence of cell surface sialic acid sensitized cells to intoxication by three of the four CDTs tested. Surprisingly, fucosylated N-linked glycans and glycolipids, previously implicated in CDT-host interactions, were not required for intoxication by any of the CDTs tested. Finally, altering host-cellular cholesterol, also previously implicated in CDT binding, affected intoxication by only a subset of CDTs tested. The findings presented here provide insight into the molecular and cellular basis of CDT-host interactions.

2.2 INTRODUCTION

Cytolethal distending toxins (CDTs) are members of a group of bacterial toxins and effectors called “cyclomodulins” that interfere with the eukaryotic cell

cycle rather than inducing overt cytotoxicity (Nougayrede et al., 2005; Oswald et al., 2005). Inhibiting cell cycle disrupts many of the normal functions of rapidly dividing eukaryotic cells, including lymphocytes and epithelial cells, which provide immunity and physical barriers to microbial pathogens (Pickett and Whitehouse, 1999; Purdy et al., 2000; Shenker et al., 2001). Thus, it is not surprising that *cdt* genes are found in a diverse group of Gram-negative pathogens that colonize different niches within the host. While a growing body of evidence supports the importance of CDTs in bacterial virulence and host-pathogen interactions (Smith and Bayles, 2006), the manner in which individual CDTs interact with and intoxicate host cells remains poorly understood.

CDTs are AB_2 toxins, consisting of a hetero-trimeric complex of three proteins (CdtA, CdtB, and CdtC) at a 1:1:1 molar ratio (Frisk et al., 2001; Pickett et al., 1996; Pickett and Whitehouse, 1999). The current model is that CdtA and CdtC are the binding “B” moieties that collaborate to facilitate binding and entry of the catalytic “A” subunit, CdtB, into mammalian cells. CdtB shares a common tertiary structure with deoxyribonuclease I (DNase I) and phosphatidylinositol 3,4,5-triphosphate (PI-3,4,5-P_3) phosphatase enzymes and displays both activities in cell-free systems (Elwell et al., 2001; Elwell and Dreyfus, 2000; Lara-Tejero and Galan, 2000; Nesic et al., 2004; Shenker et al., 2007). It is not currently known which activity is of greater importance, and this may depend on the specific toxin and/or the host target cell type (Rabin et al., 2009; Shenker et al., 2007). CdtB enzymatic activity induces cell cycle arrest predominantly at the G_2/M transition, resulting in cellular distension and

ultimately cell death (Johnson and Lior, 1988a; Pickett and Whitehouse, 1999; Thelestam and Frisan, 2004).

Consistent with their proposed roles as binding subunits, CdtA and/or CdtC increase the ability of CdtB to associate with host cells and greatly enhance intoxication (Akifusa et al., 2005; Akifusa et al., 2001; Cao et al., 2005; Deng and Hansen, 2003; Frisk et al., 2001; Lee et al., 2003; McSweeney and Dreyfus, 2004, 2005; Mise et al., 2005; Nesic and Stebbins, 2005). The identification of ricin-like lectin domains in CdtA and CdtC from structural and biochemical data first suggested that these subunits may interact with carbohydrates on the cell surface (Hu et al., 2006; Lara-Tejero and Galan, 2001; Nesic et al., 2004). Consistent with this hypothesis, CDT produced by *E. coli* (Ec-CDT) was reported to require N-linked glycoproteins for binding and subsequent intoxication of HeLa cells (McSweeney and Dreyfus, 2005). Moreover, Ec-CDT bound fucose *in vitro,* and fucose-specific lectins blocked Ec-CDT-mediated cell cycle arrest, presumably by preventing binding of toxin to its receptor. These findings suggested that fucose might serve as a binding determinant for Ec-CDT. Similarly, host glycans were reported to support *A. actinomycetemcomitans* (Aa-CDT) intoxication. Specifically, Aa-CDT bound three glycosphingolipids, G_{M1}, G_{M2} and G_{M3}, and intoxication of human monocytic U937 cells was blocked by pre-incubation of toxin with liposomes that contained G_{M3} (Mise et al., 2005). In addition, the CdtA subunit of Aa-CDT bound to the glycoprotein thyroglobulin (Cao et al., 2005). However, the functional significance of this binding is unknown because mutants that failed to bind thyroglobulin retained near wildtype activity in intoxication assays.

In addition to a proposed role for host glycans in CDT binding, Aa-CdtC was recently demonstrated to possess a functional cholesterol recognition/interaction amino acid consensus (CRAC) motif important for binding of toxin to cholesterol-rich microdomains (Boesze-Battaglia et al., 2009). However, it is not clear how CdtC binding to cholesterol relates to the previously proposed roles for glycolipids or glycoproteins. Further, it is not known whether CDTs from other bacteria possess a functional CRAC motif important for cellular binding and intoxication.

In order to determine if CDTs from various pathogens utilize similar host factors for intoxication, we set out to determine the role of several classes of cell surface biomolecules (i.e. glycoproteins, glycosphingolipids, cholesterol, etc.) in intoxication by four CDTs. We chose to investigate two highly conserved CDTs, Aa-CDT and *H. ducreyi* CDT (Hd-CDT), which share 91.9% and 93.5% amino acid identity in their CdtA and CdtC subunits, respectively (Pickett and Whitehouse, 1999)(Figure 2.1). In addition, we chose two CDTs, Ec-CDT and *C. jejuni* CDT (Cj-CDT), whose amino acid sequences are divergent (<30% amino acid identity between each other or with Aa/Hd-CDT). These four toxins were selected based on their relative sequence divergence as well as the host niche occupied by the respective CDT-producing pathogen. Specifically, CDTs from two enteric pathogens (*E. coli* and *C. jejuni*), an oral pathogen (*A. actinomycetemcomitans*), and a pathogen responsible for a sexually transmitted disease (*H. ducreyi*), were investigated.

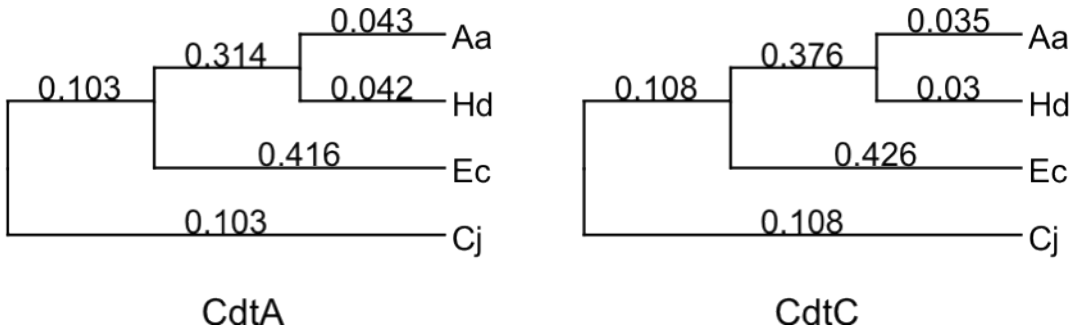

Figure 2.1 Dendogram of CdtA and CdtC proteins.
CdtA and CdtB proteins sequences were aligned with ClustalW using BLOSUM 30 similarity matrix and a midpoint rooted dendogram was constructed using MacVector version 7.2. Numbers indicate relative evolutionary distance.

Our results reveal differences in the ability of each of these four CDTs to intoxicate host cells depending on presence or absence of specific cell surface biomolecules. Furthermore, glycans previously implicated in CDT-host interactions were not required for intoxication by any of the toxins tested. Therefore, we propose that individual CDTs utilize distinct host factors in order to efficiently intoxicate target cells.

2.3 RESULTS

2.3.1 CDTs display differential target cell preferences.

CDTs are able to intoxicate a wide variety of cell types derived from multiple species and progenitor tissues, indicating that each individual CDT utilizes receptor(s) and entry processes that are conserved among different hosts and target cells (Pickett and Whitehouse, 1999). In order to test if host factors required for intoxication are shared between different CDTs, we set out to quantify the level of sensitivity to Ec-, Hd-, Aa-, and Cj-CDTs in a series of diverse cell lines. We intoxicated Chinese hamster ovary (CHO-K1) and HeLa cells, which represent epithelial cells commonly used for CDT studies, as well as T-cells (OT-1) and macrophage-like cells (RAW 264.7 and IC-21), which are proposed to be important targets for CDTs *in vivo* (Shenker et al., 2000). In addition, we intoxicated 3T3 fibroblasts and Y-1 adrenal cells, which were reported to be resistant to Ec-, Hd- and Cj-CDTs (Cope et al., 1997; Cortes-Bratti et al., 1999; Johnson and Lior, 1988a, b).

Phosphorylation of the histone protein H2AX is a characteristic of double-stranded DNA breaks and has been used to monitor CDT intoxication (Li et al.,

2002). Therefore, CDT intoxication was assayed by immunofluorescence staining for phosphorylated H2AX (phospho-H2AX) followed by laser scanning cytometry. As predicted, 3T3 fibroblasts derived from NIH or Balb/c mice, as well as Y-1 cells, were highly resistant to Ec-, and Hd-CDT intoxication (Figure 2.2). This result was not due to an altered DNA damage response, as all cell lines tested induced phospho-H2AX in response to ultraviolet light-mediated DNA damage (data not shown). Consistent with its high sequence similarity with Hd-CDT, Aa-CDT was also ineffective at inducing H2AX phosphorylation in 3T3 or Y-1 cells (Figure 2.1, 2.2). Surprisingly, Cj-CDT efficiently intoxicated all three of these cell lines (Figure 2. 2), demonstrating for the first time that CDTs derived from different bacteria display variable target cell tropism.

These data combined with the fact that the CdtB subunits from these four CDTs display similar enzymatic activities *in vitro* [1] support a model whereby Cj-CDT utilizes a receptor and/or entry pathway that is distinct from the three other toxins (Aa-, Hd-, and Ec-CDTs). Further, Ec-CDT efficiently intoxicated CHO-K1 cells but displayed low–to–undetectable activity on all other cell types. This result was opposite the pattern seen with Cj-CDT, which efficiently intoxicated all cell types except CHO-K1 (Figure 2.2). Although Aa- and Hd-CDTs were poorly active against 3T3 and Y-1 cells, these two toxins were more active than Ec- or Cj-CDTs on CHO-K1 and HeLa cells.

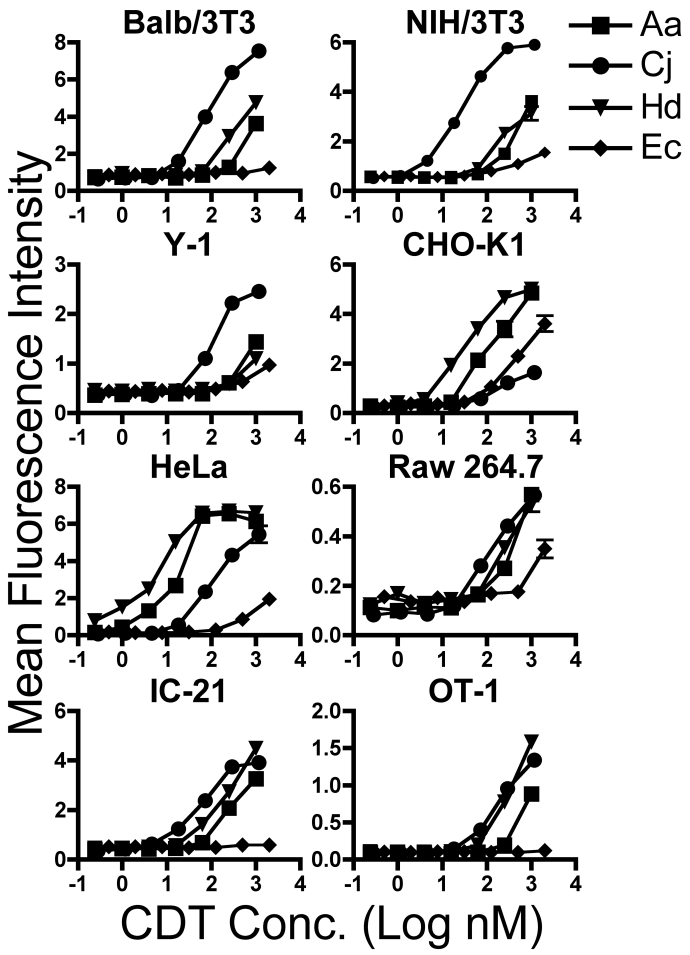

Figure 2.2 Differential sensitivity of cell lines to divergent CDTs.
Cells from indicated lines were seeded on 384-well plates, intoxicated for 24 h, fixed, permeabilized and probed with anti-phospho H2AX antibodies followed by Alexa Fluor 488 labeled goat anti-rabbit antibodies. Nuclei were identified by staining with Hoechst. The relative level of activated H2AX per cell nucleus was determined by measuring Alexa Fluor 488 and Hoechst fluorescence intensity by laser scanning cytometry. Results are plotted as mean Alexa Fluor 488 fluorescence intensity per nucleus from triplicate samples +/- SEM. Results are representative of three independent experiments.

Taken together, these data suggest that Aa- and Hd-CDT utilize a common set of host factors for intoxication that are distinct from those utilized by either Ec-CDT or Cj-CDT. Further, Ec-CDT appears to interact with host cells in manner that is distinct from Cj-, Aa- and Hd-CDTs.

2.3.2 Differential roles for cholesterol and glycoproteins in CDT intoxication.

Cholesterol was recently reported as a direct binding determinant for Aa-CDT (Boesze-Battaglia et al., 2009), and cholesterol-rich microdomains (e.g. “rafts”) were previously demonstrated to be required for binding and intoxication by Aa- and Hd-CDT (Boesze-Battaglia, 2006; Boesze-Battaglia et al., 2006; Guerra et al., 2005). Thus, we sought to determine if cholesterol is important for intoxication of CHO-K1 cells by all CDTs. CDT-mediated cell cycle arrest in G2/M was measured by staining with the DNA-binding dye propidium iodide (PI) followed by flow cytometry to determine DNA content. Intoxication by Aa-, Hd-, and Ec-CDT was enhanced by cholesterol loading (Figure 2.3A), indicating that these three toxins may bind directly to cholesterol and/or utilize lipid rafts for entry. Again, Cj-CDT behaved differently as cell cycle arrest with this toxin was not enhanced by cholesterol loading (Figure 2.3A).

We next examined the role of host glycoproteins, which were previously implicated as important determinants for intoxication by Ec-CDT and Aa-CDT (Cao et al., 2005; McSweeney and Dreyfus, 2005). N-linked glycans represent a common form of glycoprotein linkage and consist of carbohydrate covalently linked to an asparagine side chain.

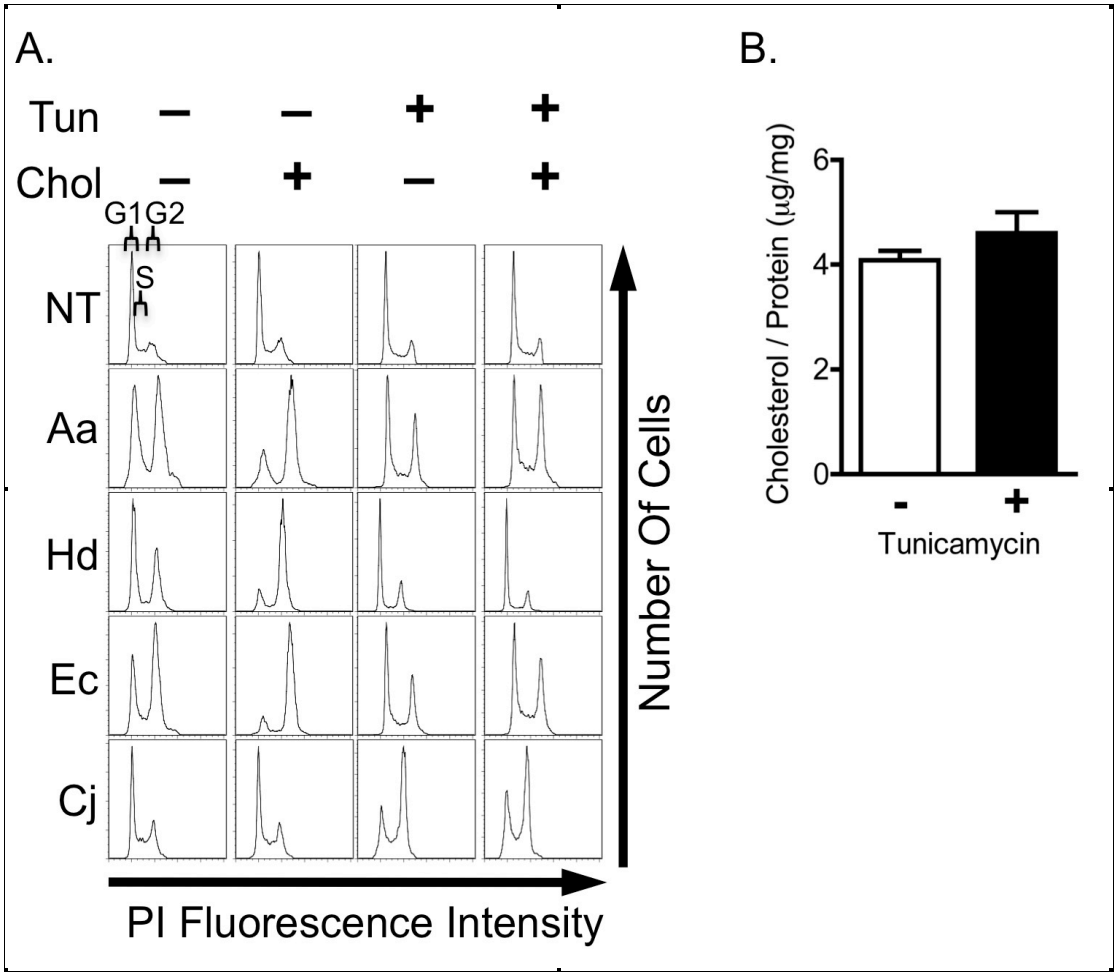

Figure 2.3 CDT intoxication of tunicamycin-treated and cholesterol-loaded CHO-K1 cells.

(A) CHO-K1 cells were treated with 0.5 μg/mL tunicamycin for 2 days, and/or incubated with 2 mg/mL MβCD conjugated cholesterol for 30 min prior to intoxication. Cells were incubated with toxin for 10 min, then washed and incubated for a further 24 h. DNA content was determined by PI staining and flow cytometry. Histograms indicate the number of cells (y-axis) at a given PI fluorescence intensity (x-axis), with the left hand peak representing cells in G0/G1 phase of cell cycle, the peak on the right representing cells in G2/M and the area between peaks representing cells in S phase as indicated in the top left histogram. (B) Total cellular cholesterol was quantified and normalized to total protein in CHO-K1 cells treated with tunicamycin. Average values calculated from triplicate samples +/- SEM are shown. (A, B) Results are representative of at least three independent experiments.

McSweeney and Dreyfus reported that treatment with tunicamycin resulted in diminished intoxication by Ec-CDT, leading them to concluded that N-linked glycans are required for this toxin (McSweeney and Dreyfus, 2005). Tunicamycin blocks the addition of the dolichol pyrophosphate precursor (Glc3Man9GlcNAc2) to asparagine side chains in the endoplasmic reticulum, thereby inhibiting all N-linked glycosylation (Zhou et al., 2005). Although tunicamycin is widely used to block the synthesis of N-linked glycans, there are several caveats in its use. Specifically, tunicamycin has been shown to block cholesterol biosynthesis by inhibiting the rate-limiting enzyme HMG CoA reductase. Furthermore, the absence of glycosylation induced by tunicamycin can result in misfolding of host-proteins and decreased presentation of these proteins on the cell surface (Volpe and Goldberg, 1983; Zhou et al., 2005). To define the effects of tunicamycin on intoxication, we asked whether this drug inhibits intoxication by all four CDTs, and explored the mechanism by which this inhibition occurs.

CHO-K1 cells were pretreated with tunicamycin, then intoxicated with each CDT for 24 h. Inhibition of N-linked glycosylation by tunicamycin was confirmed using the FITC labeled plant lectin, *Pisum sativum* agglutin (PSA) (data not shown). As expected, cells treated with tunicamycin were less sensitive to intoxication by Ec-CDT (Figure 2.3A). In addition, tunicamycin-treated cells were less sensitive to Aa- and Hd-CDTs (Figure 2.3A). Surprisingly, tunicamycin treatment enhanced intoxication by Cj-CDT (Figure 2.3A), once more implicating this toxin as having distinct host cell requirements for intoxication.

Interestingly, tunicamycin inhibited host cell sensitivity to the same three CDTs that utilize cholesterol for intoxication (Figure 2.3A). Therefore, we sought to determine if tunicamycin decreases sensitivity to Aa-, Hd-, and Ec-CDT through cholesterol depletion. Direct measurement of cellular cholesterol shows that levels of this lipid were unchanged by tunicamycin under the conditions tested here (Figure 2.3B). Furthermore, cholesterol supplementation did not reverse resistance to intoxication observed in tunicamycin treated cells (Figure 2.3A). Together, these results suggest that the primary effect of tunicamycin in our experimental system is on inhibition of glycosylation. However, it is not clear from these data whether the block to CDT intoxication results from loss of specific glycans that are required for toxin interactions, or whether decreased glycosylation in the presence of tunicamycin leads to misfolding and/or destabilization of a protein that is required by CDTs.

In order to test a direct role for specific glycans, we employed a panel of highly characterized glycan-deficient mutant CHO cells (Patnaik and Stanley, 2006). Mutant cell lines with well defined deficiencies in N-, O-, or lipid-linked glycans (Figure 2.4A) were challenged with each of the four CDTs for 24 h, stained with PI, and DNA content was measured by flow cytometry. As a control, the predicted glycan structures for each mutant (Figure 2.4A) were confirmed using the appropriate glycan-binding FITC-labeled plant lectins (data not shown). Surprisingly, although several of the mutant cell lines have drastically truncated glycans (Patnaik and Stanley, 2006), none displayed resistance to any CDT tested (Figure 2.4B).

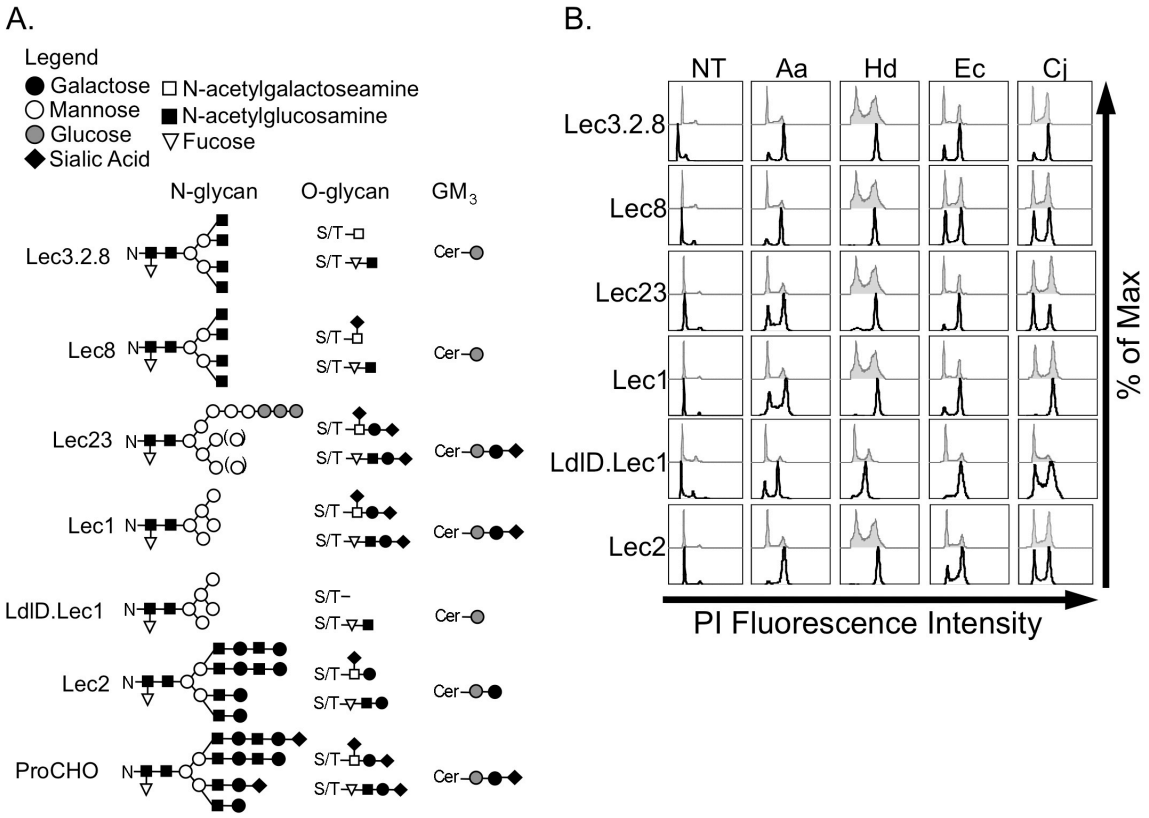

Figure 2.4 CDT intoxication of CHO glycosylation mutants.
(A) Predicted N- and O-linked glycan and glycolipid structures (Adapted from (Patnaik and Stanley, 2006)). G_{M3} is the predominant glycolipid in CHO cells; therefore, the mutant structures are based on G_{M3}. (B) Cells were intoxicated for 24 h, stained with PI and subjected to flow cytometry. Black histograms represent intoxicated loss of function mutants and grey shaded histograms represent the intoxicated parental ProCHO controls. Results are representative of at least three independent experiments.

Further, the mutant cell lines with the greatest defects in N-linked glycans (Lec1) or N- and O-linked glycans (ldlD.Lec1) demonstrated increased sensitivity to all four CDTs (Figure 2.4B). Increased sensitivity to Aa-, Hd-, and Ec-CDT in cells lacking complex or hybrid N-glycans (e.g. Lec1 and Lec23) was confirmed by treating ProCHO cells with the α-mannosidase I inhibitor, kifunensine, which blocks trimming of mannose on N-linked glycans and therefore results in high-mannose containing N-linked glycans (data not shown). Taken together, these data indicate that the four CDTs tested do not require mature host cell N- or O-glycan structures for intoxication.

Of note, the Lec cell intoxication data support the previous claim that absence of sialic acid results in more efficient intoxication by CDT (McSweeney and Dreyfus, 2005). It was previously reported that enzymatic removal of terminal sialic acid with neuraminidase resulted in increased sensitivity to Ec-CDT (McSweeney and Dreyfus, 2005). However, the extent of sialic acid removal in this study was not quantified, and the acidic pH required for neruaminidase activity may lead to secondary effects on cell surface proteins and/or cell health. Here we used a genetic approach to determine if reduced sialylation results in increased sensitivity to Ec-CDT, and extended the study to test the remaining three CDTs. CHO Lec2 cells lack the sialic acid transporter and are therefore unable to sialylate any of their glycans. Consistent with sialic acid blocking toxin interactions of some, but not all CDTs, Lec2 cells displayed increased sensitivity to Aa- Hd- and Ec-CDT. FITC-labeled WGA was used to confirm the cell surface sialic acid deficiency in these cell lines (data not shown). An inhibitory role of sialic acid was further supported by the increased

sensitivity of LdlD.Lec1 cells, which also lack terminal sialic acid due to the absence of sialotransferrase substrates.

In addition to addressing a potential role for glycans, analysis of the mutant CHO intoxication data provided further evidence that Aa-, Hd-, Ec-, and Cj-CDTs utilize divergent host determinants. When compared to the parental ProCHO cells, all of the Lec mutants tested were hypersensitive to Aa- and Hd-CDT (Figure 2.4B), supporting the hypothesis that these two CDTs have similar requirements for intoxication. In contrast, the intoxication profile for Cj-CDT on this panel of cells was markedly different, with Lec8, Lec23, and Lec2 cells being equally sensitive to this toxin when compared to parental ProCHO cells. These results further support the notion that Cj-CDT utilizes unique host determinants. Further, because Lec8, Lec23, and Lec2 cells were equally sensitive to Cj-CDT when compared to parental ProCHO cells, hypersensitivity to Aa- and Hd-CDT in these mutant cell lines is toxin-specific and does not derive from non-specific effects in these mutant cells (e.g. altered growth rates, DNA damage response, etc.). The Ec-CDT intoxication profile was unique, being similar to Cj-CDT in that Lec8 showed no change in sensitivity, and similar to Aa- and Hd-CDT in that Lec3.2.8, Lec23, and Lec2 cells showed increased sensitivity.

2.3.3 Fucosylated glycans are not required for intoxication by CDTs.

It was previously suggested that fucosylated glycans contribute to CDT binding based on findings that Ec-CDT bound directly to agarose-coupled fucose, and fucose-specific lectins blocked CdtA/C binding to HeLa cells, resulting in

decreased CDT activity (McSweeney and Dreyfus, 2005). Although data presented above indicate that complex N-linked glycans are not required for efficient CDT–host interactions (Figure 2.4), they do not rule out a potential role for fucose-modified glycans in conferring sensitivity to this family of toxins. Specifically, CHO cells contain N-linked glycans with fucose attached to the first (reducing) N-acetylglucosamine in the core glycan structure (Figure 2.4A), and this modification is maintained at reduced levels in Lec1 (Lin et al., 1994), but is absent following tunicamycin treatment. In order to test a role for fucosylated glycans in sensitivity to CDTs, we employed the mutant CHO cell line Lec13, which is deficient in the biosynthesis of fucose and therefore has reduced fucosylation of all glycans. Contrary to what was expected, Lec13 cells showed no alteration in sensitivity to any of the four CDTs tested (Figure 2.5A). Therefore, fucosylated glycans are not required for CDT intoxication.

The sensitivity of Lec13 cells to CDTs did not, however, address the question of whether terminally fucosylated glycans may serve to enhance intoxication. CHO-K1 cells express only two fucosyltransferase (*Fut*) genes, *Fut8*, which adds α1-6 fucose to the core of the N-linked glycan, and an O-fucosyltransferase that adds fucose directly to Ser/Thr residues on proteins. Many other cell types modify glycan structures by adding fucose to the terminal (non-reducing) end of N-, O-, and lipid-linked glycans through the activities of eight separate fucosyltransferases (FUT1-7, and FUT9) (Becker and Lowe, 2003).

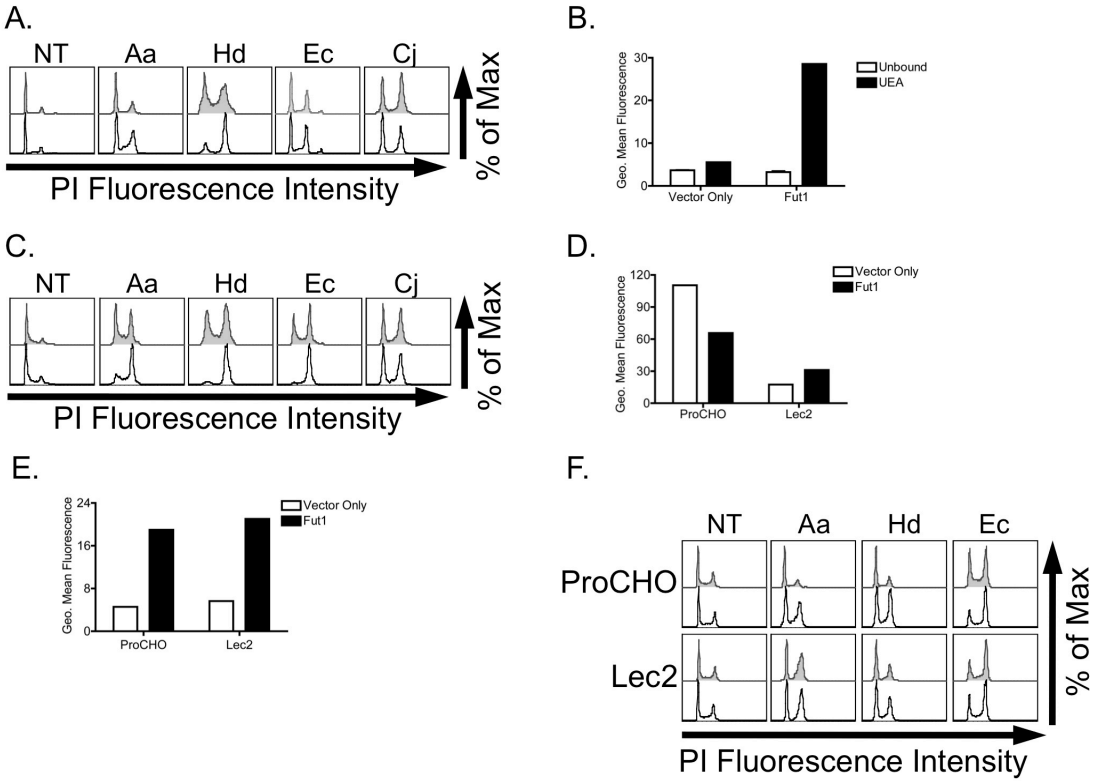

Figure 2.5. Role of fucose in CDT intoxication.
(A) CDT intoxication of the fucose biosynthetic mutant (Lec13) cells. Cells were grown in media containing dialysed serum for 2 days, intoxicated with CDT for 24 h, stained with PI and subjected to flow cytometry. Black histograms represent intoxicated Lec13 cells and grey shaded histograms are intoxicated parental ProCHO cells. (B) UEA binding of *Fut1* expressing CHO-K1 cells. Cells transduced with *Fut1*-encoding or empty vectors were detached with EDTA, washed and bound with FITC-conjugated UEA lectin for 15 min at room temperature. After three successive washes, the cells were resuspended in PBS + 1% formaldehyde and subjected to flow cytometry. Data represent geometric mean fluorescence of 10^4 cells. (C) CHO-K1 cells were transduced with a retroviral vector encoding *Fut1* (black histograms) or empty vector (grey histrograms), intoxicated for 24 h, stained with PI and subjected to flow cytometry. (D, E) ProCHO and Lec2 cells transduced with *Fut1*-encoding or empty vectors were bound with (D) FITC-conjugated WGA, or (E) FITC-conjugated UEA, washed and subjected to flow cytometry, as in (B). (F) CDT intoxication of parental (ProCHO) or sialic acid transporter mutant (Lec2) cells transduced with *Fut1* encoding (black histograms) or empty (grey histograms) retroviral vectors. Transduced cells were intoxicated for 24 h, stained with PI and subjected to flow cytometry. Results are representative of at least three independent experiments.

To test whether fucosylated glycans can enhance CDT intoxication, cDNAs encoding *Fut1-7* and *Fut9* were subcloned into retroviral vectors that were used to transduce CHO-K1 cells either individually or pairwise. Expression of all *Futs,* except *Fut2,* gave rise to the expected fucose modification profiles as judged by binding to fluorescently labeled plant lectins and antibodies (Figure 2.5B and data not shown) (Lofling et al., 2008). All cell lines were incubated with each CDT and evaluated for G_2/M arrest. Interestingly, overexpression of *Fut1*, but no other *Fut*, resulted in an increase in sensitivity to Aa-, Hd-, and Ec-CDTs (Figure 2.5C). Furthermore, co-expression of any of the *Fut* genes (*Fut3-7* and *9*) in conjunction with *Fut1* did not further sensitize CHO-K1 cells to CDT intoxication (data not shown).

The finding that *Fut1* overexpression led to enhanced sensitivity to a subset of CDTs is consistent with a role for α1,2 fucosylated glycans in host-toxin interactions. However, an alternative explanation is that expression of *Fut1* alters host glycan structures in ways other than addition of fucose. Indeed, it was previously demonstrated that expression of *Fut1* reduces sialic acid on N-linked glycans (Mathieu et al., 2004). Consistent with this, expression of *Fut1* in parental ProCHO cells resulted in decreased presentation of sialic acid (Figure 2.5D). Because a reduction in sialic acid levels led to increased sensitivity to the same group of CDTs affected by *Fut1* expression (compare Lec2 cells, Figure 2.4), we questioned whether *Fut1*-dependent hypersensitivity to CDT derived from the addition of fucose or the absence of sialic acid. To test this, we transduced sialic acid transporter-deficient CHO Lec2 cells with a retroviral vector encoding *Fut1* and intoxicated with each CDT. Activity of *Fut1* in transduced Lec2 cells and the

transduced parental ProCHO cell line was confirmed using a fluorescently labeled fucose-specific plant lectin (Figure 2.5E). Whereas ProCHO cells expressing *Fut1* were hypersensitive to CDTs, Lec2 cells expressing *Fut1* displayed no increase in sensitivity to intoxication (Figure 2.5F). Therefore, increased sensitivity associated with *Fut1* expression derives from loss of sialic acid and not from gain of fucosylation. Taken together, these data support a model where, contrary to previous reports, fucosylated glycans are not required for cellular intoxication by Ec-CDT or any of the other CDTs tested.

2.3.4 Glycolipid deficiency does not decrease sensitivity to CDT.

Next, we wished to address the proposed role of glycolipids in sensitivity to CDTs. An earlier study suggested that the glycosphingolipid G_{M3} functions as a receptor for Aa-CDT (Mise et al., 2005). Notably, G_{M3} is the predominant glycosphingolipid on CHO-K1 cells and consists of sialic acid (Neu5Ac), galactose (Gal), glucose (Glc) and ceramide (Cer) in the structure Neu5Acα2-3Galβ1-4Glcβ1-1Cer (Figure 2.4A)(Patnaik and Stanley, 2006). Therefore, mutant CHO cells defective in sialic acid (Lec2) or galactose (Lec8) modifications of glycoconjugates are predicted to lack G_{M3}. Surprisingly, neither Lec2 nor Lec8 cells displayed resistance to Aa-CDT, or any of the other three CDTs tested (Figure 2.4B). In fact, Lec2 cells displayed increased sensitivity to Aa-, Hd- and Ec-CDTs, and Lec8 cells were slightly more sensitive to Aa- and Hd-CDTs (Figure 2.4B).

Although these data indicate that the terminal saccharides of G_{M3} are not essential for conferring cell sensitivity, it is possible that the glucosylceramide core of

G_{M3} is important for intoxication. To evaluate this, we preincubated CHO-K1 cells with the glucosylceramide biosynthesis inhibitor PPMP, then challenged with each CDT. As with Lec2 and Lec8 cells (Figure 2.4), CHO-K1 cells treated with PPMP displayed increased sensitivity to Ec-, Aa- and Hd-CDT (Figure 2.6A), a result opposite of that expected if G_{M3} were a receptor. Interestingly, PPMP also increased sensitivity of CHO-K1 cells to Cj-CDT, a result not predicted by the Lec mutants. Taken together, these results suggest that contrary to previous reports, G_{M3} is not likely to function as a receptor for Aa-CDT, nor any of the three other CDTs tested. To further validate this result, a mutant CHO cell line deficient in synthesis of all sphingolipids (LY-B)(Hanada et al., 1998) was incubated with each CDT. Consistent with the Lec cell and PPMP data, LY-B cells displayed increased sensitivity to all CDTs (Figure 2.6B). These data suggest that G_{M3}, or any other glycosphingolipid, is not required for conferring sensitivity to any of the CDTs studied here.

2.4 DISUCSSION

CDTs are expressed by several distantly related Gram-negative bacterial pathogens that occupy very different ecological niches and cause distinct diseases. Here we tested whether host cellular factors previously implicated in CDT-host interactions were required for cellular intoxication by CDTs derived from four bacterial pathogens that cause periodontal disease, gastroenteritis or chancroid. Surprisingly, we found that mature N-linked as well as O-, or lipid-linked glycans are not required for intoxication by any of the CDTs tested.

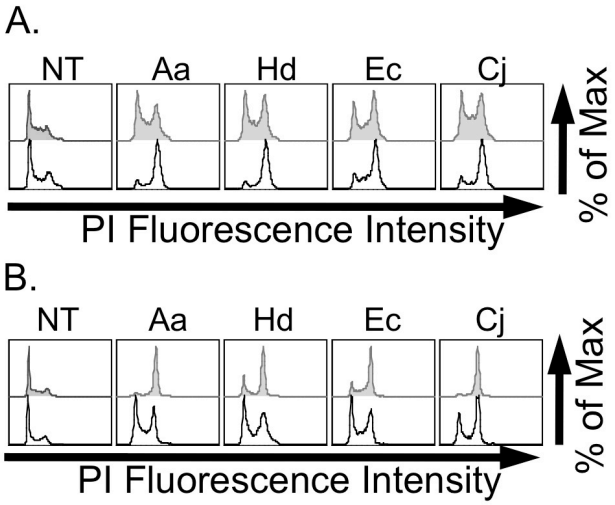

Figure 2.6 Role of glycolipids in CDT intoxication.
(A) Cells were treated with 5 μM PPMP for ten days, intoxicated with CDT for 24 h, stained with PI and subjected to flow cytometry. Black histograms are intoxicated PPMP treated cells and grey shaded histograms are untreated controls. (B) Lipid glycosylation mutant cells (LY-B; black histograms) or the cDNA complemented counterpart (Ly-BcLCB1; grey histograms) were intoxicated with CDT for 24 h, stained with PI and subjected to flow cytometry. Results are representative of at least three independent experiments.

Further, these four CDTs could be categorized into three groups based on their relative abilities to intoxicate a variety of wild type and mutant host-cell types. We report that Aa- and Hd-CDTs behave similarly, while CDTs derived from *E. coli* and *C. jejuni* display distinct host cell preferences (Table 2.1). These findings are consistent with the degree of amino acid similarity and indicate that CDTs derived from different pathogens possess unique requirements to intoxicate host cells and may have different receptors.

Prior studies with Ec- and Aa-CDTs supported a role for host carbohydrates in CDT interactions (McSweeney and Dreyfus, 2005; Mise et al., 2005). Here, we used a genetic approach to directly test the requirement of specific host glycans by employing cell lines with known glycan deficiencies. Surprisingly, mutant CHO cells that lack N-linked complex and hybrid carbohydrates (Figure 2.4) or cells that lack glycosphingolipids (Figure 2.6) were more sensitive to the CDTs tested. Hypersensitivity likely derives from the loss of sialic acid, a common feature of the Lec mutants tested here, and the only defect in Lec2 cells (Figure 2.4). This result is in agreement with the previous finding that removal of sialic acid with neuraminidase leads to increased sensitivity to Ec-CDT (McSweeney and Dreyfus, 2005). The negative charge associated with sialic acid may act to inhibit CDTs, a conclusion further supported by the finding that mutant CHO cells lacking negatively charged glycosaminoglycans (i.e. pgsA-745 and pgsD-677)(Esko et al., 1985; Lidholt et al., 1992) are hypersensitive to all CDTs studied here (data not shown).

Table 2.1 Summary of differences between CDTs.

Toxin	Target Cell Preference	TunicamycIn Treatment	Cholesterol Addition	Sialic Acid Deficiency	Galactose Transporter Deficiency	Glycolipid Deficiency
Aa	Highly active on most cell types	–	+	+	+	+
Hd	Highly active on most cell types	–	+	+	+	+
Ec	Most active on CHO-K1 cells	–	+	+	0	+
Cj	Active on 3T3 and Y-1 cells	+	0	0	0	+

+ Increased sensitivity
– Decreased sensitivity
0 No change

The difference in sensitivity of tunicamycin-treated and mutant Lec cell lines provides insight into toxin-host interactions and can be explained by one of two models. First, it is possible that the immature high-mannose and/or core glycan structure present on Lec1, ldlD.Lec1 and Lec23 cells, but absent following tunicamycin treatment contributes to sensitivity to Aa-, Hd-, and Ec-CDTs. However, excess mannose or mannans did not block CDT intoxication (data not shown). Further, multiple attempts to identify Ec-CDT binding to over 300 individual glycan structures using glycan arrays revealed no consistent or detectable interactions [2]. A second possibility is that the polypeptide component of glycoproteins, rather than glycans themselves, serve as host determinants for CDT-sensitivity and that these proteins require glycan modification for proper folding and cell-surface presentation (Zhou et al., 2005). Indeed, Carette and colleagues recently identified a host membrane protein, TMEM181, which supports intoxication by Ec-CDT and may serve as a receptor for this toxin (Carette et al., 2009).

It is striking that our results appear to contradict previously reported roles for fucosylated glycans and for G_{M3} (McSweeney and Dreyfus, 2005; Mise et al., 2005). The former may be explained by differences in toxins utilized. Specifically, *E. coli* can encode multiple distinct CDTs. While McSweeney and Dreyfus studied type II Ec-CDT, results presented here are based on the closely related but distinct type III toxin. Discrepancies regarding PPMP-mediated inhibition of G_{M3} may be partly explained by the fact that inhibition of glycolipid synthesis in monocytes, the cell type utilized by Mise *et al,* leads to altered trafficking following endocytosis and targeting of lipid-raft associated proteins to lysosomes (Sillence et al., 2002). Trafficking of

CDT to the lysosomes rather than the ER in PPMP-treated monocytes could have lead to the previously reported results. However, Mise and colleagues also reported that glycolipid-deficient LY-B cells were resistant to Aa-CDT, in contrast to results presented here. Furthermore, Carette *et al.* recently reported that cells containing retroviral insertions in sphingomyelin synthase were resistant to Ec-CDT (Carette et al., 2009). LY-B cells used in our studies were originally isolated based on having deficiency in sphingomyelin content (Hanada et al., 1998). While the source of these discrepancies is still unclear, our conclusions are supported by multiple lines of evidence obtained with Lec2, Lec8, Lec3.2.8, LY-B and PPMP-treated cells, all of which are deficient in G_{M3} and display increased sensitivity to one or more CDTs (Figure 2.4B).

In summary, the results presented here show that CDTs derived from different pathogens utilize distinct host factors for intoxication. This tropism seems to correlate with the amino acid sequence of the CDT binding subunits as opposed to bacterial niche. Although *A. actinomycetemcomitans* and *H. ducreyi* have different niches, the binding subunits of the CDTs they encode share high levels of amino acid identities and they respond similarly to alterations in host factors such as glycans, cholesterol content and cell lineage. Conversely, *E. coli* and *C. jejuni* have similar niches but their binding subunits are quite different, leading to divergent target cell preferences. Future efforts to identify receptors for CDTs will provide insight into cellular and tissue tropism, and may thus shed light on host interactions associated with CDT-producing pathogens.

2.5 EXPERIMENTAL PROCEDULRES

Cell Culture

Pro⁻CHO (ProCHO), Pro⁻Lec8.D3 (Lec8), Pro⁻Lec23.11C (Lec23), Pro⁻Lec3.2.8 3B (Lec3.2.8), LdlD.Lec1, Pro⁻Lec1.3C (Lec1), cells were provided by Pamela Stanley (Albert Einstein College of Medicine)(Chen and Stanley, 2003; Hong et al., 2004; Oelmann et al., 2001; Stanley, 1989). Pro⁻Lec13 (Lec13), Pro⁻Lec2 (Lec2) and CHO-K1 mutants defective in proteoglycan biosynthesis, PgsA745 and PgsD677 (Esko et al., 1985; Lidholt et al., 1992), were provided by Jeff Esko (UCSD). Balb/3T3 clone A31 and CHO-K1 cells were a gift from John Young (Salk Institute). Y-1 cells were provided by Edward McCabe (UCLA). OT-1 cells were provided by Carrie Miceli (UCLA). HeLa, NIH/3T3, IC-21 and Raw 264.7 cells were obtained from ATCC. Unmutagenized CHO-K1 and ProCHO, glycosylation mutant CHO and Y-1 cells were cultivated in F-12 media (Invitrogen) supplemented with 10% fetal bovine serum (FBS; Atlanta Biologicals), 100 U/mL penicillin, 100 µg/mL streptomycin and 5 mM L-glutamine (PSG; Invitrogen). Lec13 and ldlD.Lec1 cells were cultured for two days prior to intoxication in F-12 containing 10% FBS dialyzed against phosphate buffered saline (PBS). HeLa, NIH/3T3, Balb/3T3, and Raw 264.7 cells were cultured in Dulbeco's minimum essential medium (DMEM; Invitrogen) supplemented with 10% FBS and PSG. IC-21 and OT-1 cells were cultivated in RPMI and IMDM, respectively, supplemented with 10% FBS and PSG. All cells were cultured at 37°C in a humid atmosphere containing 5% CO2.

CDT cloning, expression and purification

Cloning and expression of CDTs was based on the method previously described (Nesic et al., 2004). Cultures of A. actinomycetemcomitans (Y4) and E. coli (S5) were obtained from ATCC and C. jejuni (81-176) from Patricia Guerry (Naval Medical Research Center; Silver Spring, MD). Genomic DNA was purified from mid-log-phase cultures using the Wizard DNA Purification kit (Promega). Genomic DNA of H. ducreyi (35000HP) was obtained from ATCC. cdtA, cdtB, and cdtC genes (Aa GI: 3786340, Hd GI: 2102681, Ec GI: 2218088 and Cj GI: 15791399) were PCR amplified using primers corresponding to the 5' and 3' ends of each gene (Table 2.2). These primers were engineered such that 5' NdeI and 3' BamHI restriction sites (underlined in table 2.2) were incorporated into the amplicon. Each PCR product was purified using the QIAquick PCR purification kit (Qiagen). The purified amplicons and pET15b vector were digested with NdeI and BamHI (New England Biolabs) to generate directional annealing sites. Digested vector and amplicons were ligated and electroporated into E. coli DH5α. The integrity of each gene was confirmed by DNA sequencing. E. coli BL21(DE3) strains transformed with cdt expression plasmids were grown in Luria-Bertani broth containing 100 µg/ml ampicillin (LB+amp) at 37°C with continuous aeration. Starter cultures were diluted 1:400 into fresh LB+amp and grown until the optical density at 600 nm reached 0.4 – 0.6 at which point expression of Cdt was induced by addition of 0.25 mM IPTG (Fisher).

Table 2.2 Primer sequences for PCR amplification of CDT.

Primer	Direction	Primer Sequence (5' – 3')
Aa-CdtA	forward	GGAGTTCCATATGAGTGACTATTCTCAGCCTG
Aa-CdtA	reverse	CGGGATCCTTAATTAACCGCTGTTGC
Aa-CdtB	forward	GGAGTTCCATATGAACTTGAGTGATTTCAAAGTAGC
Aa-CdtB	reverse	CGGGATCCTTAGCGATCATGAACAAAACTAACAGG
Aa-CdtC	forward	GGAGTTCCATATGGAATCAAATCCTGATCCG
Aa-CdtC	reverse	CGGGATCCTTAGCTACCCTGATTTCTCC
Hd-CdtA	forward	GGAGTTCCATATGAATGACTATTCTCAACCTGAATCTC
Hd-CdtA	reverse	CGGGATCCTTAATTAACCGCTGTTGC
Hd-CdtB	forward	GGAGTTCCATATGAACTTGAGTGACTTCAAAGTAG
Hd-CdtB	reverse	CGGGATCCTTAGCGATCACGAACAAAACTAACAG
Hd-CdtC	forward	GGAGTTCCATATGGAATCAAATCCTGATCCGAC
Hd-CdtC	reverse	CGGGATCCTTAGCTACCCTGATTTCTTC
Ec-CdtA	forward	GGAGTTCCATATGCATCTTGACCCCAAAG
Ec-CdtA	reverse	CGGGATCCTCATTGTTCGCCTCCTG
Ec-CdtB	forward	GGAGTTCCATATGGATTTAACTGATTTTCGCGTTG
Ec-CdtB	reverse	CGGGATCCTTATCGTCTGGAAACG
Ec-CdtC	forward	GGAGTTCCATATGGTCAATAATCAGATAGATGAGTTAG
Ec-CdtC	reverse	CGGGATCCTTAAATAACAGGAGATTCTGTATTTAATG
Cj-CdtA	forward	GGAGTTCCATATGTGTTCTTCTAAATTTGAAAATGTAAATCC
Cj-CdtA	reverse	CGGGATCCTCATCGTACCTCTCC
Cj-CdtB	forward	GGAGTTCCATATGAATTTAGAAAATTTTAATGTTGGCACTTGG
Cj-CdtB	reverse	CGGGATCCCTAAAATTTTCTAAAATTTACTGGAAAATGATCTGAAAC
Cj-CdtC	forward	GGAGTTCCATATGACTCCTACTGGAGATTTGAAAGATTTTACC
Cj-CdtC	reverse	CGGGATCCTTATTCTAAAGGGGTAGCAGC

Cultures were grown for an additional 3 h and then harvested by centrifugation at 5,000 x g for 10 min at 4°C. The cell pellets were resuspended in 20 mL PBS (8 g NaCl, 0.2 g KCl, 0.2 g KH2PO4, and 1.15 g Na2HPO4·7H2O in 1 L) containing 8 M urea and disrupted by sonication (six 30 s cycles at 23 kHz and 30 W) using Model 100 Sonic Dismembrator (Fisher). Cell lysates were then clarified by centrifugation at 16,000 x g for 30 min at 4°C. Supernatants containing proteins were incubated with 3 mL of TALON Metal Affinity Resin (Clontech) overnight with gentle rotation at 4°C. The resin was washed with buffer A (8 M urea, 20 mM HEPES, 200 mM NaCl, pH 7.5) and eluted with buffer A + 100 mM EDTA. Protein concentrations were quantified using the Bradford Protein Assay and purity was estimated by SDS-PAGE. Proteins were stored in elution buffer at -20°C. At time of use, proteins were diluted to 100 µg/ml with buffer A and dialyzed against buffer B (20 mM HEPES, 200 mM NaCl, 5% Glycerol, 2.5 mM DTT, pH 7.5) using 6-8 kDa MWCO membranes (Spectrum Labs). Two final buffer changes were conducted in 3 L volumes of PBS containing 5% glycerol and 2.5 mM DTT.

Intoxication of mammalian cells with CDTs

Mammalian cells were trypsinized, counted and allowed to adhere overnight in 6- or 384-well plates. The following day, media was removed and toxin-containing media was added for 10 min or 24 h as indicated in the figure legends. The concentration of toxin was selected to illustrate the presence or absence of a genetic or pharmacological effect on intoxication (Aa-CDT: 2-200nM; Hd-CDT: 0.1-75nM; Ec-CDT: 5-900nM; Cj-CDT: 50-1500nM). Twenty-four hours after toxin addition, cells were analyzed for phosphorylation of H2AX or cell cycle arrest as described

below. All results presented are representative of three or more independent experiments.

Histone H2AX assay

Cells were intoxicated for 24 h in clear bottom 384-well plates then fixed with 2% formaldehyde, quenched with 100 mM glycine and permeabilized with ice-cold methanol. The cells were subsequently blocked with 3% BSA / 0.3% Triton X-100 and incubated with rabbit anti-phospho-H2AX antibody (Cell Signal Technologies) overnight at 4°C. After washing, cells were incubated with Alexa Fluor 488-labeled goat anti-rabbit antibody (Invitrogen) for 1 h at room temperature, washed and counterstained with 1 μg/mL Hoechst 33342 (Invitrogen). Cytometric acquisition was performed on four 20X scan fields using an iCys laser scanning cytometer (CompuCyte) equipped with Argon and Violet diode lasers. Cytometric data analysis was conducted with iCys version 3.4 software (CompuCyte).

Cell cycle analysis

CHO glycosylation mutants and unmutagenized parental strains were intoxicated in 6-well plates for either 10 min or 24 h, then washed with Dulbecco's PBS (DPBS, Cellgro), detached with 0.05% trypsin/EDTA (Invitrogen), washed again with DPBS and permeabilized with 60% ethanol for 30 min on ice. After washing again, cells were stained with a 50 μg/mL propidium iodide (PI) solution containing 1 mg/mL sodium citrate, 0.3% NP-40, and 20 μg/mL RNase-A. The fluorescence was quantified for 10^4 cells using a FACSCalibur flow cytometer (Becton Dickinson) with

CellQuest acquisition software (Becton Dickinson). Flow cytometry data were subsequently analyzed using FloJo analysis software (Tree Star).

Fluorescent lectin binding

Cell surface glycan presentation was measured using the FITC conjugated lectins (EY Laboratories) Concanavalin A (ConA), Griffonia simplicifolia lectin (GS-II), Lens culinaris agglutin (LCA), Maclura pomifera agglutin (MPA), Phaseolus vulgaris agglutin (PHA), Pisum sativum agglutin (PSA), Ulex europus agglutin (UEA), and wheat germ agglutin (WGA). Cells were detached as described above, mixed with an equal volume of complete media containing FBS, washed with DPBS and resuspended in DPBS containing the manufacturer recommended concentration of FITC labeled lectin at room temperature for 15 min. Cells were washed with DPBS three times and resuspended in DPBS containing 1% formaldehyde (EMD). Fluorescence was quantified as described above.

N-linked glycosylation inhibitor treatment, and cholesterol loading

To inhibit N-linked glycosylation, CHO-K1 cells were cultured in the presence of 10 µg/mL tunicamycin (Sigma Aldrich) for two days prior to intoxication. For cholesterol loading of CHO cells, 15 mg of cholesterol (Sigma Aldrich) was solubilized by dissolving 15 mg in 0.4 mL methanol:chloroform (2:1), then adding dropwise into 20 mL PBS containing 0.37 g methyl-beta-cyclodextrin (MβCD; Sigma Aldrich) and stirred for 2 h at 80°C. The solution was dried in a rotary-evaporator and resuspended in 6 mL F-12 media (2.5 mg/mL cholesterol final). Cells were washed

in serum free F-12 media, incubated in solubilized cholesterol for 1 h, and washed in complete F-12 media three times. Following tunicamycin treatment, cholesterol loading, or both, the cells were intoxicated for 10 min, followed by a 24 h incubation, and analyzed for cell cycle arrest as described above.

Cholesterol was quantified by the use of Amplex Red reagent (Invitrogen). Cells were washed three times in PBS and detached using 1 mM EDTA in PBS. After centrifugation, cells were lysed by resuspension in 100 mM KH2PO4, 50 mM NaCl, 5 mM cholic acid and 0.1% Triton X-100 and subjected to three freeze thaw cycles. Lysates were added to an equal volume of the working Amplex Red assay buffer (prepared according to manufacturers instructions). Fluorescence was measured with a Flexstation II microplate reader (Molecular Devices) using excitation at 560 nm and detection at 590 nm. Cholesterol levels were determined by comparing fluorescence values to a standard curve and normalizing to protein content as determined by BioRad Protein Assay.

Fucosyltransferase studies

Fucosyltransferase 1 (Fut1) cDNA was PCR amplified from pCDM7 (Larsen et al., 1990)(provided by John Lowe, Case Western Reserve University) using the forward primer, CCCCTCGAGATGTGGCTCCGGAGCCAT and the reverse primer, CCCGAATTCTCAAGGCTTAGCCAATGTCC. The amplicon was digested with XhoI and EcoRI (engineered restriction sites are underlined in primer sequences), gel purified, and ligated with T4 DNA ligase (New England Biolabs) into the retroviral vector pMSCVpuro (Clontech). A similar subcloning strategy was undertaken for

Fut2-9. Plasmid DNA was purified and transfected into human 293 cells along with MLV gag/pol and VSV-G expression plasmids as previously described (Bradley et al., 2003). Forty-eight hours later, resulting retroviral particles were harvested, filter sterilized, diluted 1:1 in fresh media with 8 μg/mL polybrene (Sigma Aldrich) and used to transduce cells in a 6-well plate. Cells were incubated with viral particles overnight. After 48 h, infected cells were selected in medium containing 5 μg/mL puromycin.

Glycosphingolipid studies

In order to deplete glycosylated sphingolipids, CHO-K1 cells were cultured in the presence of 5 μM 1-phenyl-2-palmitoylamino-3-morpholino-1-propanol (PPMP; Sigma Aldrich) for 10 days then intoxicated for 24 h. Cell lines deficient in serine-palmitoyl transferase (LY-B) and the complimented counterpart LY-B/cLCB1 were obtained from RIKEN cell bank. These cells were cultured in F-12 media containing PSG, 10 μM sodium oleate, 1X nutridoma (Roche) and 0.1% fatty acid free bovine serum albumin (Sigma Aldrich) for two days prior to intoxication.

2.6 ACKNOWLEDGEMENTS

We thank Dr. David Smith and members of the Consortium of Functional Glycomics Core H for helpful discussion and glycan array screening. We thank Drs. Pamela Stanley and Jeff Esko for glycan-deficient mutant cell lines, and Dr. Esko and Dr. Linda Baum for expert consultation. Finally, we thank Dr. Baum for critical reading of the manuscript. This work was supported by NIH awards T32DE007296 (A.E.), F31AI061837 (F.J.M.-A.), and AI59095 (S.R.B.).

Footnotes

[1] Amandeep Gargi, Brendon Powers, and Steven R. Blanke data not shown.

[2] Unpublished. Data available at

http://www.functionalglycomics.org/glycomics/publicdata/primaryscreen.jsp

2.7 BIBLIOGRAPHY

Akifusa, S., Heywood, W., Nair, S.P., Stenbeck, G., and Henderson, B. (2005). Mechanism of internalization of the cytolethal distending toxin of Actinobacillus actinomycetemcomitans. Microbiology *151*, 1395-1402.

Akifusa, S., Poole, S., Lewthwaite, J., Henderson, B., and Nair, S.P. (2001). Recombinant Actinobacillus actinomycetemcomitans cytolethal distending toxin proteins are required to interact to inhibit human cell cycle progression and to stimulate human leukocyte cytokine synthesis. Infect Immun *69*, 5925-5930.

Becker, D.J., and Lowe, J.B. (2003). Fucose: biosynthesis and biological function in mammals. Glycobiology *13*, 41R-53R.

Boesze-Battaglia, K. (2006). Isolation of membrane rafts and signaling complexes. Methods Mol Biol *332*, 169-179.

Boesze-Battaglia, K., Besack, D., McKay, T., Zekavat, A., Otis, L., Jordan-Sciutto, K., and Shenker, B.J. (2006). Cholesterol-rich membrane microdomains mediate cell cycle arrest induced by Actinobacillus actinomycetemcomitans cytolethal-distending toxin. Cell Microbiol *8*, 823-836.

Boesze-Battaglia, K., Brown, A., Walker, L., Besack, D., Zekavat, A., Wrenn, S., Krummenacher, C., and Shenker, B.J. (2009). Cytolethal distending toxin induced cell cycle arrest of lymphocytes is dependent upon recognition and binding to cholesterol. J Biol Chem.

Bradley, K.A., Mogridge, J., Jonah, G., Rainey, A., Batty, S., and Young, J.A. (2003). Binding of anthrax toxin to its receptor is similar to alpha integrin-ligand interactions. J Biol Chem *278*, 49342-49347.

Cao, L., Volgina, A., Huang, C.M., Korostoff, J., and DiRienzo, J.M. (2005). Characterization of point mutations in the cdtA gene of the cytolethal distending toxin of Actinobacillus actinomycetemcomitans. Mol Microbiol *58*, 1303-1321.

Carette, J.E., Guimaraes, C.P., Varadarajan, M., Park, A.S., Wuethrich, I., Godarova, A., Kotecki, M., Cochran, B.H., Spooner, E., Ploegh, H.L.*, et al.* (2009).

Haploid genetic screens in human cells identify host factors used by pathogens. Science *326*, 1231-1235.

Chen, W., and Stanley, P. (2003). Five Lec1 CHO cell mutants have distinct Mgat1 gene mutations that encode truncated N-acetylglucosaminyltransferase I. Glycobiology *13*, 43-50.

Cope, L.D., Lumbley, S., Latimer, J.L., Klesney-Tait, J., Stevens, M.K., Johnson, L.S., Purven, M., Munson, R.S., Jr., Lagergard, T., Radolf, J.D.*, et al.* (1997). A diffusible cytotoxin of Haemophilus ducreyi. Proc Natl Acad Sci U S A *94*, 4056-4061.

Cortes-Bratti, X., Chaves-Olarte, E., Lagergard, T., and Thelestam, M. (1999). The cytolethal distending toxin from the chancroid bacterium Haemophilus ducreyi induces cell-cycle arrest in the G2 phase. J Clin Invest *103*, 107-115.

Deng, K., and Hansen, E.J. (2003). A CdtA-CdtC complex can block killing of HeLa cells by Haemophilus ducreyi cytolethal distending toxin. Infect Immun *71*, 6633-6640.

Elwell, C., Chao, K., Patel, K., and Dreyfus, L. (2001). Escherichia coli CdtB mediates cytolethal distending toxin cell cycle arrest. Infect Immun *69*, 3418-3422.

Elwell, C.A., and Dreyfus, L.A. (2000). DNase I homologous residues in CdtB are critical for cytolethal distending toxin-mediated cell cycle arrest. Mol Microbiol *37*, 952-963.

Esko, J.D., Stewart, T.E., and Taylor, W.H. (1985). Animal cell mutants defective in glycosaminoglycan biosynthesis. Proc Natl Acad Sci U S A *82*, 3197-3201.

Frisk, A., Lebens, M., Johansson, C., Ahmed, H., Svensson, L., Ahlman, K., and Lagergard, T. (2001). The role of different protein components from the Haemophilus ducreyi cytolethal distending toxin in the generation of cell toxicity. Microb Pathog *30*, 313-324.

Guerra, L., Teter, K., Lilley, B.N., Stenerlow, B., Holmes, R.K., Ploegh, H.L., Sandvig, K., Thelestam, M., and Frisan, T. (2005). Cellular internalization of cytolethal distending toxin: a new end to a known pathway. Cell Microbiol *7*, 921-934.

Hanada, K., Hara, T., Fukasawa, M., Yamaji, A., Umeda, M., and Nishijima, M. (1998). Mammalian cell mutants resistant to a sphingomyelin-directed cytolysin. Genetic and biochemical evidence for complex formation of the LCB1 protein with the LCB2 protein for serine palmitoyltransferase. J Biol Chem *273*, 33787-33794.

Hong, Y., Sundaram, S., Shin, D.J., and Stanley, P. (2004). The Lec23 Chinese hamster ovary mutant is a sensitive host for detecting mutations in alpha-glucosidase I that give rise to congenital disorder of glycosylation IIb (CDG IIb). J Biol Chem *279*, 49894-49901.

Hu, X., Nesic, D., and Stebbins, C.E. (2006). Comparative structure-function analysis of cytolethal distending toxins. Proteins *62*, 421-434.

Johnson, W.M., and Lior, H. (1988a). A new heat-labile cytolethal distending toxin (CLDT) produced by Campylobacter spp. Microb Pathog *4*, 115-126.

Johnson, W.M., and Lior, H. (1988b). A new heat-labile cytolethal distending toxin (CLDT) produced by Escherichia coli isolates from clinical material. Microb Pathog *4*, 103-113.

Lara-Tejero, M., and Galan, J.E. (2000). A bacterial toxin that controls cell cycle progression as a deoxyribonuclease I-like protein. Science *290*, 354-357.

Lara-Tejero, M., and Galan, J.E. (2001). CdtA, CdtB, and CdtC form a tripartite complex that is required for cytolethal distending toxin activity. Infect Immun *69*, 4358-4365.

Larsen, R.D., Ernst, L.K., Nair, R.P., and Lowe, J.B. (1990). Molecular cloning, sequence, and expression of a human GDP-L-fucose:beta-D-galactoside 2-alpha-L-fucosyltransferase cDNA that can form the H blood group antigen. Proc Natl Acad Sci U S A *87*, 6674-6678.

Lee, R.B., Hassane, D.C., Cottle, D.L., and Pickett, C.L. (2003). Interactions of Campylobacter jejuni cytolethal distending toxin subunits CdtA and CdtC with HeLa cells. Infect Immun *71*, 4883-4890.

Li, L., Sharipo, A., Chaves-Olarte, E., Masucci, M.G., Levitsky, V., Thelestam, M., and Frisan, T. (2002). The Haemophilus ducreyi cytolethal distending toxin activates sensors of DNA damage and repair complexes in proliferating and non-proliferating cells. Cell Microbiol *4*, 87-99.

Lidholt, K., Weinke, J.L., Kiser, C.S., Lugemwa, F.N., Bame, K.J., Cheifetz, S., Massague, J., Lindahl, U., and Esko, J.D. (1992). A single mutation affects both N-acetylglucosaminyltransferase and glucuronosyltransferase activities in a Chinese hamster ovary cell mutant defective in heparan sulfate biosynthesis. Proc Natl Acad Sci U S A *89*, 2267-2271.

Lin, A.I., Philipsberg, G.A., and Haltiwanger, R.S. (1994). Core fucosylation of high-mannose-type oligosaccharides in GlcNAc transferase I-deficient (Lec1) CHO cells. Glycobiology *4*, 895-901.

Lofling, J., Diswall, M., Eriksson, S., Boren, T., Breimer, M.E., and Holgersson, J. (2008). Studies of Lewis antigens and H. pylori adhesion in CHO cell lines engineered to express Lewis b determinants. Glycobiology *18*, 494-501.

Mathieu, S., Prorok, M., Benoliel, A.M., Uch, R., Langlet, C., Bongrand, P., Gerolami, R., and El-Battari, A. (2004). Transgene expression of alpha(1,2)-fucosyltransferase-I (FUT1) in tumor cells selectively inhibits sialyl-Lewis x expression and binding to E-selectin without affecting synthesis of sialyl-Lewis a or binding to P-selectin. Am J Pathol *164*, 371-383.

McSweeney, L.A., and Dreyfus, L.A. (2004). Nuclear localization of the Escherichia coli cytolethal distending toxin CdtB subunit. Cell Microbiol *6*, 447-458.

McSweeney, L.A., and Dreyfus, L.A. (2005). Carbohydrate-binding specificity of the Escherichia coli cytolethal distending toxin CdtA-II and CdtC-II subunits. Infect Immun *73*, 2051-2060.

Mise, K., Akifusa, S., Watarai, S., Ansai, T., Nishihara, T., and Takehara, T. (2005). Involvement of ganglioside GM3 in G(2)/M cell cycle arrest of human monocytic cells induced by Actinobacillus actinomycetemcomitans cytolethal distending toxin. Infect Immun *73*, 4846-4852.

Nesic, D., Hsu, Y., and Stebbins, C.E. (2004). Assembly and function of a bacterial genotoxin. Nature *429*, 429-433.

Nesic, D., and Stebbins, C.E. (2005). Mechanisms of assembly and cellular interactions for the bacterial genotoxin CDT. PLoS Pathog *1*, e28.

Nougayrede, J.P., Taieb, F., De Rycke, J., and Oswald, E. (2005). Cyclomodulins: bacterial effectors that modulate the eukaryotic cell cycle. Trends Microbiol *13*, 103-110.

Oelmann, S., Stanley, P., and Gerardy-Schahn, R. (2001). Point mutations identified in Lec8 Chinese hamster ovary glycosylation mutants that inactivate both the UDP-galactose and CMP-sialic acid transporters. J Biol Chem *276*, 26291-26300.

Oswald, E., Nougayrede, J.P., Taieb, F., and Sugai, M. (2005). Bacterial toxins that modulate host cell-cycle progression. Curr Opin Microbiol *8*, 83-91.

Patnaik, S.K., and Stanley, P. (2006). Lectin-resistant CHO glycosylation mutants. Methods Enzymol *416*, 159-182.

Pickett, C.L., Pesci, E.C., Cottle, D.L., Russell, G., Erdem, A.N., and Zeytin, H. (1996). Prevalence of cytolethal distending toxin production in Campylobacter jejuni and relatedness of Campylobacter sp. cdtB gene. Infect Immun *64*, 2070-2078.

Pickett, C.L., and Whitehouse, C.A. (1999). The cytolethal distending toxin family. Trends Microbiol *7*, 292-297.

Purdy, D., Buswell, C.M., Hodgson, A.E., McAlpine, K., Henderson, I., and Leach, S.A. (2000). Characterisation of cytolethal distending toxin (CDT) mutants of Campylobacter jejuni. J Med Microbiol *49*, 473-479.

Rabin, S.D., Flitton, J.G., and Demuth, D.R. (2009). Aggregatibacter actinomycetemcomitans cytolethal distending toxin induces apoptosis in nonproliferating macrophages by a phosphatase-independent mechanism. Infect Immun *77*, 3161-3169.

Shenker, B.J., Dlakic, M., Walker, L.P., Besack, D., Jaffe, E., LaBelle, E., and Boesze-Battaglia, K. (2007). A novel mode of action for a microbial-derived immunotoxin: the cytolethal distending toxin subunit B exhibits phosphatidylinositol 3,4,5-triphosphate phosphatase activity. J Immunol *178*, 5099-5108.

Shenker, B.J., Hoffmaster, R.H., McKay, T.L., and Demuth, D.R. (2000). Expression of the cytolethal distending toxin (Cdt) operon in Actinobacillus actinomycetemcomitans: evidence that the CdtB protein is responsible for G2 arrest of the cell cycle in human T cells. J Immunol *165*, 2612-2618.

Shenker, B.J., Hoffmaster, R.H., Zekavat, A., Yamaguchi, N., Lally, E.T., and Demuth, D.R. (2001). Induction of apoptosis in human T cells by Actinobacillus actinomycetemcomitans cytolethal distending toxin is a consequence of G2 arrest of the cell cycle. J Immunol *167*, 435-441.

Sillence, D.J., Puri, V., Marks, D.L., Butters, T.D., Dwek, R.A., Pagano, R.E., and Platt, F.M. (2002). Glucosylceramide modulates membrane traffic along the endocytic pathway. J Lipid Res *43*, 1837-1845.

Smith, J.L., and Bayles, D.O. (2006). The contribution of cytolethal distending toxin to bacterial pathogenesis. Crit Rev Microbiol *32*, 227-248.

Stanley, P. (1989). Chinese hamster ovary cell mutants with multiple glycosylation defects for production of glycoproteins with minimal carbohydrate heterogeneity. Mol Cell Biol *9*, 377-383.

Thelestam, M., and Frisan, T. (2004). Cytolethal distending toxins. Rev Physiol Biochem Pharmacol *152*, 111-133.

Volpe, J.J., and Goldberg, R.I. (1983). Effect of tunicamycin on 3-hydroxy-3-methylglutaryl coenzyme A reductase in C-6 glial cells. J Biol Chem *258*, 9220-9226.

Zhou, F., Xu, W., Hong, M., Pan, Z., Sinko, P.J., Ma, J., and You, G. (2005). The role of N-linked glycosylation in protein folding, membrane targeting, and substrate binding of human organic anion transporter hOAT4. Mol Pharmacol *67*, 868-876.

CHAPTER 3

FORWARD GENETIC SCREEN TO IDENTIFY HOST GENES REQUIRED FOR CDT INTOXICATION

3.1 BACKGROUND

Using genetics to elucidate the host processes that pathogens take advantage of yields an understanding of pathogenesis from the host's perspective. Most recent efforts to combat disease have focused on inhibiting bacterial or viral growth; however, these efforts have been met with emergence of antibiotic resistant and antiviral resistant pathogens. Further, in cases where bacterial toxins are the main factor for disease, antibiotics may have no effect late in disease progression because toxemia may progress even after bacteria have been cleared by antibiotics (Smith and Keppie, 1954). In these cases only an antitoxin or inhibition of a host process that supports intoxication can reverse the disease. Therefore, identifying the host factors and processes that support pathogenesis can yield targets for inhibitors that would benefit the host.

Forward genetics is a general term applied to the investigation of the genetic basis of an observed phenotype. Forward genetic methods predate the advent of modern molecular biology; naturally occurring or induced mutations were mapped by crossbreeding mutant organisms with interesting phenotypes with other individuals that carried distinct traits. This was done to determine the how frequently the two traits were co-inherited, thereby yielding a relative distance between the two genes based on the rate of meiotic recombination between the two loci. This field was greatly benefited by Hermann J. Muller's (1890-1976) discovery in 1927 that mutations could be induced by treating *Drosophilia* fruit flies with X-rays (Muller, 1927). Muller went on to investigate the genetic components that drive biological processes and his investigations provided a framework for future geneticists. Similar

to Muller, mutagenesis is still applied to whole organisms with some success. Most notable is the use of N-ethyl-N-nitrosourea (ENU) to mutagenize mice, an approach utilized by Bruce Beutler, who studies innate immune pathways and is credited with the discovery of Toll-like receptors by positional cloning (Poltorak et al., 1998).

Geneticists have also investigated the use of forward genetics in cultured mammalian cells because of their relative ease of manipulation and propagation. The methods that result in unbiased mutations provide the greatest advantages because they provide broad and diverse mutational coverage of the genome. However, due to the diploid nature of most mammalian cell lines, inducing mutations that result in genetic knockouts is difficult because mutation must occur simultaneously in both copies of the same gene. Inducing random mutations at a frequency high enough to result in two mutations in both copies of the same gene would result in mutations in many unintended loci.

The discovery of RNA interference (RNAi) to knockdown gene expression was initially lauded as a great advance; however, the use of RNAi in forward genetic screens has many caveats. First, off-target effects occur when the siRNA molecule has homology to unintended genes, causing knockdown in expression of secondary genes. siRNAs may cross react with unintended targets with as little as 11 matched bases, resulting in direct silencing of non-targeted genes (Jackson et al., 2003). Second, similar RNAi screens performed independently result in high degrees of variability (Bushman et al., 2009; Goff, 2008). Third, RNAi technology is inherently inefficient, thus prompting the community to call its use genetic “knockdown” rather than “knockout”. Even commercial entities rarely advertise greater than 90%

reduction of endogenous transcript levels. For some phenotypes, the efficiency of RNAi may be sufficient; however, easy identification of other phenotypes may require near complete knockdown.

The use of genetically haploid cells provides the advantage of easy genetic manipulation to produce knockdowns. One common somatic cell genetic tool is the use of yeast during the haploid phase of the life cycle. Although yeast are eukaryotic organisms that are good models to study somatic mutations, the use of mammalian cells would be preferable if the intent is to make a discovery about the mammalian host-pathogen relationship. A good mammalian alternative to yeast is the use of CHO cells, as they are partially hemizygous. However, the fraction of the genome that is haploid is undefined and moreover, different CHO cell lines may contain various degrees of hemizygosity and may be haploid in different parts of the genome. The discovery of a genetically heterogeneous human leukemia cell line (KBM-7) has sparked some recent advances in forward genetics (Kotecki et al., 1999). An isolated subclone of this cell line retains genomic stability for at least 8 months in culture. These cells are haploid for the entire genome, except for chromosome 8.

Murine leukemia virus (MLV) can be used to mutagenize mammalian cells by integrating into the genome and causing insertional mutations; however, such an approach has one major limitation. This approach is unable to identify essential genes that are required for intoxication because mutagenesis of such genes would result in death. A method that could conditionally shut down gene expression temporarily would provide the advantage of being able to identify genes that the cell

could survive without for short periods of time. Indeed, such a system exists. The SILENCE system causes tetracycline dependent genetic silencing by inducing heterochromatin formation at genetic sites near proviral integrations (Banks and Bradley, 2007). Using this method, cells can be cultured in the absence of tetracycline for short periods of time, phenotypically selected and then tetracycline can be added back to cells to resume expression of the essential gene.

3.2 RESULTS

Chemical mutagenesis was performed to obtain CDT resistant mutants. CHO pgsA-745 (A745) cells were utilized as the parental cell line for two reasons. First, CHO cells are partially hemizygous; they are monoploid for a portion of the genome, facilitating knockout mutations with a single genetic lesion. Second, A745 cells were previously mutagenized and selected to be proteoglycan deficient (Esko et al., 1985), resulting in high sensitivity to CDT intoxication (Eshraghi et al., 2010) and facilitating selection with minimal toxin concentration.

To induce mutations, ten pools of A745 cells were treated with the frameshift mutagen ICR191 at a concentration high enough to induce 90% death (Bradley et al., 2001). These pools were mutagenized twice further to obtain ten pools mutagenized once, twice or three times, totaling thirty pools (Figure 3.1). The pools mutagenized once and twice were seeded at 1 x 10^6 cells per 10-centimeter plate.

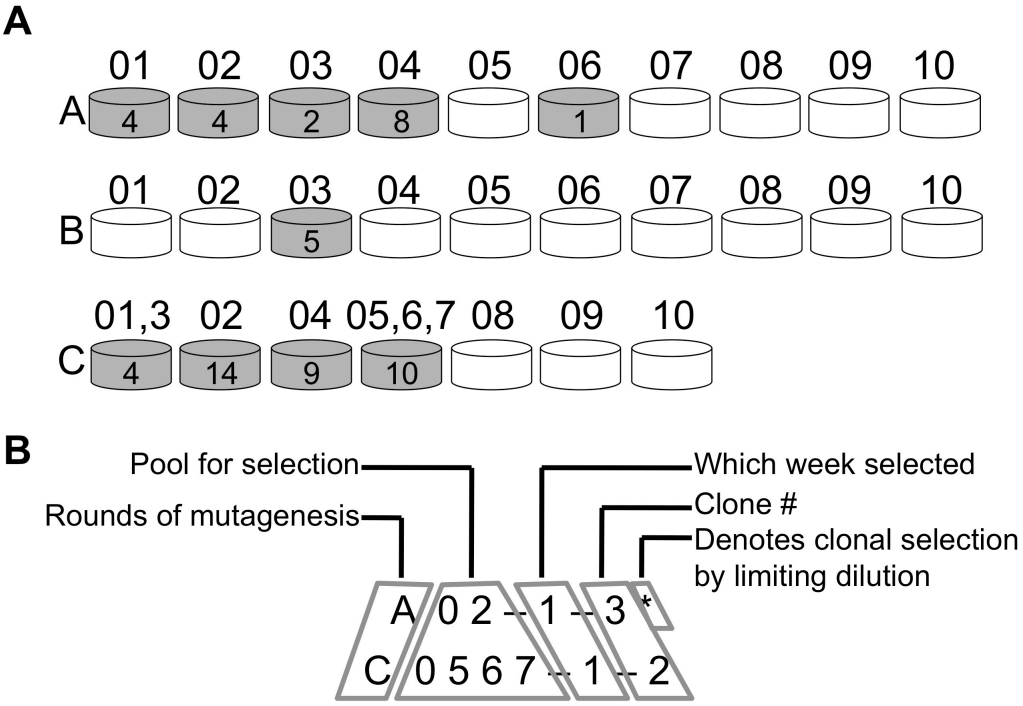

Figure 3.1 Selection of Aa-CDT resistant clones and nomenclature.
(A) Aa-CDT resistant clone selection scheme. Letters denote rounds of mutagenesis (A=1, B=2 and C=3 rounds). Numbers above cylinders indicate mutagenized pools. Grey cylinders represent pools that yielded resistant clones and numbers within grey cylinders indicate number of resistant clones isolated per pool. (B) Nomenclature of Aa-CDT resistant clones. Two examples of clone names are presented. The first letter and subsequent number indicate number of mutagenesis rounds and pool selected from. The number between the dashes represents the week the clone was selected. The last number is the clone number. The presence of an asterisk denotes that clonal selection was performed by limiting dilution, not by picking from a colony.

In the 10 pools mutagenized three times, there were very few cells in pools #1, 3, 5, 6 and 7, so pools 1, 3 and 5, 6, 7 were combined for a total of 7 pools. In total, 10, 10 and 7 pools mutagenized once, twice or three times, respectively, were selected with 20nM Aa-CDT, a concentration high enough to cause death in parental A745 cells. After growth for 10-14 days, colonies were picked or limiting dilutions were performed to obtain single cell clones of Aa-CDT resistant. These clones were grown to approximately 20% confluence in 6 well plates and reselected with Aa-CDT; all clones survived reselection. In total, 61 Aa-CDT resistant clones were selected, expanded and frozen down for further analysis (Table 3.1).

In order to begin characterization of the chemically mutagenized Aa-CDT resistant clones, their sensitivity to Aa-CDT was assessed. The resistant clones were thawed in groups of six to nine, seeded into 96 well plates at 2 x 10^4/well and intoxicated with a titration of Aa-CDT along with A745 cells as a control. Forty-eight hours after intoxication, the cells were stained with cell permeable Hoechst and fluorescent cells were counted automatically by using laser scanning cytometry. The forty-eight hour intoxication allowed for cell cycle arrest in intoxicated cells without significant death in sensitive cells at the highest concentrations, allowing the measurement of intoxication by assaying for blocked proliferation. Compared to controls, resistance among the 61 clones ranged from 13 to 170-fold. (Figure 3.2.1 – 3.2.8)

Table 3.1 List of chemically mutagenized Aa-CDT resistant mutants.

Clone name(s)	#	Clone name(s)	#
A01-1-1	39	C02-1-3*	31
A01-1-2	40	C02-1-4*	36
A01-1-3*	48	C02-2-1	7
A01-1-4*	55	C02-2-2*	26
A02-1-1	41	C02-2-3*	35
A02-1-2	42	C02-3-1*	30
A02-1-3*	59	C02-4-1	13
A02-1-4*; CHO-CDT^{R}A2	61	C02-4-2	17
A03-1-1	49	C02-4-3	28
A03-1-2	50	C02-4-4*	32
A04-1-1	43	C02-5-1*	29
A04-1-2	44	C02-5-2*	33
A04-1-3	45	C04-1-1	9
A04-1-4	46	C04-1-2	12
A04-1-5	51	C04-1-3*	23
A04-1-6	56	C04-2-1	20
A04-1-7*	57	C04-2-2*	21
A04-1-8*	60	C04-3-1	11
A06-1-1*	58	C04-3-2	18
B03-1-1	38	C04-4-1	10
B03-1-2*	47	C04-5-1	16
B03-1-3*	52	C0567-1-1	3
B03-1-4*	53	C0567-1-2	4
B03-1-5*	54	C0567-1-3	5
C013-1-1	15	C0567-1-4	6
C013-1-2*	34	C0567-1-5*	22
C013-1-3*	37	C0567-2-1	1
C013-2-1	27	C0567-2-2	2
C02-1-1	19	C0567-2-3	8
C02-1-2	24	C0567-2-4	14
		C0567-2-5*	25

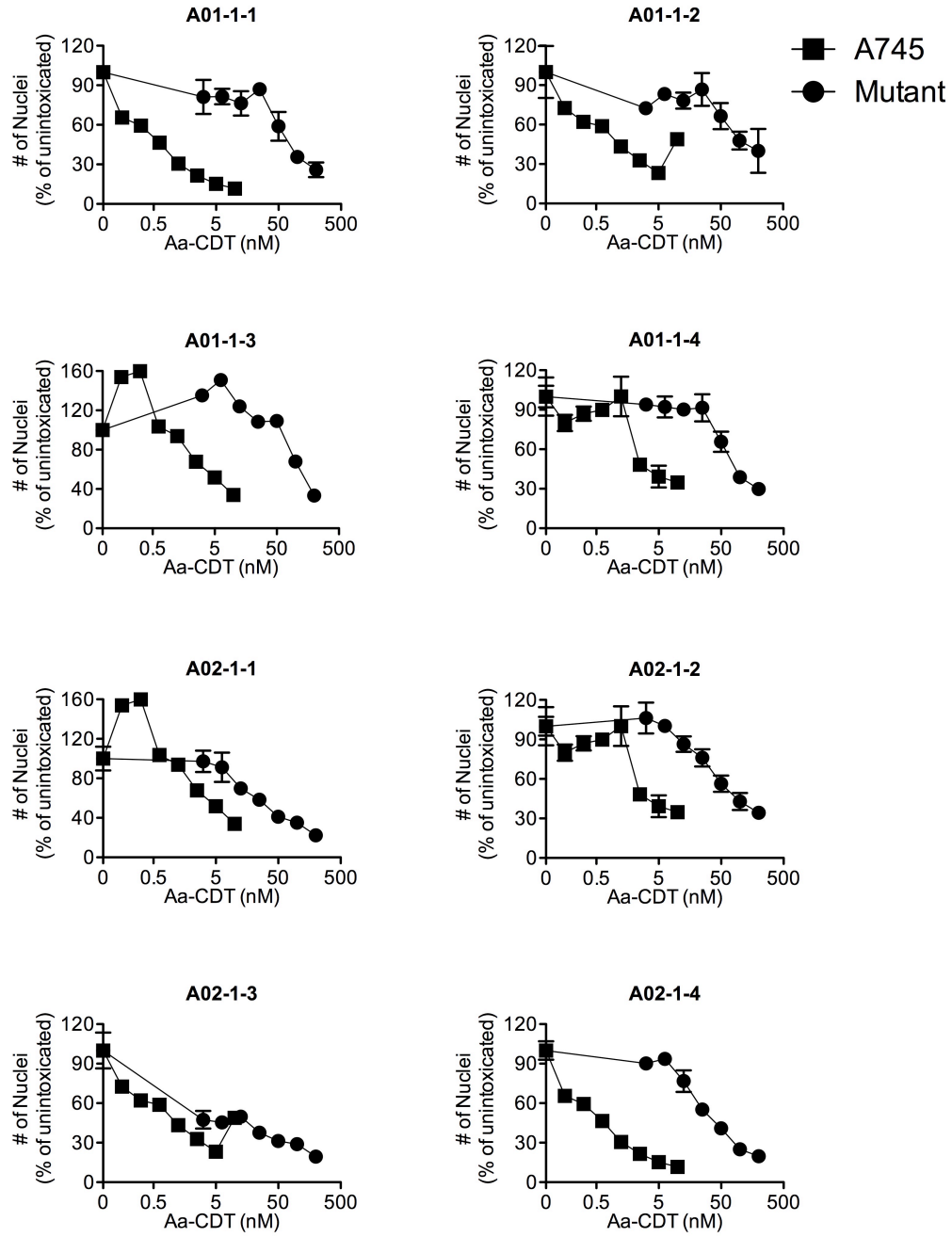

Figure 3.2.1 Aa-CDT intoxication of chemically mutagenized clones.
A745 and chemically mutagenized clones were intoxicated with a titration of Aa-CDT for 48 hours, stained with Hoechst and nuclei were counted by laser scanning cytometry. The number of nuclei was normalized to unintoxicated control.

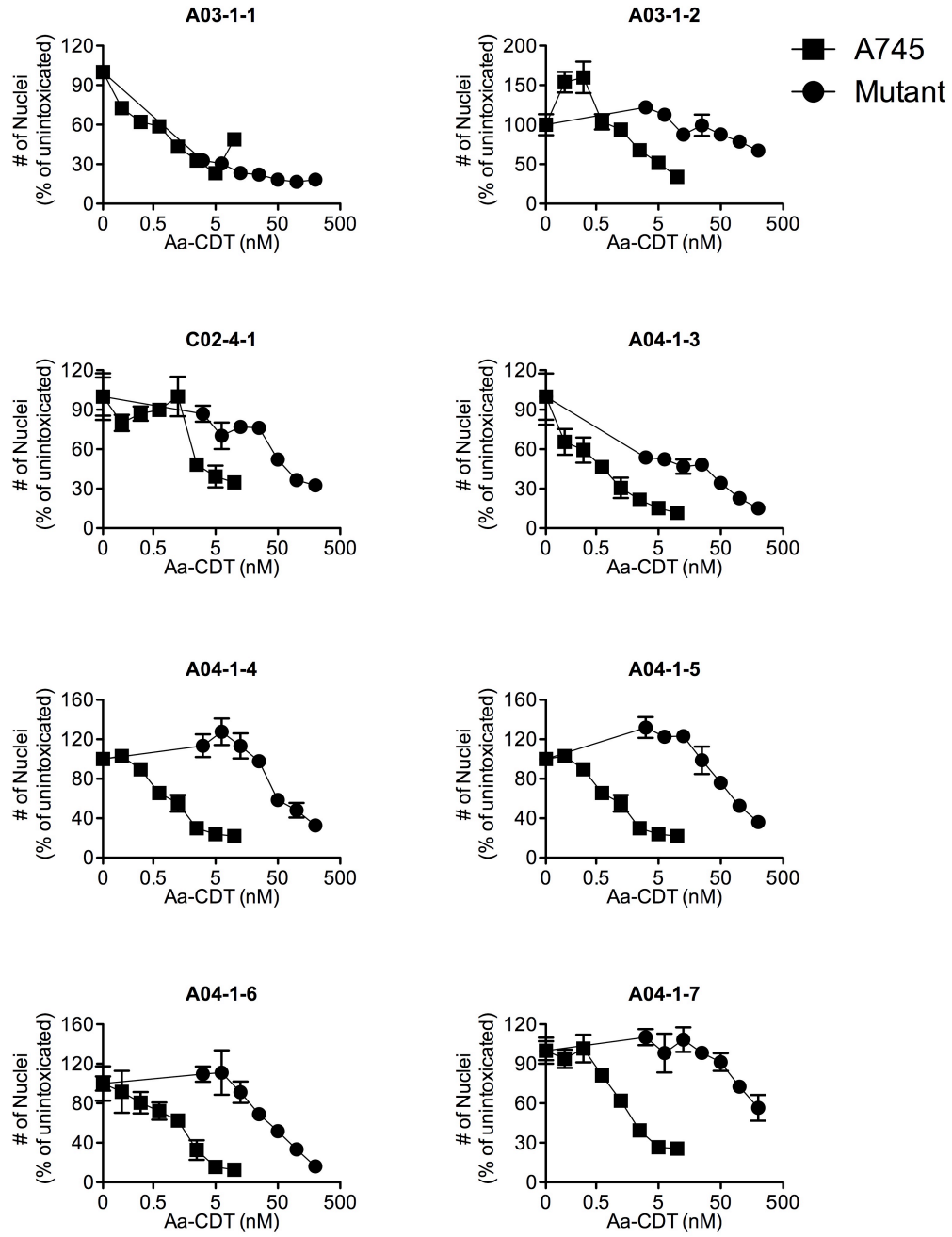

Figure 3.2.2 Aa-CDT intoxication of chemically mutagenized clones.
A745 and chemically mutagenized clones were intoxicated with a titration of Aa-CDT for 48 hours, stained with Hoechst and nuclei were counted by laser scanning cytometry. The number of nuclei was normalized to unintoxicated control.

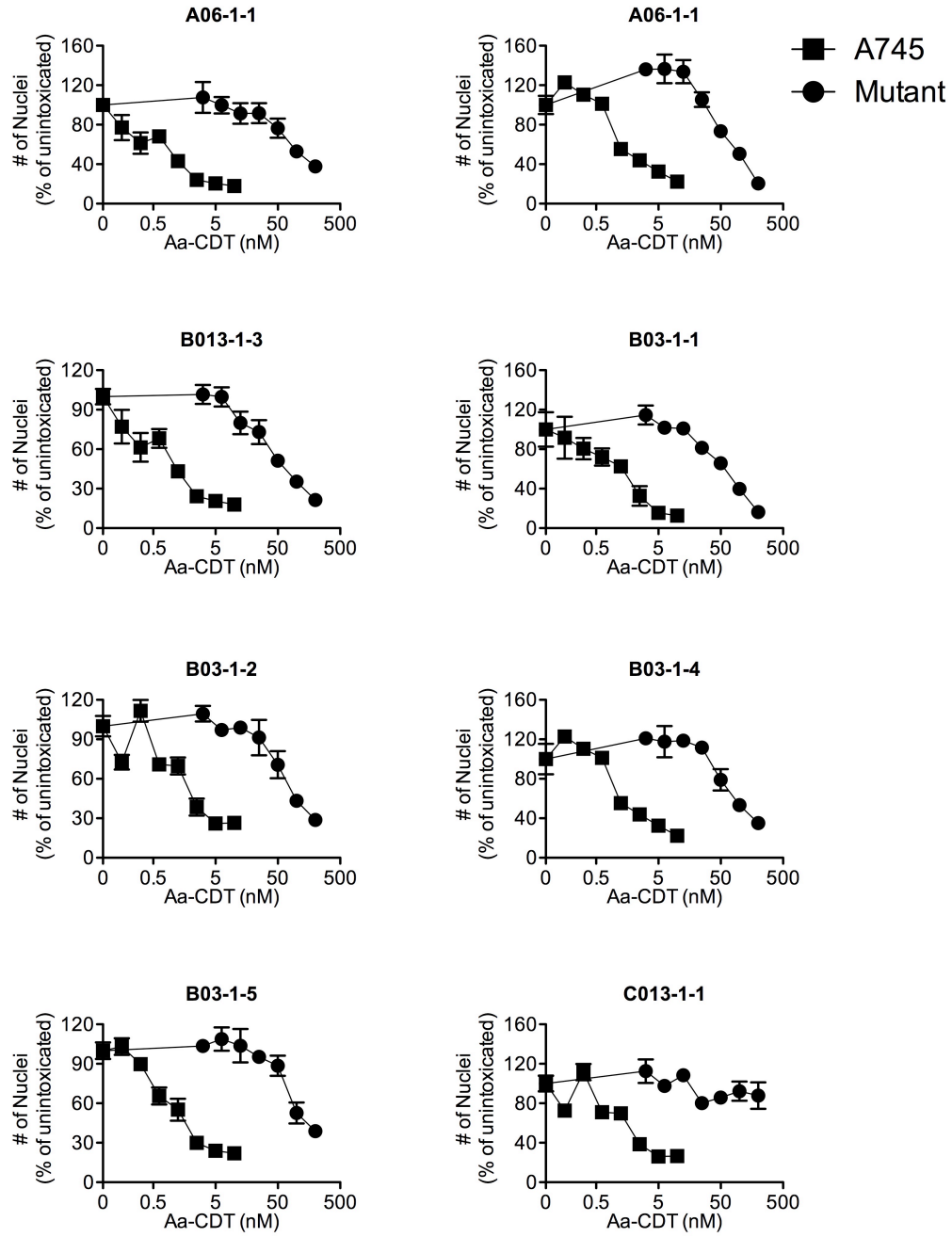

Figure 3.2.3 Aa-CDT intoxication of chemically mutagenized clones.
A745 and chemically mutagenized clones were intoxicated with a titration of Aa-CDT for 48 hours, stained with Hoechst and nuclei were counted by laser scanning cytometry. The number of nuclei was normalized to unintoxicated control.

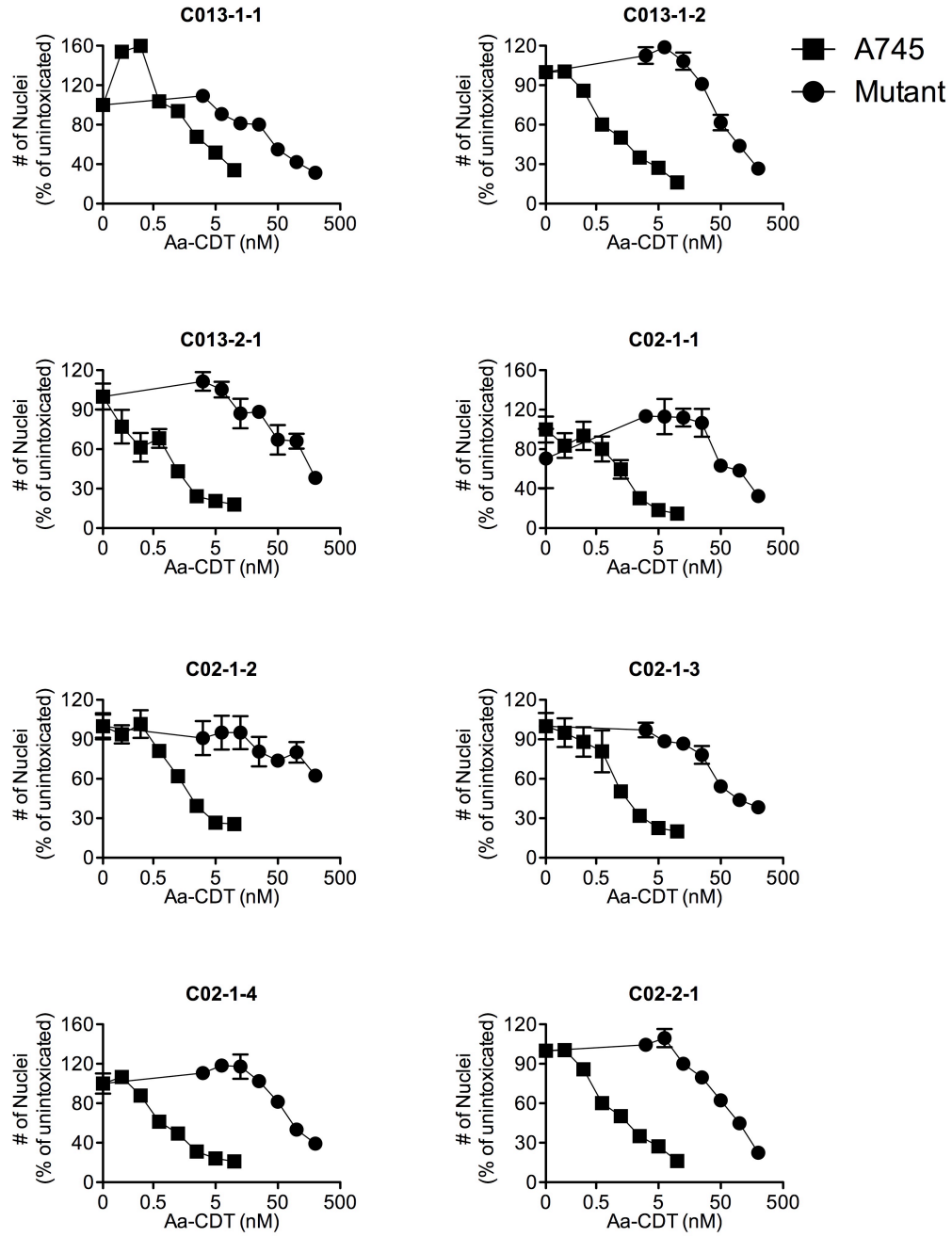

Figure 3.2.4 Aa-CDT intoxication of chemically mutagenized clones.
A745 and chemically mutagenized clones were intoxicated with a titration of Aa-CDT for 48 hours, stained with Hoechst and nuclei were counted by laser scanning cytometry. The number of nuclei was normalized to unintoxicated control.

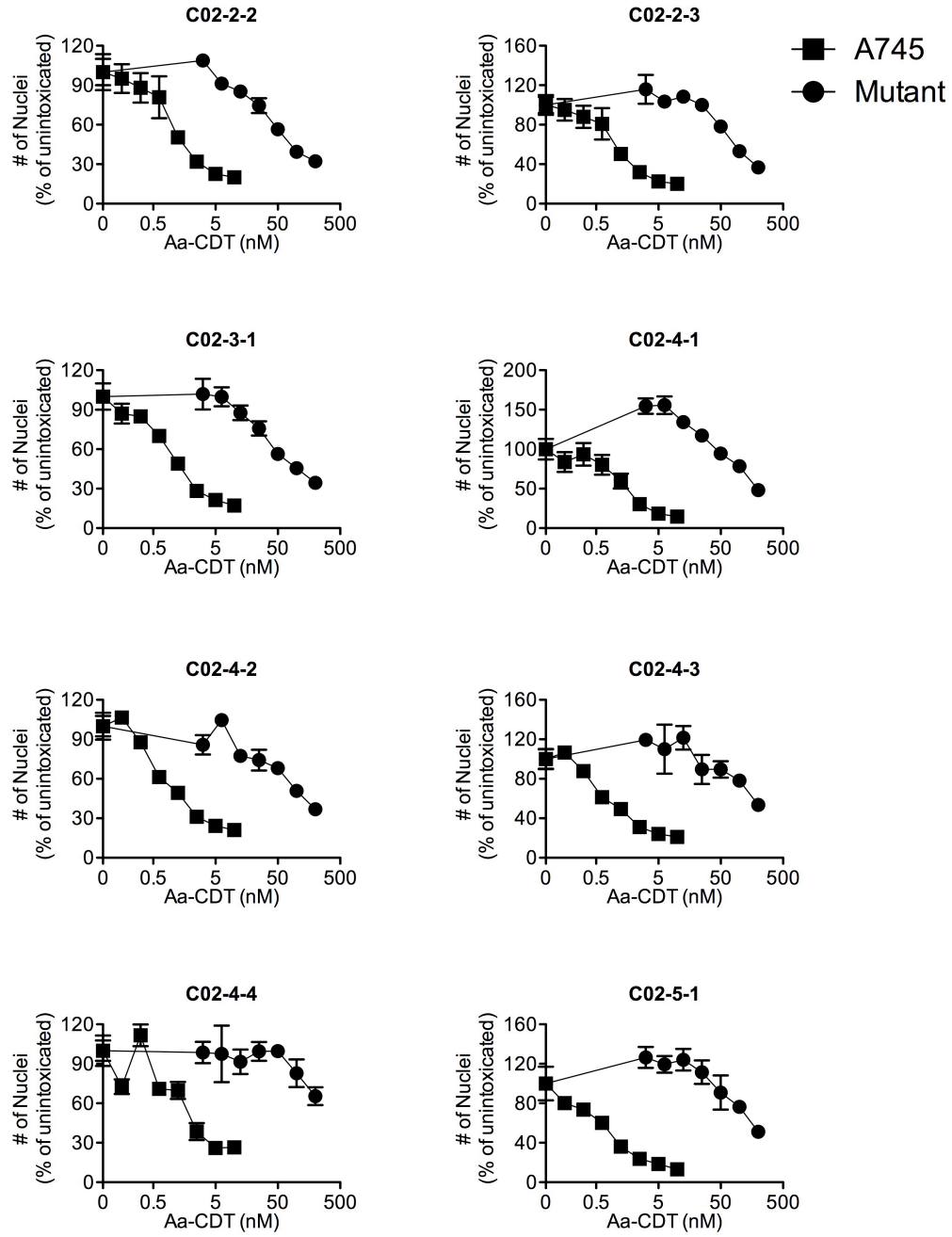

Figure 3.2.5 Aa-CDT intoxication of chemically mutagenized clones.
A745 and chemically mutagenized clones were intoxicated with a titration of Aa-CDT for 48 hours, stained with Hoechst and nuclei were counted by laser scanning cytometry. The number of nuclei was normalized to unintoxicated control.

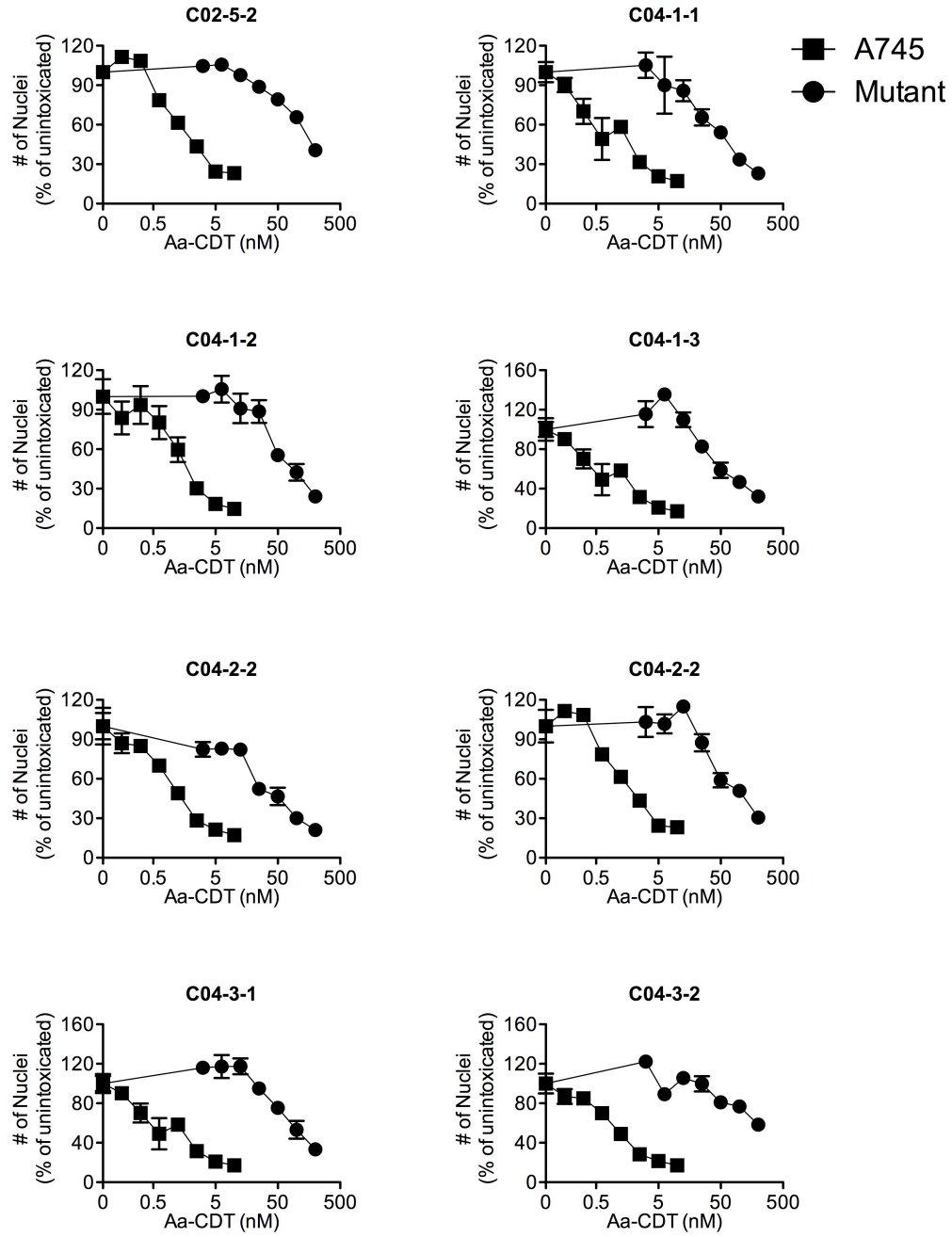

Figure 3.2.6 Aa-CDT intoxication of chemically mutagenized clones.
A745 and chemically mutagenized clones were intoxicated with a titration of Aa-CDT for 48 hours, stained with Hoechst and nuclei were counted by laser scanning cytometry. The number of nuclei was normalized to unintoxicated control.

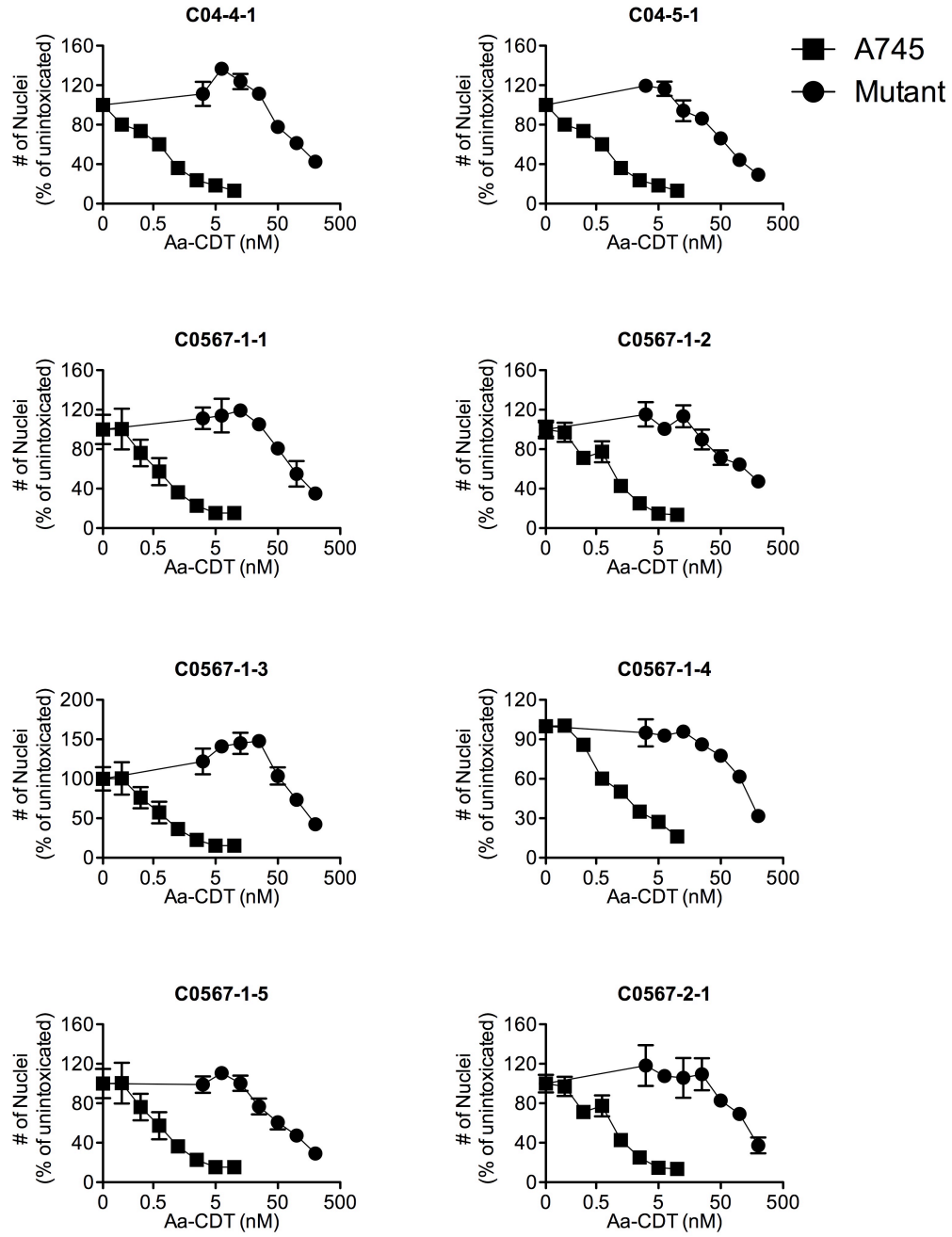

Figure 3.2.7 Aa-CDT intoxication of chemically mutagenized clones.
A745 and chemically mutagenized clones were intoxicated with a titration of Aa-CDT for 48 hours, stained with Hoechst and nuclei were counted by laser scanning cytometry. The number of nuclei was normalized to unintoxicated control.

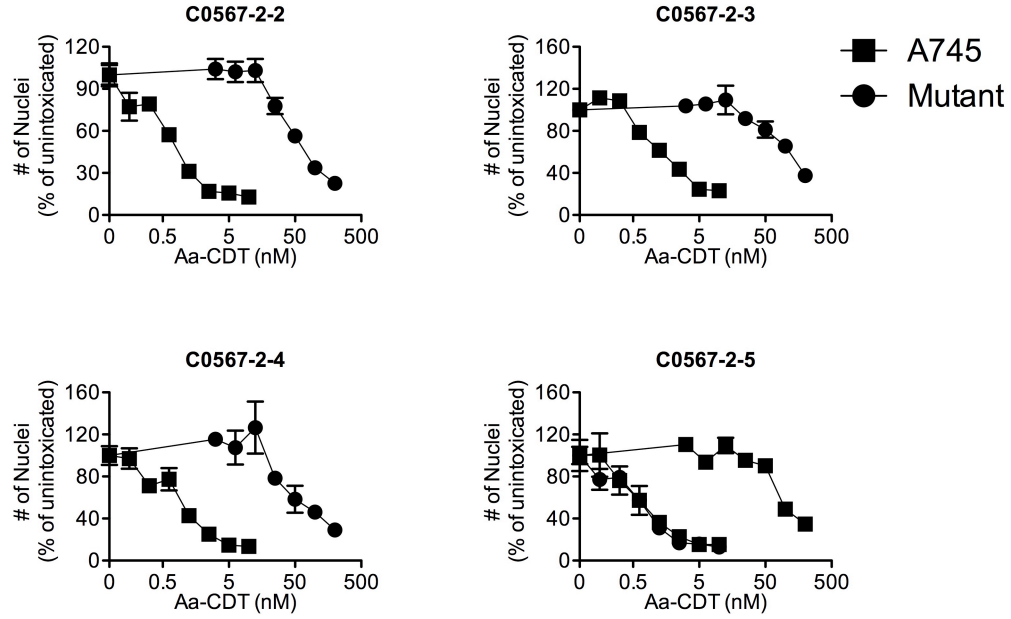

Figure 3.2.8 Aa-CDT intoxication of chemically mutagenized clones.
A745 and chemically mutagenized clones were intoxicated with a titration of Aa-CDT for 48 hours, stained with Hoechst and nuclei were counted by laser scanning cytometry. The number of nuclei was normalized to unintoxicated control.

The identification of a cell surface receptor would be a major advance in the understanding of the mechanism for CDT intoxication. Therefore, the resistant clones were assayed for ability to bind biotinylated Aa-CDT in order to find a resistant clone that lacked receptor. Biotinylation had no effect on Aa-CDT as shown by equivalent intoxication caused by biotinylated and non-biotinylated Aa-CDT. The binding constant (K_d) was measured to be 370nM on A745 cells (Figure 3.3); therefore, the binding assays were performed at 300 – 450nM in order to provide maximum change in signal with small changes in binding. None of the 61 clones had a considerable loss of binding for Aa-CDT; therefore, none were thought to be mutants for receptor (Figure 3.4).

In the preliminary stages of screening, the C02-2-2* clonal cell line was characterized further. These cells displayed altered morphology; approximately one third of the cells displayed a rounded morphology (Figure 3.5). After intoxication with Aa-CDT for 48 hours, A745 cells display a marked distention; however, C02-2-2* cells were unaffected (Figure 3.5). Interestingly, C02-2-2* cells were resistant to Aa-CDT, Hd-CDT and Ec-CDT; however, they were equally sensitive or slightly more sensitive to Cj-CDT (Figure 3.6). This supports the conclusion outlined in Chapter 2 that host factors that support sensitivity to Cj-CDT are different from those that might support the others. Since glycosylation was thought to play a role in CDT binding, the ability of C02-2-2* cell to bind fluorescently labeled plant lectins was assayed. Interestingly, C02-2-2* cells displayed greater binding to all lectins tested (Figure 3.7), suggesting that increased glycosylation may play a role in the CDT resistance of this clone.

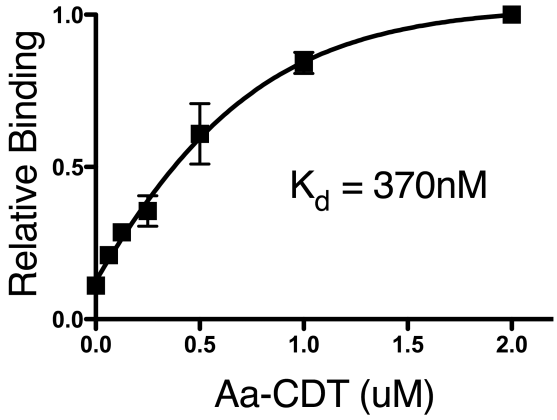

Figure 3.3 Measurement of the binding constant of biotinylated Aa-CDT. The binding constant for biotinylated Aa-CDT was measured using a cell based ELISA approach (cELISA) (Bag et al., 1993). A745 cells were seeded (1 x 10^3/well) in 384 well plates and allowed to adhere overnight. They were bound with biotinylated Aa-CDT for 45 minutes on ice, washed thoroughly, fixed, bound with streptavidin HRP, and washed thoroughly again. Detection of binding was performed through a chromogenic substrate, tetramethylbenzidine.

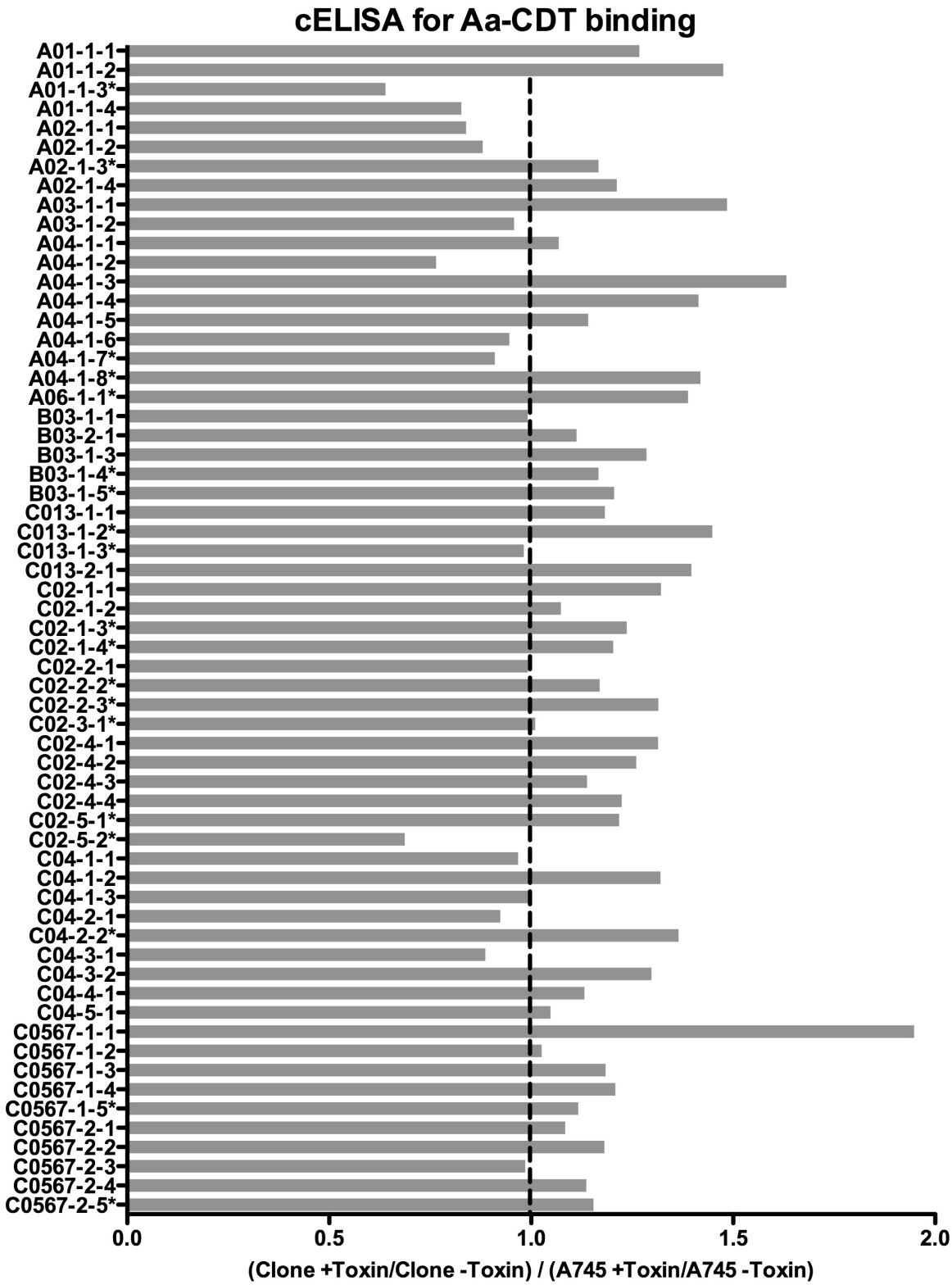
cELISA for Aa-CDT binding
A01-1-1
A01-1-2
A01-1-3*
A01-1-4
A02-1-1
A02-1-2
A02-1-3*
A02-1-4
A03-1-1
A03-1-2
A04-1-1
A04-1-2
A04-1-3
A04-1-4
A04-1-5
A04-1-6
A04-1-7*
A04-1-8*
A06-1-1*
B03-1-1
B03-2-1
B03-1-3
B03-1-4*
B03-1-5*
C013-1-1
C013-1-2*
C013-1-3*
C013-2-1
C02-1-1
C02-1-2
C02-1-3*
C02-1-4*
C02-2-1
C02-2-2*
C02-2-3*
C02-3-1*
C02-4-1
C02-4-2
C02-4-3
C02-4-4
C02-5-1*
C02-5-2*
C04-1-1
C04-1-2
C04-1-3
C04-2-1
C04-2-2*
C04-3-1
C04-3-2
C04-4-1
C04-5-1
C0567-1-1
C0567-1-2
C0567-1-3
C0567-1-4
C0567-1-5*
C0567-2-1
C0567-2-2
C0567-2-3
C0567-2-4
C0567-2-5*
0.0
0.5
1.0
1.5
2.0
(Clone +Toxin/Clone -Toxin) / (A745 +Toxin/A745 -Toxin)

Figure 3.4 Binding of biotinylated Aa-CDT to chemically mutagenized clones.
Parental A745 cells or chemically mutagenized Aa-CDT resistant clones were seeded (1 x 10^3/well) in 384-well plates and allowed to adhere overnight. They were bound with biotinylated Aa-CDT for 45 minutes on ice, washed thoroughly, fixed, bound with streptavidin HRP, and washed thoroughly again. Detection of binding was performed through a chromogenic substrate, tetramethylbenzidine. Average signal from wells with biotinylated Aa-CDT was normalized to the average signal from wells without toxin. This was further normalized to the same normalized value obtained from parental A745 cells. The vertical line represents normalized A745/normalized A745.

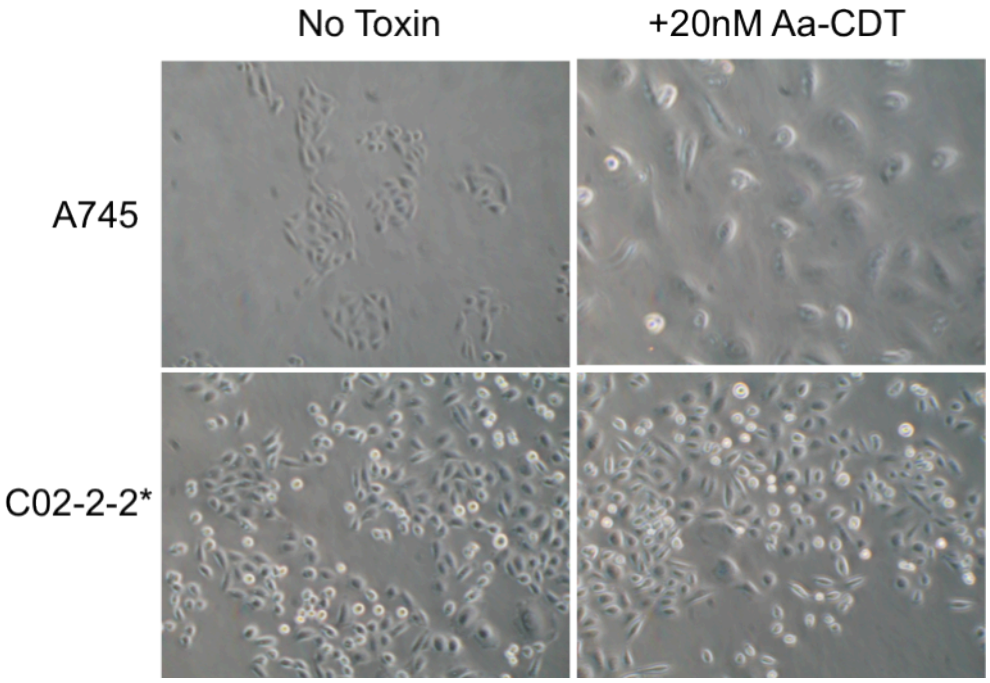

Figure 3.5 Aa-CDT intoxication of C02-2-2*.
A745 and C02-2-2* cells were seeded in 6 well plates (2.5 x 10^5/well) allowed to adhere overnight and intoxicated with 20nM Aa-CDT for 48 hours. Phase contrast microscopy was performed to obtain the images.

A

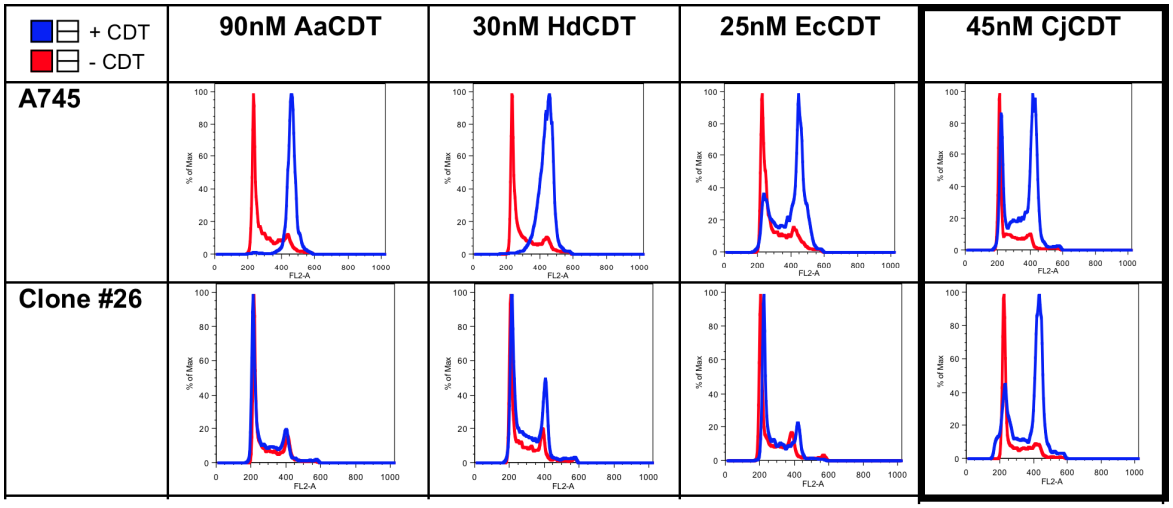

B

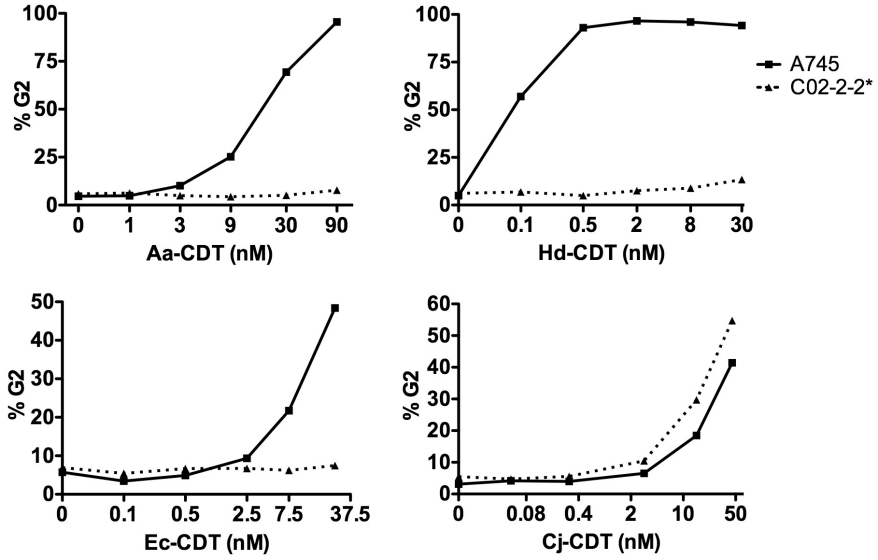

Figure 3.6 Intoxication of C02-2-2* (Clone #26) with multiple CDTs.
(A) A745 and C02-2-2* cells were seeded in 6 well plates (2.5 x 10^5/well) allowed to adhere overnight and intoxicated with 90nM Aa-CDT, 30nM Hd-CDT, 25nM Ec-CDT and 45nM Cj-CDT for 48 hours. After intoxication, the cells were removed, fixed, permeabelized and stained with propidium iodide to stain DNA. Flow cytometric analysis was performed on 1 x 10^4 cells to obtain cell cycle profiles. (B) Experiment performed as in (A), but with a titration of CDT.

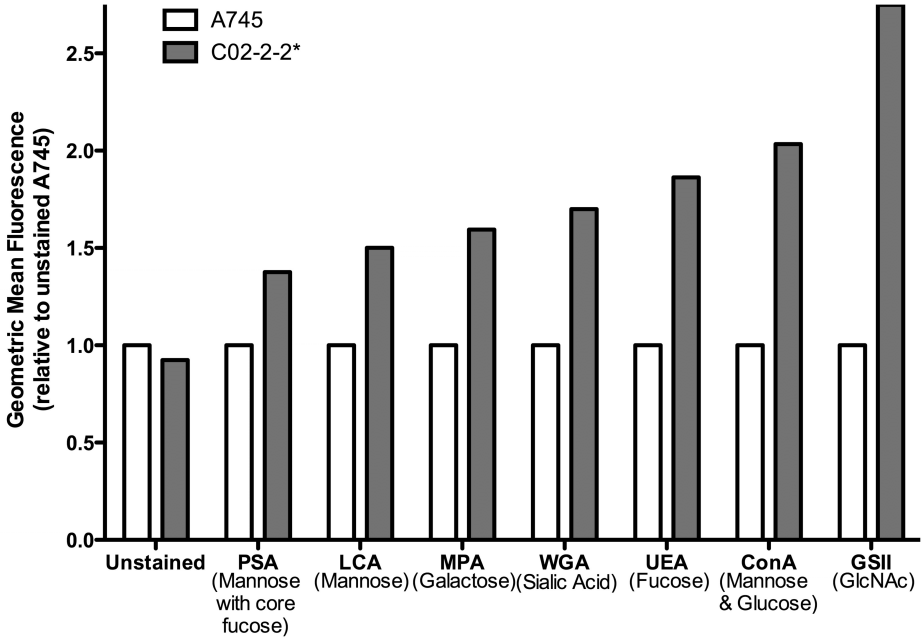

Figure 3.7 Fluorescent lectin binding to C02-2-2* cells.
A745 and C02-2-2* cells were detached from 10 centimeter tissue culture plates with PBS+1mM EDTA, washed with media and bound to fluorescent lectins for one hour. After thorough washing, cells were fixed and 1 x 10^4 cells were analyzed by flow cytometry to obtain geometric mean fluorescence.

Further, we had previously shown that decreased cell surface sialic acid, as judged by decreased binding by fluorescently labeled wheat germ agglutinin (WGA), was correlated with increased sensitivity to CDT (Chapter 2). Consistent with that finding, C02-2-2* cells display increased cell surface sialic acid and resistance to CDT. Moving forward, a strategy was formed to aid in choosing which of the 61 clones to further characterize.

A number of factors were considered in order to select which mutants to further characterize. First, the list of clones was limited to those subjected to mutagenesis only once to limit the number of genetic lesions the clones might have. Second, the most Aa-CDT resistant clone was selected from each of the five mutagenized pools that yielded resistant clones. Third, these five clones were intoxicated with multiple CDTs to determine their resistance phenotypes. Two distinct phenotypes were present. Four of these clones, A01-1-3, A02-1-4, A04-1-1 and A06-1-1, were resistant to Aa-CDT, Hd-CDT and Ec-CDT, but relatively sensitive to Cj-CDT, similar to C02-2-2* (Figure 3.8). In contrast, A03-1-2 cells were relatively sensitive to Aa-CDT, Hd-CDT and Ec-CDT and resistant to Cj-CDT. The concentration of Aa-CDT used in this assay was higher than that used to select the cells, which explains the sensitivity to intoxication displayed in these cells in this assay. The response to DNA damage induced by ultraviolet (UV) radiation was judged by an immunofluorescence assay for phosphorylated histone H2AX. All five of the clones possessed the ability to phosphorylate histones in response to UV, suggesting that the CDT resistance of these cells did not result from deficiencies in DNA damage response (Figure 3.9).

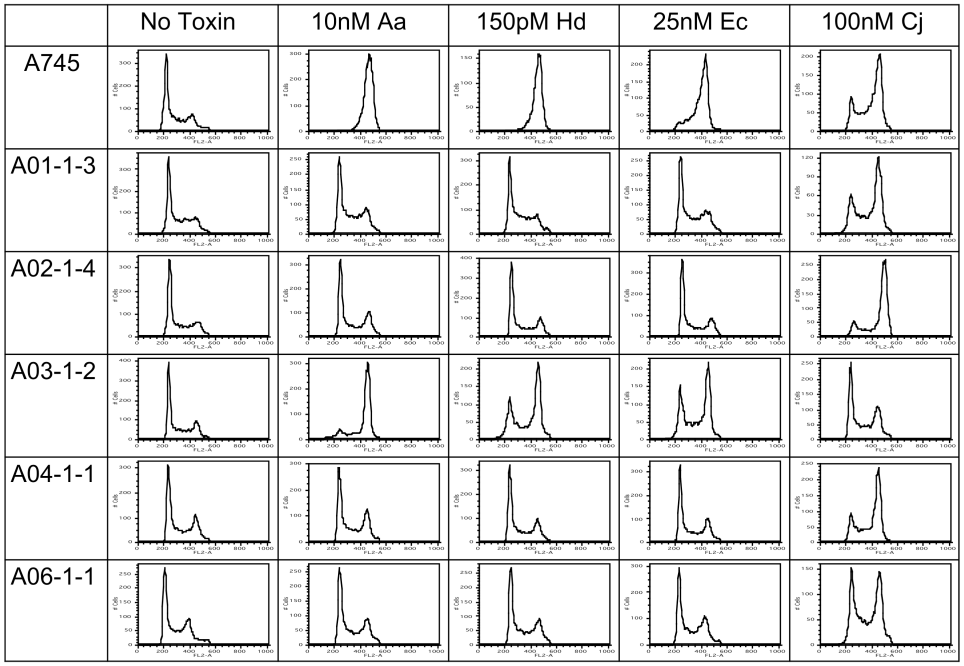

Figure 3.8 CDT intoxication of chemically mutagenized clones.
Partental A745 and chemically mutagenized clones were seeded in 6 well plates (2 x 10^5/well) allowed to adhere overnight and intoxicated with 10nM Aa-CDT, 150pM Hd-CDT, 25nM Ec-CDT and 45nM Cj-CDT for 48 hours. After intoxication, the cells were removed, fixed, permeabelized and stained with propidium iodide to stain DNA. Flow cytometric analysis was performed on 1 x 10^4 cells to obtain cell cycle profiles.

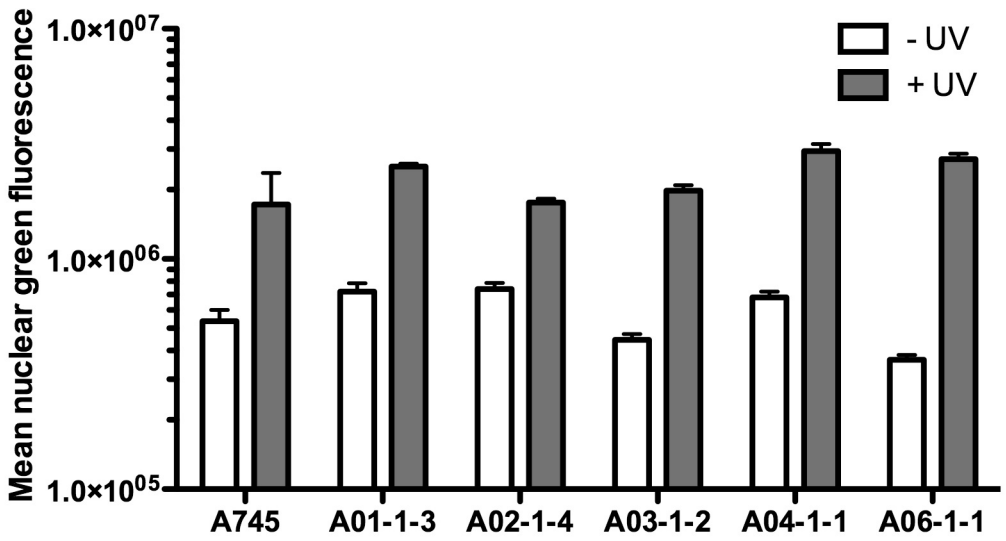

Figure 3.9 UV mediated H2AX phosphorylation in chemically resistant clones.
A745 and chemically mutagenized CDT resistant clones were exposed to UV for five minutes and incubated for 4 hours, followed by an immunofluorescence assay for phosphorylated H2AX and laser scanning cytometry to quantify nuclear fluorescence.

H2AX phosphorylation in response to a titration of Aa-CDT was also assessed. Interestingly, A03-1-2 cells displayed H2AX phosphorylation in response to Aa-CDT, while the others did not (Figure 3.10). This suggests that the deficiency in A03-1-2 cells is downstream of CDT trafficking to the nucleus and induction of DNA damage response, and the other mutants represent mutations upstream of trafficking to the nucleus. Since the identification of genes that regulate CDT trafficking would provide the greatest impact for the CDT field, the most resistant of these four clones, A02-1-4, was selected for further characterization.

In order to identify the genetic deficiency in A02-1-4 cells by complementation, a diminishing cDNA pool approach was utilized. This approach took advantage of a commercially prepared human cDNA library generated from HeLa cells, which are highly sensitive to Aa-CDT. The HeLa cell library, pLib (Clontech), is packaged in a retroviral vector for efficient transduction, and was previously used to identify the anthrax toxin receptor ANTXR1/TEM8 (Bradley et al., 2001). The pLib library was utilized in a diminishing pool approach as described for successful cloning of TNF/NGF as a receptor for herpes virus simplex virus-1 (Montgomery et al., 1996). The cDNA library (complexity of 10^7 individual cDNAs) was sub-divided into 50 individual pools in order to reduce complexity by 50-fold. Plasmid DNA was mini-prepped separately from each of the 50 pools and joined into ten separate pools (complexity of 2×10^6 per joined pool) and retroviral particles were generated. The particles transduced into 2×10^5 A02-1-4 cells at a multiplicity of infection of 10 and incubated for 48 hours to allow expression.

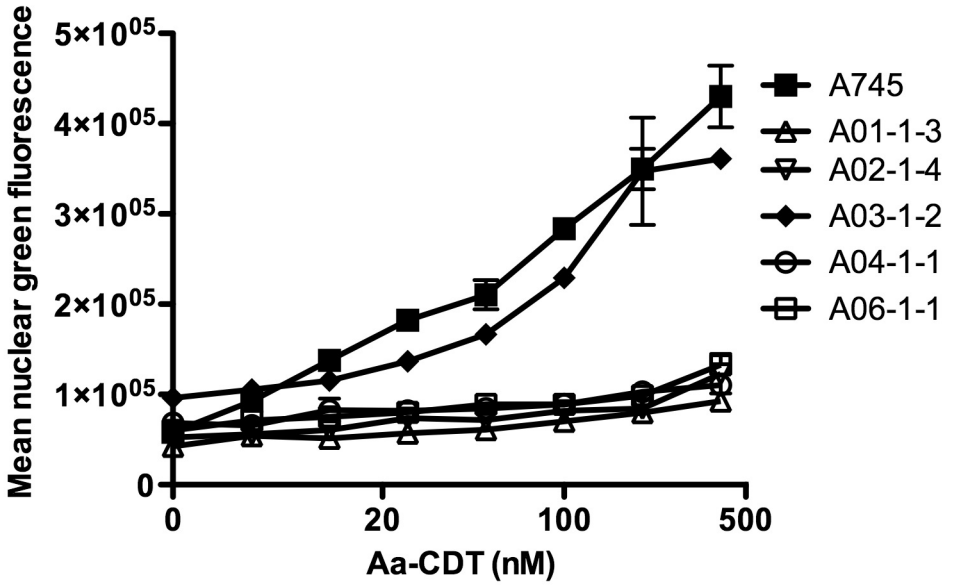

Figure 3.10 Aa-CDT mediated H2AX phosphorylation in chemically mutagenized resistant clones.
A745 and chemically mutagenized CDT resistant clones were intoxicated with Aa-CDT for 4 hours, followed by an immunofluorescence assay for phosphorylated H2AX and laser scanning cytometry to quantify nuclear fluorescence.

Following transduction, the cells were intoxicated, immunostained for phosphorylated H2AX and analyzed by laser scanning cytometry. Unfortunately, complemented cells were not detected (data not shown).

Since the diminishing cDNA pool approach was unsuccessful, a second strategy using an arrayed cDNA library was utilized to identify genes that are able to complement A02-1-4 resistance. The mammalian gene collection (MGC) is an arrayed cDNA library consisting of approximately 3 x 10^4 expression plasmids, curated as E. coli glycerol stocks containing unique cDNAs individually arrayed in a 96-well plates. The UCLA Molecular Screening Shared Resource performed informatic analysis on the MGC library cDNA sequences to identify cDNAs that are not expressable due to incomplete ORFs or containing sequences that didn't produce full-length alignments to sequences in the RefSeq database. Subsequently, the entire library was more stringently curated by re-arraying to contain only full-length, expression ready cDNAs. DNA was isolated from the more stringently curated library using high throughput minipreps and this DNA was quantified, normalized and spotted into 384-well plates. This DNA was transfected into A02-1-4 cells in duplicate and the cells were intoxicated with Aa-CDT. After intoxication, the cells were immunostained for phosphorylated H2AX and automated microscopy was performed to identify complementing cDNAs After screening approximately 3.7 x 10^3 cDNAs, nineteen "hits" were identified to increase phosphorylation of H2AX in one of the two duplicates (Table 3.2).

Table 3.2 "hits" from arrayed cDNA screen to find cDNAs complementing sensitivity to A02-1-4 cells.

#	Accession	Gene synonym	Description	Source plate	Source well	Replicate
1	BC000917	LOC100130526, MYC	similar to ORF 114| Similar to ORF 114	1	G8	A
2	BC008191	CYTH3, PSCD3	Cytohesin 3| pleckstrin homology, Sec7 and coiled-coil domains 3	1	F19	B
3	BC011373	KRT8	Keratin 8	1	G17	B
4	BC010839	RPN1	ribophorin I, (cDNA clone MGC:5072)	2	G9	B
5	BC010330	1810043G02Rik	RIKEN cDNA 1810043G02 gene, (cDNA clone MGC:6530)	2	L23	B
6	BC003494	Pofut2	Protein O-fucosyltransferase 2	2	P21	B
7	BC005493	1110005A03Rik, LOC100043293, Sfrs2	RIKEN cDNA 1110005A03 gene, splicing factor, arginine/serine-rich 2 (SC-35), (cDNA clone MGC:7377)	3	C21	A
8	BC002082	Fabp3	Fatty acid binding protein 3, muscle and heart, (cDNA clone MGC:6249)	3	H13	B
9	BC008116	Gmppa	GDP-mannose pyrophosphorylase A, (cDNA clone MGC:7719)	4	I6	B
10	BC003736	Trappc3	trafficking protein particle complex 3, (cDNA clone MGC:5818)	4	O17	B
11	BC008511	Eif3s4	eukaryotic translation initiation factor 3, subunit 4 (delta), (cDNA clone MGC:5726)	5	N15	B
12	BC011048	EWSR1	Ewing sarcoma breakpoint region 1, transcript variant EWS, (cDNA clone MGC:16900)	6	H15	B
13	BC012860	GEFT	RhoA/RAC/CDC42 exchange factor, transcript variant 2, (cDNA clone MGC:18298)	6	I10	B
14	BC015801	PROS1	protein S (alpha), (cDNA clone MGC:9207)	7	F10	B
15	BC005622	Exosc9	exosome component 9, (cDNA clone MGC:11686)	8	H12	A
16	BC015904	MRPL10	mitochondrial ribosomal protein L10, transcript variant 1, (cDNA clone MGC:17973)	8	C7	B
17	BC005682	Derl2	Der1-like domain family, member 2, (cDNA clone MGC:11613)	8	D19	B
18	BC009121	Amy1	amylase 1, salivary, (cDNA clone MGC:11568)	9	C22	B
19	BC010540	C11orf2, C11orf3	chromosome 11 open reading frame2, (cDNA clone MGC:17523)	10	A22	B

The plasmids encoding these cDNAs were purified from the glycerol stock library and used to transfect A02-1-4 cells with either 25 or 55ng of DNA, then intoxicated with 20nM Aa-CDT and immunostained for phosphorylation of H2AX. In the cells transfected with 25ng, the cDNAs encoding Derl2 and Amy1 caused significantly increased sensitivity to Aa-CDT (Figure 3.11A). In the cells transfected with 55ng, the cDNAs encoding 18010043G02Rik, Pofut2 (protein O-fucosyltransferase 2), Sfrs2 (serine/argenine-rich splicing factor 2), GEFT (rho guanine nucleotide exchange factor 25), PROS1 (protein S alpha), Exosc9 (exosome component 9), MRPL10 (mitochondrial ribosomal protein L10), Derl2 (Derlin-2) and Amy1 (Amylase-1) caused significantly increased sensitivity to Aa-CDT (Figure 3.11B). Of these, PROS1, Derl2 and Amy1 produced the greatest increase in intoxication. Since Derl2 and Amy1 produced increased sensitivity at both cDNA concentrations, these are most likely to be true hits. A subsequent independent experiment confirmed that Derl2 is a *bona fide* requirement for CDT intoxication (discussed in chapter 5).

3.3 DISCUSSION

In order to generate candidate genes required for CDT intoxication, the forward genetic screen presented above produced a number of CDT-resistant mutants. The phenotypic differences between the mutants subjected to only one round of mutagenesis suggests that a single treatment with ICR-191 was sufficient to create several independent CDT-resistant mutants.

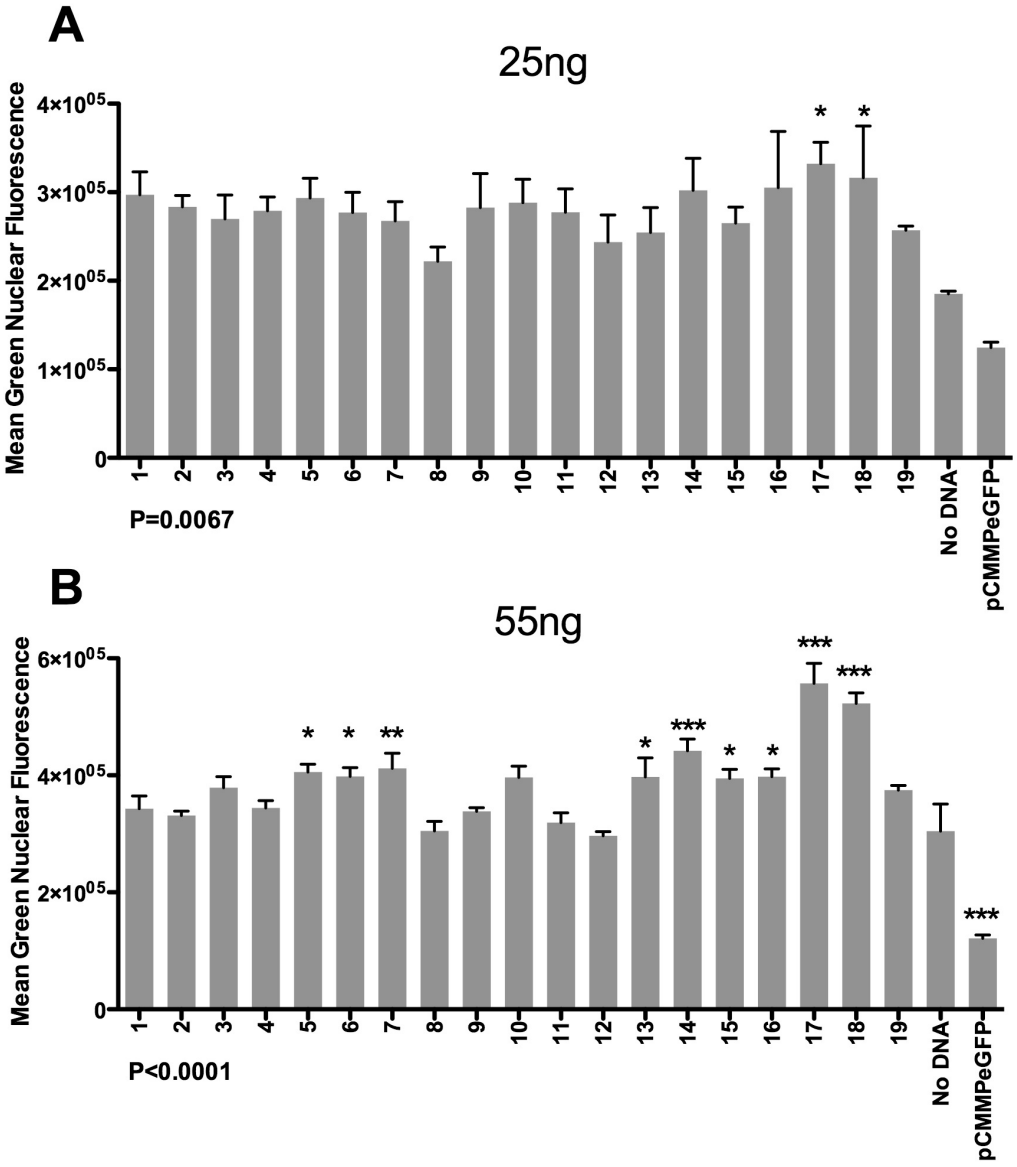

Figure 3.11 Follow up analysis of cDNA "hits" in A02-1-4 cells.
cDNA "hits" obtained in the cDNA screen were transfected into A02-1-4 cells at (A) 25ng/well or (B) 55ng/well and intoxicated with 20nM Aa-CDT followed by immunofluorescence for phosphorylated histone H2AX and laser scanning cytometry to quantify nuclear fluorescence. Error bars represent standard error, P values are from one way ANOVA analyses and asterisks denote significant differences from No DNA group by Dunnett's multiple comparison test.

In general, additional rounds of mutagenesis did not yield clones with greater levels of resistance to CDT. Therefore, we focused our characterization on clones resulting from a single round of ICR191 treatment to minimize potential complications resulting from excess mutagenesis.

Since Aa-CDT bound to all 61 of the mutants, none of them are likely to be deficient in receptor. Several reasons may explain the lack of a receptor mutant. It is possible that the screen did not reach saturation. Second, it is possible that two cell surface proteins are independently sufficient for CDT binding. If this were the case, a receptor mutant would be extremely difficult to isolate using a forward genetics because two independent mutations in the required genes would have to occur to result in loss of binding. Third, it is possible that the gene encoding the receptor is present in a diploid part of the CHO genome. A previous report showed that five rounds of ICR-191 mutagenesis of a diploid cell line allowed recovery of an appreciably higher number of mutants than just one round, suggesting biallelic mutations after five rounds (McKendry et al., 1991). Based on this report, we postulated that three rounds of mutagenesis would allow for biallelic mutations in partially hemizygous CHO cells; however, without careful quantitation, we cannot be certain.

The CDT-resistant mutants were either resistant to Aa-CDT, Hd-CDT and Ec-CDT, but sensitive to Cj-CDT or vise versa. The second chapter outlines several host factors that follow the same pattern. This correlates with the divergent binding subunits of Cj-CDT and is consistent with the hypothesis that different host factors are required for intoxication by Cj-CDT.

Four of the CDT-resistant clones subjected to one round of mutagenesis failed to phosphorylate histone H2AX in response to Aa-CDT, even though they were able to do so in response to UV. These four clones all bound CDT to their cell surface equivalently. This suggests that these four clones are deficient in the intoxication pathway somewhere between binding and induction of DNA damage responses. Although these four clones were isolated from independent pools mutagenized separately, is possible that they are deficient in the same step. Further characterization is necessary to determine if they are genetically and phenotypically distinct. The one mutant that retained the ability to phosphorylate H2AX in response to Aa-CDT likely was deficient in a process downstream of ATM activation. This clone may be of interest to those in the DNA damage response field because it may indentify a gene required for DNA damage-mediated cell cycle arrest or apoptosis.

The cDNA complementation screen on A02-1-4 cells identified 19 cDNAs that had the ability to complement Aa-CDT sensitivity; however, none of these hits occurred in duplicate, which lowers the confidence in the hits being genuine. Further analysis of these 19 hits revealed that between 2 and 9 of them are able to cause increased sensitivity in A02-1-4 cells. One possibility is that expression of these cDNAs causes increased sensitivity because they complement the deficiency in A02-1-4 cells. A second possibility is that that the proteins that are encoded by these cDNAs are required for intoxication and are present in limiting quantities; therefore, increased expression would result in increased sensitivity to CDT. This can be tested by assessing the ability of such cDNAs to cause increased CDT sensitivity in parental A745 cells. It is interesting to note that the two cDNAs that

caused increased CDT sensitivity are Derl2 and Amy1. Thorough characterization of Derl2 in the mechanism of CDT intoxication is the subject of chapter 5. Over-expression of Amy1 may affect sensitivity to CDT in an alternative fashion: Amy1 expression may not be required for sensitivity to CDT and endogenous expression may not be limiting in the intoxication pathway. Amylase-1 is classically known to breaks down long chain carbohydrates into more simple sugars by hydrolyzing α1,4 glycosidic bonds. If overexpression of this protein leads to degradation of cell surface glycoconjugates, this could lead to increased sensitivity to CDT. This would be consistent with the results discussed in chapter 2, where it was shown that genetic mutants deficient in glycosylation are hypersensitive to CDT intoxication.

3.4 EXPERIMENTAL PROCEDURES

Intoxication of Mammalian Cells with CDTs

Mammalian cells were trypsinized, counted, and allowed to adhere overnight. The following day, medium was removed and toxin-containing medium was added for 24 - 48 hours as indicated in the figure legends. Intoxicated cells were analyzed as described below.

Immunofluorescence for phosphorylated histone H2AX

Cells were intoxicated in clear bottom 384-well plates then fixed with 2% formaldehyde, quenched with 100 mM glycine, and permeabilized with ice cold methanol. The cells were subsequently blocked with 3% bovine serum albumin/0.3% Triton X-100 and incubated with rabbit anti-phospho-H2AX antibody (Cell Signal

Technologies) overnight at 4 °C. After washing, cells were incubated with Alexa Fluor 488-labeled goat anti-rabbit antibody (Invitrogen) for 1 hour at room temperature, washed, and counterstained with 1 µg/ml Hoechst 33342 (Invitrogen). Cytometric acquisition was performed on four 20X scan fields using an iCys laser scanning cytometer (CompuCyte) equipped with argon and violet diode lasers. Cytometric data analysis was conducted with iCys version 3.4 software (CompuCyte). Alternatively, immunofluorescence stained 384-well plates were analyzed by automated fluorescence microscopy on an ImageXpress^{Micro} and scored using MetaXpress® automated image analysis software (Molecular Devices, Inc.).

Cell cycle analysis

After intoxication, cells were washed with Dulbecco's PBS (DPBS, Cellgro), detached with 0.05% trypsin/EDTA (Invitrogen), washed again with DPBS, and permeabilized with 60% ethanol for 30 minutes on ice. After washing again, cells were stained with a 50 µg/ml propidium iodide (PI) solution containing 1 mg/ml sodium citrate, 0.3% Nonidet P-40, and 20 µg/ml RNase-A. The fluorescence was quantified for 10^4 cells using a FACSCalibur flow cytometer (BD Biosciences) with CellQuest acquisition software (BD Biosciences). Flow cytometry data were subsequently analyzed using FloJo analysis software (Tree Star).

Measurement of viability

Viability was quantified by using ATPlite reagent (Perkin Elmer) according to manufacturer recommendations. Intoxication data obtained by ATPlite reagent was

normalized by dividing the luminescence relative light unit (RLU) signal of each replicate by the average of the unintoxicated control cells.

Measurement of proliferation

Proliferation was measured by staining the cells with 1 μg/ml Hoechst 33342 (Invitrogen) and counting nuclei by laser scanning cytometry. Acquisition was performed on four 20X scan fields using an iCys laser scanning cytometer (CompuCyte) equipped with argon and violet diode lasers. Cytometric data analysis was conducted with iCys version 3.4 software (CompuCyte).

Fluorescent Lectin Binding

Cell surface glycan presentation was measured using the FITC-conjugated lectins (EY Laboratories) concanavalin A, Griffonia simplicifolia lectin, Lens culinaris agglutinin, Maclura pomifera agglutinin, Phaseolus vulgaris agglutinin, Pisum sativum agglutinin, Ulex europus agglutinin (UEA), and wheat germ agglutinin. Cells were detached as described above, mixed with an equal volume of complete media containing FBS, washed with DPBS, and resuspended in DPBS containing the manufacturer-recommended concentration of FITC-labeled lectin at room temperature for 15 minutes. Cells were washed with DPBS three times and resuspended in DPBS containing 1% formaldehyde (EMD Chemicals). Fluorescence was quantified as described above.

cELISA

Cells were allowed to adhere onto 384-well plates, bound to biotinylated Aa-CDT for 45 minutes on ice, thoroughly washed, fixed, then bound with streptavidin-horse radish peroxidase (HRP) and thoroughly washed again (Bag et al., 1993). Binding was detected via a chromogenic substrate for HRP, tetramethylbenzidine (TMB).

DNA Transfection

DNA was incubated with polyethyleneimine (PEI) in serum free media for 20 minutes at room temperature. Pre-seeded cells were rinsed with serum free media and then the media was replaced with media containing 20% serum. An equal volume of DNA/PEI mixture was added to result in 10% serum. The cells were allowed to express the DNA 24-48 hours prior to intoxication.

cDNA complementation screen

DNA was isolated from the more stringently curated MGC library using high throughput minipreps and this DNA was quantified, normalized and spotted into 384-well plates. Fugene 6 transfection reagent (Roche) was added to the plates to form DNA-transfection reagent complexes and these complexes were reverse transfected into A02-1-4 cells in duplicate. The cells were allowed to express cDNAs for 48 hours then intoxicated with 20nM Aa-CDT, a dose that reliably distinguished mutant from WT. Twenty-four hours post-intoxication, cells were immunostained for phosphorylated H2AX and counterstained with Hoechst. Automated fluorescence

microscopy was performed on the 384-well plates and automated scoring was completed using automated image analysis (MetaXpress©; Molecular Devices, Inc).

3.5 BIBLIOGRAPHY

Bag, P.K., Ramamurthy, T., and Nair, U.B. (1993). Evidence for the presence of a receptor for the cytolethal distending toxin (CLDT) of Campylobacter jejuni on CHO and HeLa cell membranes and development of a receptor-based enzyme-linked immunosorbent assay for detection of CLDT. FEMS Microbiol Lett *114*, 285-291.

Banks, D.J., and Bradley, K.A. (2007). SILENCE: a new forward genetic technology. Nat Methods *4*, 51-53.

Bradley, K.A., Mogridge, J., Mourez, M., Collier, R.J., and Young, J.A. (2001). Identification of the cellular receptor for anthrax toxin. Nature *414*, 225-229.

Bushman, F.D., Malani, N., Fernandes, J., D'Orso, I., Cagney, G., Diamond, T.L., Zhou, H., Hazuda, D.J., Espeseth, A.S., Konig, R.*, et al.* (2009). Host cell factors in HIV replication: meta-analysis of genome-wide studies. PLoS Pathog *5*, e1000437.

Eshraghi, A., Maldonado-Arocho, F.J., Gargi, A., Cardwell, M.M., Prouty, M.G., Blanke, S.R., and Bradley, K.A. (2010). Cytolethal distending toxin family members are differentially affected by alterations in host glycans and membrane cholesterol. J Biol Chem *285*, 18199-18207.

Esko, J.D., Stewart, T.E., and Taylor, W.H. (1985). Animal cell mutants defective in glycosaminoglycan biosynthesis. Proc Natl Acad Sci U S A *82*, 3197-3201.

Goff, S.P. (2008). Knockdown screens to knockout HIV-1. Cell *135*, 417-420.

Jackson, A.L., Bartz, S.R., Schelter, J., Kobayashi, S.V., Burchard, J., Mao, M., Li, B., Cavet, G., and Linsley, P.S. (2003). Expression profiling reveals off-target gene regulation by RNAi. Nat Biotechnol *21*, 635-637.

Kotecki, M., Reddy, P.S., and Cochran, B.H. (1999). Isolation and characterization of a near-haploid human cell line. Exp Cell Res *252*, 273-280.

McKendry, R., John, J., Flavell, D., Muller, M., Kerr, I.M., and Stark, G.R. (1991). High-frequency mutagenesis of human cells and characterization of a mutant unresponsive to both alpha and gamma interferons. Proc Natl Acad Sci U S A *88*, 11455-11459.

Montgomery, R.I., Warner, M.S., Lum, B.J., and Spear, P.G. (1996). Herpes simplex virus-1 entry into cells mediated by a novel member of the TNF/NGF receptor family. Cell *87*, 427-436.

Muller, H.J. (1927). Artificial Transmutation of the Gene. Science *66*, 84-87.

Poltorak, A., He, X., Smirnova, I., Liu, M.Y., Van Huffel, C., Du, X., Birdwell, D., Alejos, E., Silva, M., Galanos, C.*, et al.* (1998). Defective LPS signaling in C3H/HeJ and C57BL/10ScCr mice: mutations in Tlr4 gene. Science *282*, 2085-2088.

Smith, H., and Keppie, J. (1954). Observations on experimental anthrax; demonstration of a specific lethal factor produced in vivo by Bacillus anthracis. Nature *173*, 869-870.

CHAPTER 4

INVESTIGATION OF TMEM181 AS A RECEPTOR FOR Ec-CDT

4.1 INTRODUCTION

The discovery of a human leukemia cell line (KBM-7) that is haploid for the entire genome except chromosome 8 has sparked some recent advances in forward genetics and the CDT field (Carette et al., 2009; Carette et al., 2011; Kotecki et al., 1999). KBM-7 cells were used to identify host factors that are required for CDT intoxication. A Murine Stem Cell Virus (MSCV) based gene trap vector was used to mutagenize KBM-7 cells and select Ec-CDT resistant clones (Carette et al., 2009). Fourteen Ec-CDT resistant clonal cell lines were isolated. After using inverse PCR to map the proviral integration sites from these 14 cell lines, 11 of the clones had were found to have proviral integrations in the gene encoding sphingomyelin synthase 1 (SGMS1) and three integrations were found in TMEM181, a putative G-protein coupled receptor. Complementation with the corresponding cDNAs resulted in renewed sensitivity to Ec-CDT. Mutation of the SGMS1 gene resulted in reduced levels of plasma membrane sphingomyelin as judged by resistance to lysenin, a sphingomylein specific pore-forming toxin. Depletion of plasma membrane sphingomyelin alters lipid raft structure, which may impede CDT receptor clustering, a necessary event in clathrin mediated endocytosis. Cholesterol depletion-mediated resistance to CDT may function through the same mechanism (Guerra et al., 2005).

The second gene identified to support sensitivity to Ec-CDT, TMEM181, is a putative G-protein coupled receptor with 7 or 8 transmembrane domains (Figure 4.1). TMEM181 mutant and wildtype cells had similar sensitivity to lysenin, suggesting that the mechanism of CDT resistance was through a pathway distinct from that of SGMS1.

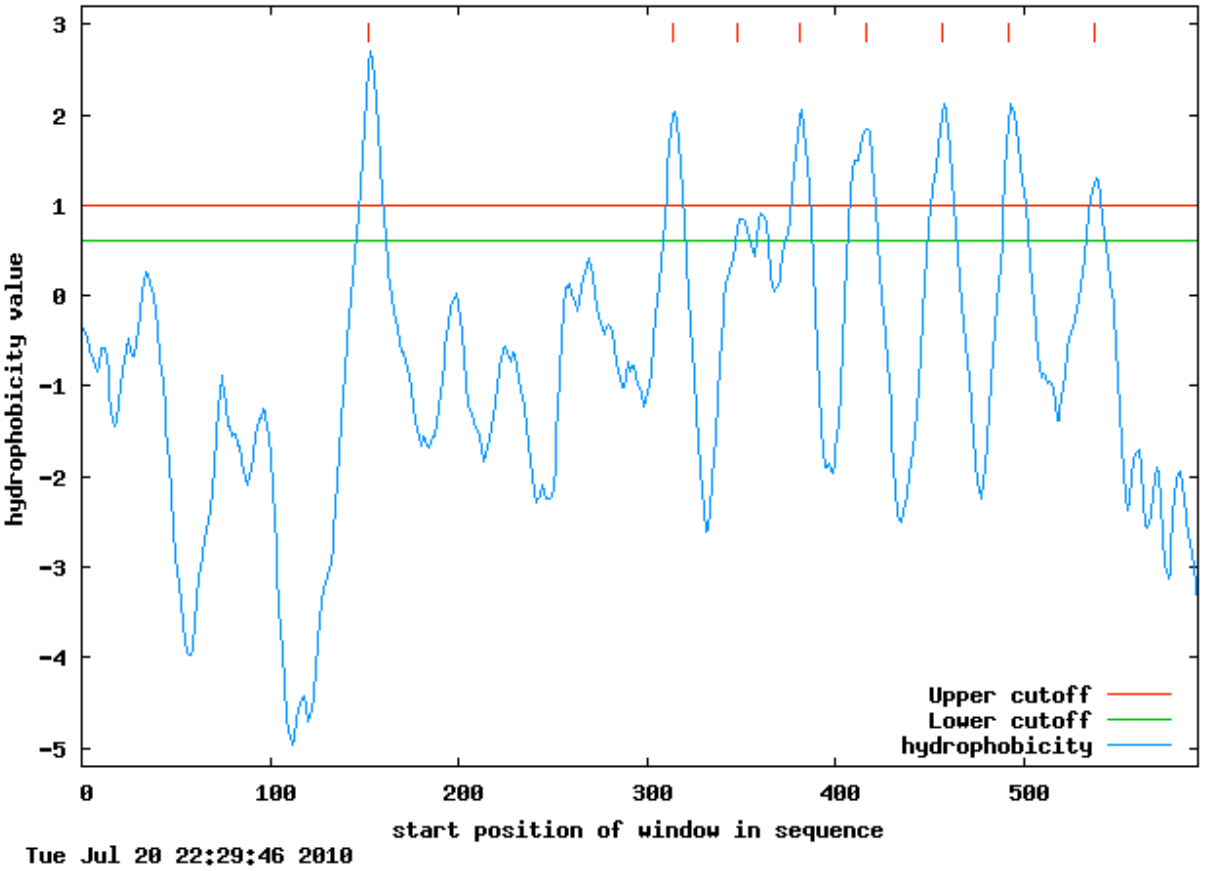

Figure 4.1 Prediction of transmembrane domains in TMEM181.
In silico prediction of hydrophobic transmembrane domains in TMEM181 based on the TMpred server (Hoffmann et al., 1993). Seven transmembrane domains are predicted, similar to other G-protein coupled receptors, based on a high stringency. If the stringincy is lowered, it is possible that it contains 8 transmembrane domains.

Coimmunoprecipitation was used to show that Ec-CDT interacts with TMEM181. Flag tagged Ec-CDT was immobilized on anti-FLAG beads and incubated with lysates from naïve KBM-7 cells or from KBM-7 cells expressing HA tagged TMEM181. Anti-HA signal was present only when CDT was immobilized on the beads, demonstrating a specific interaction between Ec-CDT and TMEM181. Overexpression of TMEM181 in human cervical carcinoma HeLa cells, mouse embryonic fibroblast NIH3T3 cells and human osteosarcoma U2OS cells increased their sensitivity to CDT, suggesting that TMEM181 levels are limiting for intoxication.

There is some evidence that TMEM181 is present on the cell surface and is glycosylated. Glycosylated TMEM181 was found on the surface of mouse embryonic stem cells, differentiating embryoid bodies and neural progenitors (Wollscheid et al., 2009). Mouse embryonic stem cells were treated with a gentle oxidizer followed by linking exposed oxidized cell surface sialic acids to a biotinylation reagent specific for aldehydes. Then, the cells were lysed and biotinylated proteins were captured on beads, released with PNGaseF and subjected to LC/MS-MS analysis to determine the identity of cell surface glycoproteins. Indeed, *in silico* analysis identifies N-linked glycosylation sites on TMEM181 (Figure 4.2). Coupled with my interest of the lectin folds in the CDT binding subunits (Chapter 2), I set out to test the hypothesis that TMEM181 is a receptor for EcCDT and determine the role of N-linked glycosylation in TMEM181 function as a CDT receptor.

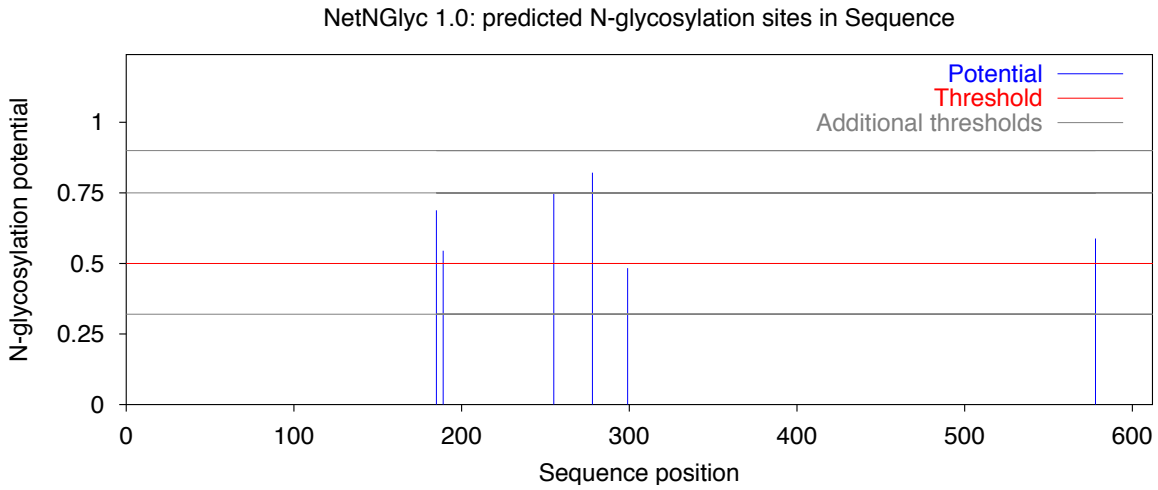

Figure 4.2 Prediction of N-linked glycosylation sites in TMEM181.
In silico prediction of N-linked glycosylation sites in TMEM181 based on the NetNGlyc 1.0 server (Gupta et al., 2004). Five predicted potential glycosylation sites are shown as blue lines above a critical threshold of 0.5, identified with a red line.

4.2 RESULTS

In order to subclone the *TMEM181* gene, the mammalian gene collection (MGC) was queried to determine if either mouse or human TMEM181 was present in the library. Performing a search for "TMEM181" returned one mouse and four human clones (Table 4.1). *E. coli* glycerol stocks containing vectors encoding these cDNAs were obtained from the Molecular Screening Shared Resource (MSSR), grown and their DNA was isolated and sequenced. The TMEM181 mRNA, TMEM181 putative open reading frame (ORF) and cDNA sequences were aligned using Sequencher. Two of the cDNAs (clone IDs 4952 and 24667) had no homology to any of the other sequences. The three remaining cDNAs aligned to the 3' end of the TMEM181 mRNA (accession number NM_020823.1); however, none of these sequences overlapped with the putative ORF (Figure 4.3), making these cDNAs useless for protein expression. Multiple attempts to PCR amplify the TMEM181 ORF from either a cDNA library constructed from HeLa cells (pLIB; Clontech) or a cDNA library constructed from human skeletal muscle (Invitrogen) failed. Further, attempts at PCR amplification of the TMEM181 ORF from homemade cDNA libraries constructed from Jurkat cells, HeLa cells, mouse liver (gift from Dr. A. Jake Lusis lab) and Chinese hamster ovary (CHO-K1) cells failed. Due to the difficulty in subcloning this gene, the TMEM181 ORF was codon optimized for maximal expression in hamster cells and this optimized sequence was custom synthesized (Genewiz).

Table 4.1 TMEM181 cDNA clones selected from the mammalian gene collection (MGC).

Open Biosystems Clone ID	Species	Donor Gender / Tissue	Gene Definition	Accession List	Clone Type
4952	Homo sapiens	Unknown / retinoblastoma	Transmembrane protein 181	BC033450, BE784310	Putative Full Length
24667	Mus musculus	Unknown / retina	Predicted gene, 547127| similar to KIAA1423 protein| transmembrane protein 181	BC032285, BI730638	Putative Full Length
6894005	Homo sapiens	Both / Brain	Transmembrane protein 181	BC044210, BI916908	Putative Full Length
6901219	Homo sapiens	Male / Sciatic nerv	Transmembrane protein 181	BC046100, BQ925083	Putative Full Length
7374956	Homo sapiens	Female / leiomyosarcoma	Transmembrane protein 181	BC058328, BU521426	Putative Full Length

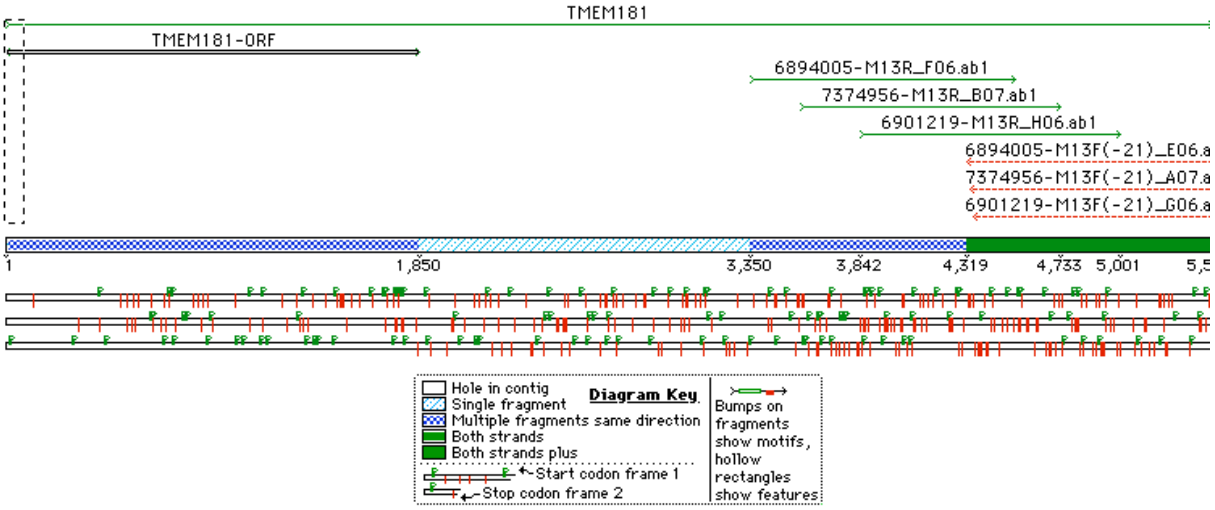

Figure 4.3 Alignment of the MGC TMEM181 cDNAs to the TMEM181 mRNA. Three cDNAs align to the 3' end of the TMEM181 mRNA, but none of these overlap with the TMEM181 ORF.

After custom synthesis of TMEM181, gateway cloning (Invitrogen) was performed to move the gene into a donor vector and subsequently several expression vectors. Expression of one of these vectors resulted in TMEM181 fused to a Bioease tag (Invitrogen), which results in endogenous biotinylation of the expressed protein. Precipitation of the biotinylated protein from transfected 293 cells was performed with streptavidin coated beads. Half of the beads were treated with PNGaseF and a western blot was performed to determine if PNGaseF treatment resulted in altered mobility due to removal of carbohydrates (Figure 4.4). The altered mobility induced by PNGaseF treatment revealed that TMEM181 was indeed N-glycosylated.

In order to determine if glycosylation has an effect on the ability of TMEM181 to serve as a receptor for CDT, site directed mutagenesis was utilized to mutate the five putative asparagine glycosylation sites to glutamines (N185Q, N189Q, N255Q, N278Q and N578Q). The wildtype TMEM181 was cloned into several destination vectors that appended various tags to the N- and C-terminus of TMEM181. First TMEM181 was cloned into a retroviral vector that appended a Bioease tag (Invitrogen) that results in endogenously biotinylated TMEM181. Retroviral particles were made from this vector and these particles were used to transduce CHO-K1 cells and subsequently selected with antibiotic to ensure expression. In addition, the retroviral vector was transiently transfected into CHO-K1 cells with polyethyleneimine (PEI).

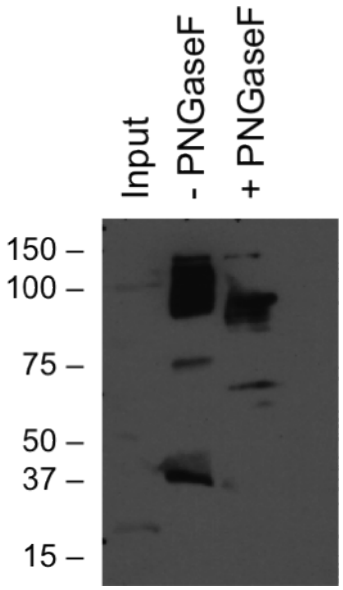

Figure 4.4 TMEM181 is N-glycosylated.
Expression of TMEM181 with a Bioease tag, followed by precipitation with streptavidin coated beads and treatment with PNGaseF reaveals that TMEM181 is N-glycosylated.

After the transduced cells were selected and 48 hours after transfection, the cells were lysed and analyzed by western blot by using streptavidin HRP to query expression of biotinylated TMEM181. There were a number of background bands present, but both transduced and transfected cells revealed a band at approximately 100kDa, consistent with TMEM181 expresssion (Figure 4.5). After confirming expression of TMEM181 in CHO-K1 cells by transfection, TMEM181 was cloned into several other vectors. The first two applied six N-terminal myc tags and three N-terminal FLAG tags and the last was an untagged retroviral vector. Transfecting these four TMEM181 expressing constructs into CHO-K1 cells and intoxicating with Ec-CDT did not result in increased sensitivity (Figure 4.6). This experiment was run several times, with similar results.

Comprehensive evaluation of the report by Carette and colleagues (2009) revealed that complementation of Ec-CDT resistant KBM-7 mutants was performed with a truncated version of TMEM181. Based on the primer sequences used for PCR amplification in the TMEM181 subcloning process, the first 420 base pairs of sequence is deleted from the full length putative open reading frame (Figure 4.7). To test whether the 420 base pair N-terminal deletion may induce hypersensitivity to Ec-CDT as they had previously shown, a TMEM181 version (TMEM181Δ1-140) identical to the published isoform was cloned into a retroviral vector and transduced into HeLa cells. Transduction was performed with high and low volumes of viral particles (representing high and low multiplicities of infection) and transduced cells were selected with antibiotic to ensure expression.

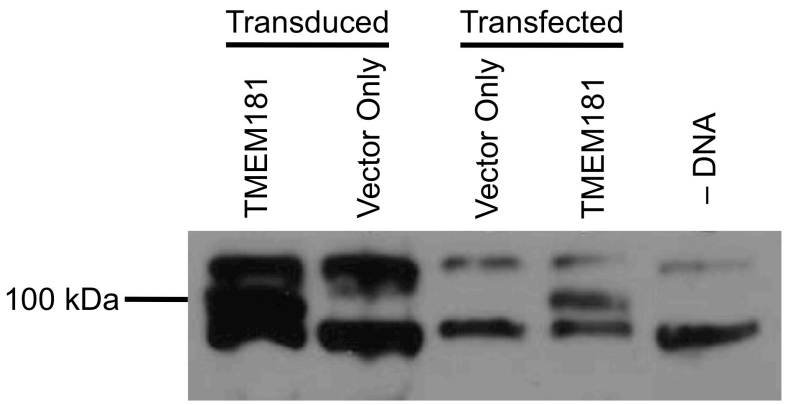

Figure 4.5 Bioease tagged TMEM181 is expressed by transduction and transfection.
CHO-K1 cells were transduced or transfected with Bioease tagged TMEM181 expressing vector and lysed. Lysates were subjected to western blot with streptavidin-HRP. Basted on size, the band at 100 kDA is likely TMEM181.

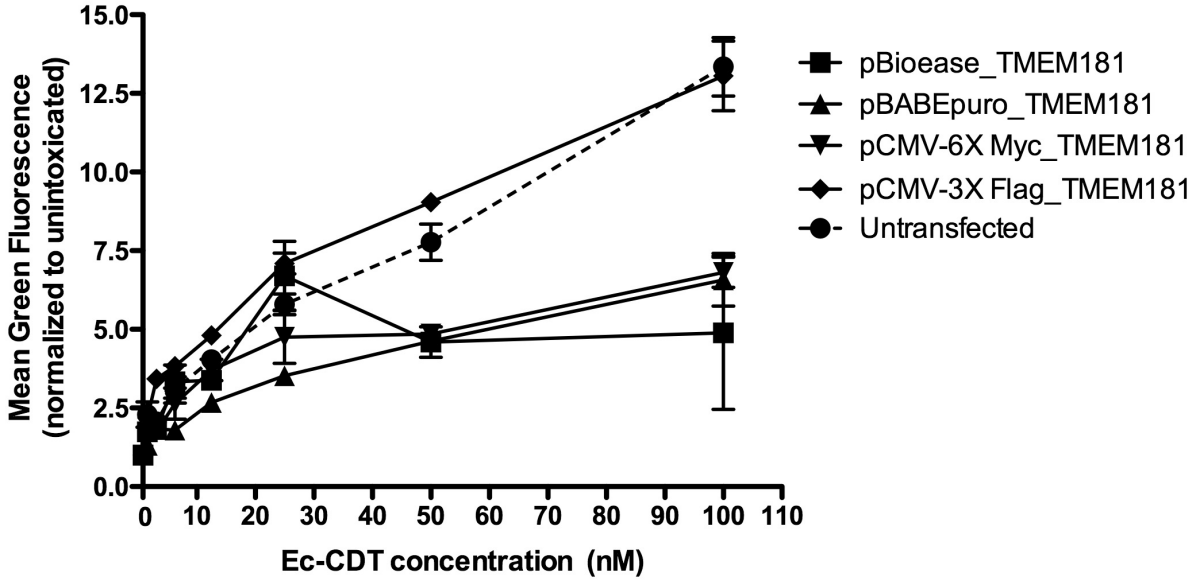

Figure 4.6 Transfection with various TMEM181 constructs does not result in increased sensitivity to Ec-CDT.
CHO-K1 cells were transfected with various TMEM181 constructs and subsequently intoxicated with Ec-CDT. Sensitivity to CDT was quantified by immunofluorescence for phosphorylated H2AX and analyzed by laser scanning cytometry.

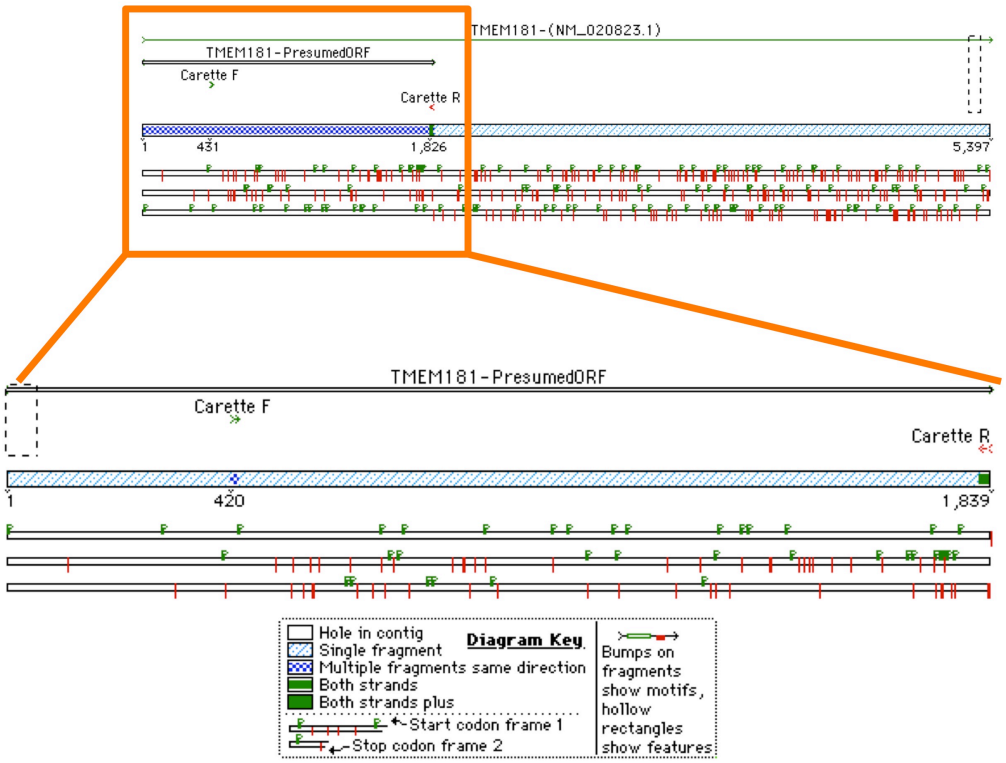

Figure 4.7 Mapping of Carette 2009 TMEM181 primers on the TMEM181 mRNA and presumed ORF.

Mapping the primers that Carette et al. (2009) used to clone the cDNA that they used to complement their Ec-CDT resistant KBM-7 mutants reveals that the cDNA they used had a 420 base pair N-terminal truncation.

These cells were seeded into 384- and 24-well plates and were intoxicated with a titration of CDT. Similar to the experiment performed by Carette et al. (2009), the intoxication progressed for five days and then the cells in the 24-well plate were stained with crystal violet for gross observation of adherent cells. A more quantitative viability assay was performed on the cells intoxicated in the 384-well plate. Consistent with our previous results, expression of either the full length or the truncated version of TMEM181 was unable to increase sensitivity to Ec-CDT (Figure 4.8).

4.3 DISCUSSION

The inconsistency between the results presented here and those presented by Carette et al. (2009) are curious. In the experiments where TMEM181 was expressed in CHO-K1 cells, it is possible that hypersensitivity was not observed because TMEM181 may be limiting in HeLa, NIH3T3 and U2OS cells, but endogenous levels in CHO-K1 cells are sufficient for intoxication. However, many of the experiments performed here overexpressed various forms of TMEM181 in HeLa cells and found no increase in sensitivity, as was previously shown. In total, two undergraduates under my direction and I performed approximately 40 experiments to test if overexpression of TMEM181 results in increased sensitivity to CDT; however, the published finding was not repeated. One disparity exists between experiments performed in our lab and those reported.

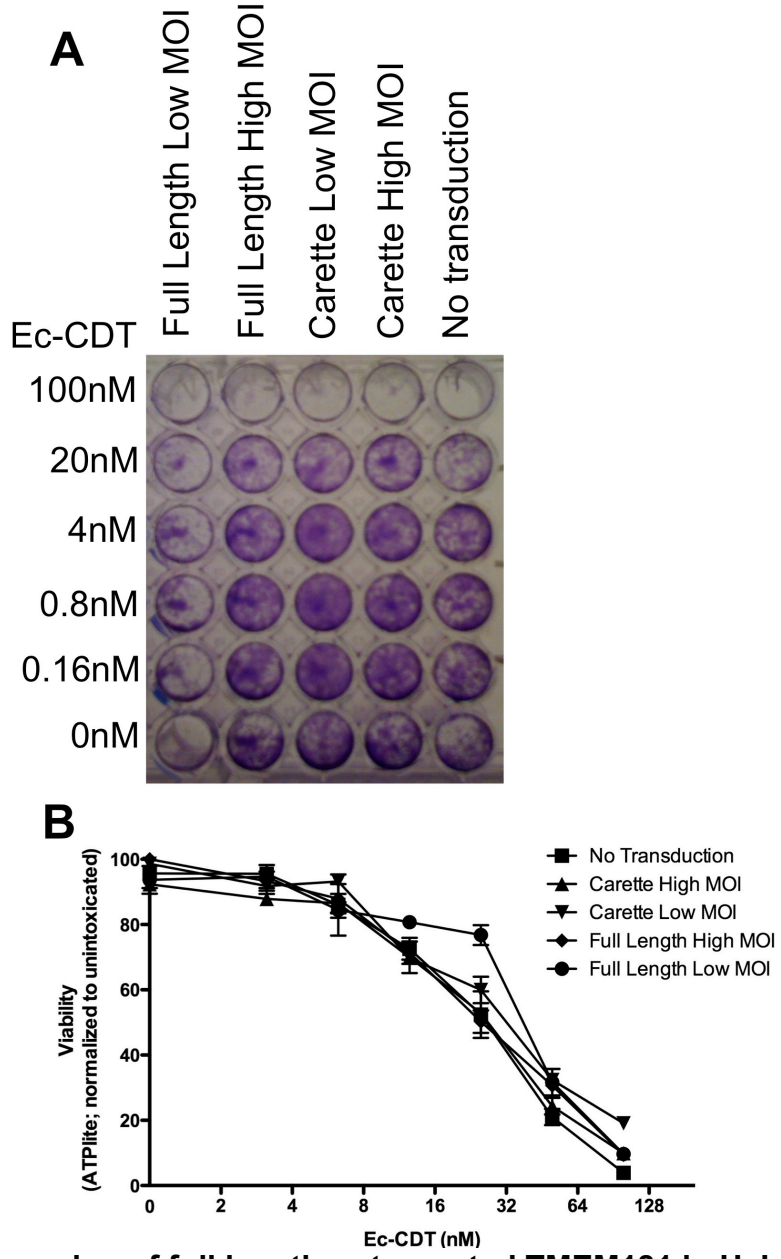

Figure 4.8 Expression of full length or truncated TMEM181 in HeLa cells does not increase sensitivity to Ec-CDT.

HeLa cells were transduced with either truncated TMEM181 (identical to the one used by Carette 2009) or full length TMEM181 at high or low MOI. Following selection, the cells were seeded into 24- and 384-well plates and intoxicated for five days. (A) The 24-well plate was stained with crystal violet to show adherent viable cells. (B) ATPlite viability assay was performed on the 384-well plate to provide quantitative data.

The TMEM181 cDNA used for expression by Carette et al. was subcloned from KBM-7 mRNA and ours was custom synthesized as an expression optimized human TMEM181 sequence obtained from NCBI. It is possible that the KBM-7 cDNA has a variation that supports CDT intoxication, while the sequence that we have does not. The only way to test this is to obtain the cDNA from the authors of the previous study; however, attempts to obtain materials from the corresponding author and coauthors went unanswered or were met with polite declinations.

4.4 EXPERIMENTAL PROCEDURES

Intoxication of Mammalian Cells with CDTs

Mammalian cells were trypsinized, counted, and allowed to adhere overnight. The following day, medium was removed and toxin-containing medium was added for 24 - 48 hours as indicated in the figure legends. Intoxicated cells were analyzed as described below.

Immunofluorescence for phosphorylated histone H2AX

Cells were intoxicated in clear bottom 384-well plates then fixed with 2% formaldehyde, quenched with 100 mM glycine, and permeabilized with ice cold methanol. The cells were subsequently blocked with 3% bovine serum albumin/0.3% Triton X-100 and incubated with rabbit anti-phospho-H2AX antibody (Cell Signal Technologies) overnight at 4 °C. After washing, cells were incubated with Alexa Fluor 488-labeled goat anti-rabbit antibody (Invitrogen) for 1 hour at room temperature, washed, and counterstained with 1 μg/ml Hoechst 33342 (Invitrogen).

Cytometric acquisition was performed on four 20X scan fields using an iCys laser scanning cytometer (CompuCyte) equipped with argon and violet diode lasers. Cytometric data analysis was conducted with iCys version 3.4 software (CompuCyte). Alternatively, immunofluorescence stained 384-well plates were analyzed by automated fluorescence microscopy on an ImageXpress^{Micro} and scored using MetaXpress® automated image analysis software (Molecular Devices, Inc.).

Measurement of viability

Viability was quantified by using ATPlite reagent (Perkin Elmer) according to manufacturer recommendations. Intoxication data obtained by ATPlite reagent was normalized by dividing the luminescence relative light unit (RLU) signal of each replicate by the average of the unintoxicated control cells.

DNA Transfection

DNA was incubated with polyethyleneimine (PEI) in serum free media for 20 minutes at room temperature. Pre-seeded cells were rinsed with serum free media and then the media was replaced with media containing 20% serum. An equal volume of DNA/PEI mixture was added to result in 10% serum. The cells were allowed to express the DNA 24-48 hours prior to intoxication.

Preparation of retroviral particles and transduction

Plasmid DNA was purified and transfected into human 293 cells along with murine leukemia virus gag/pol and vesicular stomatitis virus G-spike protein

expression plasmids as previously described (Bradley et al., 2003). Forty-eight hours later, resulting retroviral particles were harvested, filter-sterilized, diluted in fresh media with 8 µg/ml Polybrene (Sigma-Aldrich), and used to transduce cells in a 6-well plate. Cells were incubated with viral particles overnight. After 48 hours, transduced cells were selected in medium containing antibiotic.

4.5 BIBLIOGRAPHY

Bradley, K.A., Mogridge, J., Jonah, G., Rainey, A., Batty, S., and Young, J.A. (2003). Binding of anthrax toxin to its receptor is similar to alpha integrin-ligand interactions. J Biol Chem *278*, 49342-49347.

Carette, J.E., Guimaraes, C.P., Varadarajan, M., Park, A.S., Wuethrich, I., Godarova, A., Kotecki, M., Cochran, B.H., Spooner, E., Ploegh, H.L.*, et al.* (2009). Haploid genetic screens in human cells identify host factors used by pathogens. Science *326*, 1231-1235.

Carette, J.E., Guimaraes, C.P., Wuethrich, I., Blomen, V.A., Varadarajan, M., Sun, C., Bell, G., Yuan, B., Muellner, M.K., Nijman, S.M.*, et al.* (2011). Global gene disruption in human cells to assign genes to phenotypes by deep sequencing. Nat Biotechnol *29*, 542-546.

Guerra, L., Teter, K., Lilley, B.N., Stenerlow, B., Holmes, R.K., Ploegh, H.L., Sandvig, K., Thelestam, M., and Frisan, T. (2005). Cellular internalization of

cytolethal distending toxin: a new end to a known pathway. Cell Microbiol *7*, 921-934.

Gupta, R., Jung, E., and Brunak, S. (2004). Prediction of N-glycosylation sites in human proteins.

Hoffmann, I., Clarke, P.R., Marcote, M.J., Karsenti, E., and Draetta, G. (1993). Phosphorylation and activation of human cdc25-C by cdc2--cyclin B and its involvement in the self-amplification of MPF at mitosis. Embo J *12*, 53-63.

Kotecki, M., Reddy, P.S., and Cochran, B.H. (1999). Isolation and characterization of a near-haploid human cell line. Exp Cell Res *252*, 273-280.

Wollscheid, B., Bausch-Fluck, D., Henderson, C., O'Brien, R., Bibel, M., Schiess, R., Aebersold, R., and Watts, J.D. (2009). Mass-spectrometric identification and relative quantification of N-linked cell surface glycoproteins. Nat Biotechnol *27*, 378-386.

CHAPTER 5

DERLIN-2 IS REQUIRED FOR INTOXICATION BY CYTOLETHAL DISTENDING TOXIN

Aria Eshraghi[1], Emily Jin-Kyung Kim[1], Batcha Tamilselvam[2], Julia C. Kulik[1], Amandeep Gargi[2], Robert Damoiseaux[3], Steven R. Blanke[2] and Kenneth A. Bradley[1,3 *]

[1] Department of Microbiology, Immunology and Molecular Genetics, University of California, Los Angeles; Los Angeles, CA 90095 USA

[2] Department of Microbiology, Institute for Genomic Biology, University of Illinois, Urbana; Urbana, IL 61801 USA

[3] California NanoSystems Institute, University of California, Los Angeles, CA; Los Angeles, CA 90095 USA

CONTACT

* Corresponding author

kbradley@microbio.ucla.edu; phone (310) 206-7465

609 Charles E. Young Drive East, Los Angeles, CA 90095

RUNNING TITLE

Derlin-2 is required for CDT intoxication

5.1 ABSTRACT

Intracellular acting protein exotoxins produced by bacteria and plants are important molecular determinants that drive numerous human diseases. A subset of these toxins, the cytolethal distending toxins (CDTs), are encoded by several Gram-negative pathogens and have been proposed to enhance virulence by allowing evasion of the immune system. These toxins are retrograde trafficked from the cell surface through the Golgi apparatus and into the ER where they face the formidable challenge of translocation across the ER membrane to gain access to their downstream cellular target. Despite the absolute requirement for translocation across the ER membrane, the mechanism is poorly understood. The ER-associated degradation (ERAD) pathway is presumed to be important; however, the details of the mechanism and even the proteins involved are largely unknown. Here we show that Derlin-2 (Derl2), a central component of the host ERAD machinery, is required for intoxication by retrograde trafficking CDTs. The mechanism of Derl2-dependent of escape of CDTs from the ER is distinct from previously described Derl2-dependent retrotranslocation of ERAD substrates. Specifically, we show that two independent requirements for Derl2-mediated ERAD of misfolded proteins, a conserved WR motif and interaction with the AAA-ATPase p97, are dispensable for retrotranslocation of CDT and another retrograde trafficking toxin, ricin. This previously undescribed mechanism demonstrates a novel Derl2-dependent ERAD pathway exploited by retrograde trafficking toxins.

5.2 AUTHOR SUMMARY

Cytolethal distending toxins (CDTs) are produced by several bacterial pathogens and increase the ability of these bacteria to cause disease. After binding to a cell surface receptor and being internalized, CDTs are trafficked through the Golgi apparatus and into the endoplasmic reticulum (ER) where they must translocate across the ER membrane to gain access to their intracellular target; however, this translocation process is poorly understood for CDTs and other toxins that are similarly trafficked. It is presumed that these retrograde trafficking toxins take advantage of a host cellular process, called ER-associated degradation (ERAD), that is utilized to translocate misfolded ER lumenal proteins through the ER membrane for degradation in the cytosol by the proteosome. This report shows that the protein Derlin-2 (Derl2), which is involved in ERAD of misfolded proteins, is required for intoxication by CDT. The absence of this protein results in the inability of CDT to be translocated out of the ER and cause intoxication of the host cell. Further, two Derl2 functional domains that are required for ERAD of misfolded proteins are dispensable for intoxication by CDT. This paper demonstrates a novel mechanism exploited by retrograde trafficking toxins.

5.3 INTRODUCTION

Cytolethal distending toxins (CDTs) are produced by a variety of Gram-negative pathogens and belong to a larger, emerging group of intracellular-acting "cyclomodulins" whose expression is associated with increased persistence, invasiveness and/or severity of symptoms (Ahmed et al., 2001; Fox et al., 2004; Ge et al., 2005; Ge et al., 2007; McAuley et al., 2007; Purdy et al., 2000; Young et al., 2004). Rather than inducing overt cytotoxicity and tissue damage, cyclomodulins drive more subtle alterations in the host through changes in cell cycle progression. CDTs cause DNA damage in susceptible mammalian cells, resulting in the induction of DNA repair signaling mechanisms including phosphorylation of the histone H2AX, cell cycle arrest at the G_2/M interface and disruption of cytokinesis (Gargi et al., 2012). In cultured cells, the DNA damage response ultimately leads to apoptotic cell death, while *in vivo*, persistent DNA damage may give rise to infection-associated oncogenesis (Guidi et al., 2013). Although the cellular response to CDTs is well characterized (Gargi et al., 2012; Guerra et al., 2011), the mechanism by which CDTs bind to host cells and ultimately gain access to their nuclear target is less clear.

CDTs generally function as complexes of three protein subunits, encoded by three contiguous genes (*cdtA*, *cdtB*, *cdtC*) in a single operon (Thelestam and Frisan, 2004). Consistent with the AB model of intracellular acting toxins (Blanke, 2006), CdtB functions as the enzymatic A-subunit and possesses DNase I-like activity responsible for inducing DNA damage within the nuclei of intoxicated cells (Elwell and Dreyfus, 2000; Lara-Tejero and Galan, 2000). CdtA and CdtC are thought to

function together as the cell-binding B-moiety of AB toxins to deliver CdtB into cells (Cao et al., 2008; Cao et al., 2005; McSweeney and Dreyfus, 2005; Nesic and Stebbins, 2005). Inhibiting the cell cycle interferes with many functions of rapidly dividing eukaryotic cells, including lymphocytes and epithelial cells, which play a role in immunity and provide a physical barrier to microbial pathogens (Pickett and Whitehouse, 1999; Purdy et al., 2000; Shenker et al., 2001). Thus, it is not surprising that CDTs are expressed by a diverse group of Gram-negative pathogens that colonize different niches within the host, including the oral pathogen *Aggregatibacter actinomycetemcomitans*, the sexually transmitted pathogen *Haemophilus ducreyi*, and the gastrointestinal pathogens, *Escherichia coli* and *Campylobacter jejuni*. CDT is associated with virulence in several human pathogens; however, little is known about the mechanism of intoxication.

Studies to elucidate the trafficking of bacterial and plant toxins in mammalian cells have revealed novel and unexpected mechanisms by which pathogens subvert existing host systems, and in doing so have provided valuable insights into the mechanisms and pathways underlying the entry of extracellular molecules into the cytosol (Sandvig and van Deurs, 2005). Since CDTs are the first known bacterial effectors targeted to the host cell nucleus (Nishikubo et al., 2003), they present the opportunity to reveal novel trafficking pathway usurped by bacterial virulence factors (Carette et al., 2011). To exert their cyclomodulatory effects on cells, CDTs must be taken up from the cell surface and transported intracellularly in a manner that ultimately results in localization to the nucleus. Similar to Shiga toxin, cholera toxin, *Pseudomonas aeruginosa* exotoxin A, and ricin, CDT is retrograde trafficked through

the Golgi and into the ER where it is thought to be translocated across the ER membrane to gain access to the cytosol or nucleus (Damek-Poprawa et al., 2012; Guerra et al., 2009; Guerra et al., 2005). Retrograde trafficking toxins do not possess the ability to translocate themselves across the ER membrane and must therefore rely on host cellular processes to access their intracellular targets. The escape of retrograde trafficking toxins from the ER is thought to occur via ER-associated degradation (ERAD), a mechanism utilized for retrotranslocation of misfolded proteins for proteosomal degredation. However, the molecular details and mechanism by which CDTs are translocated across the host membrane to gain access to the cytosol and/or nucleus are poorly understood (Damek-Poprawa et al., 2012; Guerra et al., 2009; Guerra et al., 2005). The core machinery driving ERAD in mammalian cells consists of the Hrd1/Sel1L ubiquitin ligases, the Derlin family of proteins and may also involve Sec61 (Hebert et al., 2010). Here we provide the first demonstration of an ERAD component, Derl2, whose absence results in a complete block to intoxication by a retrograde trafficking toxin in mammalian cells.

5.4 RESULTS

5.4.1 Derl2 is Required for Intoxication by CDT

In order to identify genes that confer sensitivity to CDT, we utilized two forward somatic cell genetic approaches. First, we utilized the frameshift mutagen ICR-191 to induce mutations in ten separate pools of CHO-pgs A745 cells (A745). Each pool of 1 x 10^6 cells was selected with 20 nM *A. actinomycetemcomitans* CDT (Aa-CDT), a toxin concentration high enough to cause death in parental cells. Five of

the ten pools yielded Aa-CDT resistant clones; the most resistant clone isolated (CHO-CDT^{R}A2) was resistant to the highest dose of Aa-CDT tested (Figure 5.1A). Interestingly, CHO-CDT^{R}A2 cells were also resistant to the highest dose of *H. ducreyi* CDT (Hd-CDT) tested (Figure 5.1B) and more modestly resistant to CDTs from *E. coli* (Ec-CDT)(Figure 5.1C) and *C. jejuni* (Cj-CDT)(Figure 5.1D). To identify the gene responsible for CDT resistance in CHO-CDT^{R}A2 cells, we utilized a high throughput cDNA expression-based complementation approach. A custom cDNA library consisting of approximately 3.7 x 10^3 arrayed clones was prepared from the mammalian gene collection. Plasmid DNA was isolated from the library, normalized for concentration, plated into 384-well plates and reverse transfected into CHO-CDT^{R}A2 cells. After 72 hours, the transfected cells were intoxicated with 20 nM Aa-CDT and immunostained using fluorescent α-pH2AX antibodies to identify activation of CDT-mediated DNA damage response. Cells were stained with Hoechst 33342 to enumerate nuclei, imaged by automated fluorescence microscopy and scored using automated image analysis software. We identified *Mus musculus Derlin-2* (Genbank ID: BC005682), a gene involved in the ER-associated degradation (ERAD) pathway, as able to complement the sensitivity of CHO-CDT^{R}A2 cells to Aa-CDT. CHO-CDT^{R}A2 cells were transduced with a retroviral vector encoding Derl2 to verify this finding and test whether Derl2 was able to complement resistance to the remaining three CDTs. CHO-CDT^{R}A2 cells expressing Derl2 regained sensitivity to all four CDTs tested to near parental levels (Figure 5.1A-D).

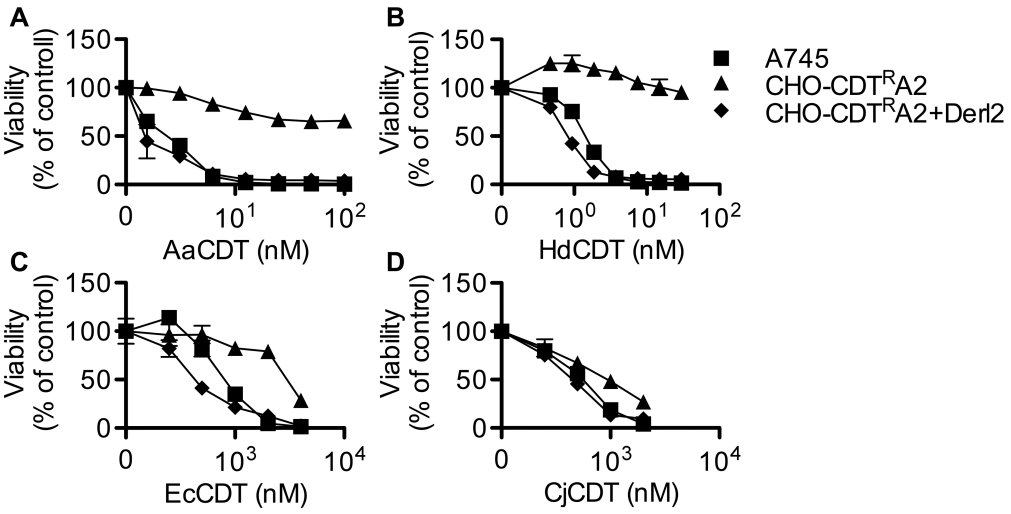

Figure 5.1 The chemically mutagenized clone, CHO-CDT^{R}A2, is resistant to CDT and complemented by expression of Derl2.
Parental A745 cells, chemically induced mutant CHO-CDT^{R}A2 cells, and CHO-CDT^{R}A2 cells expressing Derl2 were seeded in a 384-well plate (1 x 10^3 cells/well) and allowed to adhere overnight, followed by 48 hour intoxication with Aa-CDT (a), Hd-CDT (b), Ec-CDT (c) and Cj-CDT (d) and quantitation of viability using ATPlite 1-step reagent (Perkin Elmer). Data are representative of at least three independent experiments performed in triplicate, percent viability is normalized to unintoxicated controls and error bars indicate standard error.

In a parallel effort to identify genes required for CDT intoxication, a retroviral mutagenesis approach was employed (Banks and Bradley, 2007). Approximately 1 x 10^7 A745 cells expressing the tetracycline repressor protein fused to the Krüppel associated box from human *Kox1* (A745TKR) were transduced with murine leukemia virus (MLV) at a multiplicity of infection of 0.1 and selected with 5 nM Hd-CDT, a toxin concentration high enough to cause death in parental cells. Two independent pools produced Hd-CDT-resistant clones. Subsequent characterization of one clone from each pool, CHO-CDT^{R}C1 and CHO-CDT^{R}F1, revealed that they were resistant to the highest concentrations of the four CDTs tested (Figure 5.2A-D). The site of mutational proviral integration was determined using a combination of sequence capture, inverse PCR and sequencing (Banks and Bradley, 2007). Proviral integration sites in the mutants were distinct; the mutagenic integration in CHO-CDT^{R}C1 cells occurred between the first and second *Derl2* exons and occurred in the opposite orientation in CHO-CDT^{R}F1 cells between the fourth and fifth *Derl2* exons (Figure 5.2E). Overexpression of Derl2 in these mutants complemented sensitivity to all CDTs tested (Figure 5.2A-D; Figure 5.3). In contrast, Derl1 overexpression in CHO-CDT^{R}C1 cells had no effect on sensitivity to Hd-CDT (Figure 5.2F). Both CHO-CDT^{R}C1 and CHO-CDT^{R}F1 mutant cells displayed decreased Derl2 expression by immunoprecipitation followed by western blot (Figure 5.2G). Targeted knockdown of Derl2 by siRNA treatment of HeLa cells confirmed that Derl2 deficiency led to resistance to Hd-CDT and demonstrated that this requirement for Derl2 was not exclusive to Chinese hamster ovary cells (Figure 5.2H).

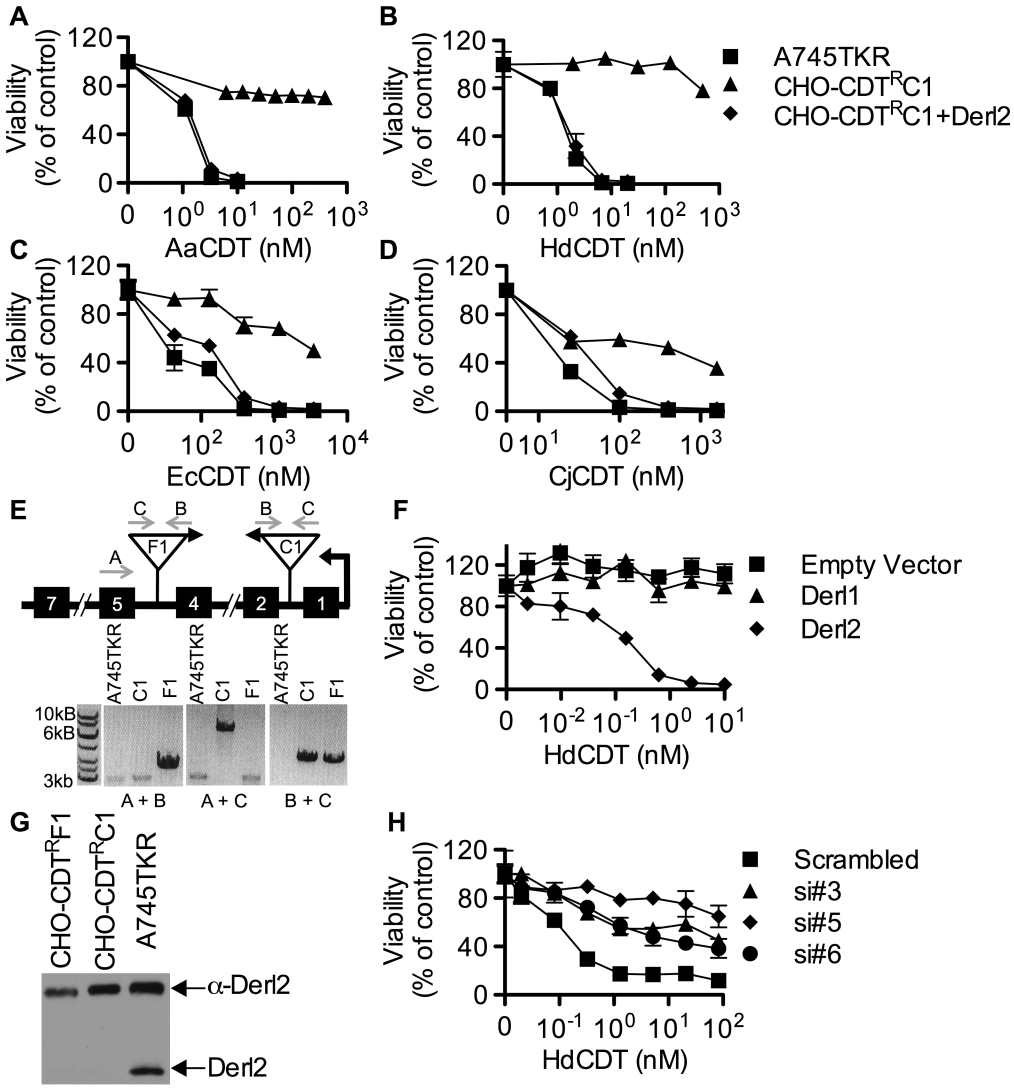
A
Viability (% of control)
AaCDT (nM)
B
HdCDT (nM)
A745TKR
CHO-CDTRC1
CHO-CDTRC1+Derl2
C
EcCDT (nM)
D
CjCDT (nM)
E
A
B
C
F1
C1
7
5
4
2
1
10kB
6kB
3kb
A745TKR
C1
F1
A + B
A + C
B + C
F
Empty Vector
Derl1
Derl2
HdCDT (nM)
G
CHO-CDTRF1
CHO-CDTRC1
A745TKR
α-Derl2
Derl2
H
Scrambled
si#3
si#5
si#6
HdCDT (nM)

Figure 5.2 Derl2 is required for CDT intoxication.
Viability of parental A745TKR cells, retrovirally induced mutant CHO-CDT^{R}C1 cells, and CHO-CDT^{R}C1 cells expressing Derl2 after intoxication with Aa-CDT (a), Hd-CDT (b), Ec-CDT (c) and Cj-CDT (d). Intoxication was performed similar to figure 5.1. (e) Diagrammatic representation of the Derl2 open reading frame with boxes representing exons, gray arrows representing primers, and upside down triangles representing proviral insertions. PCR amplification of genomic DNA from parental A745TKR, CHO-CDT^{R}C1 and CHO-CDT^{R}F1 cells using primers detailed in the diagram. (f) Overexpression of Derl1 does not complement resistance to CDT. Derl1 deficient CHO-CDT^{R}C1 cells expressing empty vector, Derl1, and Derl2 were intoxicated with Hd-CDT, similar to figure 5.1. (g) Immunoprecipitation western blot of Derl2 from parental and mutant cells. Western blot was performed on Derl2 antibody-precipitated protein from normalized cell lysates. (h) Derl2 knockdown in HeLa cells causes resistance to Hd-CDT. HeLa cells were transfected with scrambled siRNA or siRNAs targeting human Derl2, followed by intoxication with Hd-CDT, similar to figure 5.1. Data are representative of at least three independent experiments performed in triplicate, percent viability is normalized to unintoxicated controls and error bars indicate standard error.

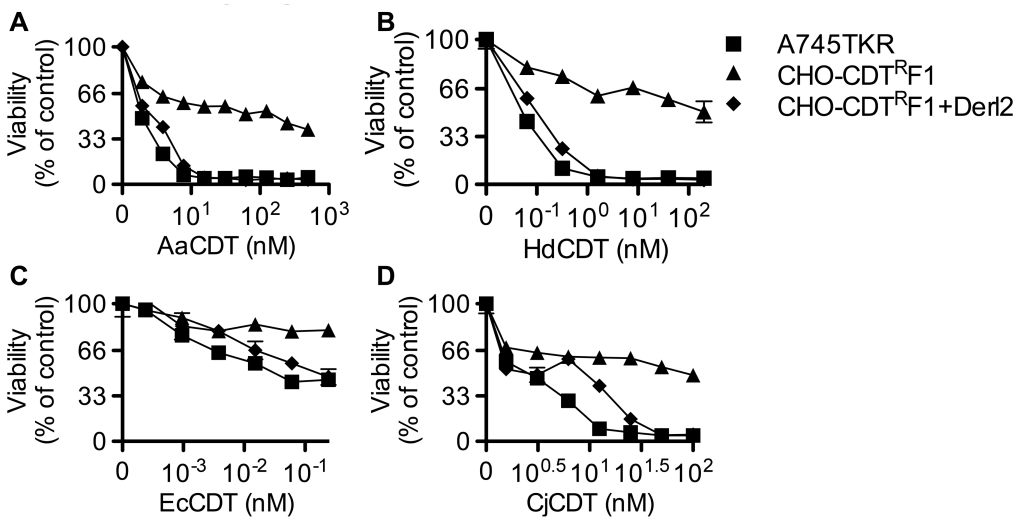

Figure 5.3 The retrovirally mutagenized Derl2 deficient CHO-CDT^{R}F1 cell line is resistant to CDT.

Viability of parental A745TKR cells, retrovirally induced mutant CHO-CDT^{R}F1 cells, and CHO-CDT^{R}F1 cells expressing Derl2 after intoxication with Aa-CDT (a), Hd-CDT (b), Ec-CDT (c) and Cj-CDT (d). Intoxication was performed similar to figure 5.1, data are representative of at least three independent experiments performed in triplicate, percent viability is normalized to unintoxicated controls and error bars indicate standard error.

5.4.2 Derl2 is Required for Translocation of CdtB from the ER

Although Derlins have been most intensely studied as important factors in the translocation of ERAD substrates, these proteins have also been implicated in the trafficking of the plant toxin ricin from endosomes to the Golgi apparatus (Dang et al., 2011). To identify which step of the CDT retrograde trafficking pathway was blocked in Derl2-deficient cells, the intracellular trafficking of Hd-CDT in parental A745TKR and mutant CHO-CDT^{R}C1 cells was assessed as a function of time. After 10 min of intoxication, Hd-CdtB was clearly internalized into all the cell types (Figure 5.4, 5.5). However, after 60 min, significantly more CdtB had localized to the nucleus of the parental A745TKR cells, than in the Derl2-deficient CHO-CDT^{R}C1 and CHO-CDT^{R}F1 cells (Figure 5.4, 5.5). In the CHO-CDT^{R}C1 and CHO-CDT^{R}F1 cells, Hd-CdtB was clearly localized to the ER, even after 60 min, but nearly absent within the ER of the parental A745TKR cells (Figure 5.4, 5.5). Together, these data support a model that Derl2 is required for retrograde translocation of Hd-CdtB from the ER lumen.

5.4.3 Retrotranslocation of CdtB is Distinct from Previously Characterized ERAD Substrates

Derlins have been implicated in retrotranslocation of misfolded proteins out of the ER [30,31]. In order to evaluate whether Derl2 might function by a similar mechanism to retrotranslocate CDTs, we investigated the importance of several Derlin functional motifs required for the retrotranslocation of previously characterized ERAD substrates.

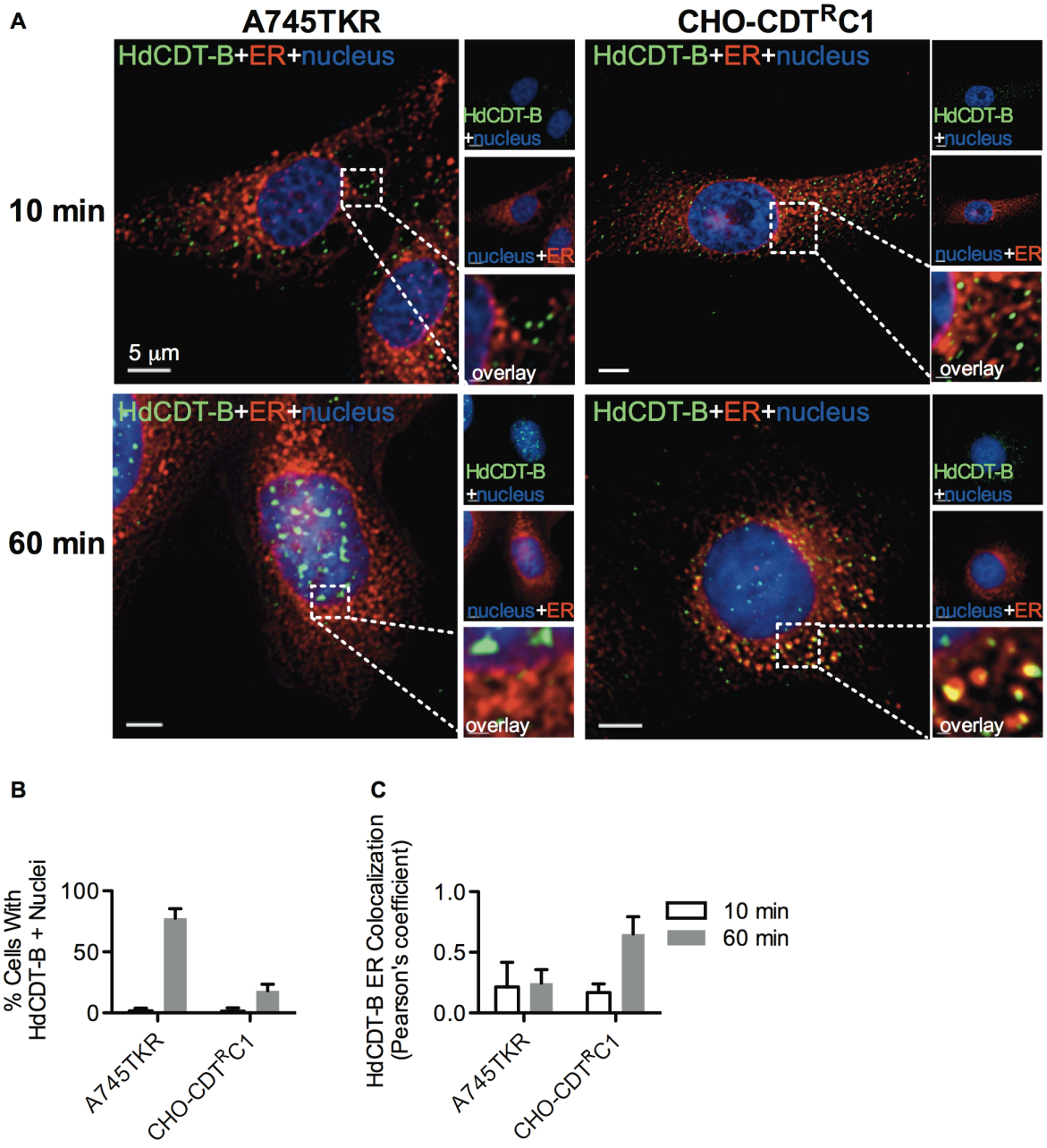
A
A745TKR
CHO-CDTRC1
10 min
60 min
HdCDT-B+ER+nucleus
HdCDT-B +nucleus
nucleus+ER
overlay
5 μm
B
% Cells With HdCDT-B + Nuclei
100
50
0
A745TKR
CHO-CDTRC1
C
HdCDT-B ER Colocalization (Pearson's coefficient)
1.0
0.5
0.0
10 min
60 min

Figure 5.4. Retrograde trafficking of Hd-CDT in Derl2 deficient cells is blocked at the endoplasmic reticulum.
(a) A745TKR and CHO-CDT^{R}C1 cells were incubated with Hd-CDT on ice, washed and incubated at 37 °C for 10 or 60 min. Cells were then fixed and stained with DAPI (nuclei, blue), Concanavalin A (ER, red) and α-Hd-CdtB (green) antibody. White scale bars indicate 5 μm. (b,c) Quantification of microscopy results comparing the percentage of cells with at least one green puncta localized to the nucleus or Pearson's coefficient values indicating colocalization of the Hd-CdtB signal with the ER marker. Images and quantitation are representative of those collected from a total of 30 randomly chosen cells analyzed during three independent experiments and error bars represent standard deviations.

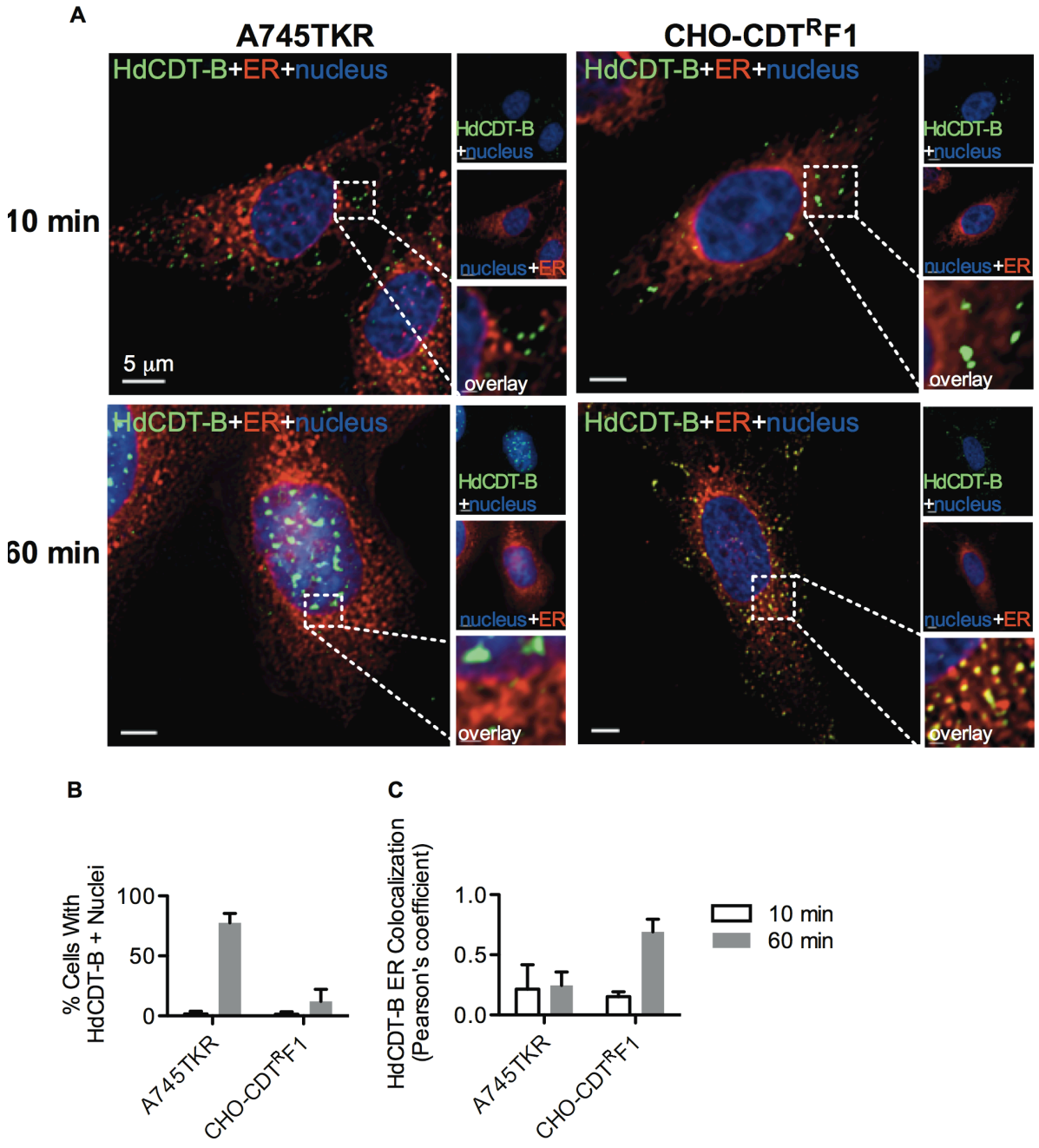
A
A745TKR
CHO-CDTRF1
10 min
60 min
HdCDT-B+ER+nucleus
HdCDT-B +nucleus
nucleus+ER
overlay
5 μm
B
% Cells With HdCDT-B + Nuclei
100
50
0
A745TKR
CHO-CDTRF1
C
HdCDT-B ER Colocalization (Pearson's coefficient)
1.0
0.5
0.0
10 min
60 min

Figure 5.5. Similar to CHO-CDT^{R}C1 cells, Hd-CDT trafficking in the CHO-CDT^{R}F1 cell line is blocked at the endoplasmic reticulum.
(a) A745TKR and CHO-CDT^{R}F1 cells were incubated with Hd-CDT on ice, washed and incubated at 37 °C for 10 or 60 min. Cells were then fixed and stained with DAPI (nuclei, blue), Concanavalin A (ER, red) and α-Hd-CdtB (green) antibody. White scale bars indicate 5 μm. (b,c) Quantification of microscopy results comparing the percentage of cells with at least one green puncta localized to the nucleus or Pearson's coefficient values indicating colocalization of the Hd-CdtB signal with the ER marker. Images and quantitation are representative of those collected from a total of 30 randomly chosen cells analyzed during three independent experiments and error bars represent standard deviations. A745TKR data from figure 5.4 is shown for comparison.

A carboxyl terminal SHP box (FxGxGQRn, where n is a non-polar residue) was recently demonstrated to be required for the interaction of Derlins with the AAA ATPase p97 [32], which provides energy to extract ERAD substrates from the lumen into the cytosol [33,34,35]. To assess the importance of p97-Derl2 interactions for the escape of CdtB from the cytosol, we overexpressed Derl2 with a deletion of the C-terminus (Derl2ΔC) that removes the SHP box. Additionally, we overexpressed a dominant negative form of Derl2 with a C-terminal GFP tag (Derl2-GFP)[26,30]. Similar to what had been shown previously for Derl2ΔC [32], we found that p97 was unable to bind Derl2-GFP (Figure 5.6A). Surprisingly, these studies revealed that despite failing to interact with p97, Derl2-GFP and Derl2ΔC both supported intoxication by CDT (Figure 5.6B-D). These results suggest that CDTs have evolved to use a Derl2-dependent retrotranslocation pathway that is independent of interaction between Derl2 and p97.

We next evaluated the importance of a second functional domain required for Derl2-mediated retrotranslocation of ERAD substrates. Derlins were recently classified as members of the rhomboid protease family of proteins, although they lack key residues required for proteolytic activity (Greenblatt et al., 2011). Rhomboid proteases are unique in that they contain an aqueous membrane-embedded cavity that allows for hydrolytic catalysis within the lipid bilayer (Wang et al., 2006). Similar to other rhomboid proteases, Derl2 contains a “WR motif” (Q/ExWRxxS/T) in the sequence between the first and second transmembrane domains.

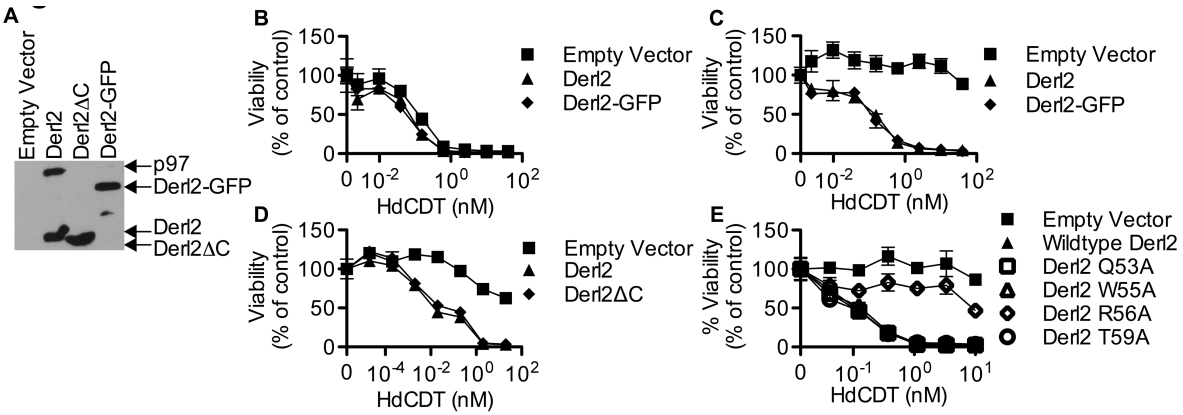

Figure 5.6 The interaction of Derl2 and p97 is not required for CDT intoxication.

(a) Derl2-GFP fails to bind p97, similar to Derl2ΔC. 293 cells were transfected with vectors encoding S-tagged versions of the indicated forms of Derl2. After 3 days, the cells were lysed and western blot was performed on S-protein precipitates with α-p97 and α-S-tag antibodies (b) Overexpression of Derl2-GFP does not affect Hd-CDT intoxication of parental A745TKR cells. Parental A745TKR cells expressing empty vector, Derl2 or Derl2-GFP were intoxicated with Hd-CDT, similar to figure 5.1. (c) Derl2-GFP complements the Hd-CDT resistance of CHO-CDT^{R}C1 to the same level as does Derl2. CHO-CDT^{R}C1 cells expressing empty vector, Derl2 and Derl2-GFP were intoxicated similar to figure 5.1. (d) Derl2ΔC complements the resistance to Hd-CDT. CHO-CDT^{R}C1 cells expressing empty vector, Derl2 and Derl2ΔC were intoxicated similar to figure 5.1. (e) The Derl2 WR motif is not required for intoxication by Hd-CDT. CHO-CDT^{R}C1 cells expressing empty vector, wildtype Derl2, Derl2 Q53A, Derl2 W55A, Derl2 R56A and Derl2 T59A were intoxicated similar to figure 5.1. Data are representative of at least three independent experiments performed in triplicate, percent viability is normalized to unintoxicated controls and error bars indicate standard error.

This WR motif protrudes laterally into the bilayer and plays a role in rearrangement of the local lipid environment (Wang et al., 2006; Wu et al., 2006). Mutation of WR motif residues in Derl1 renders it unable to retrotranslocate a constitutively misfolded protein to the cytosol for proteosomal degradation; in fact, overexpression of a Derl1 WR motif point mutant acts in a dominant negative fashion (Greenblatt et al., 2011). To test for a role for the WR motif in CDT entry, Derl2 variants with single point mutations in the residues that comprise the WR motif were expressed in Derl2 deficient CHO-CDT^{R}C1 cells. Expression of Derl2 variants Q53A, W55A and T59A complemented the resistance to Hd-CDT in CHO-CDT^{R}C1 cells to the same levels as that of wildtype Derl2 (Figure 5.6E). A single point mutant in the WR domain (R56A) failed to complement CHO-CDT^{R}C1 cells (Figure 5.6E), but this mutant was not expressed (Figure 5.7), and therefore no conclusion can be made regarding a role for this residue. These data suggests that although the WR motif is required for retrotranslocation of misfolded proteins by Derl1 (Greenblatt et al., 2011), it is not required for retrotranslocation of CDT.

5.4.4 Role for Derl2 in Intoxication by Ricin

Similar to CDT, several other protein toxins such as ricin, *Pseudomonas aeruginosa* exotoxin A, Shiga toxin and cholera toxin rely on retrograde trafficking from the cell surface through the ER in order to gain access to the cytoplasm (Sandvig and van Deurs, 2005; Slominska-Wojewodzka et al., 2006).

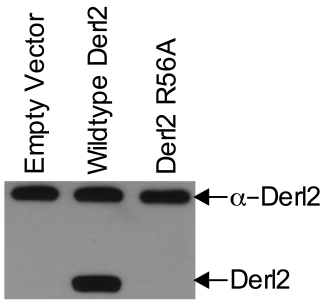

Figure 5.7 Derl2 R56A is not expressed in CHO-CDT^{R}C1 cells.
Western blot was performed on α-Derl2-precipitated protein from normalized cell lysates from CHO-CDT^{R}C1 cells transduced with empty vector, wildtype Derl2 or Derl2 R56A.

Recently, RNAi-mediated repression of members of the Derlin family was shown to cause a slight resistance to ricin (Dang et al., 2011; Moreau et al., 2011) via reduced trafficking from endosomes to the Golgi (Dang et al., 2011). Similarly, the Derl2 deficient mutant cell line CHO-CDT^{R}C1 displayed four-fold resistance to ricin, which was complemented by transduction with Derl2 (Figure 5.8A). This low-level resistance to ricin suggests that Derl2 contributes to, but is not an absolute requirement for ricin intoxication. In contrast, a high level of resistance to CDT resulted from Derl2 deficient CHO-CDT^{R}C1 and CHO-CDT^{R}F1 cells. This difference between ricin and CDT may result from the distinct steps of intoxication in which Derl2 functions to support cellular entry of these toxins (Dang et al., 2011). Interestingly, the novel SHP box- and WR motif-independence characterized for CDT was shared with ricin. Derl2ΔC and Derl2 WR mutants were able to restore sensitivity to Derl2 deficient CHO-CDT^{R}C1 cells (Figure 5.8B-C), suggesting that Derl2 may have multiple functions that are independent of the conserved WR motif and SHP box-mediated interactions with p97.

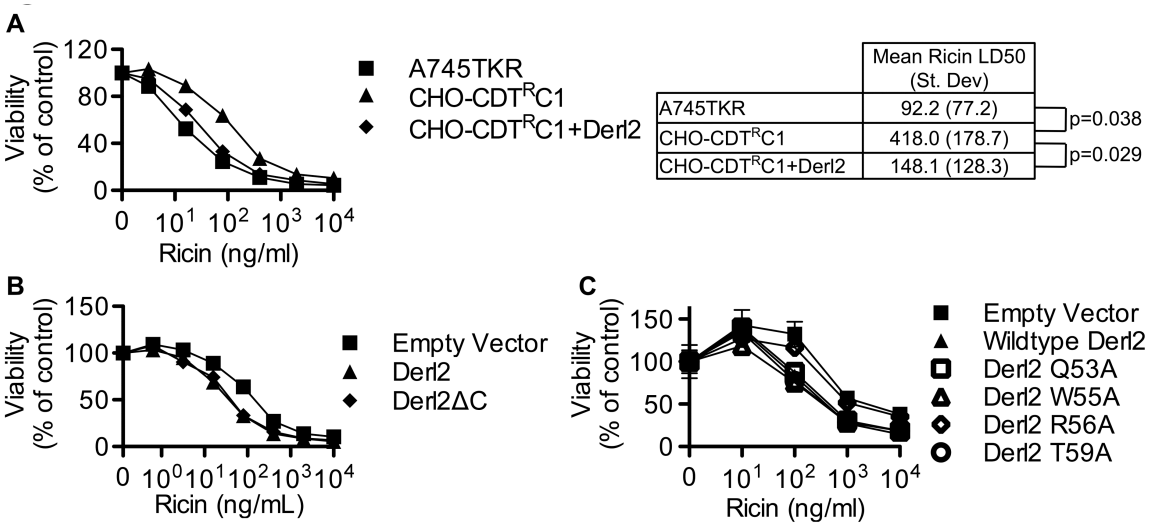

Figure 5.8 Derl2 deficiency causes resistance to ricin, independent of the interaction with p97 and the WR motif.

(a) Derl2 deficiency causes resistance to ricin. A745TKR cells, CHO-CDT^{R}C1 cells, and CHO-CDT^{R}C1 cells expressing Derl2 were seeded in a 384-well plate (1 x 10^3 cells/well) and allowed to adhere overnight, followed by 48 hour intoxication with ricin and quantitation of viability using ATPlite 1-step reagent (Perkin Elmer). Ricin LD_{50} values were calculated from three independent experiments and paired t-test was performed to calculate two tailed p-values. (b) Derl2ΔC complements the resistance to ricin. CHO-CDT^{R}C1 cells expressing empty vector, Derl2 and Derl2ΔC were intoxicated similar to (a). (c) The Derl2 WR motif is not required for intoxication by ricin. CHO-CDT^{R}C1 cells expressing empty vector, wildtype Derl2, Derl2 Q53A, Derl2 W55A, Derl2 R56A and Derl2 T59A were intoxicated similar to (a). Data are representative of at least three independent experiments performed in triplicate, percent viability is normalized to unintoxicated controls and error bars indicate standard error.

5.5 DISCUSSION

In order to gain access to their intracellular targets, retrograde trafficking toxins bind the plasma membrane, are endocytosed and trafficked though endosomes, the Golgi and ultimately the ER. At this point they must cross the formidable barrier posed by the host cellular membrane. The mechanism of this translocation across the ER membrane is poorly understood, but the current dogma is that retrograde trafficking toxins commandeer the host ERAD pathway to cross the ER membrane, thereby gaining access to the cytosol. This model is supported by studies on ricin and Shiga toxin that revealed roles for proteins involved in substrate recognition and unfolding of ERAD substrates (Day et al., 2001; Slominska-Wojewodzka et al., 2006; Spooner et al., 2004). In addition, Sec61 and members of the HRD ubiquitin ligase complex, Hrd1 and Sel1L, were shown to contribute to retrotranslocation of ricin (Li et al., 2010; Redmann et al., 2011; Simpson et al., 1999). However, a role for the core ERAD machinery in retrotranslocation of all other retrograde trafficking toxins is largely unknown. A genome-wide RNAi screen recently found that knockdown of the Sec61 translocon resulted in reduced intoxication by *Pseudomonas aeruginosa* exotoxin A and Shiga toxin (Moreau et al., 2011). However, repression of Sec61 may have indirect effects on retrotranslocation by reducing levels of proteins required for ERAD (Simpson et al., 1999). Knockdown of Derlins 1-3 led to resistance to ricin (Moreau et al., 2011), though it was recently shown that Derlins support ricin intoxication by affecting endosome to Golgi trafficking upstream of ERAD (Dang et al., 2011). Derl1 was also implicated in

retrotranslocation of cholera toxin (Bernardi et al.; Dixit et al., 2008); however, recent data question the relevance of Derl1 in cholera intoxication (Saslowsky et al., 2010). Here we provide evidence that a core component of the ERAD machinery, Derl2, is required for retrotranslocation of four distinct CDTs. This represents the first example of an ERAD component whose repression leads to complete resistance to retrograde trafficking toxins.

In addition to identifying Derl2 as a novel host factor usurped by CDTs to gain access to the host cytosol, the studies presented here provide insight into the mechanism by which Derlin-GFP fusions act as dominant negative proteins. These constructs have been used to study the role of Derlin family members in retrograde translocation of misfolded proteins, cytomegalovirus mediated degradation of class I MHC, infection by murine polyomavirus, and intoxication by ricin and cholera toxin (Bernardi et al., 2008; Greenblatt et al., 2011; Lilley et al., 2006; Lilley and Ploegh, 2004; Slominska-Wojewodzka et al., 2006); however, the mechanism by which these constructs inhibit ERAD function was unknown. Interestingly, overexpression of Derl1-GFP or Derl2-GFP was previously shown to have no effect on ricin or CDT intoxication of HeLa cells (Guerra et al., 2005; Slominska-Wojewodzka et al., 2006). Similarly, we found that overexpression of Derl2-GFP had no effect on CDT intoxication of parental A745TKR cells (Figure 4b). Rather, overexpression of Derl2-GFP actually complemented sensitivity to CDT in Derl2-deficient CHO-CDT^{R}C1 cells. Expression of Derl2ΔC complemented resistance to both ricin and CDT. The data presented here suggest that Derlin-GFP constructs act in a dominant negative manner by blocking interactions mediated by the C-terminus such as SHP box-

mediated interactions with p97, and therefore may only exert dominant negative effects on ERAD and trafficking processes that require these interactions.

Previous somatic cell genetic screens identified twelve host genes required for intoxication by CDT and ricin, but failed to identify Derl2 (Carette et al., 2009; Carette et al., 2011). The reason for this difference is unclear, though any single genetic model system is unlikely to provide a complete picture of such a complex biological process. Indeed, the host genes identified thus far only begin to explain the host processes required for cellular binding and entry by CDTs. Only two host genes identified thus far, sphingomyelin synthase 1 (SGMS1)(Carette et al., 2011) and Derl2 (Fig's 1, 2), are required for intoxication by all four CDTs described here. Future studies will likely identify many more host requirements for this family of toxins and provide further insight into their cellular entry pathways.

5.6 EXPERIMENTAL PROCEDURES

Tissue Culture

Chinese hamster ovary cells (CHO) and CHO derivatives were maintained in F-12 media (Gibco) supplemented with 10% fetal bovine serum (Sigma Aldrich), 100 U/ml penicillin, 100 µg/ml streptomycin, 5 mM L-glutamine (Invitrogen) and 1 µg/ml doxycycline (Sigma Aldrich). HeLa cells (American Type Culture Collection) were maintained in Dulbecco's Modified Eagle Medium (DMEM; Cellgro) containing 25 mM HEPES, 4.5 g/l sodium pyruvate, 4.5 g/l glucose, 10% fetal bovine serum (Sigma Aldrich), 100 U/ml penicillin, 100 µg/ml streptomycin, and 5 mM L-glutamine (Invitrogen). 293 cells (American Type Culture Collection) were maintained similar to

HeLa, but with the addition of 1% non-essential amino acids (Gibco). All cells were cultured at 37ºC in a humid atmosphere containing 5% CO_2.

Selection of CDT-resistant clones

To isolate chemically mutagenized CDT-resistant clones, ten pools of CHO-pgs A745 cells (A745, provided by Jeff Esko, UCSD) were treated with ICR191 (Sigma Aldrich) at a concentration high enough to kill 90% of the cells (Bradley et al., 2001). The resulting cells were counted, seeded at 1 x 10^6 cells per 10 cm plate and selected with 20 nM Aa-CDT. Resulting resistant cells were subjected to limiting dilutions to obtain single cell clones, expanded and reselected with Aa-CDT.

Selection of retrovirally mutagenized CDT-resistant clones was performed similar to Banks and Bradley (Banks and Bradley, 2007). Briefly, an Hd-CDT-sensitive clonal A745 cell line expressing tetR-KRAB (A745TKR) was established. Ten pools of 1 x 10^6 A745TKR parental cells were mutagenized by transduction with murine leukemia virus encoding the transcription response element $TetO_7$ in the long terminal repeat (pCMMP.GFP-NEO-TRE) at a multiplicity of infection of 0.1. These pools were transcriptionally repressed at proviral integration sites for 96 hours in the absence of doxycycline then selected with 5nM Hd-CDT for 24 h. After selection, two of the ten pools yielded colonies; these colonies were picked, expanded and reselected with Hd-CDT. None of the CDT-resistant clones displayed doxycycline dependant sensitivity to CDT, so they were further maintained in the presence of doxycycline.

Intoxication assays

Mammalian cells were trypsinized, counted and seeded at approximately 1 x 10^3 cells per well in 384-well plates. The following day, medium was removed and toxin containing medium was added for 48 h, followed by addition of ATPlite 1-step reagent (Perkin Elmer). Recombinant CDTs were cloned, expressed, and purified as described previously (Eshraghi et al., 2010) and ricin was purchased commercially (List Biological Laboratories). Each biological replicate intoxication was performed in triplicate. Analysis of intoxication was performed either by quantitation of pH2AX immunofluorescence (as described previously (Eshraghi et al., 2010)) or by using ATPlite reagent (Perkin Elmer) according to manufacturer recommendations. Intoxication data obtained by ATPlite reagent was normalized by dividing the luminescence relative light unit (RLU) signal of each replicate by the average of the unintoxicated control cells. All results presented are representative of at least three biological replicates.

Sequence capture mediated inverse PCR

In order to identify the location of the provirus in the CDT-resistant clones, genomic DNA was purified from each clone according to manufacturer recommendations (Qiagen), followed by digestion of 2 µg of genomic DNA with BamHI restriction enzyme (New England Biolabs). Digested genomic DNA was purified by column chromatography (Qiagen) and resuspended in 100 mM Tris-HCl, 150 mM NaCl, 50 mM EDTA, pH 7.5, containing 10 pmol biotinylated oligonucleotide complimentary to the 3' pCMMP long terminal repeat (Sigma Aldrich;

[Biotin]GTACCCGTGTTCTCAATAAACCCTC). The samples were heated to 95 ºC for 5 minutes then plunged on ice, followed by end over end rotation at 55 ºC for 14 hours.

Streptavidin coated magnetic beads were washed three times with 10 mM Tris-HCl, 2 M NaCl, 1 mM EDTA, pH 7.5 and added to the samples. Samples were vortexed for 0.5 hours at room temperature then the beads were immobilized on a magnet and supernatant removed, followed by three washes with 5 mM Tris-HCl, 1 M NaCl, 0.5 mM EDTA, pH 7.5 and resuspension in 100 µL water. The tubes were heated to 95 ºC in the presence of the magnet and the supernatant was removed and self-circularized with T4 DNA ligase according to manufacturer recommendations (Fermentas). PCR was performed using the following primers (GAGGGTTTATTGAGAACACGGGTAC and GTGATTGACTACCCGTCAGCGGGGTC) followed by nested PCR with the following primers (CGAGACCACGAGTCGGATGCAACTGC and GTTCCTTGGGAGGGTCTCCTCTG). Amplicons were run in a 1% agarose gel, bands were cut out, column purified (Qiagen) and sequenced (Genewiz).

Subcloning and Expression of Derlins

Murine Derl1 and Derl2 cDNA was subcloned by PCR amplifying using the following primers (restriction sites and kozak consensus sequences shown underlined and capitalized, respectively): Derl1 forward aaaagatctTCCACCATGtcggacatcggggactggttcagg; Derl1 reverse aaactcgagctggtctccaagtcggaagc; Derl2 forward

aaaagatctTCCACCATGgcgtaccagagcctccggctgg; Derl2 reverse aaactcgagcccaccaaggcgctggccctcacc. The amplicons and the empty retroviral vector pMSCVpuro (Clontech) were digested with BglII and XhoI (New England Biolabs), gel purified (Qiagen) and ligated with T4 DNA ligase (Fermentas).

In order to generate retrovirus, plasmid DNA was purified and transfected into human 293 cells along with MLV gag/pol and vesicular stomatitis virus G-spike protein expression plasmids, as previously described (Banks and Bradley, 2007). 48 and 72 hours later, resulting retroviral particles were harvested, filter sterilized and used to transduce target cells in the presence of 8 µg/ml polybrene (Sigma Aldrich).

PCR confirmation of MLV integration at Derl2 locus

In order to confirm that the MLV proviral integration occurred at the Derl2 locus, PCR amplification was performed on the genomic DNA from the retrovirally induced CDT resistant clones and the parental A745TKR cells. The primers used for amplification annealed to the fifth exon in the Derl2 open reading frame (CCATGAGCACCCAGGGCAGG) and either forward proviral elements (TGATCGCGCTTCTCGTTGGG) or reverse proviral elements (AGCGCATCGCCTTCTATCGC).

Immunoprecipitation western blot

Approximately 1 x 10^7 cells were lysed in 1% digitonin, 25 mM Tris-HCl, 150 mM NaCl, 5 mM EDTA, 1 U/ml DNAse (Promega), and protease inhibitors (Roche), pH 7.0. The lysates were centrifuged at 14,000 x G and supernatants were mixed

with 1 µg/ml α-Derl2 antibody (Sigma Aldrich) and incubated overnight at 4 °C with agitation. Protein-A sepharose beads (Santa Cruz Biotechnology) were washed, blocked with 5% bovine serum albumin (EMD Millipore) and incubated with the lysates for 1 hour at room temperature with agitation. Following incubation, the beads were washed three times, mixed with SDS reducing buffer and subjected to SDS-PAGE followed by transfer to PVDF membranes. Membranes were probed with α-Derl2 antibody followed by HRP conjugated α-rabbit antibody (Invitrogen) to allow detection.

siRNA

In a six well plate, 10 pmol of siRNAs targeting Derl2 (Qiagen) or scrambled siRNA (Ambion) were added to 5 µL Lipofectamine RNAiMax (Invitrogen) in a total volume of 500 µL OptiMEM media (Gibco), mixed thoroughly and incubated at room temperature for 15 min. HeLa cells were trypsinized, counted, diluted in DMEM containing 12% fetal bovine serum and 1.5 x 10^5 cells were added to the plate in a total volume of 2 ml, resulting in a total concentration of 5 nM siRNA. Two days after siRNA transfection, the cells were trypsinized, counted, reseeded into a 384-well plate and intoxicated as described above.

Fluorescence Microscopy

Cells on 8 well-chambered slides (Nunc; Rochester, NY) were pre-chilled on ice, and after 30 minutes further incubated on ice with 200 nM Hd-CDT for 30 minutes. The monolayers were washed with ice-cold PBS pH 7.4 (Lonza,

Walkersville, MD), and then incubated at 37 °C with complete medium. After 60 minutes at 37 °C, the cells were washed with ice-cold PBS pH 7.4, and fixed with ice-cold 2% formaldehyde (Sigma). After fixing for 30 min at room temperature, the cells were permeabilized by incubating in PBS 7.4 containing 0.1% Triton X-100 for 15 minutes, and blocked with 3% BSA (Sigma) for 30 minutes. To probe for Hd-CdtB localization to the nucleus, cells were incubated with rabbit polyclonal α-Hd-CdtB antibodies (generated by Immunological Resource Center, University of Illinois, Urbana, IL) at 4 °C overnight, followed by incubation with goat α-rabbit Alexa Fluor 488-labeled antibody (Invitrogen) at room temperature for 2 hours. The cells were counter stained for the nucleus and endoplasmic reticulum with DAPI (Invitrogen) and Concanavalin A conjugated with Alexa Fluor 594 (Invitrogen), respectively, for 30 minutes at room temperature. The slides were mounted with ProLong Gold antifade reagent (Invitrogen) and images were collected using DIC/fluorescence microscopy and deconvoluted by using SoftWoRX constrained iterative deconvolution tool (ratio mode), and analyzed using Imaris 5.7 (Bitplane AG, Zurich, Switzerland). For each cell, images were collected from an average of 30 z-planes, each at a thickness of 0.2 μm. Nuclear localization analysis was conducted by using the DeltaVision SoftWoRx 3.5.1 software suite. For nuclear localization, the percentage of Hd-CdtB localization into nucleus in parental and Derl2 deficient cells were calculated from approximately 30 cells from each group over three independent experiments. To test the colocalization of Hd-CdtB with the endoplasmic reticulum, results were expressed as the localization index, which was derived from calculating the Pearson's coefficient of correlation values, which

represent the colocalization of Hd-CdtB and the ER in each z plane of the cell. In these studies, a localization index value of 1.0 indicates 100% localization of Hd-CdtB to the ER, whereas a localization index of 0.0 indicates the absence of Hd-CdtB localization to the ER. The localization index was calculated from the analysis of a total of 30 images collected over three independent experiments.

Coimmunoprecipitation of Derl2 and p97

HEK293 cells were trypsinized, counted, seeded at 1 x 10^6 per 10 cm plate and allowed to adhere overnight. The following day, the standard calcium phosphate method was used to transfect 10 µg of plasmid DNA into the 293 cells. 72 hours post-transfection, the cells were lysed in 1% digitonin lysis buffer (as described above). S-protein agarose beads were blocked in 5% bovine serum albumin for 1 hour and incubated with the lysates overnight at 4 °C. The beads were washed with 0.1% digitonin, 25 mM Tris-HCl, 150 mM NaCl, 5 mM EDTA, pH 7.0 and protease inhibitors and then mixed with 1X SDS reducing buffer. Samples were subjected to SDS-PAGE, transferred to PVDF membranes then probed with rabbit α-S-tag antibody (Cell Signal Technologies) and mouse α-p97 antibody (Santa Cruz Biotechnology).

Statistical Analysis

The half maximal lethal dose (LD_{50}) of ricin intoxication was calculated by log transforming ricin concentrations and calculating sigmoidal variable slope dose response curves using the least squares (ordinary) fitting method. Paired t-tests

were performed on average LD_{50} values calculated from three independent experiments performed in triplicate to determine two tailed p-values. Data analysis was performed using Prism version 5.0d (GraphPad software).

5.7 BIBLIOGRAPHY

Ahmed, H.J., Svensson, L.A., Cope, L.D., Latimer, J.L., Hansen, E.J., Ahlman, K., Bayat-Turk, J., Klamer, D., and Lagergard, T. (2001). Prevalence of cdtABC genes encoding cytolethal distending toxin among Haemophilus ducreyi and Actinobacillus actinomycetemcomitans strains. J Med Microbiol *50*, 860-864.

Banks, D.J., and Bradley, K.A. (2007). SILENCE: a new forward genetic technology. Nat Methods *4*, 51-53.

Bernardi, K.M., Forster, M.L., Lencer, W.I., and Tsai, B. (2008). Derlin-1 facilitates the retro-translocation of cholera toxin. Mol Biol Cell *19*, 877-884.

Blanke, S.R. (2006). Portals and Pathways: Principles of Bacterial Toxin Entry into Host Cells. Microbe *1*, 26-32.

Bradley, K.A., Mogridge, J., Mourez, M., Collier, R.J., and Young, J.A. (2001). Identification of the cellular receptor for anthrax toxin. Nature *414*, 225-229.

Cao, L., Bandelac, G., Volgina, A., Korostoff, J., and DiRienzo, J.M. (2008). Role of aromatic amino acids in receptor binding activity and subunit assembly of the

cytolethal distending toxin of Aggregatibacter actinomycetemcomitans. Infect Immun *76*, 2812-2821.

Cao, L., Volgina, A., Huang, C.M., Korostoff, J., and DiRienzo, J.M. (2005). Characterization of point mutations in the cdtA gene of the cytolethal distending toxin of Actinobacillus actinomycetemcomitans. Mol Microbiol *58*, 1303-1321.

Carette, J.E., Guimaraes, C.P., Varadarajan, M., Park, A.S., Wuethrich, I., Godarova, A., Kotecki, M., Cochran, B.H., Spooner, E., Ploegh, H.L.*, et al.* (2009). Haploid genetic screens in human cells identify host factors used by pathogens. Science *326*, 1231-1235.

Carette, J.E., Guimaraes, C.P., Wuethrich, I., Blomen, V.A., Varadarajan, M., Sun, C., Bell, G., Yuan, B., Muellner, M.K., Nijman, S.M.*, et al.* (2011). Global gene disruption in human cells to assign genes to phenotypes by deep sequencing. Nat Biotechnol *29*, 542-546.

Damek-Poprawa, M., Jang, J.Y., Volgina, A., Korostoff, J., and DiRienzo, J.M. (2012). Localization of Aggregatibacter actinomycetemcomitans cytolethal distending toxin subunits during intoxication of live cells. Infect Immun *80*, 2761-2770.

Dang, H., Klokk, T.I., Schaheen, B., McLaughlin, B.M., Thomas, A.J., Durns, T.A., Bitler, B.G., Sandvig, K., and Fares, H. (2011). Derlin-dependent retrograde transport from endosomes to the Golgi apparatus. Traffic *12*, 1417-1431.

Day, P.J., Owens, S.R., Wesche, J., Olsnes, S., Roberts, L.M., and Lord, J.M. (2001). An interaction between ricin and calreticulin that may have implications for toxin trafficking. J Biol Chem *276*, 7202-7208.

Dixit, G., Mikoryak, C., Hayslett, T., Bhat, A., and Draper, R.K. (2008). Cholera toxin up-regulates endoplasmic reticulum proteins that correlate with sensitivity to the toxin. Exp Biol Med (Maywood) *233*, 163-175.

Elwell, C.A., and Dreyfus, L.A. (2000). DNase I homologous residues in CdtB are critical for cytolethal distending toxin-mediated cell cycle arrest. Mol Microbiol *37*, 952-963.

Eshraghi, A., Maldonado-Arocho, F.J., Gargi, A., Cardwell, M.M., Prouty, M.G., Blanke, S.R., and Bradley, K.A. (2010). Cytolethal distending toxin family members are differentially affected by alterations in host glycans and membrane cholesterol. J Biol Chem *285*, 18199-18207.

Fox, J.G., Rogers, A.B., Whary, M.T., Ge, Z., Taylor, N.S., Xu, S., Horwitz, B.H., and Erdman, S.E. (2004). Gastroenteritis in NF-kappaB-deficient mice is produced with

wild-type Camplyobacter jejuni but not with C. jejuni lacking cytolethal distending toxin despite persistent colonization with both strains. Infect Immun *72*, 1116-1125.

Gargi, A., Reno, M., and Blanke, S.R. (2012). Bacterial toxin modulation of the eukaryotic cell cycle: are all cytolethal distending toxins created equally? Front Cell Infect Microbiol *2*, 124.

Ge, Z., Feng, Y., Whary, M.T., Nambiar, P.R., Xu, S., Ng, V., Taylor, N.S., and Fox, J.G. (2005). Cytolethal distending toxin is essential for Helicobacter hepaticus colonization in outbred Swiss Webster mice. Infect Immun *73*, 3559-3567.

Ge, Z., Rogers, A.B., Feng, Y., Lee, A., Xu, S., Taylor, N.S., and Fox, J.G. (2007). Bacterial cytolethal distending toxin promotes the development of dysplasia in a model of microbially induced hepatocarcinogenesis. Cell Microbiol *9*, 2070-2080.

Greenblatt, E.J., Olzmann, J.A., and Kopito, R.R. (2011). Derlin-1 is a rhomboid pseudoprotease required for the dislocation of mutant alpha-1 antitrypsin from the endoplasmic reticulum. Nat Struct Mol Biol *18*, 1147-1152.

Guerra, L., Cortes-Bratti, X., Guidi, R., and Frisan, T. (2011). The biology of the cytolethal distending toxins. Toxins (Basel) *3*, 172-190.

Guerra, L., Nemec, K.N., Massey, S., Tatulian, S.A., Thelestam, M., Frisan, T., and Teter, K. (2009). A novel mode of translocation for cytolethal distending toxin. Biochim Biophys Acta *1793*, 489-495.

Guerra, L., Teter, K., Lilley, B.N., Stenerlow, B., Holmes, R.K., Ploegh, H.L., Sandvig, K., Thelestam, M., and Frisan, T. (2005). Cellular internalization of cytolethal distending toxin: a new end to a known pathway. Cell Microbiol *7*, 921-934.

Guidi, R., Guerra, L., Levi, L., Stenerlow, B., Fox, J.G., Josenhans, C., Masucci, M.G., and Frisan, T. (2013). Chronic exposure to the cytolethal distending toxins of Gram-negative bacteria promotes genomic instability and altered DNA damage response. Cell Microbiol *15*, 98-113.

Hebert, D.N., Bernasconi, R., and Molinari, M. (2010). ERAD substrates: which way out? Semin Cell Dev Biol *21*, 526-532.

Lara-Tejero, M., and Galan, J.E. (2000). A bacterial toxin that controls cell cycle progression as a deoxyribonuclease I-like protein. Science *290*, 354-357.

Li, S., Spooner, R.A., Allen, S.C., Guise, C.P., Ladds, G., Schnoder, T., Schmitt, M.J., Lord, J.M., and Roberts, L.M. (2010). Folding-competent and folding-defective forms of ricin A chain have different fates after retrotranslocation from the endoplasmic reticulum. Mol Biol Cell *21*, 2543-2554.

Lilley, B.N., Gilbert, J.M., Ploegh, H.L., and Benjamin, T.L. (2006). Murine polyomavirus requires the endoplasmic reticulum protein Derlin-2 to initiate infection. J Virol *80*, 8739-8744.

Lilley, B.N., and Ploegh, H.L. (2004). A membrane protein required for dislocation of misfolded proteins from the ER. Nature *429*, 834-840.

McAuley, J.L., Linden, S.K., Png, C.W., King, R.M., Pennington, H.L., Gendler, S.J., Florin, T.H., Hill, G.R., Korolik, V., and McGuckin, M.A. (2007). MUC1 cell surface mucin is a critical element of the mucosal barrier to infection. J Clin Invest *117*, 2313-2324.

McSweeney, L.A., and Dreyfus, L.A. (2005). Carbohydrate-binding specificity of the Escherichia coli cytolethal distending toxin CdtA-II and CdtC-II subunits. Infect Immun *73*, 2051-2060.

Moreau, D., Kumar, P., Wang, S.C., Chaumet, A., Chew, S.Y., Chevalley, H., and Bard, F. (2011). Genome-wide RNAi screens identify genes required for Ricin and PE intoxications. Dev Cell *21*, 231-244.

Nesic, D., and Stebbins, C.E. (2005). Mechanisms of assembly and cellular interactions for the bacterial genotoxin CDT. PLoS Pathog *1*, e28.

Nishikubo, S., Ohara, M., Ueno, Y., Ikura, M., Kurihara, H., Komatsuzawa, H., Oswald, E., and Sugai, M. (2003). An N-terminal segment of the active component of the bacterial genotoxin cytolethal distending toxin B (CDTB) directs CDTB into the nucleus. J Biol Chem *278*, 50671-50681.

Pickett, C.L., and Whitehouse, C.A. (1999). The cytolethal distending toxin family. Trends Microbiol *7*, 292-297.

Purdy, D., Buswell, C.M., Hodgson, A.E., McAlpine, K., Henderson, I., and Leach, S.A. (2000). Characterisation of cytolethal distending toxin (CDT) mutants of Campylobacter jejuni. J Med Microbiol *49*, 473-479.

Redmann, V., Oresic, K., Tortorella, L.L., Cook, J.P., Lord, M., and Tortorella, D. (2011). Dislocation of ricin toxin A chains in human cells utilizes selective cellular factors. J Biol Chem *286*, 21231-21238.

Sandvig, K., and van Deurs, B. (2005). Delivery into cells: lessons learned from plant and bacterial toxins. Gene Ther *12*, 865-872.

Saslowsky, D.E., Cho, J.A., Chinnapen, H., Massol, R.H., Chinnapen, D.J., Wagner, J.S., De Luca, H.E., Kam, W., Paw, B.H., and Lencer, W.I. (2010). Intoxication of zebrafish and mammalian cells by cholera toxin depends on the flotillin/reggie proteins but not Derlin-1 or -2. J Clin Invest *120*, 4399-4409.

Shenker, B.J., Hoffmaster, R.H., Zekavat, A., Yamaguchi, N., Lally, E.T., and Demuth, D.R. (2001). Induction of apoptosis in human T cells by Actinobacillus actinomycetemcomitans cytolethal distending toxin is a consequence of G2 arrest of the cell cycle. J Immunol *167*, 435-441.

Simpson, J.C., Roberts, L.M., Romisch, K., Davey, J., Wolf, D.H., and Lord, J.M. (1999). Ricin A chain utilises the endoplasmic reticulum-associated protein degradation pathway to enter the cytosol of yeast. FEBS Lett *459*, 80-84.

Slominska-Wojewodzka, M., Gregers, T.F., Walchli, S., and Sandvig, K. (2006). EDEM is involved in retrotranslocation of ricin from the endoplasmic reticulum to the cytosol. Mol Biol Cell *17*, 1664-1675.

Spooner, R.A., Watson, P.D., Marsden, C.J., Smith, D.C., Moore, K.A., Cook, J.P., Lord, J.M., and Roberts, L.M. (2004). Protein disulphide-isomerase reduces ricin to its A and B chains in the endoplasmic reticulum. Biochem J *383*, 285-293.

Thelestam, M., and Frisan, T. (2004). Cytolethal distending toxins. Rev Physiol Biochem Pharmacol *152*, 111-133.

Wang, Y., Zhang, Y., and Ha, Y. (2006). Crystal structure of a rhomboid family intramembrane protease. Nature *444*, 179-180.

Wu, Z., Yan, N., Feng, L., Oberstein, A., Yan, H., Baker, R.P., Gu, L., Jeffrey, P.D., Urban, S., and Shi, Y. (2006). Structural analysis of a rhomboid family intramembrane protease reveals a gating mechanism for substrate entry. Nat Struct Mol Biol *13*, 1084-1091.

Young, V.B., Knox, K.A., Pratt, J.S., Cortez, J.S., Mansfield, L.S., Rogers, A.B., Fox, J.G., and Schauer, D.B. (2004). In vitro and in vivo characterization of Helicobacter hepaticus cytolethal distending toxin mutants. Infect Immun *72*, 2521-2527.

5.8 ACKNOWLEDGMENTS

The authors declare that there are no conflicts of interest. This work was supported by the US National Institutes of Health (T32DE007296 and F31DE022485 to A.E. and R01GM098756 to K.A.B and S.R.B).

Chapter 6

Contributions to the field and future directions

The research presented in this dissertation has enhanced the understanding of multiple steps in the CDT intoxication pathway. The second chapter provided evidence that cell surface glycans do not serve as receptors for CDT. This challenged the previous dogma in the CDT field, which was based on hypotheses formed by several groups suggesting that the CDT binding subunits may bind host cell glycoconjugates {Hu, 2006;Hu, 2006;lara-tejero, 2001;Nesic,2004;Mcsweeney, 2005;Mise, 2005}. Work discussed in the fourth chapter tested the ability of a cell surface protein, previously identified in a screen for host factors that support CDT sensitivity {Carette, 2009}, to serve as a receptor for Ec-CDT. Data from numerous experiments with various forms of the protein tagged at either the N- or C-terminus suggest that overexpression of TMEM181 does not lead to increased sensitivity to CDT and question the model that this molecule is a receptor for Ec-CDT. Chapter 3 described the characterization of mutants isolated from a forward genetic screen and revealed that several were deficient in CDT trafficking between binding to the cell surface and trafficking to the nucleus, while another had a deficiency downstream of DNA damage that allowed it to escape apoptosis. Finally, by identifying Derl2 as required for CDT intoxication, chapter 5 showed that CDT utilizes the ERAD pathway to translocate out of the ER. Further, I show two Derl2 motifs that are required for ERAD of misfolded proteins and other retrograde trafficking toxins {Greenblat, 2011;Ye, 2001;Sato, 2006;Kothe, 2005} are not required for CDT translocation, suggesting that this is a novel mechanism of retrotranslocation in mammalian cells.

Advances in the understanding of CDT binding to the cell surface

Identification and characterization of factors that support binding to the cell surface has been an active area of investigation since the discovery of CDTs. Several reports have outlined the ability of host plasma membrane cholesterol, cell surface glycoproteins and glycosphingolipids to serve as receptors for CDT. By testing the ability of cholesterol supplementation to increase host cell sensitivity, I found that increasing plasma cholesterol resulted in increased sensitivity to some CDTs, but not to Cj-CDT. Subsequently, it was shown that cholesterol depletion results in resistance to Cj-CDT {Lin, 2011}. This suggests that plasma membrane cholesterol is important to intoxication by most, if not all, CDTs. Perturbations in plasma membrane cholesterol may alter lipid raft structure, which is required for CDT internalization {Guerra, 2005; Boesze-Battaglia, 2006;Carette, 2009}. It is yet unclear if alterations in sensitivity to CDT arise solely from cholesterol dependent changes in binding or if altering lipid raft structure also plays a role. The identification of a cholesterol recognition amino acid consensus (CRAC) sequence in Aa-CdtC and a non-traditional CRAC sequence in CdtC from *Haemophilus parasuis* suggests that cholesterol may play a role in the binding of CDTs to the host cell surface {Boesze-Battaglia, 2009;Zhou, 2012}. It is possible that other CDTs also contain non-traditional CRAC motifs, but have yet to be found. The presence of of non-traditional CRAC sequences in Hd-CDT and Ec-CDT would provide a mechanism behind the increased sensitivity of cholesterol-supplemented cells

presented in this dissertation. Regardless, these data indicate that host cellular cholesterol is an important factor governing sensitivity to several CDTs.

Prior to the work described in this dissertation, the dogma in the CDT field was that cell surface glycoconjugates were required for CDT binding. The CDT binding subunits contain lectin folds, similar to ricin, and a glycosylation inhibitor, tunicamycin, resulted in reduced sensitivity to CDT {Nesic, 2004;McSweeney, 2005}. Further, CDT had previously been shown to bind fucose and a fucose-specific lectin reduced sensitivity to CDT {McSweeney, 2005;Cao, 2005}. By using an exhaustive panel of genetically and phenotypically defined mutant cell lines deficient in glycosylation, I showed that no single class of glycoconjugate, including fucosylated glycans, were required for intoxication by CDT and therefore glycans do not serve as the sole receptor for CDT. In fact, many of these mutants that display reduced presentation of cell surface carbohydrates were hypersensitive to CDT. Further characterization revealed that mutants deficient in just terminal sialic acid were hypersensitive to Aa-CDT, Hd-CDT and Ec-CDT, suggesting that sialic acid may block access to the CDT receptor. Although fucose deficient cells were not resistant to intoxciation, overexpression of fucosyltransferase 1 resulted in hypersensitivity to CDT. By expressing fucosyltransferase 1 in parental and sialic acid deficient mutant cells, I characterized the mechanism behind fucosyltransferase 1-dependent hypersensitivity as being due to decreased cell surface sialic acid when fucosyltransferase was overexpressed. The identification of a cell surface receptor would allow the ability to test if sialic acid does, in fact, block access of CDT to the receptor.

One reason behind the investigation of glycans as CDT receptors was the ability of the glycosylation inhibitor tunicamycin to make cells resistant to CDT intoxication. Prior to the research presented in this dissertation, tunicamycin was shown to inhibit cholesterol biosynthesis; therefore, I hypothesized that tunicamycin could cause resistance to CDT via depletion of cholesterol. However, in my experimental system, tunicamycin had no effect on cellular cholesterol levels under conditions in which it caused resistance to CDT. This suggests that tunicamycin-dependent resistance to CDT may be due to a requirement for the CDT receptor to be glycosylated for proper folding and presentation on the cell surface. Again, the identification of a *bona fide* cell surface CDT receptor would allow the ability to test the requirement of the CDT receptor for glycosylation for proper folding and presentation on the cell surface.

Interestingly, although glycans may not serve as receptors for CDT, it seems that they potentiate sensitivity to CDT. The data above indicates that decreased cell surface presentation of complex glycans results in hypersensitivity to CDT. One of the CDT-resistant mutants isolated by chemical mutagenesis and selection with Aa-CDT, C02-2-2, was hyperglycosylated as judged by increased binding by seven fluorescently labeled lectins. Further, expression of Amylase-1 cDNA was shown to increase sensitivity to Aa-CDT, possibly via hydrolysis of higher order cell surface glycans to more simple carbohydrates. These data suggest that there is an inverse correlation between glycosylation and sensitivity to CDT.

When the paper identifying TMEM181 as the receptor for Ec-CDT was published {Carette, 2009}, the bacterial toxin community saw this as a big advance

for the CDT field. However, this paper and a second one in 2011 identifying a number of other host factors required for CDTs {Carette, 2011} lacked thorough mechanistic characterization. Since then, there have been no further reports showing how these genes support CDT intoxication. Although there were slight differences between the reported TMEM181 cDNA that caused hypersensitivity to Ec-CDT and the one we had custom synthesized, we were unable to show TMEM181 dependent hypersensitivity to CDT in over 40 experiments using various forms of TMEM181 with different tags at the N- and C-termini. Future studies to characterize the influence of TMEM181 expression on CDT intoxication would benefit the CDT community, as it seems that TMEM181 may not be a receptor

Advances in the understanding of CDT trafficking from the plasma membrane to the nucleus

In chapter 3, a forward genetic screen was performed, resulting in isolation of 61 CDT-resistant mutants with varying levels of resistance to Aa-CDT. All of these clones bound to Aa-CDT at equivalent or greater levels than parental cells. Five of these clones were characterized further to find that all of them had competent DNA damage responses, as judged by UV dependent phosphorylation of histone H2AX. Four of these mutants failed to induced phosphorylation of histone H2AX in response to CDT intoxication, suggesting that they were deficient in CDT trafficking from the plasma membrane to the nucleus. Further characterization of the mutant that displayed CDT-dependent H2AX phosphorylation but was able to avoid apoptosis could be interesting for the DNA damage community because this mutant

could identify a gene involved in DNA damage-mediated apoptosis. Based on these five clones, the predominant block to intoxication in the mutant clones appears to be at the level of trafficking from the plasma membrane to the nucleus.

Advances in the understanding of retrotranslocation of CDT from the ER lumen

Two independent forward genetic screens reported here identified Derl2 as a gene required for CDT intoxication. First, screening for cDNAs that were able to complement a chemically mutagenized CDT-resistant clone identified Derl2 as a cDNA that was able to increase sensitivity to Aa-CDT. Second, I discovered that Derl2 is required for CDT intoxication by retrovirally mutagenizing CHO cells, selecting with Hd-CDT and subsequently mapping of proviral integration sites. In both cases, the Derl2 deficient cells were resistant to the four CDTs tested. The requirement of Derl2 for CDT intoxication was not exclusive to CHO cells as siRNA-mediated knockdown of Derl2 in HeLa cells also resulted in CDT resistance. This work further characterized differences between Derl2 and a related protein, Derl1, by showing that they are not functionally redundant. Derl2 deficiency led to the inability of CDT to translocate out of the ER, which is consistent with previous reports outlining the role of derlin proteins in ERAD. This data demonstrated for the first time that CDT utilizes the ERAD pathway to escape from the lumen of the ER.

Motifs required for Derl2 mediated retrotranslocaton of other substrates were found to be dispensable for CDT intoxication. Expression of Derl2 with mutations in the WR domain, which facilitates a membrane embedded hydrophilic loop and is required for retrotranslocation of misfolded proteins, supports CDT intoxication in

Derl2 deficient cells at the same level as wildtype Derl2. Likewise, expression of a Derl2 C-terminal deletion, lacking a SHP box which mediates interaction with the AAA ATPase p97 to supply energy for dislocation, supports CDT intoxication at the same level as wildtype Derl2. This work has benefited the ERAD field by demonstrating for the first time a WR domain-independent function of Derl2. Further, this is the first time that Derl2 dependent retrotranslocation has been shown to be independent of interaction with p97.

Several plant and bacterial toxins are retrograde trafficked from the plasma membrane through the Golgi and ER before entering the cytosol. The current dogma is that these toxins utilize ERAD to gain access to downstream targets in the cytosol; however, the details of this mechanism and even the proteins involved are poorly defined. Data presented in chapter 6 suggest that other retrograde trafficking toxins, such as the plant toxin ricin, may also utilize Derl2 in a WR domain and p97 independent manner for trafficking.

Derlin C-terminal fusions with GFP/YFP have been widely used as dominant negative constructs to determine if various processes require derlin proteins. Derl2-GFP was previously reported to have no effect on CDT intoxication, leading to the conclusion that derlins are not involved in sensitivity to this family of toxins; however, the data presented in chapter 5 convincingly show that CDT retrotranslocation is Derl2 dependent. Further data presented in chapter 5 shows that the addition of GFP to the C-terminal tail of Derl2 resulted in the inability to bind p97. Expression of Derl2-GFP in Derl2-replete cells had no effect on CDT intoxication because the CDT intoxication mechanism is dependent on Derl2 but in a fashion independent of Derl2

interacting with p97. This suggests that although Derlin-GFP/YFP fusions may serve as dominant negative proteins for p97 dependent processes, they do not do so for p97 independent processes.

There is some contention in the CDT field about the mechanism of CDT trafficking from the lumen of the ER to the nucleus. One report suggests a direct ER to nucleus route. Another report identifies a nuclear localization signal on Ec-CDT, suggesting that CDT translocates to the cytoplasm and is subsequently trafficked to the nucleus via the nuclear pore complex. However, to date no reports have directly shown that CDT is trafficked through the cytoplasm. This is a gap in knowledge that if addressed would greatly benefit the CDT field. Since previous Derl2 substrates have been shown to traffic to the cytoplasm, the data presented here supports the latter model, but biochemical evidence of CDT trafficking through the cytoplasm would be the most convincing evidence. Further characterization of the interaction between Derl2 and CDT, i.e. whether direct interaction occurs and if so identification of amino acids involved, will provide a more mechanistic understanding of the role of Derl2 in retrotranslocation of CdtB.

Lastly, an animal model should be utilized to address the clinical significance of Derl2 in CDT intoxication. Several animal models have been used successfully in the CDT field and could be applied to Derl2 knockout mice, which have previously been generated {Dougan, 2011}. CDT expressing bacteria or recombinant CDT can be orally gavaged into adult mice to see if the presence of CDT is associated with increased gastroenteritis, sloughing of intestinal mucosa, increased inflammation or bacterial invasion into extraintestinal tissues. The suckling mouse model can be

used to determine if CDT expressing Campylobacter produce a diarrheagenic response. Alternatively, CDT expressing *Haemophilus ducreyi* or isogenic mutants can be intradermally injected or placed on top of abraded skin to see if CDT plays a role in exacerbating infection in a model of chancroid.

Advances in somatic cell genetic techniques

To identify genes involved in CDT trafficking, I developed a high-throughput method of cDNA complementation. This assay represents a contribution not only to the CDT field, but also to any group using a forward genetic method that results in untagged genetic lesions (i.e. chemical mutagenesis). While this strategy is an alternative to using mixed cDNA libraries or diminishing pool methods, it still does not allow for rapid complementation of a high number of mutants. With the absence of such technology, a large effort would be required to identify the genetic deficiencies in the remaining 60 uncharacterized CDT resistant mutants. However, if primary screening were performed to increase the chances of identifying interesting genes required for CDT intoxication, the high throughput cDNA complementation strategy could be applied to a limited number of mutants.

Using high-throughput cDNA complementation, two cDNAs were found to increase sensitivity to one of the CDT-resistant clones: Derlin-2 (Derl2) and Amylase-1 (Amy1). Derl2 is part of the ERAD pathway and is discussed above. It is possible that the resistant clone may contain a mutation in Amy1; however, it is also possible that overexpression of Amy1 degrades complex carbohydrates resulting glycan deficiency mediated hypersensitivity to CDT, as was observed in chapter 2.

Further characterization of Amy1 mediated sensitivity to CDT will be fruitful for the CDT community and may support an inverse relationship between hypoglycosylation and CDT sensitivity. The high throughput screen provided several other cDNAs that were able to increase sensitivity to CDT, albeit at lower levels. This panel of cDNAs provides a list of genes that should be characterized further to determine their role in the mechanism of CDT intoxication.

Elucidation of differences in CDTs expressed by divergent pathogens

Several pieces of evidence suggested that CDTs expressed by different pathogens have distinct binding preferences and that these differences correlate with CDT binding subunit homology. The binding subunits from Aa-CDT and Hd-CDT were highly conserved while those of Ec-CDT and Cj-CDT were more distantly related. Aa-CDT and Hd-CDT have similar host cell preferences based on the intoxication of eight cell lines from diverse origins and mutants deficient in glycosylation (Chapter 2). The effect of altering specific host-cell glycans on the sensitivity to intoxication by Ec-CDT was often similar to that seen with Aa-CDT and Hd-CDT, but in other cases more closely resembled effects on Cj-CDT intoxication. Cj-CDT almost always displayed unique preferences in host glycans, with the exception of intoxicating galactose transporter deficient cells similar to Ec-CDT and glycolipid deficient cells, which were hypersensitive to all four CDTs. Characterization of five mutants from the forward genetic screen revealed two intoxication phenotypes. Four of the mutants were highly resistant to Aa-CDT, Hd-CDT and Ec-CDT and relatively sensitive to Cj-CDT. The fifth clone, A03-1-2, had

the opposite phenotype; this clone was relatively sensitive to Aa-CDT, Hd-CDT and Ec-CDT and highly resistant to Cj-CDT. Supporting these findings, a subsequent forward genetic screen identified host genes required by these four CDTs {Carette, 2011}. With the exception of one gene that was required by all four CDTs, the required genes were unique to each CDT, in concordance with the model presented above. These data suggest that CDTs derived from different pathogens likely utilize distinct host factors for intoxication. This tropism correlates with the amino acid sequences of the CDT binding subunits as opposed to bacterial niche. Although *A. actinomycetemcomitans* and *H. ducreyi* have different niches, the binding subunits of the CDTs they encode share high levels of amino acid identities, and they respond similarly to alterations in host factors. Conversely, *E. coli* and *C. jejuni* have similar niches, but their binding subunits are quite different, leading to divergent target cell preferences. Future efforts to identify and characterize host factors required for intoxication by these CDTs will elucidate different mechanisms of intoxication.

APPENDIX

CELLULAR INTERACTIONS OF THE CYTOLETHAL DISTENDING TOXINS FROM ESCHERICHIA COLI AND HAEMOPHILUS DUCREYI

CELLULAR INTERACTIONS OF THE CYTOLETHAL DISTENDING TOXINS FROM *ESCHERICHIA COLI* AND *HAEMOPHILUS DUCREYI*

Amandeep Gargi[‡], Batcha Tamilselvam[‡], Brendan Powers[‡], Michael G. Prouty[‡1], Tommie Lincecum[§2], Aria Eshraghi[¶], Francisco J. Maldonado-Arocho[¶3], Brenda A. Wilson[‡†], Kenneth A. Bradley[¶], and Steven R. Blanke[‡†4]

From the [‡]Department of Microbiology, [†]Institute for Genomic Biology, University of Illinois, Urbana, Illinois, [§]Department of Biology and Biochemistry, University of Houston, Houston, Texas, and [¶] Department of Microbiology, Immunology and Molecular Genetics, University of California, Los Angeles, Los Angeles, California

Running Title: Distinct cell interactions of *E. coli* and *H. ducreyi* CDTs

[1] Current address: Department of Enterics/Infectious Disease Directorate, Naval Medical Research Center, Silver Springs, MD. [2] Current address: Life Technologies Corporation, Carlsbad, CA. [3] Current address: Department of Molecular Biology and Microbiology, Tufts University School of Medicine Boston, MA.

[4] To whom correspondence should be addressed: B103 CLSL, 601 South Goodwin Avenue, Urbana, IL 61801. Tel.: 217-244-2412; Fax: 217-244-6697; E-mail: sblanke@illinois.edu.

Key words: cytolethal distending toxin, *Haemophilus ducreyi*, *Escherichia coli*, toxin trafficking, toxin uptake, toxin internalization, DNase, cell cycle arrest

Background: Cytolethal distending toxins (CDTs) produced by pathogenic bacteria are genotoxic.
Results: CDTs exploit two different endocytic pathways to reach the nucleus.
Conclusion: Individual members of the CDT superfamily interact with host cells by distinct mechanisms.
Significance: Learning how CDTs interact with and modulate host cells and tissues is critical for understanding the strategies used by pathogenic bacteria during infection.

SUMMARY

The cytolethal distending toxins (CDTs) comprise a subclass of intracellular-acting genotoxins produced by many Gram-negative pathogenic bacteria that disrupt the normal progression of the eukaryotic cell cycle. Here, the intoxication mechanisms of CDTs from *Escherichia coli* (Ec-CDT) and *Haemophilus ducreyi* (Hd-CDT), which share limited amino acid sequence homology, were directly compared. Ec-CDT and Hd-CDT shared comparable *in vitro* DNase activities of the CdtB subunits, saturable cell surface binding with comparable affinities, and the requirement for an intact Golgi complex to induce cell cycle arrest. In contrast, disruption of endosome acidification blocked Hd-CDT-mediated cell cycle arrest and toxin transport to the endoplasmic reticulum (ER) and nucleus, while having no effects on Ec-CDT. Phosphorylation of the histone protein H2AX, as well as nuclear localization, were inhibited for Hd-CdtB, but not Ec-CdtB, in cells expressing dominant negative Rab7 (T22N) suggesting that Hd-CDT, but not Ec-CDT, is trafficked through late endosomal vesicles. In support of this idea, significantly more Hd-CdtB than Ec-CdtB co-localized with Rab9, which is enriched in late endosomal compartments. Competitive binding studies suggested that Ec-CDT and Hd-CDT bind to discrete cell surface determinants. These results suggest that Ec-CDT and Hd-CDT are transported within cells by distinct pathways, possibly mediated by their interaction with different receptors at the cell surface.

The cytolethal distending toxins (CDTs) comprise a family of multi-subunit bacterial genotoxins that modulate the eukaryotic cell cycle (1-5). CDT-mediated cell cycle arrest and the disruption of cytokinesis have been proposed to alter the normal barrier and immune functions of both epithelial cells and lymphocytes (3). Animal model studies as well as the association of *cdt* gene carriage in disease-causing bacteria from human isolates both support the importance of CDTs for the virulence strategies of specific pathogens (6,7).

Most CDTs function as assembled complexes of three protein subunits, encoded by three contiguous genes (*cdtA*, *cdtB*, *cdtC*) within an operon (8). Consistent with the canonical AB model of intracellular acting toxins (9), CdtB appears to function as the enzymatic A-subunit. CdtB has DNase I-like activity (10,11) and localizes to the nucleus when expressed ectopically within the cytosol of mammalian cells (12-14), suggesting that this subunit directly causes DNA damage within the nuclei of intoxicated cells. CdtA and CdtC facilitate the delivery of CdtB into cells (15-18), although the molecular details of how these subunits facilitate the cell-surface binding, uptake, and intracellular transport of CdtB remain poorly understood.

A diverse group of Gram-negative pathogenic bacteria that colonize distinct niches within the host have been identified to possess *cdt* genes (19). The AB_2 toxin architecture as well as a number of other key structural features appear to be generally conserved across the CDT family (20), suggesting that individual toxin members may interact with and intoxicate cells in a similar fashion. However, the cellular intoxication properties of CDTs produced by different pathogenic organisms are poorly understood. Recently, the sensitivity of several cell lines to CDTs from *Aggregatibacter actinomycetemcomitans, Campylobacter jejuni, Escherichia coli*, and *Haemophilus ducreyi* were demonstrated to be differentially affected by alterations in host glycans and membrane cholesterol (21), suggesting that host cell requirements for CDT intoxication of mammalian cells may not be universally conserved. However, it remains unclear whether the overall mechanism and molecular basis of toxin binding, uptake, and intracellular transport, are broadly applicable to all members of the CDT family.

The objective of this study was to directly compare the cellular intoxication mechanisms employed by CDTs produced by *E. coli* and *H. ducreyi*, two pathogens that colonize highly divergent host niches (i.e. the intestinal and urogenital tracts, respectively). Notably, the CDTs from *E. coli* (Ec-CDT) and *H. ducreyi* (Hd-CDT) share only 22% and 19% sequence identity, respectively, in their CdtA and CdtC subunits, suggesting the possibility that these two toxins might interact with host cells in fundamentally different ways. These studies revealed differences in the cellular requirements for toxin intracellular trafficking. Moreover, Ec-CDT and Hd-CDT did not compete with each other for binding to the surface of cells, suggesting that these toxins may target and bind to discrete receptors. Overall, these studies suggest that Ec-CDT and Hd-CDT are transported within cells by distinct pathways, possibly mediated by their interaction with different receptors at the cell surface.

Experimental Procedures

Cloning of cdt genes and preparation of expression strains. The cloning of the genes encoding Ec-CDT and Hd-CDT in plasmids for recombinant expression in *E. coli* was previously described (21).

Expression and purification of recombinant Ec-CDT and Hd-CDT. Each recombinant protein was expressed and purified as previously described (21). Protein concentrations were quantified using the Bradford Protein Assay (Thermo Scientific, Rockford, IL). Recombinant proteins were used only when purified to at least 95% homogeneity, as estimated by resolving the proteins using sodium-dodecyl sulfate (SDS)-polyacrylamide gel electrophoresis (PAGE), and visualizing after staining the gels with Coomassie Brilliant Blue (Bio-Rad, Hercules, CA; data not shown). The purified, denatured subunits were stored at -20 °C in HEPES (20 mM, *N*-[2-Hydroxyethyl] piperazine-*N*-[2-ethanesulphonic acid], Calbiochem, La Jolla, CA), pH 7.5 containing urea (8 M) and NaCl (200 mM).

Ec-CDT and Hd-CDT holotoxins were prepared as previously described (22). Ec-CDT and Hd-CDT holotoxin integrity was evaluated using the dialysis retention assay, as previously described (17). Ec-CDT or Hd-CDT holotoxin (5-20 μM, 1 ml) was dialyzed (100 kDa molecular mass cut-off tubing; Spectrum Laboratories) at 4 °C against four 250 ml volumes of PBS pH 7.4 containing 5% glycerol. After 24 h, the dialyzed proteins were evaluated using SDS-PAGE followed by staining with Coomassie Brilliant blue. The gels were scanned with a CanonScan 9950F scanner (Canon, Lake Success, NY) using ArcSoft Photo Studio 5.5 software (ArcSoft, Fremont, CA). The integrity of the holotoxins was quantified by comparing the relative intensities of the bands corresponding to CdtA, CdtB, or CdtC before and after dialysis, as determined by using the UN-SCAN-IT program (Silk Scientific, Inc., Orem, UT). Individual CDT subunits, each of which has a molecular mass less than 35 kDa, were used as negative controls.

Mammalian cells. All mammalian cell cultures were maintained at 37 °C and under 5% CO_2 within a humidified environment. Human cervical cancer epithelial (HeLa) cells (CCL-2, ATCC) were maintained in Minimal Essential Medium Eagle (MEM, Mediatech, Herndon, VA) with 10% fetal bovine serum (FBS, Mediatech). Chinese hamster ovary (CHO-K1) cells (CCL-61, ATCC) were maintained in Ham's F-12K (Lonza, Walkersville, MD) with 10% FBS. Human epithelial colorectal adenocarcinoma (Caco-2) cells (HTB-37, ATCC) were maintained in MEM (Eagle) with 20% FBS. Human embryonic intestinal (INT-407) cells (CCL-6, ATCC) were maintained in basal medium eagle (Sigma) with 10% FBS. Complete medium was obtained by supplementing each medium described above with L-glutamine (2 mM, Sigma), penicillin (50 IU/ml, Mediatech), and streptomycin (50 μg/ml, Mediatech).

Cell cycle phase determination. The indicated cell lines were seeded (1.5×10^5 cells per well) in 6-well plates (Corning Inc., Corning, NY). After 18 h, the cells were further incubated in complete medium with or without Ec-CDT or Hd-CDT at the indicated concentrations, or mock incubated with PBS pH 7.4. After 48 h, the cells were analyzed for arrest at the G_2/M interface, as previously described (21). From these data, dose response curves were generated by plotting cells in G_2/M as a function of toxin concentration. From the dose response curves, we determined $CCAD_{50}$ (i.e. cell cycle arrest $dose_{50}$) values, which we defined as the toxin concentrations required to induce G_2/M arrest in 50% of the cell population not already in G_2/M.

For both Ec-CDT and Hd-CDT, preliminary studies revealed nearly identical dose response curves for G_2/M arrest in the presence or absence of the hexa-histidine tags (Fig. S4). All subsequent studies were conducted with Ec-CDT or Hd-CDT assembled from subunits that retained their respective hexa-histidine tags.

Some studies were conducted in the presence of the indicated concentrations of brefeldin A (BFA; MP Biomedicals), ammonium chloride (NH_4Cl, Sigma), bafilomycin A1 (LC Laboratories, Woburn, MA), monensin (Sigma), or nigericin (Sigma). These studies were conducted at approximately the $CCAD_{50}$ values determined for Hd-CDT and Ec-CDT in order to best assess whether each pharmacological agent inhibited, potentiated, or had no effect on toxin activity.

Flow cytometry. Analytical flow cytometry-based assays were carried out as previously described (21).

DNase assay. The relative *in vitro* DNase activities of either Ec-CdtB or Hd-CdtB were determined as described previously (10), using purified pUC19 as the substrate. Reactions were stopped at 4 h by the addition of EDTA (to a final concentration of 10 mM). DNA gel loading dye (6x; Promega) was added to each sample, and the samples were resolved by employing agarose (0.8%) gel electrophoresis using Tris-acetate-EDTA (TAE, 40 mM Tris base, Fisher Biotech, Fair Lawn, NJ; 20 mM acetic acid, Fisher Scientific; 1 mM EDTA) electrophoresis buffer with constant voltage (100 V). The gels were stained with ethidium bromide (1 μg/ml, Bio-Rad), photographed using a Gel Doc EQ system (Bio-Rad), and the relative pixel densities of

stained bands corresponding to supercoiled pUC19 were measured using UN-SCAN-IT. Relative DNase activity was calculated from the pixel densities of ethidium bromide stained bands corresponding to supercoiled pUC19, using the relationship: relative DNase activity = [(super-coiled pUC19 pixels from control reactions lacking Ec-CdtB and Hd-CdtB) – (super-coiled pUC19 pixels from reactions containing Ec-CdtB or Hd-CdtB)] / [super-coiled pUC19 pixels from control reactions lacking Ec-CdtB and Hd-CdtB]. A value of 1.0 corresponds to a complete loss of detectable supercoiled pUC19.

Biotinylation of CDTs. Ec-CDT or Hd-CDT (1 ml at 5-20 μM) in PBS pH 7.4 was incubated overnight at 4 °C with EZ Link Sulfo-NHS-LC-Biotin (10-fold molar excess, Thermo Scientific). The labeling reaction was arrested by the addition of Tris pH 8.0 (to a final concentration of 20 mM). To remove free label, the proteins were dialyzed at 4 °C against four changes of PBS pH 7.4 (250 ml each) containing 5% glycerol. Preliminary studies indicated that biotinylation reactions had no detectable effects on the capacity of either Ec-CDT or Hd-CDT to induce cell cycle arrest in G_2/M.

Internalization assay. Cells were seeded (2×10^4 per well) in 8-well chamber slides (Nunc; Rochester, NY). After 18 h, the slides were incubated on ice for 30 min. The cells were washed two times with ice-cold PBS pH 7.4, and then further incubated on ice with or without biotinylated Ec-CDT or Hd-CDT (at the indicated concentrations) in PBS pH 7.4 with bovine serum albumin (BSA, 3%, Sigma), or mock incubated in PBS pH 7.4 with BSA (3%). After 30 min of toxin pre-binding on ice, the cells were washed three times with ice-cold PBS pH 7.4.

To monitor CDT binding, the cells were immediately fixed by incubating with ice-cold 2% formaldehyde (Sigma), and then further incubated at room temperature for 30 min. To monitor CDT internalization, after 30 min of toxin pre-binding on ice, the cells were incubated with pre-warmed (37 °C) complete medium. After 10 min, the cells were washed with ice-cold PBS pH 7.4, and fixed with ice-cold 2% formaldehyde. After fixing for 30 min at room temperature, the cells were permeabilized by incubating in PBS 7.4 containing 0.1% Triton X-100 for 15 min, and blocked with 3% BSA for 30 min. To probe for biotinylated Ec-CDT or Hd-CDT, the fixed and permeabilized cells were incubated at room temperature with streptavidin conjugated with Alexa Fluor 488 (1:200 dilution in PBS 7.4; Invitrogen). After 1 h, the cells were washed 3 times with 0.1% Tween-20 (Fisher Scientific) in PBS pH 7.4. The nucleus was stained by incubating with 4',6-diamidino-2-phenylindole (DAPI; 300 nM in PBS pH 7.4, Invitrogen) for 2 min. Slides were washed 3 times with 0.1% Tween-20 in PBS pH 7.4 and air-dried. The slides were mounted with ProLong Gold antifade reagent (Invitrogen) and cured overnight. The cells were then analyzed using DIC/fluorescence microscopy.

DIC/fluorescence microscopy. Chamber slides were analyzed using a DeltaVision RT microscope (Applied Precision; Issaquah, WA), using an Olympus Plan Apo 40x oil objective with NA 1.42 and working distance of 0.17 mm DIC images were collected using a Photometrics CoolSnap HQ camera; (Photometrics, Tucson; AZ). Images were processed using SoftWoRX Explorer Suite (version 3.5.1, Applied Precision Inc). Deconvolution was carried out using SoftWoRX constrained iterative deconvolution tool (ratio mode), and analyzed using Imaris 5.7 (Bitplane AG, Zurich, Switzerland).

CDT localization to the ER. Cells were plated in an 8-well chamber slide to 30-40% confluency. After overnight incubation, cells were washed 2 times with PBS pH 7.4, followed by addition of 100 μL OPTI-MEM (Invitrogen, Grand Island, NY), and further incubated for 2 h before transfection. Approximately 30 min prior to addition to cells, the appropriate dilutions of pDsRed2-ER (0.4 μg/200 μl/well; Clontech, Mountain View, CA), which encodes RFP fused to the ER targeting sequence of calreticulin, and the ER retention sequence, KDEL; and Lipofectamine 2000 reagent (1 μl/200 μl/well; Invitrogen) complex were prepared according to the manufacturers instructions, and allowed to incubate at room temperature. After 30 min, OPTI-MEM was removed, and the plasmid DNA-

transfection mixture (100 μl) was added to each well in a drop-wise fashion with gentle agitation, and the cells were immediately incubated at 37 °C and under 5% CO_2. After 4 h, the transfection mixture was removed from the monolayers, and the cells were incubated in complete medium at 37 °C and under 5% CO_2. After overnight incubation, we typically detected 80-90% of the cells within the monolayer to be transfected based on the percentage of cells with RFP fluorescence, as determined using an Olympus CKX 41 fluorescence microscope (Olympus America Inc., Center Valley, PA).

Cells that had been transfected, as described above, with pDsRed2-ER, were pre-incubated for 30 min in the absence or presence of NH_4Cl (20 mM) at 37 °C and under 5% CO_2. The cells were then further incubated with biotinylated Ec-CDT or Hd-CDT (200 nM), and the cells were stained for each toxin as described above under "*Internalization Assay*". The cells were further stained for actin by incubating with Alexa Fluor 647-labelled phalloidin (1 U/200 μl/well; Invitrogen). Images were collected using DIC/fluorescence microscopy and deconvoluted, as described above. For each cell, images were collected from an average of 30 z-planes, each at a thickness of 0.2 μm. Localization analysis was conducted by using the co-localization module of the DeltaVision SoftWoRx 3.5.1 software suite. Results were expressed as the localization index, which was derived from calculating the Pearson's coefficient of correlation values, which in these studies was a measure of localization of the indicated CDT to the ER in each z plane of the cell. In these studies, a localization index value of 1.0 indicates 100% localization of Ec-CDT or Hd-CDT to the ER, whereas a localization index of 0.0 indicates the absence of Ec-CDT or Hd-CDT localization to the ER. The localization index was calculated from the analysis of a total of 50 images collected over three independent experiments.

Monitoring nuclear localization of Ec-CdtB or Hd-CdtB within the nuclear fraction of CDT-intoxicated cells. Cells were seeded in 100 mm culture dishes (BD Biosciences, Durham, NC). After overnight incubation, the monolayers were treated with bafilomycin A1 (20 nM) for 30 min, and further incubated with Ec-CDT or Hd-CDT (at the indicated concentrations). After 30 min, the cells were further incubated with fresh medium (not containing toxin) for an additional 210 min. After 240 min total internalization of Ec-CDT or Hd-CDT, the cells were harvested by scraping, lysed using hypotonic buffer, and fractionated as per the manufacturer's protocol (Nuclear Extract Kit, Active Motif, Carlsbad, CA). The fractionated samples were evaluated by western blotting, using rabbit polyclonal antibodies against Ec-CdtB (1:20,000 dilution; generated by Thermo Fisher Scientific Inc., Rockford, IL), or rabbit polyclonal antibodies against Hd-CdtB (1:10,000; generated by Immunological Resource Center, University of Illinois, Urbana, IL), cytosolic marker GAPDH (1:200; Abcam, Cambridge, MA), microsomal marker calnexin (1:2,000; Abcam), nuclear marker p84 (1:2,000; Abcam), and cell lysate loading control actin (1:1,000; NeoMarkers, Fremont, CA). Anti-mouse (1:2,000), and anti-rabbit (1:5,000) secondary antibodies were purchased from Pierce Protein Biology Products (Thermo Fisher Scientific Inc.). Relative amounts of CdtB were determined by densitometric analysis of the blot bands using the UN-SCAN-IT program.

H2AX activation assay. Cells were transfected with pDsRed-Rab7 DN (0.4 μg/200 μL/well), using the general transfection procedure as described above under "*CDT localization to the ER."* The transfected monolayers were incubated at 37°C with Ec-CDT (200 nM) or Hd-CDT (200 nM). After 8 hours, the cells were fixed and permeabilized as described above under "*Internalization Assay*." To monitor activation of H2AX by CDT, samples were stained overnight with a rabbit polyclonal anti-p-H2AX antibody (1:5000 dilution; Invitrogen) at 4 °C, followed by incubation with goat anti-rabbit Alexa Fluor 488 antibody (1:1000 dilution; Invitrogen) at room temperature for 2 h. The cells were further counter stained for actin by incubating with Alexa Fluor 647-labelled phalloidin (1 U/200 μl/well) and for nuclei by incubating with DAPI (1 ng/200 μl, Invitrogen) for 30 min. The slides were mounted with ProLong Gold Antifade Reagent (25 μl/well; Invitrogen). Images were collected using DIC/fluorescence microscopy and deconvoluted, as described above. For each cell, images were collected from an average of 30 z-planes, each at a

thickness of 0.2 μm. H2AX activation analysis was conducted by using the DeltaVision SoftWoRx 3.5.1 software suite. Percentage of H2AX activated cells in each group of functional and dysfunctional Rab7 cells were calculated from approximately 50 cells from each group over three independent experiments.

Monitoring nuclear localization of Ec-CdtB or Hd-CdtB using fluorescence microscopy. Cells were transfected with pDsRed-Rab7-DN (0.4 μg/200 μL/well), using the general transfection procedure as described above under "*CDT localization to the ER*" The transfected monolayers were pre-chilled for 30 min on ice and further incubated with Ec-CDT (200 nM) or Hd-CDT (200 nM) on ice for 30 min. After 60 min post internalization, the cells were fixed and permeabilized as described above under "*Internalization Assay*" To monitor Ec-CdtB or Hd-CdtB localization to the nucleus, cells were incubated with rabbit polyclonal anti-Ec-CdtB or anti-Hd-CdtB antibodies (1:2000 dilution) at 4 °C overnight, followed by incubation with goat anti-rabbit Alexa Fluor 488-labeled antibody (1:1000 dilution; Invitrogen) at room temperature for 2 h. The cells were further counter stained for the nucleus by incubating with DAPI (1 ng/200 μL, Invitrogen) for 30 min at room temperature. The slides were mounted with ProLong Gold Antifade Reagent (25 μL/well; Invitrogen). Images were collected using DIC/fluorescence microscopy and deconvoluted, as described above. For each cell, images were collected from an average of 30 z-planes, each at a thickness of 0.2 μm. Nuclear localization analysis was conducted by using the DeltaVision SoftWoRx 3.5.1 software suite. Percentage of CdtB localization into nucleus in each group of functional and dysfunctional Rab7 cells were calculated from approximately 30 cells from each group over three independent experiments.

CdtB-localization to Rab9-enriched vesicles. Pre-chilled monolayers were incubated with pre-chilled Ec-CDT (200 nM) or Hd-CDT (200 nM) on ice. After internalization, the cells were fixed and permeabilized as described above under "*Internalization Assay*." To probe the localization of CDT in Rab9 enriched vesicles, intoxicated cells were incubated with rabbit polyclonal anti-Ec-CdtB or anti-Hd-CdtB antibodies (1:2000 dilution), along with mouse monoclonal anti-Rab9 antibody (1:50 dilution; Abcam) at 4 °C overnight, followed by incubation with goat anti-rabbit Alexa Fluor 488-labeled antibody (1:1000 dilution; Invitrogen) and donkey anti-mouse Alexa Fluor 568 antibody (1:1000 dilution; Invitrogen) at room temperature for 2 h. The cells were further counter stained for actin by incubating with Alexa Fluor 647-labeled phalloidin (1 U/200 μL/well; Invitrogen) and for the nucleus by incubating with DAPI (1 ng/200 μL, Invitrogen) for 30 min at room temperature. The slides were mounted with ProLong Gold Antifade Reagent (25 μL/well; Invitrogen).

Images were collected using DIC/fluorescence microscopy and deconvoluted, as described above. For each cell, images were collected from an average of 30 z-planes, each at a thickness of 0.2 μm. Localization analysis was conducted by using the co-localization module of the DeltaVision SoftWoRx 3.5.1 software suite. Results were expressed as the localization index, which was derived from calculating the Pearson's coefficient of correlation values, which in these studies was a measure of localization of the indicated CDT to the Rab9 in each z plane of the cell. In these studies, a localization index value of 1.0 indicates 100% localization of Ec-CdtB or Hd-CdtB to Rab9, whereas a localization index of 0.0 indicates the absence of Ec-CdtB or Hd-CdtB localization to the Rab9. The localization index was calculated from the analysis of a total of 50 images collected over three independent experiments.

Cell binding assays. Mammalian cell binding assays were conducted as previously described (17,23). Cells were seeded (2×10^4/well) in 96-well plates (Fisher). After 18 h, the plates were incubated on ice. After 30 min, the cells were washed two times with ice-cold PBS pH 7.4, and then further incubated on ice with or without biotinylated Ec-CDT or Hd-CDT (at the indicated concentrations) and BSA (3%) in PBS pH 7.4, or mock incubated with BSA (3%) in PBS pH 7.4. After 1 h on ice, the cells were washed three times with ice-cold PBS pH 7.4, and then fixed by adding ice-cold 2% formaldehyde and 0.2% glutaraldehyde, and then further incubated at room

temperature. Preliminary studies indicated that maximal binding occurred between 30 and 60 min (not shown). After 15 min, the plate was washed three times with PBS pH 7.4 at room temperature, and then incubated at room temperature with streptavidin-HRP conjugate (1:15,000, GE Healthcare, Little Chalfont, Buckinghamshire, UK) in PBS pH 7.4. After 30 min, the cells were washed five times with PBS pH 7.4, and then incubated at room temperature with TMB Ultra (100 µl, Thermo Scientific). After 30 min, the supernatant from each well was removed and added to an equal volume of sulfuric acid (2 N, Mallinckrodt Baker Inc., Paris, KY) at room temperature. The optical density at 450 nm ($O.D._{450nm}$) was measured using a Biotek Synergy 2 plate reader (Biotek Instruments Inc., Winooski, VT). The $O.D._{450nm}$ measured for supernatants collected from wells containing cells incubated with PBS pH 7.4 alone (background absorbance) was subtracted from the $O.D._{450nm}$ measured for supernatants collected from wells containing cells that had been incubated with Ec-CDT or Hd-CDT. Relative binding was determined by dividing the $O.D._{450nm}$ minus background at each toxin concentration by the $O.D._{450\ nm}$ minus background at the highest concentration of toxin used in these studies (200 nM). The dissociation constants (K_d) were calculated by non-linear regression of the curve generated from plotting relative binding as a function of toxin concentration, using GraphPad Prism (Version 4.03, GraphPad Software, La Jolla, CA). Competitive binding assays were conducted as described above, except in the absence or presence of 100-fold molar excess of the specified non-biotinylated proteins.

Effects of lectin binding on CDT binding. Cell monolayers were prepared as described above under "*Cell binding assays*." Pre-chilled cells were pre-treated on ice with Euonymus Europaeus Agglutinin lectin (EEA, EY Labs, San Mateo, CA; 40 µg/ml). After 30 min, the cells were further incubated on ice with or without biotinylated Ec-CDT (100 nM) or Hd-CDT (100 nM) and BSA (3%) in PBS pH 7.4, or mock incubated with BSA (3%) in PBS pH 7.4, in the presence, or absence of 40 µg/ml EEA. After 30 min on ice, the cells were washed, fixed, and analyzed as described above under "*Cell binding assays*."

Statistics. Unless otherwise indicated, each experiment was performed at least three independent times, each time in triplicate. Statistical analyses were performed using Microsoft Excel (Version 11.0, Microsoft, Redmond, WA) or GraphPad. The *Q*-test was performed to eliminate data that were statistical outliers (24). Error bars represent standard deviations. All *P* values were calculated with the Student's *t*-test using paired, two-tailed distribution. A *P* value of less than 0.05 indicated that differences in the specified data were considered statistically significant.

RESULTS

Evaluating the relative sensitivities of mammalian cell lines to Ec-CDT and Hd-CDT. A recent study (21) reported that considerably lower concentrations of Hd-CDT than Ec-CDT were required to induce phosphorylation of the histone protein H2AX, a marker of DNA damage, in HeLa, CHO-K1, Balb/3T3, Y-1 cells, OT-1, NIH/3T3, IC-21, and Raw 264.7 cells. To evaluate the relationship between these results and the capacity of Ec-CDT or Hd-CDT to induce G_2/M cell cycle arrest, one of several possible downstream consequences of H2AX activation, we measured cell cycle progression in HeLa and CHO-K1 cells, which have been commonly used as models for studying the function of bacterial toxins, including CDTs (25-36), as a function of Ec-CDT or Hd-CDT concentrations. From the dose response curves, we determined $CCAD_{50}$ (i.e. cell cycle arrest $dose_{50}$) values, which we defined as the toxin concentrations required to induce G_2/M arrest in 50% of the cell population not already in G_2/M. These studies revealed that substantially lower concentrations of Hd-CDT than Ec-CDT were required to induce G_2/M cell cycle arrest in HeLa cells (Fig. S1A, B). For HeLa cells, $CCAD_{50}$ values of 4 pM and 100 nM were determined for Hd-CDT (Fig. S1A) and Ec-CDT (Fig. S1B), respectively, indicating that Hd-CDT is approximately 2.5×10^4-fold more potent towards HeLa cells than Ec-CDT. In contrast, CHO-K1 cells required only 70-fold higher concentrations of Ec-CDT than Hd-CDT, with $CCAD_{50}$ values of 7 nM and 0.1 nM, respectively (Fig. S1C, D). These results are consistent with

those of the previous study (21), which reported that HeLa and CHO-K1 cells required approximately 1.0 x 10^4- and 50-fold higher concentrations, respectively, of Ec-CDT than Hd-CDT to induce H2AX phosphorylation.

We also compared the relative sensitivities towards Hd-CDT and Ec-CDT using two intestinal cell lines (Caco-2, INT-407 cells), which had not been evaluated in the previous study (21). These studies revealed that Caco-2 (Fig. S1E, F) and INT-407 cells (Fig. S1G, H) were both arrested at the G_2/M interface at considerably lower concentrations of Hd-CDT than Ec-CDT. However, these cell lines again varied in their relative susceptibilities to the two toxins. Caco-2 cells required approximately 3 x 10^2-fold higher concentrations of Ec-CDT ($CCAD_{50}$ = 3 nM) than Hd-CDT ($CCAD_{50}$ = 10 pM), whereas INT-407 cells required approximately 7 x 10^3-fold higher concentrations of Ec-CDT ($CCAD_{50}$ = 40 nM) than Hd-CDT ($CCAD_{50}$ = 6 pM).

To evaluate the possibility that differences in holotoxin stability might underlie the highly divergent cellular potencies of Ec-CDT and Hd-CDT, we investigated the assembly of the heterotrimeric complexes using the dialysis retention assay (17,37). These studies revealed that approximately 60-99% Ec-CDT or Hd-CDT were assembled into holotoxins, as indicated by their retention within dialysis tubing with a molecular weight cutoff of approximately 100 kDa (Fig. S2), while CdtC (Fig. S2) or CdtA or CdtB (data not shown) were not retained. Even in the worst-case scenarios (e.g. 60% holotoxin assembly), the large differences in potencies robustly measured for these two toxins (more than 10^4-fold greater activity for Hd-CDT than Ec-CDT on HeLa cells) cannot readily be attributed to the inability of the holotoxins to assemble.

Relative in vitro DNase activities of Ec-CdtB and Hd-CdtB. CDT-dependent G_2/M arrest of intoxicated cells has been attributed to the activation of cellular DNA repair pathways (38,39) in response to the DNase I-like enzymatic activity associated with the CdtB subunit of several CDTs, including Ec-CDT (10,11) and Hd-CDT (40). To evaluate whether or not differences in the sensitivities of HeLa cells to Ec-CDT and Hd-CDT might be associated with the intrinsic catalytic properties of the CdtB subunits of each toxin, the *in vitro* DNase activities of the purified recombinant Ec-CdtB and Hd-CdtB subunits (in the absence of CdtA and CdtC) were compared. These studies revealed that both Ec-CdtB and Hd-CdtB demonstrated similar DNase activity in a dose-dependent manner (Fig. 1). Consistent with previous reports (11,17,40), Ec-CdtA, Ec-CdtC, Hd-CdtA, or Hd-CdtC did not yield detectable DNase activity (data not shown). These results support the idea that the disparity in cellular potencies of Ec-CDT and Hd-CDT are not likely due to intrinsic divergence in the DNase activities between these toxins' catalytic subunits.

Both Ec-CDT and Hd-CDT are taken up from the plasma membrane into cells within 10 min. Several studies have reported that ectopic expression of CdtB within mammalian cells is sufficient to induce cell cycle arrest in G_2/M, even in the absence of CdtA and CdtC (11,13,38,41), strongly supporting a model that CdtB acts from an intracellular location. To evaluate the possibility that differences in cell sensitivity to Ec-CDT and Hd-CDT may be due to large disparities between the times required for toxin uptake from the cell surface, we examined the internalization of both toxins into HeLa cells using DIC/fluorescence microscopy. These experiments revealed that under conditions non-permissive for cell entry (4 °C), both Ec-CDT and Hd-CDT were visible at the cell surface (Fig. S3A, C), indicating that both toxins were bound to the plasma membrane. When the temperature was raised to 37 °C to induce conditions permissive for uptake, both toxins were visible within the cell after just 10 min (Fig. S3B, D), indicating that Ec-CDT and Hd-CDT were both efficiently internalized from the plasma membrane into cells.

Effect of BFA on toxin-induced G_2/M cell cycle arrest. Hd-CDT mediated cell cycle arrest has been demonstrated to be sensitive to the action of BFA, which disrupts retrograde protein transport from the Golgi complex to the ER (42,43), suggesting that this toxin is trafficked by a retrograde mechanism (9). Because the importance of an intact Golgi complex for intoxication of cells with Ec-CDT had not been previously studied,

toxin-mediated cell cycle arrest of HeLa cells was evaluated in the presence or absence of BFA and at approximately the respective $CCAD_{50}$ values of each toxin (e.g. 5 pM for Hd-CDT, and 100 nM for Ec-CDT). These studies revealed that for Ec-CDT, as well as for Hd-CDT, toxin-mediated G_2/M cell cycle arrest was blocked by BFA (Fig. 2A, B), which supports a model that both toxins are trafficked to the ER via the Golgi complex.

Effects of endosomal acidification inhibitors on toxin-induced G_2/M cell cycle arrest. The finding that Ec-CDT and Hd-CDT-mediated G_2/M cell cycle is blocked in the presence of BFA prompted us to further evaluate host cell requirements associated with transport from the cell surface to the ER. Transport of a subset of intracellular acting bacterial toxins within the cell requires the lowering of pH within the lumen of endocytic compartments (9). While an earlier study (42) reported that Hd-CDT mediated G_2/M cell cycle arrest in HeLa cells was inhibited by several agents that block endosome acidification, the requirement for endosome acidification associated with Ec-CDT mediated G_2/M cell cycle arrest had not previously been reported. As previously demonstrated (42), Hd-CDT mediated G_2/M cell cycle arrest in HeLa cells was inhibited (Fig. 3A, B) by the lysosomotropic amine, ammonium chloride (44). In contrast, Ec-CDT mediated cell cycle arrest was not blocked in the presence of NH_4Cl (Fig. 3A, B). Moreover, bafilomycin A_1, which blocks acidification of intracellular vacuoles by an alternative mechanism, inhibiting the action of vacuolar ATPases (45), also blocked Hd-CDT-mediated, but not Ec-CDT-mediated G_2/M cell cycle arrest (Fig. 3C, D). Finally, the polyether ionophore monensin, which is known to block intracellular protein transport by collapsing proton gradients as a sodium/proton antiporter (46), and, the potassium/proton carboxylic ionophore, nigericin (44), both blocked Hd-CDT-mediated, but not Ec-CDT-mediated G_2/M cell cycle arrest (Fig. 3E). The sensitivity of cells to Ec-CDT was modestly, but reproducibly, elevated in the presence of agents that block acidification of endosomal compartments (Fig. 3), but we do not currently understand the basis for the slight enhancement in Ec-CDT cellular activity.

Essentially identical results were obtained when using CHO-K1 cells in the presence of NH_4Cl, bafilomycin A1, monensin, or nigericin (data not shown), indicating that the disparate effects of agents that block endosomal acidification on Ec-CDT- or Hd-CDT-mediated cell cycle arrest in G_2/M are not idiosyncratic to HeLa cells. Additional studies confirmed that neither the cellular binding nor the uptake of either Ec-CDT or Hd-CDT into cells from the plasma membrane was affected by NH_4Cl, bafilomycin A1, monensin, or nigericin (data not shown).

To more quantitatively assess whether the presence of the His-tag on the amino-terminus of the recombinant CDT subunits might alter CDT intracellular trafficking, we compared the dose-response curves of the His-tagged and non-His-tagged forms of Ec-CDT and Hd-CDT in the presence or absence of NH_4Cl or bafilomycin A1, both of which inhibited Hd-CDT-mediated G_2/M cell cycle arrest, but not Ec-CDT-mediated G_2/M cell cycle arrest. These studies revealed that the dose response curves of the His-tagged and non-His-tagged forms of Ec-CDT and Hd-CDT were essentially identical in the presence or absence of NH_4Cl or bafilomycin A1 (Fig. S4). Taken together, these data indicated that Ec-CDT-mediated G_2/M cell cycle arrest does not require acidification of endosomal compartments, suggesting that Ec-CDT and Hd-CDT are transported from the cell surface to the ER by different pathways.

Effects of inhibiting endosomal acidification on toxin-transport to the ER. While an earlier study indicated that Hd-CDT mediated G_2/M cell cycle arrest in HeLa cells was inhibited by several agents that block endosome acidification (42), the importance of endosome acidification for localization of Ec-CDT or Hd-CDT to the ER, the organelle from which CdtB subunits have been proposed to be translocated to the cytosol (5), has not been reported. To evaluate whether acidification of endosomal vesicles is required for intracellular toxin transport to the ER, we used fluorescence microscopy to determine whether Ec-CDT or Hd-CDT localization to the ER is altered in the presence of NH_4Cl. These studies revealed that Ec-CDT localization to the ER is not visibly altered in the presence of NH_4Cl (Fig. 4A, B, E).

In contrast, Hd-CDT localization to the ER was significantly reduced in the presence of NH_4Cl (Fig. 4C, D, E). Several attempts to evaluate CDT localization specifically to the ER using biochemical fractionation approaches were inconclusive due to the inability to satisfactorily resolve the ER from other membrane-containing fractions, with the exception of the nucleus. These results indicate that transport to the ER of Hd-CDT, but not Ec-CDT, requires acidification of endosomal vesicles, and moreover, suggests that Ec-CDT and Hd-CDT may be transported to the ER via different trafficking pathways.

Effects of endosomal acidification inhibitors on CdtB localization to the nucleus. Previous reports that CdtB possesses *in vitro* DNase I-like activity (10,11) and localizes to the nucleus when expressed ectopically within the cytosol of mammalian cells (12-14), supports a model that this CDT subunit functions within the nucleus of intoxicated cells. To evaluate whether acidification of endosomal vesicles is required for intracellular toxin transport to the nucleus, we fractionated cells intoxicated for 60 min with Ec-CDT or Hd-CDT in the absence or presence of bafilomycin A1, and used western blotting to determine whether the localization of the CdtB subunit is altered when endosomal acidification was prevented. These studies revealed that most of the internalized Ec-CdtB or Hd-CdtB was associated with the nuclear fraction (Fig. 5), while neither CdtB subunit was associated with either the cytosolic or microsomal fractions. In contrast to the CdtB subunits, neither the CdtA or CdtC subunits of Ec-CDT or Hd-CDT were detected within the nuclear fractions (data not shown), which is consistent with the model that only the A fragments of retrograde-trafficked bacterial toxins are translocated out of the ER (9) and more recently, with immunofluorescence studies of the intracellular trafficking of CDT from *Aggregatibacter actinomycetemcomitans* (47).

Ec-CdtB was detected within the nuclear fractions prepared from cells that had been incubated with Ec-CDT holotoxin in the presence or absence of bafilomycin A1 (Fig. 5). In contrast, Hd-CdtB was not detected in either the nuclear fraction or whole cell lysates prepared from cells that had been incubated with Hd-CDT holotoxin in the presence of bafilomycin A1 (Fig. 5). We speculate that in the presence of bafilomycin A1, Hd-CdtB is either degraded within the endolysosomal system or, alternatively, recycled back to the cell surfaces and released, although we did not investigate either of these possibilities further. These results indicate that the transport of Hd-CdtB, but not Ec-CdtB, to the nucleus requires acidification of endosomal vesicles.

Comparing the importance of late-endosome-targeted carrier vesicle biogenesis for Ec-CDT- and Hd-CDT-mediated H2AX phosphorylation. One of the consequences resulting from inhibition of the V-ATPase-mediated pH drop is inhibition of endosomal carrier vesicle formation, which facilitates transport between endosomal compartments (48). To more directly evaluate the importance of late-endosome-targeted carrier vesicle transport for the intracellular activity of Ec-CDT or Hd-CDT, we compared toxin-dependent phosphorylation of H2AX in cells expressing a dominant negative (DN) form of Rab7, a small GTPase required for late-endosome-targeted carrier vesicle biogenesis (49). Transiently transfected HeLa cells expressing Rab7 (T22N) fused to DsRed, (DN-DsRed-Rab7 (T22N)), which is defective in nucleotide exchange and has a reduced affinity for GTP (50) were incubated with either Ec-CDT or Hd-CDT. After 8 h, the monolayers were examined using fluorescence microscopy to quantify the number of cells with phosphorylated H2AX (p-H2AX). Because approximately 40%-60% of the cells in any well were discovered to be expressing DN-DsRed-Rab7 (T22N), H2AX phosphorylation could be monitored within the same well in both transfected and non-transfected cells. These studies revealed significantly fewer DN-DsRed-Rab7 (T22N) expressing cells with p-H2AX activation than in non-transfected cells (Fig. 6), supporting the idea that toxin trafficking from early to late endosomal compartments is important for the biological activity of Hd-CDT but not Ec-CDT.

Comparing the importance of late-endosome-targeted carrier vesicle biogenesis for Hd-CdtB trafficking to the nucleus. Because the biological activity of CDTs is generally considered to require their CdtB subunits to function within the nucleus

of intoxicated cells (5), we hypothesized that DN-DsRed-Rab7 (T22N) blocked the cellular activity of Hd-CDT by inhibiting the transport of Hd-CdtB to the nucleus. To evaluate this hypothesis, the nuclear localization of Ec-CdtB and Hd-CdtB was compared within transiently transfected HeLa cells expressing DN-DsRed-Rab7 (T22N) to non-transfected HeLa cells. These studies revealed significantly less Hd-CdtB localized to the nucleus of cells expressing DN-DsRed-Rab7 (T22N) than in non-transfected cells (Fig. 7). In contrast, Ec-CdtB was localized to the nucleus to approximately the same extent in cells expressing or not expressing DN-DsRed-Rab7 (T22N) (Fig. 7), indicating that late-endosome-targeted carrier vesicle biogenesis is important for intracellular trafficking of Hd-CdtB, but not Ec-CdtB.

Comparing the localization of Ec-CDT-and Hd-CDT to Rab9-enriched vesicles. Because late-endosome-targeted carrier vesicle biogenesis is required to transport cargo from early to late vesicles within the endolysosomal system, we hypothesized that Hd-CdtB, but not Ec-CdtB is transported through late endosomal vesicles. To evaluate this hypothesis, we used fluorescence imaging to investigate the localization of Ec-CdtB and Hd-CdtB to vesicles enriched with the small GTPase Rab9, which contributes to the generation and maintenance of late endocytic compartments (51). These experiments revealed that after 30 min, visibly more Hd-CdtB co-localized with Rab9-enriched puncta than Ec-CdtB (Fig. 8), supporting the hypothesis that Hd-CdtB, but not Ec-CdtB, is transported through late endosomal vesicles. Taken together with the data presented above indicating the importance of late-endosome-targeted carrier vesicle biogenesis for Hd-CDT but not Ec-CDT, these results suggest that the catalytic CdtB subunits of these two toxins are trafficked along distinct pathways.

Relative cell binding of Ec-CDT and Hd-CDT. Analogous to all intracellular-acting bacterial exotoxins (9), CDTs must bind to the surface of target cells prior to internalization (16,52). Studies to evaluate the binding of Ec-CDT and Hd-CDT to HeLa cells as a function of toxin concentration revealed that both Ec-CDT and Hd-CDT yielded saturable binding curves (Fig. 9A, B). Moreover, the presence of a 100-fold molar excess of non-biotinylated toxins inhibited the dose-dependent cell association of biotinylated toxins, indicating that the binding of both Ec-CDT and Hd-CDT was largely specific, with K_d values for specific binding of 172 (±27) nM (Fig. 9A) and 169 (±35) nM (Fig. 9B), respectively.

Despite binding to the cell surface with similar properties, it was not clear whether Ec-CDT and Hd-CDT were binding to the same or discrete plasma membrane receptors. To differentiate between these possibilities, we evaluated whether Ec-CDT and Hd-CDT bind competitively to the surface of HeLa cells. These studies revealed that the binding of biotinylated Ec-CDT to the cell surface was inhibited to a greater extent by 100-fold molar excess of unlabeled Ec-CDT than a 100-fold molar excess of unlabeled Hd-CDT (Fig. 10A). In a similar manner, cell surface binding of biotinylated Hd-CDT was found to be inhibited to a greater extent by 100-fold molar excess of unlabeled Hd-CDT than a 100-fold molar excess of unlabeled Ec-CDT (Fig. 10B). These data suggest that while the interactions of both Ec-CDT and Hd-CDT with host cells are largely specific, the two toxins may bind to distinct cell surface components. In further support of this idea, the cell surface binding of Ec-CDT, but not Hd-CDT, was partially inhibited in the presence of EEA, a fucose-specific lectin that was previously reported to antagonize Ec-CDT binding to HeLa cells (15) (Fig. 10C).

DISCUSSION

The studies presented here revealed differences in the manner in which CDTs from two unrelated pathogenic bacteria intoxicate mammalian cells. Hd-CDT induces G_2/M cell cycle arrest at substantially lower concentrations than Ec-CDT in all tested cell lines (Fig. S1), consistent with a recent report demonstrating that Hd-CDT induces H2AX activation within cells at lower concentrations than Ec-CDT (21). The high level of dissimilarity between the protein sequences of the CdtA and CdtC subunits (22% and 19% sequence identity, respectively) does not readily

reveal the reasons underlying the divergent potencies of Ec-CDT and Hd-CDT, but is consistent with the idea that these two toxins may interact with and intoxicate cells by disparate mechanisms. Indeed, although both Ec-CDT and Hd-CDT possess similar *in vitro* DNase activities exhibited by their catalytic CdtB subunits (Fig. 1), are both efficiently taken up by cells (Fig. S3), and both require an intact Golgi complex to induce G_2/M cell cycle arrest (Fig. 2), divergence was discovered in the cellular requirements associated with intracellular toxin transport (Figs. 3-8). Hd-CDT-mediated G_2/M arrest and ER localization were inhibited by agents that prevent acidification of endosomal compartments, while Ec-CDT-mediated G_2/M arrest and ER localization were not affected.

How might the requirement for acidification of endosomal compartments relate to the cyclomodulatory activities of Ec-CDT and Hd-CDT? Intoxication of cells by a subset of intracellular-acting bacterial toxins requires a drop of the luminal pH within endosomal compartments (9,53-56), which is a normal step in vesicle maturation carried out by the proton-pumping vacuolar ATPase (V-ATPase) (57-59). For diphtheria, anthrax, or botulinum toxins, the pH drop induces conformational changes in the toxin structure required for insertion into the endosomal membrane and translocation of the catalytic fragment into the cytosol (9,60). However, preventing acidification of endosomal compartments can also stall the trafficking of proteins along the endosomal pathway, such as the mannose 6-phosphate receptor that is normally transported from late endosomal vesicles to the Golgi complex (61,62). Inhibition of the V-ATPase-mediated pH drop inhibits trafficking by blocking the formation of endosomal carrier vesicles, which facilitate transport between endosomal compartments (48). The finding that the presence of NH_4Cl or bafilomycin A1 significantly inhibited localization of Hd-CDT to the ER (Fig. 4) or nucleus (Fig. 5) respectively, suggests that Hd-CDT intoxication requires an intracellular transport pathway involving late endosomal compartments. This idea is further supported by the importance of Rab7, which regulates the biogenesis at early endosomes of transport vesicles targeted for late endosomal compartments (Fig. 6, 7), as well the co-localization of Hd-CdtB with Rab9 (Fig. 8).

In contrast, our data support a model that Ec-CDT transport to the ER occurs by a mechanism independent of late endosome-mediated trafficking. Notably, several reports have indicated that the retrograde transport mechanisms of other toxins, including Shiga toxin (63), cholera toxin (64,65), or ricin (66), are also insensitive to agents that prevent endosomal acidification, suggesting that these toxins are transported from early endocytic vesicles to the ER through a pathway that bypasses late endosomal compartments. Additional experimental work will be required to more completely define the Ec-CDT and Hd-CDT intracellular trafficking mechanisms, but we speculate that the overall pathway of Ec-CDT transport to the ER may be more similar to that used by Shiga toxin, cholera toxin, or ricin, than the pathway used by Hd-CDT.

The molecular basis underlying the putative targeting of Ec-CDT and Hd-CDT to discrete intracellular trafficking pathways is unclear. However, based on the inability of Ec-CDT or Hd-CDT to competitively bind to the surface of cells (Fig. 10A, B), we hypothesize that the two toxins utilize distinct cell surface receptors. Inhibition of the cell surface binding of Ec-CDT, but not Hd-CDT, by the fucose-specific lectin EEA (Fig. 10C) further supports this idea. Receptor recognition and binding is critical for the function of intracellular-acting toxins because the receptor, in part, functions as a molecular "carrier" whose normal uptake and trafficking through the cell directly impacts the final cellular destination of the toxin (9). A cell surface receptor for Hd-CDT has not yet been identified, but a genetic screen using the KBM7 chronic myeloid leukemia cell line revealed that a putative G protein–coupled receptor, TMEM181, contributes to cellular binding and sensitivity to Ec-CDT (67). Our competition studies (Fig. 10) suggest that Hd-CDT and Ec-CDT do not share the same receptor, but we cannot rule out the possibility of a role for TMEM181 in conferring cell sensitivity to Hd-CDT. Consistent with the idea that Ec-CDT and Hd-CDT may bind to different receptors on the surface of sensitive cells, a recent study reported that a mutant CHO cell line, characterized by abbreviated glycan sequences on membrane

glycoproteins and glycolipids, was hypersensitive to Hd-CDT, but demonstrated the same sensitivity as the parental CHO cells to Ec-CDT (21).

Comparing the molecular and structural basis for Ec-CDT and Hd-CDT receptor recognition is currently challenging because, even though the crystal structure has been solved for Hd-CDT (22), high-resolution structural data is not yet available for the Ec-CDT holotoxin. The highly dissimilar protein sequences of the CdtA and CdtC subunits of Ec-CDT and Hd-CDT are consistent with the idea that these two toxins may interact with and intoxicate cells by disparate mechanisms. Additional studies will also be required to determine whether or not differences in intracellular trafficking pathways between Ec-CDT and Hd-CDT directly contribute to the disparity in the potencies exhibited by the two toxins towards sensitive cells. Nonetheless, we speculate that differential cell surface requirements for toxin association is critical for targeting Ec-CDT and Hd-CDT to their respective uptake and intracellular trafficking pathways.

Multiple factors could potentially contribute to the differences in cellular potencies of Ec-CDT and Hd-CDT. For example, discrepancies in the cytosolic localization of the respective CdtB subunits, which is widely thought to precede localization to the nucleus, may contribute to differences in toxin potencies. In studies to compare the levels of Ec-CdtB and Hd-CdtB within the cytosol of intoxicated cells, we could not detect Ec-CdtB and Hd-CdtB by either fluorescence microscopy or cellular fractionation and western blot analysis (data not shown). We speculate that the levels of Ec-CdtB and Hd-CdtB within the cytosol in these experiments were below our detection limits. A recent study reported the detection of a fluorescent version of CdtB from *A. actinomycetemcomitans* within the cytosol and nucleus (47). On the other hand, in another recent study, the authors suggested that Hd-CdtB localization to the nucleus not require that this subunit to be first translocated to the cytosol (68).

In summary, we have identified differences in the intoxication pathways used by CDTs from pathogens that colonize two distinct niches. Because CDTs are generally believed to disrupt the normal functions of epithelial and immune cells comprising the mucosal barrier (3,4), we speculate that Ec-CDT and Hd-CDT may have evolved divergently in response to the specific tissue and cell tropisms of the pathogenic microbes that produce these toxins. Finally, these results provide experimental evidence that caution must be applied when extrapolating the properties of individual CDTs to the entire family of these toxins.

REFERENCES

1. Ohara, M., Oswald, E., and Sugai, M. (2004) Cytolethal distending toxin: a bacterial bullet targeted to nucleus. *J Biochem* **136**, 409-413
2. Ceelen, L. M., Decostere, A., Ducatelle, R., and Haesebrouck, F. (2006) Cytolethal distending toxin generates cell death by inducing a bottleneck in the cell cycle. *Microbiol Res* **161**, 109-120
3. Nougayrede, J. P., Taieb, F., De Rycke, J., and Oswald, E. (2005) Cyclomodulins: bacterial effectors that modulate the eukaryotic cell cycle. *Trends Microbiol* **13**, 103-110
4. Oswald, E., Nougayrede, J. P., Taieb, F., and Sugai, M. (2005) Bacterial toxins that modulate host cell-cycle progression. *Curr Opin Microbiol* **8**, 83-91
5. Gargi, A., Reno, M., and Blanke, S. R. (2012) Bacterial toxin modulation of the eukaryotic cell cycle: are all cytolethal distending toxins created equally? *Frontiers in cellular and infection microbiology* **2**, 124
6. Ge, Z., Schauer, D. B., and Fox, J. G. (2008) *In vivo* virulence properties of bacterial cytolethal-distending toxin. *Cell Microbiol* **10**, 1599-1607
7. Smith, J. L., and Bayles, D. O. (2006) The contribution of cytolethal distending toxin to bacterial pathogenesis. *Crit Rev Microbiol* **32**, 227-248
8. Thelestam, M., and Frisan, T. (2004) Cytolethal distending toxins. *Rev Physiol Biochem Pharmacol* **152**, 111-133
9. Blanke, S. R. (2006) Portals and Pathways: Principles of Bacterial Toxin Entry into Host Cells. *Microbe* **1**, 26-32
10. Elwell, C. A., and Dreyfus, L. A. (2000) DNase I homologous residues in CdtB are critical for cytolethal distending toxin-mediated cell cycle arrest. *Mol Microbiol* **37**, 952-963
11. Lara-Tejero, M., and Galan, J. E. (2000) A bacterial toxin that controls cell cycle progression as a deoxyribonuclease I-like protein. *Science* **290**, 354-357
12. McSweeney, L. A., and Dreyfus, L. A. (2004) Nuclear localization of the Escherichia coli cytolethal distending toxin CdtB subunit. *Cell Microbiol* **6**, 447-458
13. Nishikubo, S., Ohara, M., Ueno, Y., Ikura, M., Kurihara, H., Komatsuzawa, H., Oswald, E., and Sugai, M. (2003) An N-terminal segment of the active component of the bacterial genotoxin cytolethal distending toxin B (CDTB) directs CDTB into the nucleus. *J Biol Chem* **278**, 50671-50681
14. Wising, C., Magnusson, M., Ahlman, K., Lindholm, L., and Lagergard, T. (2010) Toxic activity of the CdtB component of *Haemophilus ducreyi* cytolethal distending toxin expressed from an adenovirus 5 vector. *Apmis* **118**, 143-149
15. McSweeney, L. A., and Dreyfus, L. A. (2005) Carbohydrate-binding specificity of the *Escherichia coli* cytolethal distending toxin CdtA-II and CdtC-II subunits. *Infection and immunity* **73**, 2051-2060
16. Cao, L., Bandelac, G., Volgina, A., Korostoff, J., and DiRienzo, J. M. (2008) Role of aromatic amino acids in receptor binding activity and subunit assembly of the cytolethal distending toxin of *Aggregatibacter actinomycetemcomitans*. *Infection and immunity* **76**, 2812-2821
17. Cao, L., Volgina, A., Huang, C. M., Korostoff, J., and DiRienzo, J. M. (2005) Characterization of point mutations in the cdtA gene of the cytolethal distending toxin of *Actinobacillus actinomycetemcomitans*. *Mol Microbiol* **58**, 1303-1321
18. Nesic, D., and Stebbins, C. E. (2005) Mechanisms of assembly and cellular interactions for the bacterial genotoxin CDT. *PLoS Pathog* **1**, e28
19. Pickett, C. L., and Whitehouse, C. A. (1999) The cytolethal distending toxin family. *Trends Microbiol* **7**, 292-297
20. Hu, X., Nesic, D., and Stebbins, C. E. (2006) Comparative structure-function analysis of cytolethal distending toxins. *Proteins* **62**, 421-434

21. Eshraghi, A., Maldonado-Arocho, F. J., Gargi, A., Cardwell, M. M., Prouty, M. G., Blanke, S. R., and Bradley, K. A. (2010) Cytolethal distending toxin family members are differentially affected by alterations in host glycans and membrane cholesterol. *J Biol Chem* **285**, 18199-18207
22. Nesic, D., Hsu, Y., and Stebbins, C. E. (2004) Assembly and function of a bacterial genotoxin. *Nature* **429**, 429-433
23. Lee, R. B., Hassane, D. C., Cottle, D. L., and Pickett, C. L. (2003) Interactions of *Campylobacter jejuni* cytolethal distending toxin subunits CdtA and CdtC with HeLa cells. *Infection and immunity* **71**, 4883-4890
24. Dixon, W. (1950) Analysis of extreme values. . *Ann Math Stat* **21**, 488-506
25. Cortes-Bratti, X., Chaves-Olarte, E., Lagergard, T., and Thelestam, M. (1999) The cytolethal distending toxin from the chancroid bacterium *Haemophilus ducreyi* induces cell-cycle arrest in the G2 phase. *J Clin Invest* **103**, 107-115
26. Gelfanova, V., Hansen, E. J., and Spinola, S. M. (1999) Cytolethal distending toxin of *Haemophilus ducreyi* induces apoptotic death of Jurkat T cells. *Infection and immunity* **67**, 6394-6402
27. Frisan, T., Cortes-Bratti, X., Chaves-Olarte, E., Stenerlow, B., and Thelestam, M. (2003) The *Haemophilus ducreyi* cytolethal distending toxin induces DNA double-strand breaks and promotes ATM-dependent activation of RhoA. *Cell Microbiol* **5**, 695-707
28. Johnson, W. M., and Lior, H. (1988) A new heat-labile cytolethal distending toxin (CLDT) produced by *Campylobacter spp*. *Microb Pathog* **4**, 115-126
29. Johnson, W. M., and Lior, H. (1988) A new heat-labile cytolethal distending toxin (CLDT) produced by *Escherichia coli* isolates from clinical material. *Microb Pathog* **4**, 103-113
30. Cope, L. D., Lumbley, S., Latimer, J. L., Klesney-Tait, J., Stevens, M. K., Johnson, L. S., Purven, M., Munson, R. S., Jr., Lagergard, T., Radolf, J. D., and Hansen, E. J. (1997) A diffusible cytotoxin of *Haemophilus ducreyi*. *Proc Natl Acad Sci U S A* **94**, 4056-4061
31. Sugai, M., Kawamoto, T., Peres, S. Y., Ueno, Y., Komatsuzawa, H., Fujiwara, T., Kurihara, H., Suginaka, H., and Oswald, E. (1998) The cell cycle-specific growth-inhibitory factor produced by *Actinobacillus actinomycetemcomitans* is a cytolethal distending toxin. *Infection and immunity* **66**, 5008-5019
32. Aragon, V., Chao, K., and Dreyfus, L. A. (1997) Effect of cytolethal distending toxin on F-actin assembly and cell division in Chinese hamster ovary cells. *Infection and immunity* **65**, 3774-3780
33. Bag, P. K., Ramamurthy, T., and Nair, U. B. (1993) Evidence for the presence of a receptor for the cytolethal distending toxin (CLDT) of *Campylobacter jejuni* on CHO and HeLa cell membranes and development of a receptor-based enzyme-linked immunosorbent assay for detection of CLDT. *FEMS Microbiol Lett* **114**, 285-291
34. Bouzari, S., and Varghese, A. (1990) Cytolethal distending toxin (CLDT) production by enteropathogenic *Escherichia coli* (EPEC). *FEMS Microbiol Lett* **59**, 193-198
35. Mayer, M. P., Bueno, L. C., Hansen, E. J., and DiRienzo, J. M. (1999) Identification of a cytolethal distending toxin gene locus and features of a virulence-associated region in *Actinobacillus actinomycetemcomitans*. *Infection and immunity* **67**, 1227-1237
36. Okuda, J., Kurazono, H., and Takeda, Y. (1995) Distribution of the cytolethal distending toxin A gene (cdtA) among species of Shigella and Vibrio, and cloning and sequencing of the cdt gene from *Shigella dysenteriae*. *Microb Pathog* **18**, 167-172
37. Cao, L., Volgina, A., Korostoff, J., and DiRienzo, J. M. (2006) Role of intrachain disulfides in the activities of the CdtA and CdtC subunits of the cytolethal distending toxin of *Actinobacillus actinomycetemcomitans*. *Infection and immunity* **74**, 4990-5002
38. Li, L., Sharipo, A., Chaves-Olarte, E., Masucci, M. G., Levitsky, V., Thelestam, M., and Frisan, T. (2002) The *Haemophilus ducreyi* cytolethal distending toxin activates sensors of DNA damage and repair complexes in proliferating and non-proliferating cells. *Cell Microbiol* **4**, 87-99
39. Hassane, D. C., Lee, R. B., and Pickett, C. L. (2003) *Campylobacter jejuni* cytolethal distending toxin promotes DNA repair responses in normal human cells. *Infection and immunity* **71**, 541-545

40. Frisk, A., Lebens, M., Johansson, C., Ahmed, H., Svensson, L., Ahlman, K., and Lagergard, T. (2001) The role of different protein components from the *Haemophilus ducreyi* cytolethal distending toxin in the generation of cell toxicity. *Microb Pathog* **30**, 313-324
41. Elwell, C., Chao, K., Patel, K., and Dreyfus, L. (2001) *Escherichia coli* CdtB mediates cytolethal distending toxin cell cycle arrest. *Infection and immunity* **69**, 3418-3422
42. Cortes-Bratti, X., Chaves-Olarte, E., Lagergard, T., and Thelestam, M. (2000) Cellular internalization of cytolethal distending toxin from *Haemophilus ducreyi*. *Infection and immunity* **68**, 6903-6911
43. Guerra, L., Teter, K., Lilley, B. N., Stenerlow, B., Holmes, R. K., Ploegh, H. L., Sandvig, K., Thelestam, M., and Frisan, T. (2005) Cellular internalization of cytolethal distending toxin: a new end to a known pathway. *Cell Microbiol* **7**, 921-934
44. Mellman, I., Fuchs, R., and Helenius, A. (1986) Acidification of the endocytic and exocytic pathways. *Annu Rev Biochem* **55**, 663-700
45. Bowman, E. J., Siebers, A., and Altendorf, K. (1988) Bafilomycins: a class of inhibitors of membrane ATPases from microorganisms, animal cells, and plant cells. *Proc Natl Acad Sci U S A* **85**, 7972-7976
46. Mollenhauer, H. H., Morre, D. J., and Rowe, L. D. (1990) Alteration of intracellular traffic by monensin; mechanism, specificity and relationship to toxicity. *Biochim Biophys Acta* **1031**, 225-246
47. Damek-Poprawa, M., Jang, J. Y., Volgina, A., Korostoff, J., and DiRienzo, J. M. (2012) Localization of *Aggregatibacter actinomycetemcomitans* cytolethal distending toxin subunits during intoxication of live cells. *Infection and immunity* **80**, 2761-2770
48. Hurtado-Lorenzo, A., Skinner, M., El Annan, J., Futai, M., Sun-Wada, G. H., Bourgoin, S., Casanova, J., Wildeman, A., Bechoua, S., Ausiello, D. A., Brown, D., and Marshansky, V. (2006) V-ATPase interacts with ARNO and Arf6 in early endosomes and regulates the protein degradative pathway. *Nat Cell Biol* **8**, 124-136
49. Vonderheit, A., and Helenius, A. (2005) Rab7 associates with early endosomes to mediate sorting and transport of Semliki forest virus to late endosomes. *PLoS biology* **3**, e233
50. Spinosa, M. R., Progida, C., De Luca, A., Colucci, A. M., Alifano, P., and Bucci, C. (2008) Functional characterization of Rab7 mutant proteins associated with Charcot-Marie-Tooth type 2B disease. *The Journal of neuroscience : the official journal of the Society for Neuroscience* **28**, 1640-1648
51. Ganley, I. G., Carroll, K., Bittova, L., and Pfeffer, S. (2004) Rab9 GTPase regulates late endosome size and requires effector interaction for its stability. *Molecular biology of the cell* **15**, 5420-5430
52. Mise, K., Akifusa, S., Watarai, S., Ansai, T., Nishihara, T., and Takehara, T. (2005) Involvement of ganglioside GM3 in G(2)/M cell cycle arrest of human monocytic cells induced by *Actinobacillus actinomycetemcomitans* cytolethal distending toxin. *Infection and immunity* **73**, 4846-4852
53. Daro, E., Sheff, D., Gomez, M., Kreis, T., and Mellman, I. (1997) Inhibition of endosome function in CHO cells bearing a temperature-sensitive defect in the coatomer (COPI) component epsilon-COP. *J Cell Biol* **139**, 1747-1759
54. Sandvig, K., and van Deurs, B. (2005) Delivery into cells: lessons learned from plant and bacterial toxins. *Gene Ther* **12**, 865-872
55. Abrami, L., Reig, N., and van der Goot, F. G. (2005) Anthrax toxin: the long and winding road that leads to the kill. *Trends Microbiol* **13**, 72-78
56. Tweten, R. K. (2005) Cholesterol-dependent cytolysins, a family of versatile pore-forming toxins. *Infection and immunity* **73**, 6199-6209
57. Sun-Wada, G. H., Wada, Y., and Futai, M. (2004) Diverse and essential roles of mammalian vacuolar-type proton pump ATPase: toward the physiological understanding of inside acidic compartments. *Biochim Biophys Acta* **1658**, 106-114

58. Sun-Wada, G. H., Wada, Y., and Futai, M. (2003) Lysosome and lysosome-related organelles responsible for specialized functions in higher organisms, with special emphasis on vacuolar-type proton ATPase. *Cell Struct Funct* **28**, 455-463
59. Nishi, T., and Forgac, M. (2002) The vacuolar (H+)-ATPases--nature's most versatile proton pumps. *Nat Rev Mol Cell Biol* **3**, 94-103
60. Montecucco, C., Papini, E., and Schiavo, G. (1994) Bacterial protein toxins penetrate cells via a four-step mechanism. *FEBS Lett* **346**, 92-98
61. Lombardi, D., Soldati, T., Riederer, M. A., Goda, Y., Zerial, M., and Pfeffer, S. R. (1993) Rab9 functions in transport between late endosomes and the trans Golgi network. *EMBO J* **12**, 677-682
62. Riederer, M. A., Soldati, T., Shapiro, A. D., Lin, J., and Pfeffer, S. R. (1994) Lysosome biogenesis requires Rab9 function and receptor recycling from endosomes to the trans-Golgi network. *J Cell Biol* **125**, 573-582
63. Mallard, F., Antony, C., Tenza, D., Salamero, J., Goud, B., and Johannes, L. (1998) Direct pathway from early/recycling endosomes to the Golgi apparatus revealed through the study of shiga toxin B-fragment transport. *J Cell Biol* **143**, 973-990
64. Lencer, W. I., Strohmeier, G., Moe, S., Carlson, S. L., Constable, C. T., and Madara, J. L. (1995) Signal transduction by cholera toxin: processing in vesicular compartments does not require acidification. *Am J Physiol* **269**, G548-557
65. Orlandi, P. A., Curran, P. K., and Fishman, P. H. (1993) Brefeldin A blocks the response of cultured cells to cholera toxin. Implications for intracellular trafficking in toxin action. *J Biol Chem* **268**, 12010-12016
66. Simpson, J. C., Dascher, C., Roberts, L. M., Lord, J. M., and Balch, W. E. (1995) Ricin cytotoxicity is sensitive to recycling between the endoplasmic reticulum and the Golgi complex. *J Biol Chem* **270**, 20078-20083
67. Carette, J. E., Guimaraes, C. P., Varadarajan, M., Park, A. S., Wuethrich, I., Godarova, A., Kotecki, M., Cochran, B. H., Spooner, E., Ploegh, H. L., and Brummelkamp, T. R. (2009) Haploid genetic screens in human cells identify host factors used by pathogens. *Science* **326**, 1231-1235
68. Guerra, L., Nemec, K. N., Massey, S., Tatulian, S. A., Thelestam, M., Frisan, T., and Teter, K. (2009) A novel mode of translocation for cytolethal distending toxin. *Biochim Biophys Acta* **1793**, 489-495

FOOTNOTES

We thank Dr. Ana Medrano for laboratory assistance. We thank Dr. Ian Gut and Dr. Prashant Jain for critical reading of the manuscript. This work was supported by grants from the National Institutes of Health R01GM098756 (K.A.B.), AI0059095 (S.R.B.), AI038396 (B.A.W.), T32DE007296 and F31DE022485 (A.E.), and, the James R. Beck Graduate Research Fellowship and Francis and Harlie Clark Graduate Student Research Award (A.G.).

FIGURE LEGENDS

FIGURE 1. ***In vitro*** **DNase activities of Ec-CdtB and Hd-CdtB**. The DNase activities of Ec-CdtB (filled triangles) and Hd-CdtB (filled circles) were determined as described under Experimental Procedures, and plotted as a function of toxin concentration. The rendered data were combined from three independent experiments, each conducted in triplicate. Error bars indicate standard deviations. Statistical significance was calculated for the differences in relative DNase activities at the indicated concentrations of Ec-CdtB and Hd-CdtB. * indicates $P < 0.05$.

FIGURE 2. **Effects of BFA on Ec-CDT- or Hd-CDT-induced cell cycle arrest**. Ec-CDT (100 nM)- or Hd-CDT (5 pM)-mediated arrest of HeLa cells in G_2/M was determined in the absence or presence of BFA (0.2 μg/ml). (A) The data are rendered as individual histograms representative of those collected during three independent experiments. Histograms indicate the number of cells (y axis, same scale for each histogram) at a given PI fluorescence intensity (x axis, same scale for each histogram), with, as indicated in the top left histogram, the left peak representing cells in G_0/G_1 phase (designated as G_1) of the cell cycle, the right peak representing cells in G_2/M (designated as G_2), and the area between the peaks representing cells in S phase (designated as S). The results are rendered as bar graphs generated from data combined from three or more independent experiments that compare the percentage of cells arrested in G_2/M in untreated cells (white bars), cells treated with either Ec-CDT or Hd-CDT, as indicated, in the absence of BFA (black bars), or cells treated with BFA in the absence or presence of Ec-CDT or Hd-CDT, as indicated (gray bars). Error bars represent standard deviations. Statistical significance was calculated for the differences between cell populations incubated in the absence or presence of BFA.

FIGURE 3. **Effects of agents that inhibit acidification of endosomal compartments on Ec-CDT- or Hd-CDT-induced cell cycle arrest**. Ec-CDT (100 nM)- or Hd-CDT (5 pM)-mediated arrest of HeLa cells in G_2/M was determined, as indicated in the absence or presence of NH_4Cl (20 mM; A, B), bafilomycin A1 (20 nM; C, D), monensin (10 nM; E), or nigericin (100 nM; E). (A, C) The data are rendered as individual histograms representative of those collected during three independent experiments. In (C), bafilomycin A1 is abbreviated as baf. A1 in the 2 lower panels. (B, D, E) The results are rendered as bar graphs generated from data combined from three independent experiments that compare the percentage of cells arrested in G_2/M phase in untreated cells (white bars), cells treated with Ec-CDT or Hd-CDT, as indicated, in the absence of pharmacological agents (black bars), or cells treated with pharmacological agents, as indicated, in the absence or presence of Ec-CDT or Hd-CDT (gray bars). Error bars represent standard deviations. Statistical significance was calculated for the differences between cell populations incubated in the absence or presence of the indicated agent.

FIGURE 4. **Effects of agents that inhibit acidification of endosomal compartments on Ec-CDT or Hd-CDT localization to the ER**. HeLa cells that had been transiently transfected with pDsRed2-ER were incubated with Ec-CDT (200 nM; A, B, E) or Hd-CDT (200 nM; C, D, E) at 37 °C for 60 min in the absence (A, C, E) or presence (B, D, E) of NH_4Cl (20 mM), were imaged using fluorescence microscopy. (A-D) Cellular actin was counterstained with phalloidin conjugated with Alexa Fluor 647. Images were representative of those collected from three independent experiments. The data were rendered as a single z-plane (5 μm depth within each cell). As labeled, green puncta indicate either Ec-CDT or Hd-CDT, red puncta indicate ER, white or blue filaments indicate actin, and Ec-CDT or Hd-CDT localized to ER is indicated by yellow puncta. White bars indicate 10 μm. The solid white boxes are digitally enlarged

images of the smaller dashed white boxes. (E) The results are rendered as a bar graph generated from data combined from three independent experiments that compare the Pearson's correlation coefficient for Ec-CdtB or Hd-CdtB co-localized with ER in cells treated with Ec-CDT or Hd-CDT, as indicated, in the absence of NH_4Cl (black bars), or cells treated with toxin, as indicated, in the presence of NH_4Cl (gray bars). Error bars represent standard deviations. Statistical significance was calculated for differences in the Pearson's correlation coefficient between cell populations incubated in the presence or absence of NH_4Cl.

FIGURE 5. **Effects of inhibiting acidification of endosomal compartments on Ec-CdtB or Hd-CdtB localization to the nucleus**. HeLa cells at 37 °C were pre-incubated for 30 min in the absence or presence of bafilomycin A1 (20 nM). The cells were then further incubated at 37 °C in the absence or presence of bafilomycin A1 (20 nM) with either Ec-CDT (100 nM) or Hd-CDT (100 nM). After 30 min, the cells were washed once with PBS pH 7.4, and then further incubated at 37 °C in the absence or presence of bafilomycin A1 (20 nM). After another 210 min, the monolayers were lysed and fractionated as described under Experimental Procedures. (A) Western blots are shown, which are representative of three independent experiments. Whole cell lysates and sub-cellular fractions were adjusted to the same volume, from which an identical volume was loaded into each well. The whole cell lysate (CL), microsomal fraction (M), nuclear fraction (N), and cytosolic fraction (CS) were each analyzed by western blot analysis for CdtB, calnexin (ER marker, representing microsomes), GAPDH (cytosolic marker), and p84 (nuclear matrix marker). Arrowheads indicate CdtB in the nuclear fraction of bafilomycin A1-treated cells. (B) Quantitative rendering of the western blot data for CdtB, as shown in Part (A), using densitometric analysis. For each toxin (Ec-CDT or Hd-CDT) and for each treatment (+/- bafilomycin A1), the data were rendered as bar graphs showing the amount of CdtB in each fraction relative to the pixels for CdtB in the cell lysate normalized to 1.0. The data are combined from 3 independent experiments. Error bars represent standard deviations. Statistical significance was calculated for the difference between amount of CdtB in whole cells lysate (black bar to the left of white), against nuclear fraction (white bar).

FIGURE 6. **Evaluating the effects of ectopic expression of dominant-negative Rab7 (T22N) on Ec-CDT- or Hd-CDT-mediated activation of H2AX**. HeLa cells that had been transiently transfected with a plasmid harboring the gene encoding dominant negative DsRed-Rab7 (T22N) (Rab7-DN) were incubated with Ec-CDT (200 nM; A, C) or Hd-CDT (200 nM; B, C) at 37 °C. After 8 h, the monolayers were fixed and imaged using fluorescence microscopy. (A and B) Cellular actin was counterstained with phalloidin conjugated with Alexa Fluor 647. Images were representative of those collected from three independent experiments. The data were rendered as a single z-plane (5 μm depth within each cell). As labeled, green puncta indicate phospho-H2AX (pH2AX), red puncta indicate Rab7-DN, white filaments indicate actin, and the blue staining indicates the nucleus. White bars indicate 10 μm. (C) Quantification of Ec-CDT- or Hd-CDT-mediated activation of H2AX. The data, which were combined from three independent experiments, are rendered as the percentage of cells within the monolayers with activated H2AX, as indicated by presence of green fluorescence within the nucleus, relative to untransfected cells.

FIGURE 7. **Effects of ectopic expression of dominant-negative Rab7 (T22N) on Ec-CdtB or Hd-CdtB localization to the nucleus**. HeLa cells that had been transiently transfected with a plasmid harboring the gene encoding dominant negative DsRed-Rab7 (T22N) (Rab7-DN), were chilled to 0 °C on ice for 30 min, and then incubated on ice with either Ec-CDT (200 nM) or Hd-CDT (200 nM), both of which had also been pre-chilled on ice. After 30 min, the cells were washed once with ice-cold PBS pH 7.4, and then further incubated at 37 °C. After 60 min, the monolayers were fixed and evaluated by

fluorescence imaging. (A and B) Images were representative of those collected from three independent experiments. The data were rendered as a single z-plane (approximately 5 μm depth within each cell). As labeled, green puncta indicate either Ec-CdtB (A) or Hd-CdtB (B), red puncta indicate cells expressing DsRed-Rab7-DN, and the blue staining indicates the nucleus. White scale bars indicate 10 μm. (C) The results are rendered as a bar graph generated from data combined from three independent experiments that compare the percentage of cells with at least one green puncta (corresponding to either Ec-CdtB (white bars) or Hd-CdtB (black bars)) localized to the nucleus in cells expressing or not expressing Rab7-DN. Error bars represent standard deviations. Statistical significance was calculated for differences in the percentage of nuclear localization of either Ec-CdtB or Hd-CdtB between cell populations expressing or not expressing DsRed-Rab7-DN.

FIGURE 8. **Evaluating the co-localization of Ec-CdtB or Hd-CdtB with Rab9**. HeLa cells that had been prechilled on ice for 30 min, were incubated on ice with either Ec-CDT (100 nM) or Hd-CDT (100 nM), each of which had also been prechilled on ice. After 30 min, the cells were washed once with PBS pH 7.4, and then further incubated at 37 °C. After 30 min, the cells were fixed and imaged using fluorescence microscopy. (A and B) Images were representative of those collected from three independent experiments. The data were rendered as a single z-plane (approximately 5 μm depth within each cell). As labeled, green puncta indicate either Ec-CdtB or Hd-CdtB, red puncta indicate Rab9, and Ec-CdtB or Hd-CdtB co-localized with Rab9 is indicated by yellow puncta. White bars indicate 10 μm. The solid white boxes are digitally enlarged images of the smaller dashed white boxes. (C) The results are rendered as a bar graph generated from data combined from three independent experiments that compare the Pearson's correlation coefficient for Ec-CdtB or Hd-CdtB co-localized with Rab9 in cells treated with Ec-CDT or Hd-CDT, as indicated. Error bars represent standard deviations. Statistical significance was calculated for differences in the Pearson's correlation coefficient between cell populations incubated with Ec-CDT or Hd-CDT.

FIGURE 9. **Cell surface binding of Ec-CDT and Hd-CDT.** The data are rendered as the relative binding after 30 min of biotinylated forms of Ec-CDT (A) or Hd-CDT (B) to HeLa cells as a function of toxin concentration (1-200 nM) in the absence (indicated on the graphs as "total binding," empty circles (A) or squares (B)) or presence (indicated on the graphs as "non-specific binding," filled triangles (A) or diamonds (B)) of 100-fold molar excess of non-biotinylated Ec-CDT (A) or Hd-CDT (B). Specific binding (indicated on the graphs as "specific binding," filled circles (A) or squares (B)) was computationally derived by subtracting the non-specific binding data from the total binding data. The normalized data from three independent experiments, each conducted in triplicate, were combined. K_d values were calculated using non-linear regression, and indicated directly on the graphs, with the error bars indicating standard deviations.

FIGURE 10. **Competitive cell surface binding of Ec-CDT and Hd-CDT in the absence or presence of cognate or non-cognate toxins.** The data are rendered as the relative binding after 30 min of Ec-CDT (A) or Hd-CDT (B) to HeLa cells as a function of toxin concentration (1-200 nM) in the presence or absence of 100-fold molar excess of non-biotinylated cognate or non-cognate toxins, as indicated. The data were normalized and combined from three independent experiments, each conducted in triplicate, and rendered as line graphs comparing the relative binding of biotinylated Ec-CDT (A) or Hd-CDT (B) in the absence or presence of 100-fold molar excess of unlabeled Ec-CDT or Hd-CDT, as indicated. Error bars are standard deviations. (C) The data are rendered as normalized relative binding of 100 nM of biotinylated Ec-CDT, or Hd-CDT to HeLa cells for 30 minutes, in the absence or presence of

the lectin EEA (40 μg/ml). Data are combined from three independent experiments, each conducted in triplicate. Error bars represent standard deviations. Statistical significance was calculated for differences in the cell-surface binding of Ec-CDT or Hd-CDT between cell populations incubated in the absence or presence of the lectin EEA

Figure 1. Gargi *et al.*, 2012

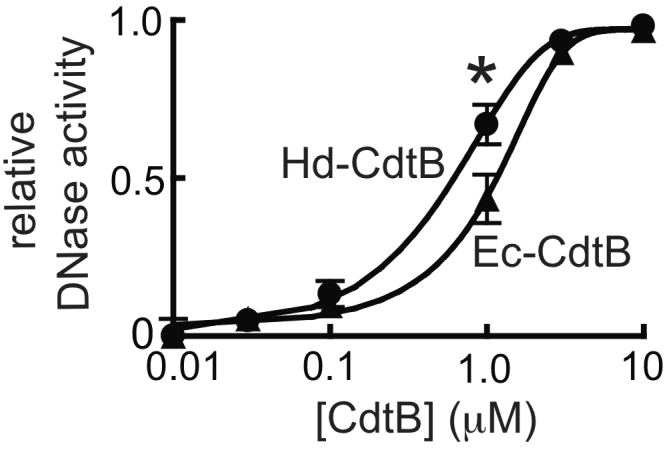

Figure 2. Gargi *et al.*, 2012

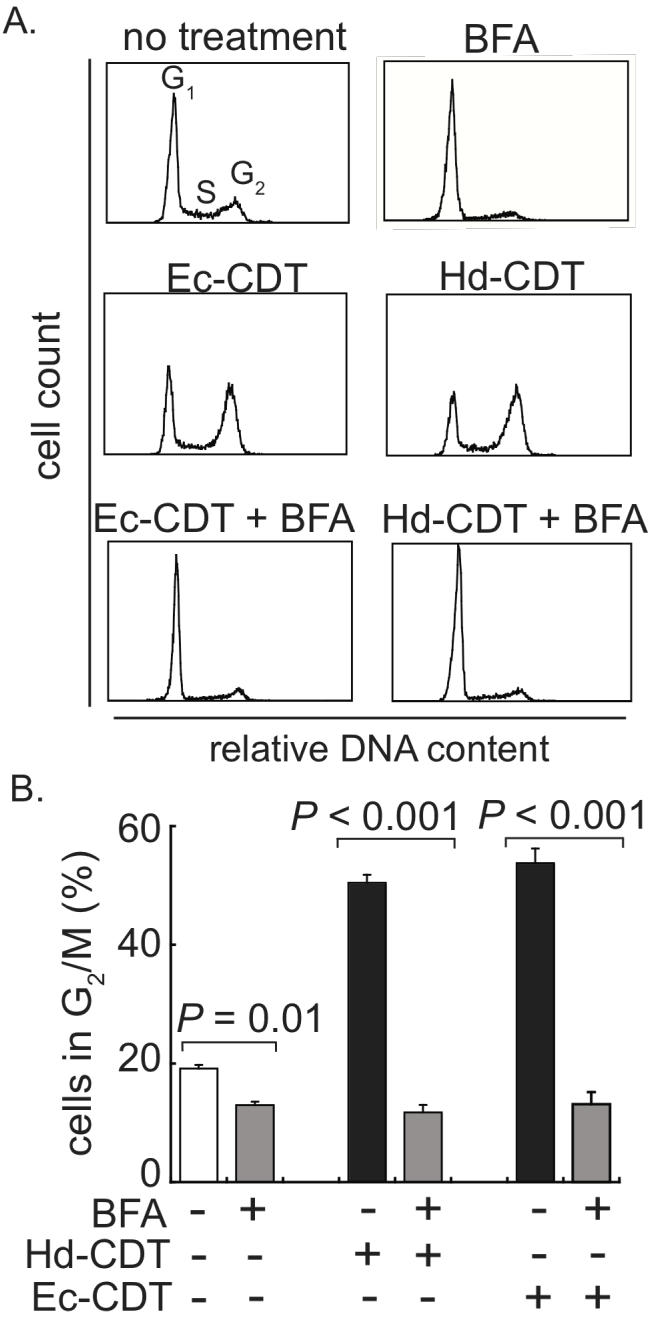

Figure 3. Gargi *et al.*, 2012

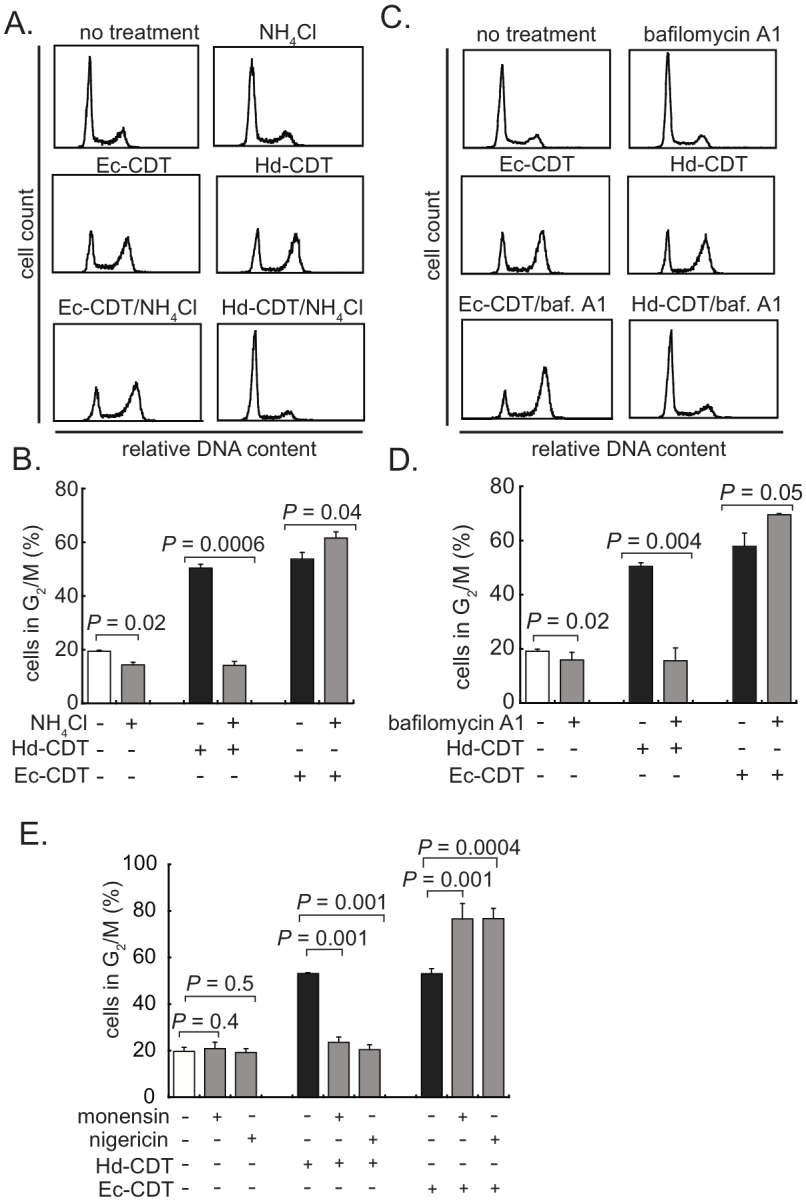

Figure 4. Gargi *et al.*, 2012

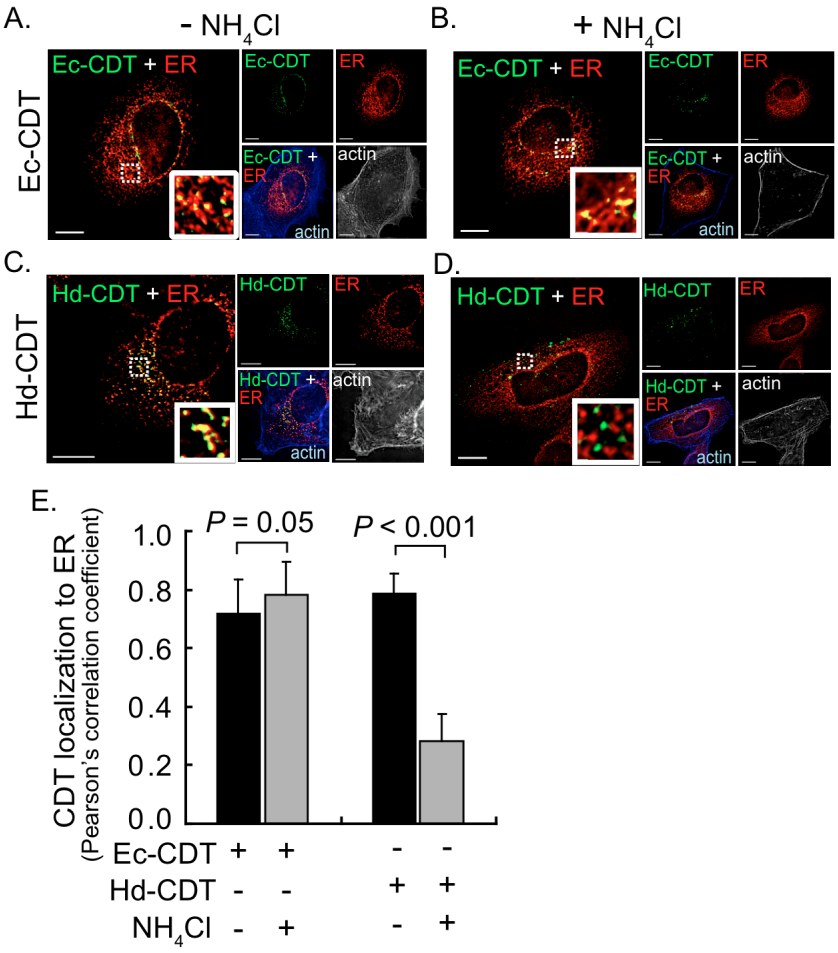

Figure 5. Gargi *et al.*, 2012

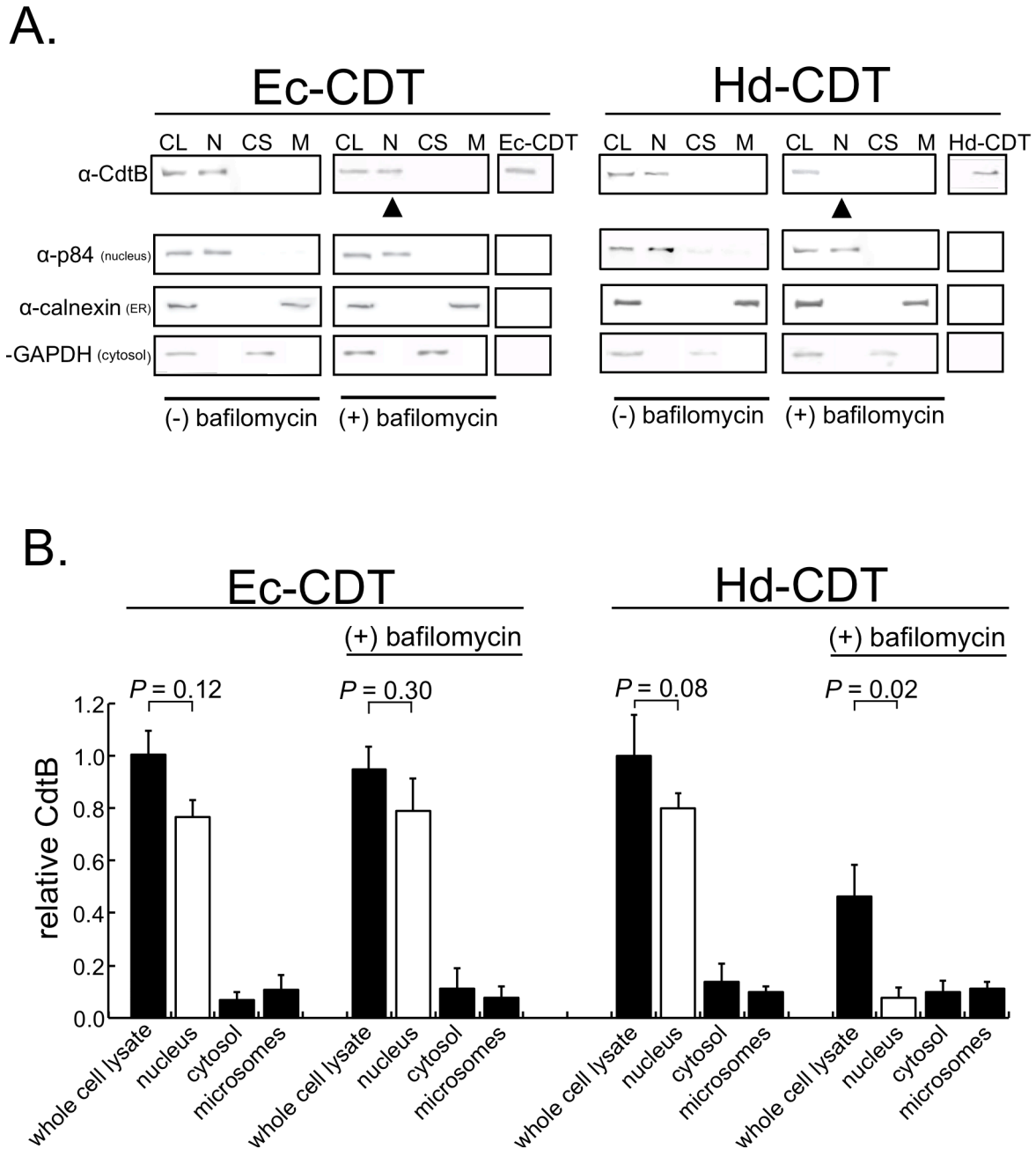

Figure 6. Gargi et al., 2012

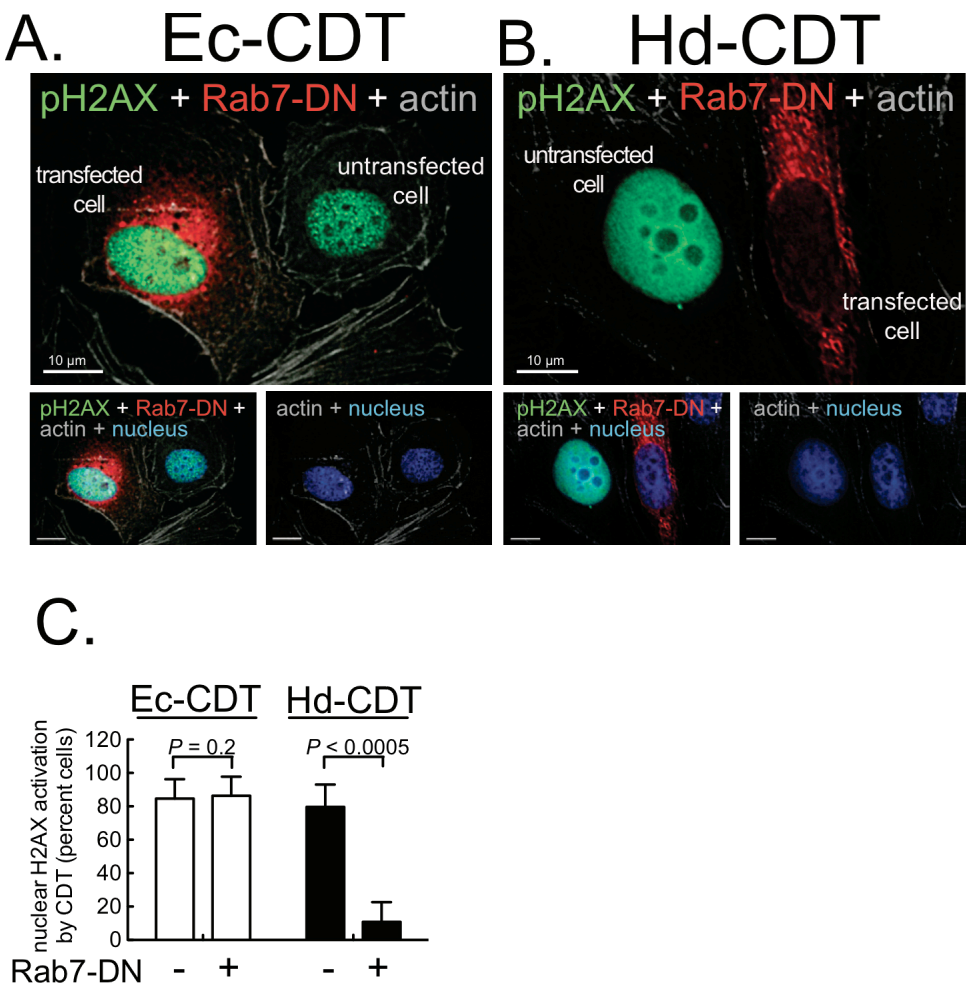

Figure 7. Gargi et al., 2012

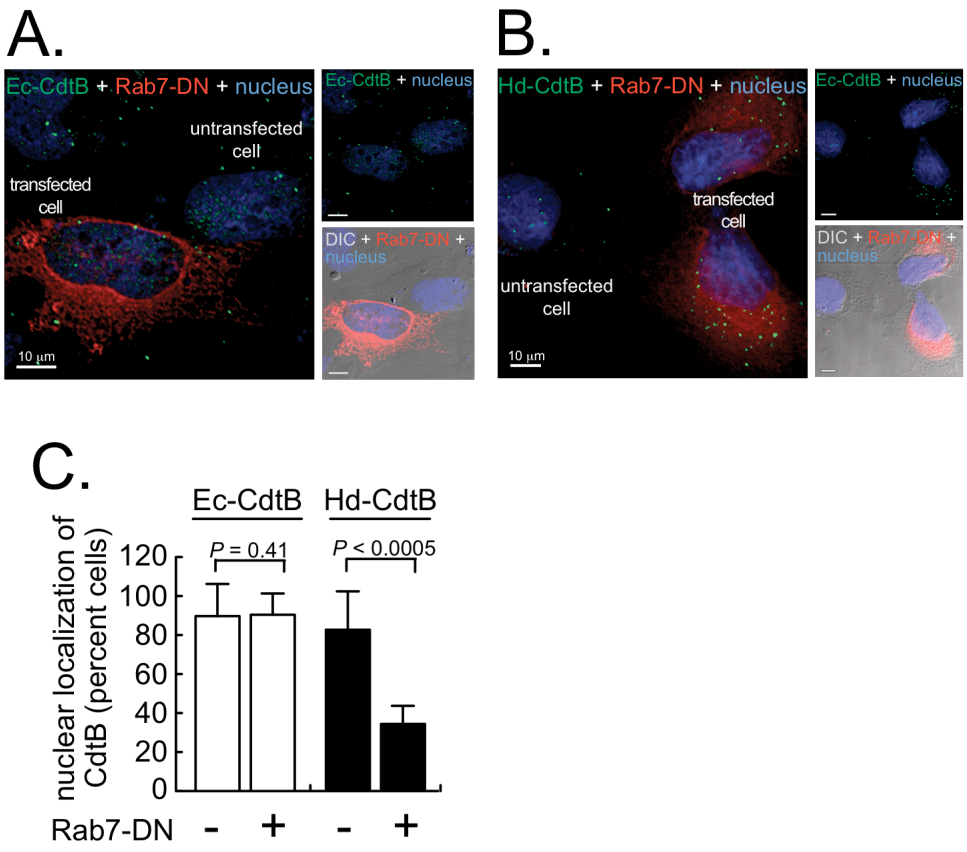

Figure 8. Gargi et al., 2012

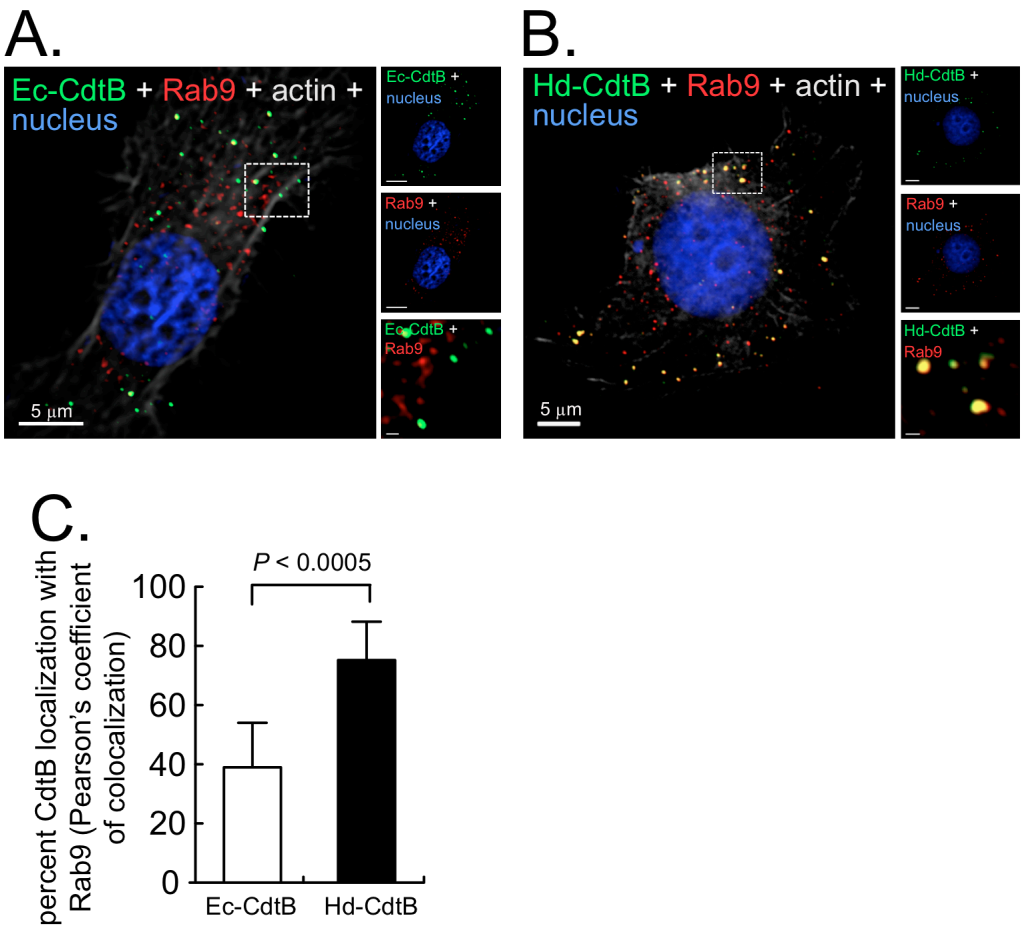

Figure 9. Gargi *et al.*, 2012

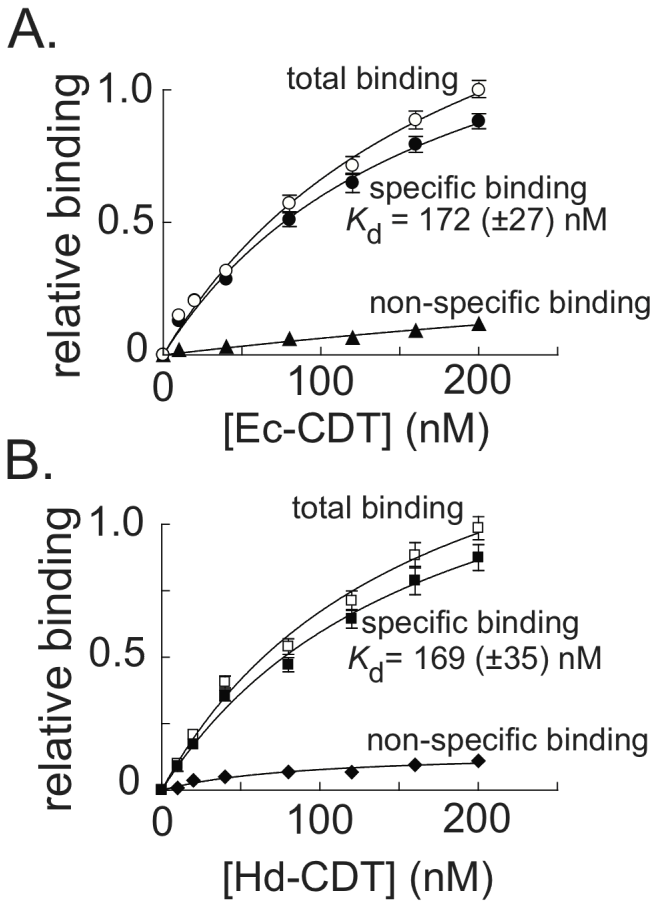

Figure 10. Gargi et al., 2012